National Library of Canada
Canadian Theses Division
Ottawa, Canada
K1A 0N4

Bibliothèque nationale du Canada
Division des thèses canadiennes

PERMISSION TO MICROFILM — AUTORISATION DE MICROFILMER

• Please print or type — Écrire en lettres moulées ou dactylographier

Full Name of Author — Nom complet de l'auteur

AGODICHUKWU SUNDAY CHUKWUEMEKA EZEUDEMBAH

Date of Birth — Date de naissance

February 4, 1945

Country of Birth — Lieu de naissance

NIGERIA

Permanent Address — Résidence fixe

c/o St James' Church, NANKA, Via Aguata L.G.A.
ANAMBRA STATE, NIGERIA

Title of Thesis — Titre de la thèse

STEADY STATE RADIAL GAS FLOW THROUGH POROUS MEDIA

University — Université

UNIVERSITY OF ALBERTA

Degree for which thesis was presented — Grade pour lequel cette thèse fut présentée

M.Sc. (Petroleum Engineering)

Year this degree conferred — Année d'obtention de ce grade

1981

Name of Supervisor — Nom du directeur de thèse

Prof. P.M. Dranchuk

Date

Dec 3, 1980

Signature

THE UNIVERSITY OF ALBERTA

STEADY STATE RADIAL GAS FLOW THROUGH POROUS MEDIA

by

© AGODICHUKWU S. C. EZEUDEMBAH

A THESIS

SUBMITTED TO THE FACULTY OF GRADUATE STUDIES AND RESEARCH
IN PARTIAL FULFILMENT OF THE REQUIREMENTS FOR THE DEGREE
OF MASTER OF SCIENCE

IN

PETROLEUM ENGINEERING

DEPARTMENT OF MINERAL ENGINEERING

EDMONTON, ALBERTA

Spring 1981

THE UNIVERSITY OF ALBERTA

RELEASE FORM

NAME OF AUTHOR AGODICHUKWU S. C. EZEUDEMBAH

TITLE OF THESIS STEADY STATE RADIAL GAS FLOW THROUGH POROUS MEDIA

DEGREE FOR WHICH THESIS WAS PRESENTED MASTER OF SCIENCE

YEAR THIS DEGREE GRANTED Spring 1981

Permission is hereby granted to THE UNIVERSITY OF ALBERTA LIBRARY to reproduce single copies of this thesis and to lend or sell such copies for private, scholarly or scientific research purposes only.

The author reserves other publication rights, and neither the thesis nor extensive extracts from it may be printed or otherwise reproduced without the author's written permission.

(SIGNED) ....

PERMANENT ADDRESS:

St. James' Church,

N A N K A, Via Aguata L.G.A.

Anambra State, N I G E R I A

DATED October 30, 1980

THE UNIVERSITY OF ALBERTA

FACULTY OF GRADUATE STUDIES AND RESEARCH

The undersigned certify that they have read, and recommend to the Faculty of Graduate Studies and Research, for acceptance, a thesis entitled STEADY STATE RADIAL GAS FLOW THROUGH POROUS MEDIA submitted by AGODICHUKWU S. C. EZEUDEMBAH in partial fulfilment of the requirements for the degree of MASTER OF SCIENCE in PETROLEUM ENGINEERING.

Prof. P. M. Dranchuk ....
Supervisor

Dr. D. L. Flock ....

Dr. R. G. Bentsen ....

Dr. N. Rajaratnam ....

Date October 30, 1980

To the memory of my father

Daniel Ogbonnaya EZEUDEMBAH

March 15, 1915 - December 27, 1979

Abstract

This work deals with the possible causes of anomalous gas flow behavior which has been observed on both Klinkenberg and visco-inertial plots at higher flow rates and pressures. In pursuance of this study, experiments were carried out at higher flow rates and pressures, and at lower flow rates and pressures, with the following objectives:

1. evaluation and re-arrangement of flow case studies for use in the experiments;
2. re-evaluations of the existing visco-inertial flow model equation which uses Forchheimer's quadratic equation;
3. consideration of stress and strain on the core during the course of radial flow under uniaxial confinement;
4. a check on the possibility of hysteresis effect.

The plot profiles, obtained by conducting the experimental runs at higher flow rates and pressures, suggest a deviation from expected profiles which fit the visco-inertial flow model equation. By analysis, and model fitting, these profiles are found to fit Forchheimer's cubic equation. The log-log plot of the friction factor against the Reynolds number suggests an existence of some term beyond the visco-inertial flow regime. The plot profiles, obtained by conducting the runs at lower flow rates and pressures, conform to the visco-inertial flow model equation. Similar anomalous flow behavior, in which the apparent gas permeability increases for increasing flow

rate, is found to be dependent on both the flow method, and the type of radial confinement used. Application of stress-strain analysis has proved to be a vital tool in the study of confining pressure effects on flow behavior. Hysteresis has been observed to be significant in the parameter estimated values.

Both Forcheimer's quadratic and cubic equations have been derived by considering Navier-Stokes equations and dimensional analysis for the quadratic case, and kinetic energy equation of mean flow and dimensional analysis for the cubic case. The cubic term is regarded as an extension to the quadratic equation at higher flow rates. The physical existence of its main parameter, gamma, together with the flow regime in which it operates, is established by consideration of the boundary layer theory to the flow problem. Properties of gamma, obtained from experiment, agree with those obtained from theory.

Similar runs were made under triaxial confinement, using a triaxial overburden radial cell. The results, however, are not conclusive due to design problems.

Acknowledgement

The author acknowledges the guidance and supervision of Professor P.M.Dranchuk in the preparation of this work. He also extends his appreciation to Drs. S.M.Farouq-Ali, R.G. Bentsen, all of this Department, and Dr. N.Rajaratnam of the Department of Civil Engineering, for their helpful comments and suggestions in parts of this work. The counsel received from Drs. D.L.Flock and F.H.Vitovec is appreciated. Acknowledgements also go to Mr. G.T.Walsh; who designed the second radial cell, Mrs. R.Mei, who typed parts of the manuscript, the general staff of this department, and the consultants at the Computing Services of this university.

The author acknowledges with appreciation the financial support, opportunity, and permission, which made this study possible. Hence, special thanks are given to the University, the Department, the Natural Sciences and Engineering Research Council (NSERC) Canada, and to the Federal Government and Peoples of the Republic of Nigeria.

Cordial and understanding atmosphere within the family contributed greatly to the completion of this work. To this effect, the author gives credit to his wife, Onyemere, his son, Udoka, and his other family members in Nigeria, who, despite the present trying period within the family, gave him full support.

Table of Contents

List of Tables

List of Figures

List of Plates

Nomenclature

a = Hydraulic resistivity in the Kozeny-Carman form, K^{-1}, in Equations 2.5, 2.22

A = Cross-sectional Area

A = Arbitrary constant vector used in Appendix B

A' = Area open to flow in Appendix A

A_1, A_2 = Arbitrary constants used in Chapter 5

b = Slippage coefficient, $[ML^{-2}T^{-2}]$, in Equation 2.7

B = Arbitrary constant vector used in Appendix B

CC1 = Coefficient of the viscous term of the general cubic flow equation, Chapter 4.

CC2 = Coefficient of the inertial term of the general cubic flow equation, Chapter 4.

CC3 = Coefficient of the cubic term of the general cubic flow equation, Chapter 4.

Cd = Orifice drag coefficient in Equations 2.30, 2.31

C_L = Laminar energy loss coefficient, in Equations 2.30, 2.31

CP = Confining pressure

C_t = Turbulent energy loss coefficient, Equations 2.30, 2.31

C_1-C_3 = Arbitrary flow physical constants in the general cubic flow equation, Chapter 4

C1-C6 = Arbitrary flow physical constants in the general cubic flow equation, Appendix A

d = Boundary layer thickness in Equation A-26

dc = Characteristic hydraulic matrix mean pore size diameter, Equations 2.30, 2.31

dm = Mean grain diameterin Equation 2.5

D = Skin frictional coefficient, dimensionless, in Appendix A

Da = Average diameter of the particles, ft, in Equations 2.26, 2.27

D,DT = Arbitrary constant vector and its transpose used in Appendix B

E = Young's Modulus in Chapter 5

E = Arbitrary constant vector used in Appendix B

f = Friction factor, in Equations 2.15, 2.16, 2.27

Fb = Inertial resistance coefficient, Beta, ft^{-1}, m^{-1}

g = Acceleration due to gravity

G = Gas Gravity in Equations 2.26, 2.27

Gs = Superficial mass velocity, $lbmass/ft^2sec$, in Equations 3.1, 3.2, 3.3

h = Height, [L]

J = Hydraulic gradient, in Equation 2.22

k = Absolute gas permeability at infinite mean pressure in Equation 2.7, $[L^2]$, md, μm^2

ka = Apparent gas permeability, calculated from Darcy's law in Equation 2.7, $[L^2]$, md, μm^2

K = Hydraulic conductivity which measures the permeability of the porous medium ,in Equation 2.5

L = Length scale in Appendix A

Le = Overall length of the porous media, ft, in Equation 3.1

m,n = Exponential values for porosity, in Equation 2.26, 2.27

m(P) = Real gas pseudo-pressure in Equation 2.12

M = Molecular weight of gas

P = Pressure at ambient condition, atm, kPa, $[ML^{-2}T^{-2}]$

Pb = Base pressure in Equation 2.12

Pe, P_2 = Outer pressure, atm, kPa, $[ML^{-2}T^{-2}]$

PEW = Coefficient of the slippage term of the general cubic flow equation, Chapter 4.

Phc = Hydrostatic rock confinement pressure, psi

Pm = Arithmetic mean flowing fluid pressure = (Pe + Pw)/2

Pnc = Net rock confinement pressure, psi

Pw, P_1 = Pressure, psi, kPa

q = Gas flow rate, Q/Area

Q = Gas flow rate, Mscf/day.

Qo = Gas flow rate, cm^3/sec, m^3/day, at standard conditions

re, r_2 = Outer radius, [L]

rw, r_1 = Inner radius, [L]

Re = Reynolds number, dimensionless.

S = Shape factor which is dependent on the shape of the grains and their structure in Equation 2.5

S′ = Shape factor for increasing inertial effect, in Equation 2.23

Sr = Principal stress in the radial direction

S+ = Principal stress in the tangential direction

Sz = Principal stress in the axial direction

T = Temperature, °R

Ta = Average temperature of flowing gas, °R

u = Velocity notation in Appendix A

U = Flow rate of displacement in Chapter 5

U = Velocity scale in Appendix A

U' = Fluctuation's velocity scale

v = Superficial gas velocity, ft/sec, Equations 2.18, 2.19, 2.20, 2.30

W = Arbitrary constant vector used in Appendix B

Wi,Wn = Arbitrary constants used in Appendix B

Wo,Wn = Arbitrary constants used in Appendix B

Wo-W_5 = Arbitrary constants used in Appendix B

Ws = Weight of flowing gas, Ib/sec, in Equations 2.26, 2.27

x = Distance between plates of orifice model, in Equations 2.30, 2.31

X = Arbitrary constant vector used in Appendix B

Y = Arbitrary constant vector used in Appendix B

Z = Compressibility factor of gas

Za = Average compressibility factor

α = Alpha, viscous coefficient, $[L^{-2}]$, K^{-1}, ft^{-2}, in Equations 2.20, 2.28

β = Beta, Inertial coefficient, $[L^{-1}]$,

γ = Gamma, Parameter in the cubic term, $[LTM^{-1}]$, $atm.cm^2.sec^3/gm^2$ = cm.sec/gm, m.sec/Kg

λ = Mean free path of the flowing gas.

μ = Gas viscosity, $[ML^{-1}T^{-1}]$, lb/ft-sec, cp, μPa.s

ν = Kinematic viscosity, $[L^{-1}]$, in Equation 2.5,

atm.sec²/gm = cm⁻¹

ν = Poisson's ratio in Chapter 5.

ε_r = Principal strain in the radial direction

ε_t = Principal strain in the tangential direction

ε_z = Principal strain in the axial direction

ρ = Density of gas, $[ML^{-3}]$

ρ_o = Density of gas at standard condition, $[ML^{-3}]$

ϕ = Porosity

Conversion Factors

To = 288.150 °K, at standard condition

Po = 1 atm = 101.325 kPa, at standard condition

Zo = approximately unity, at standard condition

gc = 32.17 lbm.ft/lbf.sec^2

R = Gas constant,

R = 1545 lbforce.ft^3/ft^2.lbmole °R

R = 82.056 atm.cm^3/gmmole °K

R = 8.3143 kPa.m^3/kgmole °K

1 cp = 10^3 μPa.s

1 darcy = 0.9869 μm^2

1 cm^3/sec = 86400x10^{-6} m^3/day

1 atm.sec^2/gm = 101.325x10^6 m^{-1}

1 atm.cm^3/gmmole°K = 0.101325 kPa.m^3/kgmole °K

1 atm.sec^3.cm^2/gm^2 = 101.325x10^5 msec/kg

1. INTRODUCTION

Considerable effort has been made to explain the phenomenon of gas flow through porous media, using Darcy's law as a fundamental equation. Problems encountered in interpretation and understanding of this phenomenon brought some necessary modifications to this law. These include a correction for gas slippage at lower flow rates, using Klinkenberg's equation. For increasing inertial effects due to higher flow rates, modification has been made by using Forchheimer's quadratic equation.

This study is an attempt to explain some of the observations made by both Piplapure(1) and Senturk(2) on Klinkenberg and visco-inertial plots at higher flow rates and pressures. They were of the general opinion that inadequate confinement pressure could be contributive to some of the observed deviations. Senturk, in addition, felt that these deviations are related to the production method of experimentation. The existing model flow equation is due to Piplapure who pointed out that it is a simplified form of a more complete equation.

It becomes, therefore, necessary that the fundamental theory of steady state radial gas flow through porous media be reviewed with the following objectives.

1.1 Objectives

The main objective is to attempt an explanation of the deviations observed on the Klinkenberg and visco-inertial plots. To effect this, experimentation is done

1. with different flow methods,
2. to span both lower and higher flow rates and pressures,
3. to study the significance of both the flow methods and hysteresis on gas flow behavior.

Secondly, the effect of confinement pressure is to be studied by analysing the stress and strain on the core sample as flow progresses.

Thirdly, there is need for reassessing the existing visco-inertial flow model equation and reviewing it for higher, increasing flow rates and pressures. In order to accomplish this, it may be necessary to study the applicability of both Forchheimer's quadratic and cubic equations to the flow data.

2. LITERATURE REVIEW

2.1 Viscous Flow Equations

As quoted by Hubbert(3), Darcy(4) determined that when water flows vertically downwards through a packed sand filter, the volumetric flux density is found to be proportional to the differential pressure gradient. This relationship, which subsequently became known as Darcy's law, is expressed by the following equation:

$$q = - K \frac{h_2 - h_1}{L} \tag{2.1}$$

where K is the constant coefficient which depends on the permeability of the sand. Numerous attempts have been made to theoretically derive this law using variables with more general physical meaning.

In 1956, Hall(5) derived the general form of Darcy's law for non-isotropic porous media from Newton's basic laws of motion and viscosity. Assuming negligible forces of inertia in the system, and continuous liquid films, he obtained the following equation

$$q = - \left(\frac{1}{\mu}\right) K \cdot (\vec{\nabla} p + \rho \vec{\nabla} gz) \tag{2.2}$$

by using a representative volume element. The permeability, K, is considered to be a tensor and gz is the potential of the gravitational force.

Hubbert(6) used the Navier-Stokes equations of motion of viscous fluids to derive Darcy's law for macroscopically homogeneous and isotropic porous medium in the form of:

$$q = Nd^2(\rho/\mu)\ [\vec{g} - \frac{1}{\rho}\,\text{grad}\ P] \qquad (2.3)$$

This is preceded by his earlier work in 1940.(7)

Irmay(8), in 1958, used both a hydraulic model and statistical methods on the Navier-Stokes equations of motion to study a one-dimensional flow of an incompressible fluid through a homogeneous and isotropic medium. At low values of Reynolds number, he derived Darcy's law in the form of:

$$q = KJ \qquad (2.4)$$

where

$$K = \frac{1}{a} = \frac{gd_m^2}{S\nu} \cdot \frac{\phi^3}{(1-\phi)^2} \qquad (2.5)$$

He further emphasized that Darcy flow through porous media is such that the total kinetic energy of flow, which is proportional to the square of the flow rate, is minimum.

The book by Scheidegger(9) gives a detailed review of various theories, models, and derivations of Darcy's law. This law is used extensively to describe the flow of fluids through porous media for the viscous laminar flow regime.

2.1.1 Gas Slippage Phenomena

Flowing gas through porous media, especially at lower pressures, yields higher permeability values than those values obtained by flowing liquid. From theory and through extensive experimentation, Klinkenberg(10) in 1941 showed this to be due to gas slippage which occurs at the fluid-solid interface. He observed that the permeability to a gas

a) is a function of the mean free path of the gas molecules.

b) depends on pressure, temperature and the nature of the gas.

c) is both dependent on the property of the porous rock and on the mean pressure at which the gas flows.

Darcy's law, for horizontal plane radial flow, and Klinkenberg's equation are, respectively:

$$-\frac{dp}{dr} = \frac{\mu}{k} q \qquad (2.6)$$

$$ka = k\left(1 + \frac{b}{P_m}\right) \qquad (2.7)$$

where

b = Slippage coefficient, expressed as

$$b = \frac{4c\bar{\lambda}}{r} P_m \qquad (2.8)$$

Combination of Equations 2.6 and 2.7 shows that both the viscous and the slippage terms are active in Darcy gas flow.

The work of Klinkenberg opened up more investigations to determine the validity and theory of gas slippage. According to this equation, a plot of ka versus 1/Pm, usually called the Klinkenberg plot, should be linear with intercept k and slope bk.

Calhoun and Yuster(11) in 1946 validated Klinkenberg's equation but pointed out that the relationship between the apparent permeability,ka, and the reciprocal of the mean pressure is not exactly linear. They concluded that permeability measurements at different pressure differentials, as stated by Klinkenberg, gave the same value of permeability as long as the mean pressure is constant.

Yuster(12), made the following observations:

1. The plot of apparent gas permeability against the reciprocal of the mean pressure is usually linear, but appreciable curvature at high mean pressures may be noticeable.
2. Using several gases on one core for the Klinkenberg plot, all the lines extrapolated to the same point at infinite pressure.
3. Apparent gas permeability increases with increase in

temperature, but its value at an infinite mean pressure is essentially independent of temperature.

Using the basic concept of kinetic theory of gases, Rose(13) validated Klinkenberg's interpretation of gas slip flow phenomena. He expressed the mean free path of the flowing gas, measured at mean pressures, in terms of temperature, T, gas constant, R, and molecular weight, M, of the gas with the following relation:

$$\lambda \quad 2.13 \frac{\mu}{P_m}\sqrt{\frac{RT}{M}} \tag{2.9}$$

By statistical averaging, Heid, McMahon, Nielsen, and Yuster(14) obtained a relationship between the absolute gas permeability, k, and the gas slippage coefficient, b, as:

$$b = 0.777k^{-0.39} \tag{2.10}$$

where b is in atmospheres and k is in millidarcies. They observed that, at higher permeabilities, small errors in permeability measurements can cause large errors in the values of b obtained, and unusually low porosity tends to give lower than average values ~~of b~~.

Dranchuk and Sadiq(15) observed that permeability obtained in a Klinkenberg extrapolation technique is invalid if the data used are not taken in the viscous flow region. They noticed a departure from linearity at high mean pressures on a Klinkenberg plot. Subsequently, they suggested that a back-pressure curve be plotted first on log-log paper in order to delineate the viscous and the visco-inertial flow regions.

Jones(16) obtained the following relation for gas slip coefficient, b(in psi), in terms of permeability, k(in md):

$$b = 6.9k^{-0.36} \tag{2.11}$$

Casse and Ramey, Jr.(17) observed that the slip coefficient varies linearly with temperature.

2.1.2 Real Gas Pseudo-Pressure

The dependence of the gas compressibility factor and viscosity on pressure was studied by Al-Hussainy, Ramey and Crawford(18). They developed the real gas pseudo-pressure as:

$$m(P) = 2\int_{P_b}^{P} \frac{P}{\mu(P)Z(P)}\,dP \tag{2.12}$$

where Pb is the base pressure. Using this potential, they proposed the following equation for steady state, isothermal, radial gas flow in the viscous region:

$$q = \frac{\pi k h T_0[m(P_e) - m(P_w)]}{T P_0 \ln \frac{r_e}{r_w}} \tag{2.13}$$

Mackett(19) considered the isothermal variation of compressibility factor and viscosity with pressure at their reduced conditions with the following integral

$$XKI = \int_0^{P_r} \frac{P_r}{Z\mu_r} \, dP_r \qquad (2.14)$$

He then concluded that under the experimental conditions in which he worked, the values obtained by using average fluid properties do not differ very appreciably from the values obtained by using the above integral.

2.2 Reynolds Number Criterion

Increasing both flow rate and flowing pressure leads to a deviation from Darcy's law, and this leads, subsequently, to departure from laminar flow. Earlier investigators(20,21,22) attributed this phenomenon to turbulent flow. Recent reasoning, which has been facilitated mainly by the study of Navier-Stokes equations of motion, attribute it to inertial effects(23,24).

Wright(25) in 1968 explained that, as flow rate increases, deviation from Darcy's law is initially due to inertial effects and at higher flow rates turbulent effects may be observed. He designated the flow regimes as: viscous, steady-inertial, transition to turbulence and full turbulence. Using this explanation, the transition from purely laminar, Darcy-type flow to fully turbulent flow, covers a wide range of flow rates.

For pipe flow, the Reynolds number is used to determine the onset of turbulence and the departure from laminar flow.

Applying this concept to flow through porous media, a need arises for a suitable cut-off value of Reynolds number which characterizes the departure from both Darcy's law and laminar flow.

Hubbert(26), using unconsolidated porous medium, came to the following conclusions:

1. For deviation from Darcy's law, Reynolds number is greater than 1.
2. Darcy's law fails when velocity is great enough to make the inertial force significant.
3. Incidence of turbulence in Darcy flow occurs at much higher velocities corresponding to very high Reynolds numbers.

Subsequently, he defined the Reynolds number as the ratio of the inertial forces to the viscous drag forces.

Linquist(27) in 1933 concluded that Darcy's law is true for Reynolds number up to 4 and, for Reynolds number between 4 and 180, he postulated the equation

$$fRe = 40Re + 2500 \qquad (2.15)$$

On the basis of his results, King(28) in 1940 concluded that Darcy's law holds for Reynolds number up to 10. For Reynolds number between 10 and 300, he postulated

$$f = 94/Re^{0.16} \qquad (2.16)$$

Collins(29) pointed out that, in sands and sandstones, the transition from laminar to turbulent flow occurs gradually at Reynolds numbers between one and ten. He added that true turbulence occurs only at higher Reynolds numbers.

Scheidegger(30) reviewed the correlations of Reynolds number and friction factors with flow regimes. He noted that there are two critical Reynolds numbers at which the flow regime changes, even though they may not be universally defined. The first change occurs when inertial effects in laminar flow become important. The second change signals real turbulence. He further stated that correlations are valid, and useful, only for application to particular systems. Caution must therefore be exercised if they are to be applied to other conditions for which they were not originally obtained.

2.3 Forchheimer's Equations

Forchheimer(31), in 1901, suggested that Darcy's law be modified for high flow rates by including a second-order term in the flow rate as follows:

$$-\frac{dP}{dx} = aq + bq^2 \tag{2.17}$$

where a and b are polynomial constants. The extra term takes care of the increasing inertial effect.

By dimensional considerations, Green, Jr. and Duwez(32) observed that for a low Reynolds number, corresponding to a low velocity, the following relation is obtained:

$$-\frac{dP}{dx} = \text{Const} \cdot \frac{\mu v}{\delta^2} \tag{2.18}$$

Identifying this equation as Darcy's law, they obtained the following relation for higher velocity:

$$-\frac{dP}{dx} = \text{Const} \cdot \frac{\rho v^2}{\delta} \tag{2.19}$$

They reasoned that

a) the losses due to the inertia of the fluid become progressively more important with increasing velocity;

b) the gradual transition from Darcy flow regime is marked by losses due to both the viscous shear in creeping flow, and to inertial effects.

Therefore, they combined the two equations to obtain a Forchheimer-type of equation

$$-\frac{dP}{dx} = \alpha\mu v + \beta\rho v^2 \tag{2.20}$$

Beta, in this equation, was previcusly known as the turbulence factor, but is now known as the inertial resistance coefficient, Fb. Kolada(33) expressed it as:

$$F_b = \frac{7.56 \times 10^8}{\phi^{1.67} k^{1.12}} \tag{2.21}$$

Senturk(34) concluded from his studies that this parameter is both a property of the flowing gas and of the porous medium.

Irmay(35) derived Forchheimer's equation for a one dimensional steady-state flow through a homogeneous isotropic medium of average grain diameter as:

$$J = aq + bq^2 \quad (2.22)$$

where

$$b = \frac{S'(1-\phi)^2}{\phi^3} \cdot \frac{1}{gd_m^2} \quad (2.23)$$

He stated that while coefficient,a, depends on both viscosity and temperature, coefficient,b, does not. For Reynolds number greater than 100, the flow becomes turbulent.

Schiedegger(36), reported that following further research, Forcheimer added a third-order term thus:

$$-\frac{dP}{dx} = aq + bq^2 + cq^3 \quad (2.24)$$

where a, b, and c are polynomial constants. He added that this equation fitted experimental data better for higher flow rates.

Basak and Soni(37), reviewing the flow relations due to both Darcy and Forchheimer, observed that while Darcy's law failed beyond Reynolds number one, the velocity gradient response is adequately represented by Forchheimer's relations. Analysing high-velocity gas flow through porous media, Firoozabadi and Katz(38) noted that there are cases where Forchheimer's quadratic equation failed to correctly fit the experimental data. They therefore suggested for such cases the use of Forchheimer's cubic equation in the following form

$$-\frac{dP}{dx} = \frac{\mu}{k} q + \beta \rho q^2 + \gamma \rho^2 q^3 \qquad (2.25)$$

2.4 Radial Visco-Inertial Flow Equations

Elenbaas and Katz(39) developed a radial turbulent gas flow equation, by assuming average values of gas viscosity, temperature and compressibility factor. For laminar and turbulent flow through unconsolidated particles, they gave, respectively, the following equations:

$$P_2^2 - P_1^2 = 8.12 \times 10^{-4} \frac{\mu Z_a T_a W_s}{D_a^2 \phi^{n-m} hG} \ln \frac{r_2}{r_1} \qquad (2.26)$$

$$P_2^2 - P_1^2 = 2.02 \times 10^{-6} \frac{W_s^2 T_a Z_a f}{D_a \phi^n h^2 G} \left(\frac{1}{r_1} - \frac{1}{r_2}\right) \qquad (2.27)$$

Furthermore, they observed that a back-pressure curve of $(Pe^2 - Pw^2)$ versus Q for a given gas well can be used to designate the different flow regimes present. Deviation of the slope of the curve at higher flow rates from unity marks the point of deviation from Darcy's law.

Using the linear equation presented by Green and Duwez(40), Cornell and Katz(41) gave a corresponding equation for radial geometry cases:

$$P_2^2 - P_1^2 = 1.5 \times 10^{-11} \frac{\alpha\mu ZTQ_o}{h} \ln \frac{r_2}{r_1} + 1.09 \times 10^{-13} \frac{\beta MQ_o^2 ZT}{h^2} \left(\frac{1}{r_1} - \frac{1}{r_2}\right) \quad (2.28)$$

Tek, Coats and Katz(42) combined both Forchheimer's quadratic equation and the modified gas law to obtain the following radial steady state turbulent gas flow equation:

$$P_2^2 - P_1^2 = \frac{1424\mu ZTQ_o}{hk} \ln \frac{r_2}{r_1} + \frac{3.161 \times 10^{-12} \beta GQ_o^2 ZT}{h^2} \left(\frac{1}{r_1} - \frac{1}{r_2}\right) \quad (2.29)$$

By using a force momentum balance on a capillary-orifice model, Crafton(43) obtained a quadratic equation similar to that of Forchheimer:

$$-\frac{dP}{dr} = \left(\frac{C_L R_e}{\pi r \phi d_c}\right) \mu v + \left(\frac{\rho C_d}{2x} + \frac{C_t}{\pi r \phi}\right) v^2 \quad (2.30)$$

where the Fb term in Forchheimer's equation is given as :

$$F_b = \frac{\rho C_d}{2x} + \frac{C_t}{\pi r \phi} \tag{2.31}$$

Fb = matrix term + "radial controlled" fluid term

Piplapure(44) obtained the following modified equation, similar to Equation 2.29, which expresses the parameters k, b, Fb simultaneously:

$$(P_e^2 - P_w^2) + 2b(P_e - P_w) = -\left[\frac{1424\bar{\mu}\bar{Z}\bar{T}Q_o}{hk} \ln\frac{r_e}{r_w} + 3.1602 \times 10^{-12}\frac{F_b G\bar{Z}\bar{T}Q_o|Q_o|}{h^2}\left(\frac{1}{r_w} - \frac{1}{r_e}\right)\right] \tag{2.32}$$

He identified them as viscous, slippage, and inertial terms respectively.

In deriving this equation, he transformed the mean pressure term in Klinkenberg's equation into its instantaneous pressure value. Subsequently, he assumed the value

$$\left[F_b\left(\frac{P_o m}{RT}\right)^2 \frac{\bar{Z}R\bar{T}}{m} \cdot \frac{Q_o|Q_o|}{(2\pi h)^2}\right] \times \frac{b}{P} \tag{2.33}$$

is sufficiently small so that it can be neglected.

3. DEVELOPMENTS FROM PREVIOUS EXPERIMENTS

3.1 Klinkenberg and Visco-Inertial Plots

It is standard practice to study and predict gas flow behavior in a porous medium under viscous and visco-inertial flow conditions by conducting a multiple-point flow test on a sample of the medium. The parameters - absolute gas permeability,k, gas slippage factor,b, and inertial resistance coefficient,Fb, - are evaluated, graphically or numerically, by using the flow equations in data analysis. Equation 2.7 yields the Klinkenberg plot for flow within the viscous region where Darcy's law is valid. The absolute gas permeability is the extrapolated value at infinite mean pressure and the gas slippage coefficient,b, is obtained from the slope. This plot departs from predicted linearity and curves downwards at higher pressures corresponding to higher flow rates.

3.1.1 Linear Geometry

Equation 2.20 represents the more general form of the second-order Forchheimer equation (Equation 2.17). Cornell and Katz(45) modifying this equation for linear geometry cases, presented it as:

$$\frac{(P_2^2 - P_1^2)Mg_c}{2L_e G_s ZRT\mu} = \alpha + \beta \frac{G_s}{\mu} \qquad (3.1)$$

In this form, a plot of the left hand side versus Gs/μ

yields the visco-inertial plot. This is a linear plot with the intercept as the reciprocal of the apparent permeability, ka, and the slope as the inertial resistance coefficient, Fb. Dranchuk and Sadiq(46) observed that this plot departs from linearity with a characteristic downward curve at lower flow rates. This, they explained, is due to gas slippage at the gas-solid interface.

From the foregoing, two methods exist for the determination of permeability of a porous medium. While the resulting values from these two methods are expected to be equal, experiments(47,48) have shown them to be different. The visco-inertial plot yields the higher value, and depending on the gas slippage coefficient, the difference can be very large. Dranchuk and Kolada(49) inferred that possibly some or all of the data may be affected by gas slippage. They therefore suggested that, in order to account for gas slippage, Equation 3.1 be modified to:

$$\frac{(P_2^2 - P_1^2)Mg_c}{2L_e ZRT\mu G_s} = \frac{1}{K(1 + \frac{b}{P_m})} + \beta \frac{G_s}{\mu} \tag{3.2}$$

or

$$\frac{(1 + \frac{b}{P_m})(P_2^2 - P_1^2)Mg_c}{2L_e ZRT\mu G_s} = \frac{1}{k} + \beta \frac{G_s}{\mu}(1 + \frac{b}{P_m}) \tag{3.3}$$

Equation 3.3 suggests a linear plot between the left hand side term and $(Gs/\mu)(1+b/Pm)$. The intercept yields the reciprocal of the absolute permeability while the slope yields the inertial resistance coefficient. This plot, known as the modified visco-inertial plot, requires that the gas slippage coefficient be known first. Dranchuk and Kolada recommended that the value of b be obtained through trial and error. This is done by repeatedly plotting both the back-pressure and the Klinkenberg plots and checking the values of b for good agreement. The final reliable value is used in Equation 3.3 to construct a modified visco-inertial plot for all the data points except those which have been found to be in the viscous region.

By expressing the unknown parameters, b, k, Fb, simultaneously, as in Equation 3.3, some possible numerical procedure for estimating these parameters may be found. Kolada, using the Newton-Raphson approximation technique, pointed out that this method requires an initial estimate of the parameters and also quasilinearization in the derivatives containing the parameters. He added that convergence is dependent on the goodness of the initial estimates, and on the algorithm used.

3.1.2 Radial Geometry

Piplapure(50) replaced both the conventional visco-inertial equation (Equation 3.1) and the modified visco-inertial equation (Equation 3.3), with the following equations:

$$-\left[\frac{(P_e^2 - P_w^2)h}{1424\bar{\mu}\bar{T}\bar{Z}Q_o}\right] = \frac{\ln \frac{r_e}{r_w}}{k} + \frac{2.2192 \times 10^{-15} F_b G \left(\frac{1}{r_w} - \frac{1}{r_e}\right) \frac{|Q_o|}{\mu}}{h} \tag{3.4}$$

$$-\frac{[(P_e^2 - P_w^2) + 2b(P_e - P_w)]h}{1424\bar{\mu}\bar{T}\bar{Z}Q_o} = \frac{\ln \frac{r_e}{r_w}}{k} + \frac{2.2192 \times 10^{-15} F_b G \left(\frac{1}{r_w} - \frac{1}{r_e}\right) |Q_o|}{h} \tag{3.5}$$

Equation 3.5 is not strictly an exact counterpart of Equation 3.3 because, as Piplapure pointed out, it is a simplified form of the complete equation. Nevertheless, the three parameters are simultaneously represented and all the treatments using Equation 3.3 are assumed to apply. Dranchuk and Piplapure(51) indicated that the viscous region can be delineated on the basis of Reynolds number which can be calculated only when k and Fb are known.

3.2 Anomalies

Some anomalous behavior in both Klinkenberg and visco-inertial plots has been reported. Kolada(52) plotted some reconstituted data of Cornell(53) and noticed that the apparent permeability, ka, decreases with mean pressure, Pm, and flow rate, Qo, at lower flow rates, and increases with them at higher flow rates. Piplapure(54) obtained a profile with an upward curve on the Klinkenberg plot, instead of a profile with the usual downward curve. The nature of these plots, he reported, caused less effective prediction of both permeability and slippage coefficient to be made. Though the runs produced peculiar Klinkenberg plots, he noticed that the resulting visco-inertial plots appeared to be normal in every respect. The runs were taken at constant upstream pressures for varying downstream pressures.

In another set of runs, taken at both constant downstream and upstream pressures, and at higher flow rates, he again reported an upward curve on the Klinkenberg plots. This meant an increase in apparent permeability with increasing mean pressure. He explained that graphical parameter estimation was still possible, but both visco-inertial plots and numerical estimations yielded negative values of the inertial resistance coefficient. Despite this, he added, conventional visco-inertial plots were smooth, and modified visco-inertial plots yielded expected linear plots. He remarked that these peculiarities may be due to the effect of confining pressure.

Similar anomalies on the Klinkenberg plots were observed by Senturk(55) on runs taken at both constant downstream and constant upstream pressures, and at constant predefined net confinement pressures. He stressed that they were found in runs on low permeability cores, and at higher mean flowing gas pressures. These anomalies, he explained, may be due to inadequate definition of the net rock confinement pressure, lack of radial confinement pressures, or the manner in which the flow tests were conducted.

3.3 Effect of Confinement Pressure

Senturk investigated more closely the effect of confinement pressure on the parameters. He defined the net confinement pressure in terms of both the hydrostatic rock confinement pressure and mean flowing fluid pressure as:

$$Pnc = Phc - Pm \tag{3.6}$$

Subsequently, he concluded that for increasing net rock confinement pressure, absolute permeability decreased, and both gas slippage and inertial resistance coeficients increased.

3.4 Evaluating the Anomalies Using the Current Theory

By Equation 2.8, gas slippage phenomenon varies inversely with the mean pressure, and can be expressed as

$$\frac{4c\bar{\lambda}}{r} = \frac{b}{P_m} \tag{3.7}$$

where b, the proportionality constant, is the gas slippage coefficient. In conjunction with Equation 2.7, gas slippage varies directly with apparent gas permeability,ka. By standard experimental procedure and from the back-pressure relationship, mean pressure increases as flow rate increases. Therefore, both mean pressure and flow rate increase for decreasing gas slippage and apparent permeability,ka. Similarly, from theory, both mean pressure and flow rate increase with increasing inertial effects.

These considerations are combined in the analysis of three data cases from the literature. The trends of ka, gas slippage, and inertial effects, are respectively followed with reference to both the flow rate,Qo, and the mean pressure,Pm. Since Pm is an independent variable in the Klinkenberg plot, and Qo is part of a dependent variable in the visco-inertial plot, evaluation of these trends may be made with respect to the viscous and the visco-inertial regions of both plots.

<u>Case 1 (Constant Pw, and Decreasing Pe):</u>

In Piplapure's data for Sample 2 Run 1,(56), Pw is held constant at atmospheric pressure while Pe is steadily decreased at constant confining pressure,CP, of 3447.4 kPa. This results in decreasing (Pe^2 - Pw^2), decreasing Pm, and decreasing flow rate,Qo. With reference to Pm, 1/Pm increases, ka increases, 1/ka decreases, slip increases, and inertial effects decrease. With reference to Qo, which decreases, ka increases, 1/ka decreases, slip increases, and inertial effects decrease. The overall trend in both regions of flow of both plots is such that for decreasing Pm and Qo, ka increases, gas slippage increases, and inertial effects decrease. Both plots should yield a profile with a downward curve and a positive slope. Figures 3.1 and 3.2 show, respectively, the Klinkenberg and visco-inertial plots from

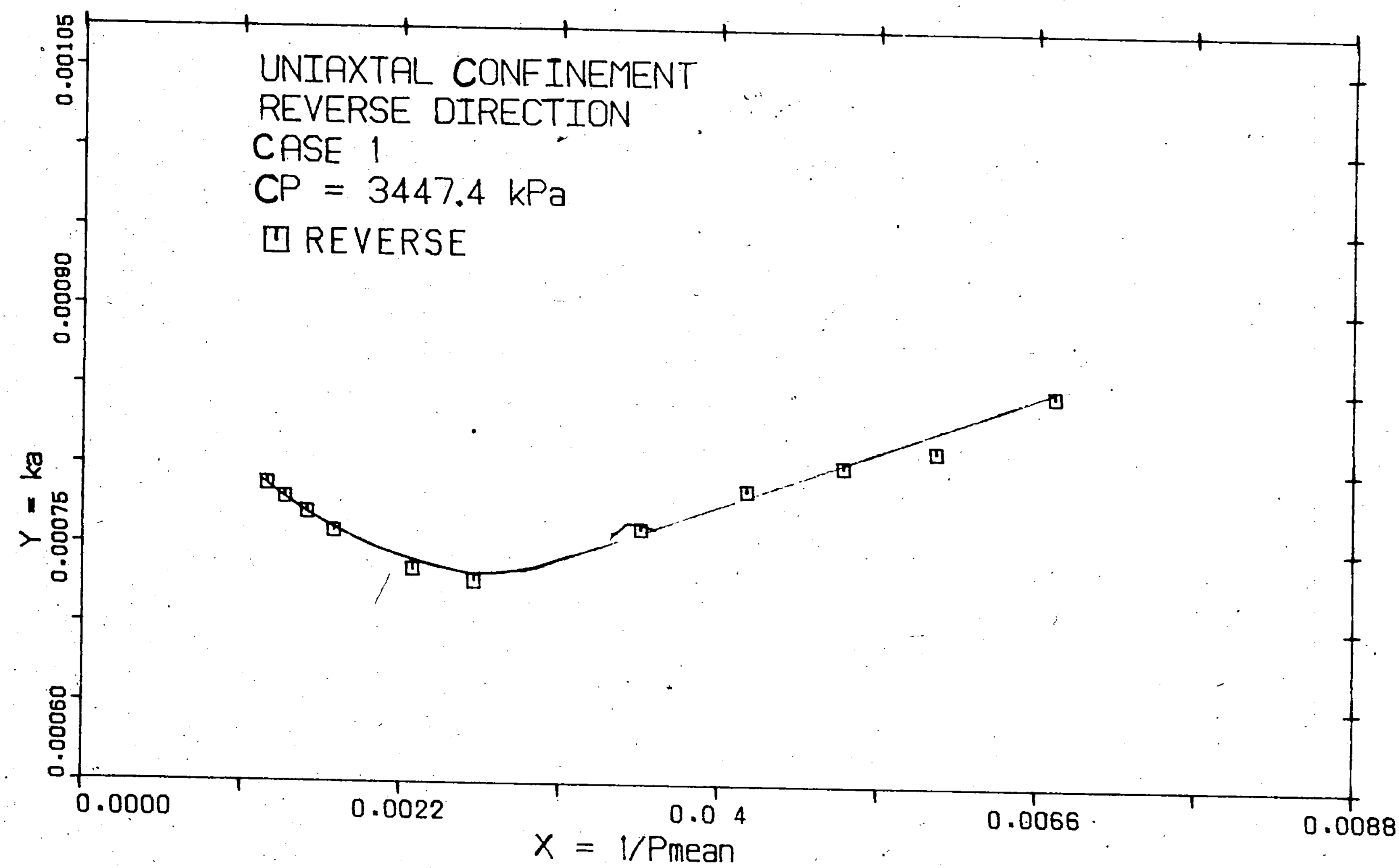

FIGURE 3-1: PIPLAPURE'S DATA KLINKENBERG PLOT

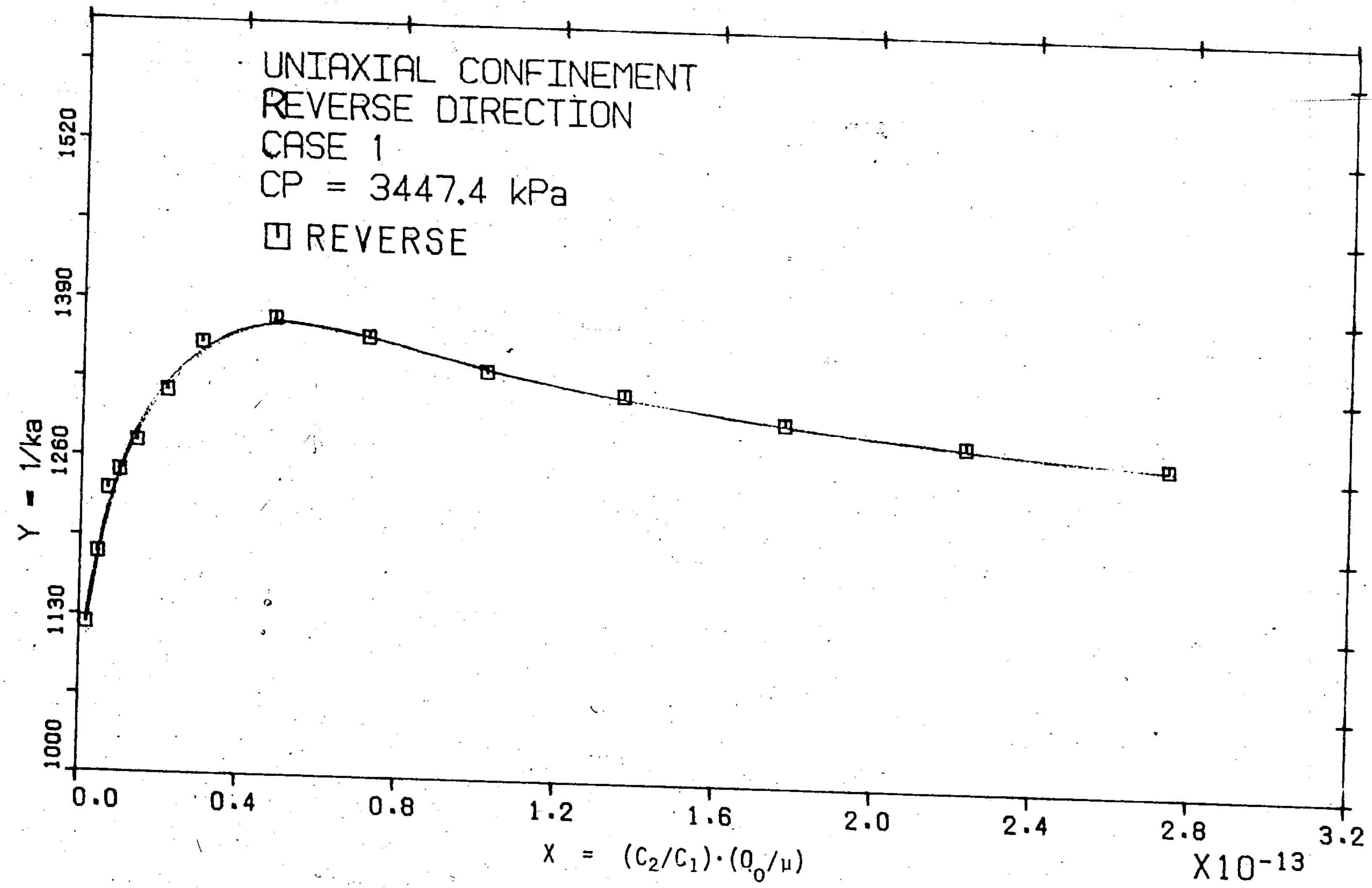

Figure 3-2: PIPLAPURE'S DATA VISCO-INERTIAL PLOT

Piplapure's data. The values of ka decrease initially, and then increase for decreasing Pm and Qo. This gives the Klinkenberg plot a concave upward profile while the visco-inertial plot gives a concave downward profile. Figure 3.3, which is the back-pressure plot, shows a decreasing slope at higher flow rates instead of an increasing slope.

Case 2 (Constant Pw and Increasing Pe):

This is Senturk's data for Sample SS-1-A, Run 2,(57) at constant confining pressure,CP, of 4136.9 kPa. The value of Pw is held constant at atmospheric pressure while Pe is steadily increased. This results in increasing (Pe^2 - Pw^2), increasing Pm, and increasing Qo. With reference to Pm, 1/Pm decreases, ka decreases, 1/ka increases, slip decreases, and inertial effects increase. With reference to Qo, which increases, ka decreases, 1/ka increases, slip decreases, and inertial effects increase. Therefore, for increasing Pm and Qo, the overall trend in both regions of both plots is such that ka decreases, gas slippage decreases, and inertial effects increase. This acts in the opposite sense to the expected trend in Case 1, even though the profiles should be similar. Figure 3.4 gives a trend similar to that of Figure 3.1 while Figure 3.5 gives a trend of decreasing ka with increasing Qo as has been predicted. The back-pressure plot in Figure 3.6 gives a lower slope at higher flow rates instead of the expected higher value.

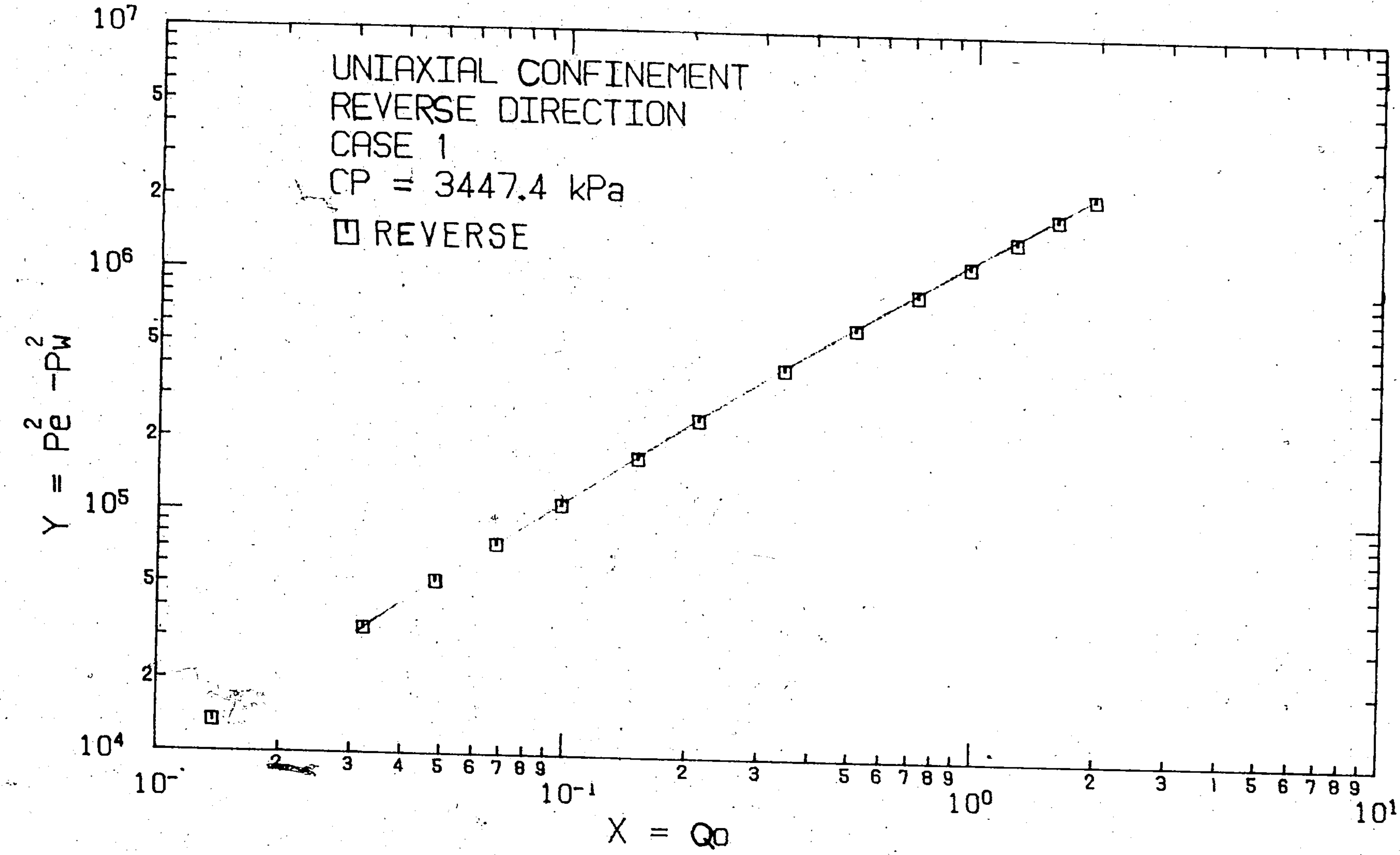

Figure 3-3: PIPLAPURE'S DATA BACK PRESSURE PLOT

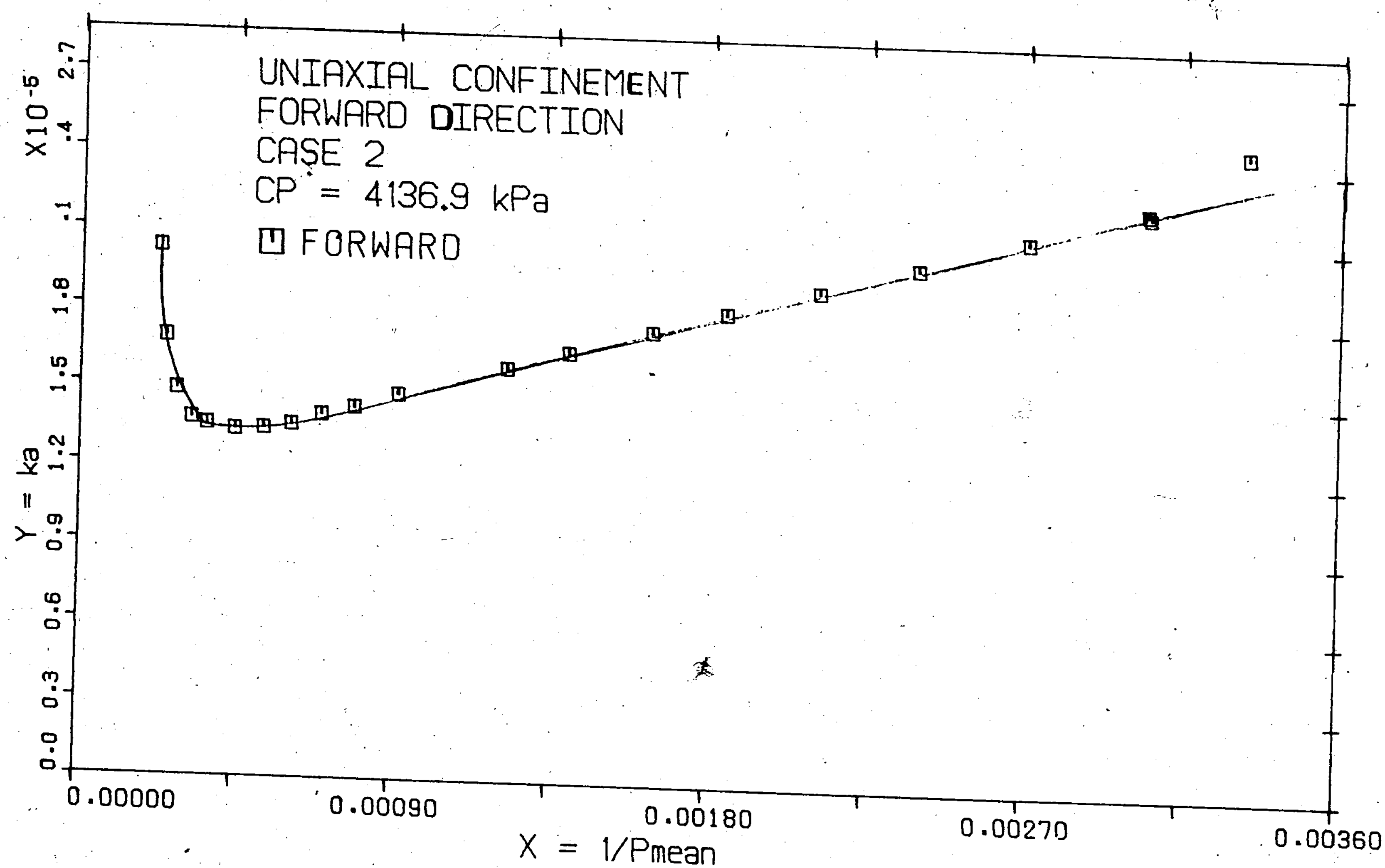

FIGURE 3-4: SENTURK'S DATA 2 KLINKENBERG PLOT

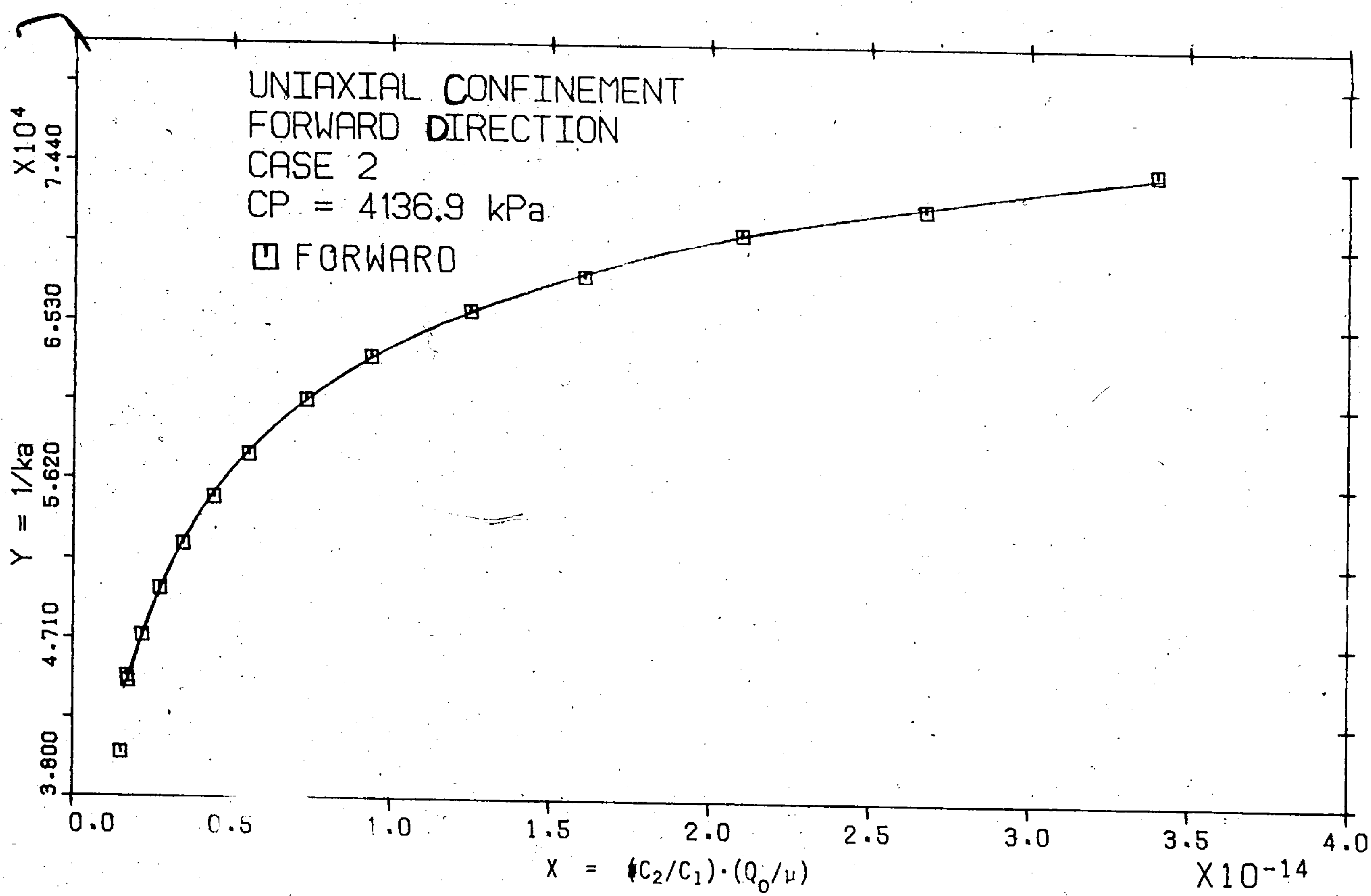

Figure 3.5: SENTURK'S DATA ... 'ISCO-INERTIAL PLOT

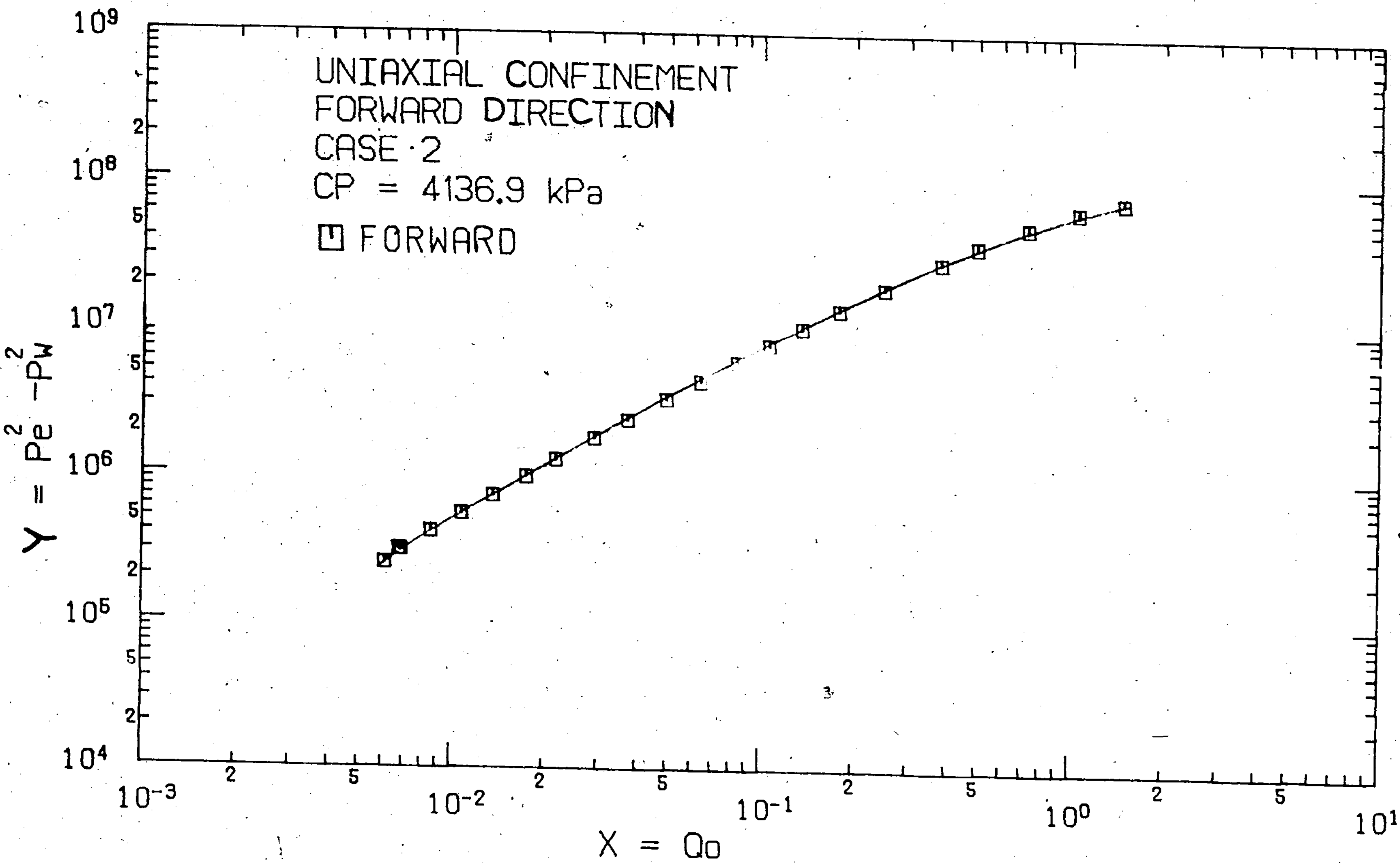

Figure 3-6: SENTURK'S DATA 2 BACK PRESSURE PLOT

Case 3 (Increasing Pw and Constant Pe):

This is taken from Senturk's data for Sample LS1, Run 5,(58) at confining pressure,CP, of 5515.8 kPa. The external pressure,Pe, is held constant at 2068.43 kPa and Pw is steadily increased. This results in decreasing (Pe^2 - Pw^2), decreasing Qo, and increasing Pm. With reference to Pm, 1/Pm decreases, ka decreases, 1/ka increases, slip decreases, and inertial effects increase. With reference to Qo, which decreases, ka increases, 1/ka decreases, slip increases, and inertial effects decrease. Since the flow condition results in increasing Pm, but decreasing Qo, the trends of ka, gas slippage, and inertial effects in both regions of both plots are expected to be opposite. Depending on the magnitude of the flow rates and pressures, the produced profile may be such that ka decreases with decreasing Qo and Pm. Figure 3.7 shows a decreasing ka for decreasing Qo and Pm, while Figure 3.8 shows a decreasing ka for increasing Qo and Pm. Figure 3.9 gives a back-pressure plot with higher slope at higher flow rate.

If, in Case 3, Pw decreases instead of increasing, for constant Pe, (Pe^2 - Pw^2) increases, Qo increases, and Pm decreases. This new case, designated as Case 4, suggests that the trends of ka, gas slippage, and inertial effects in both regions of both plots are opposite to those obtained in Case 3. Table 3.1 summarizes the effect of the flow methods on flow profiles for the cases considered.

The foregoing analysis shows that:

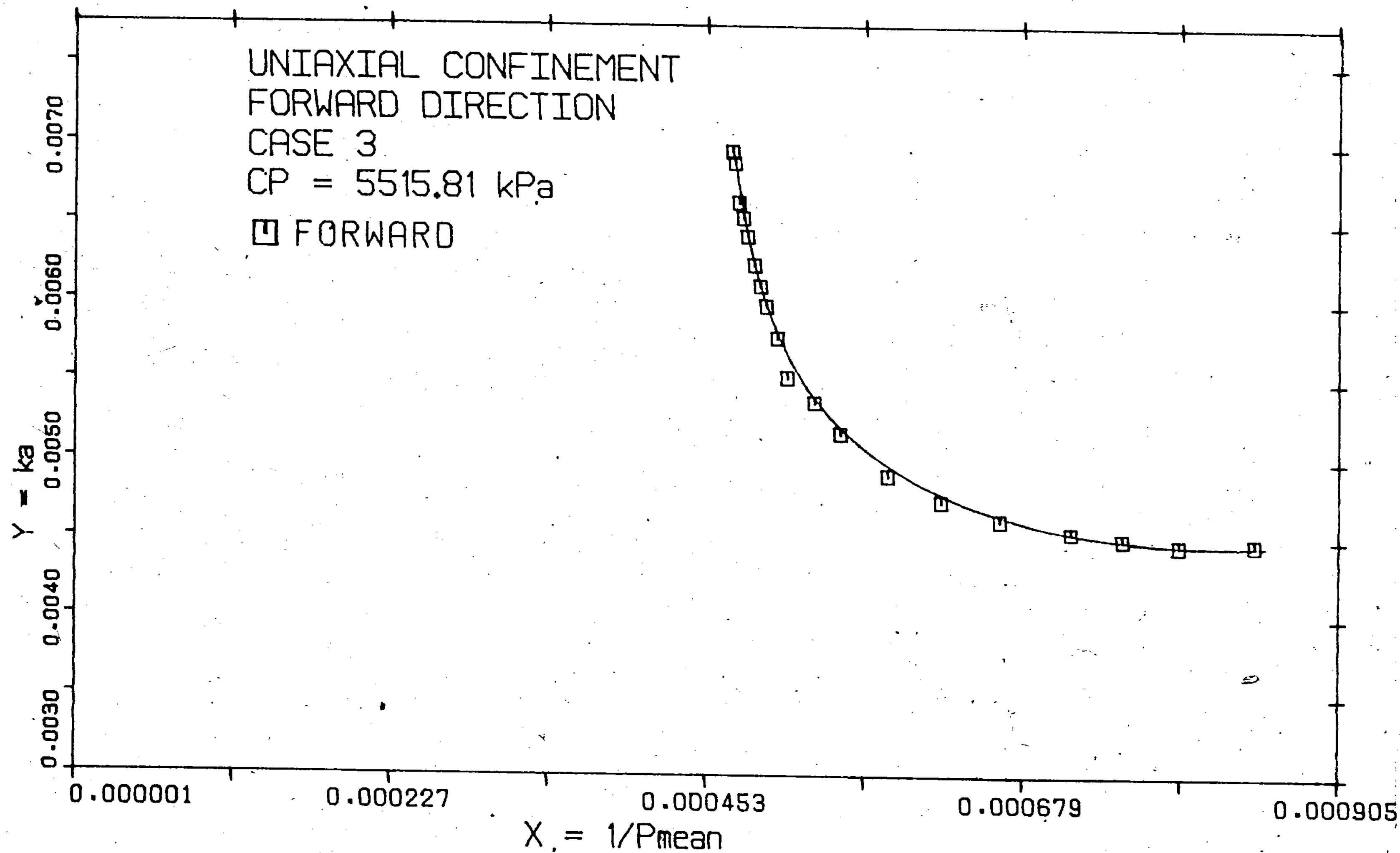

FIGURE 3-7: SENTURK'S DATA 3 KLINKENBERG PLOT

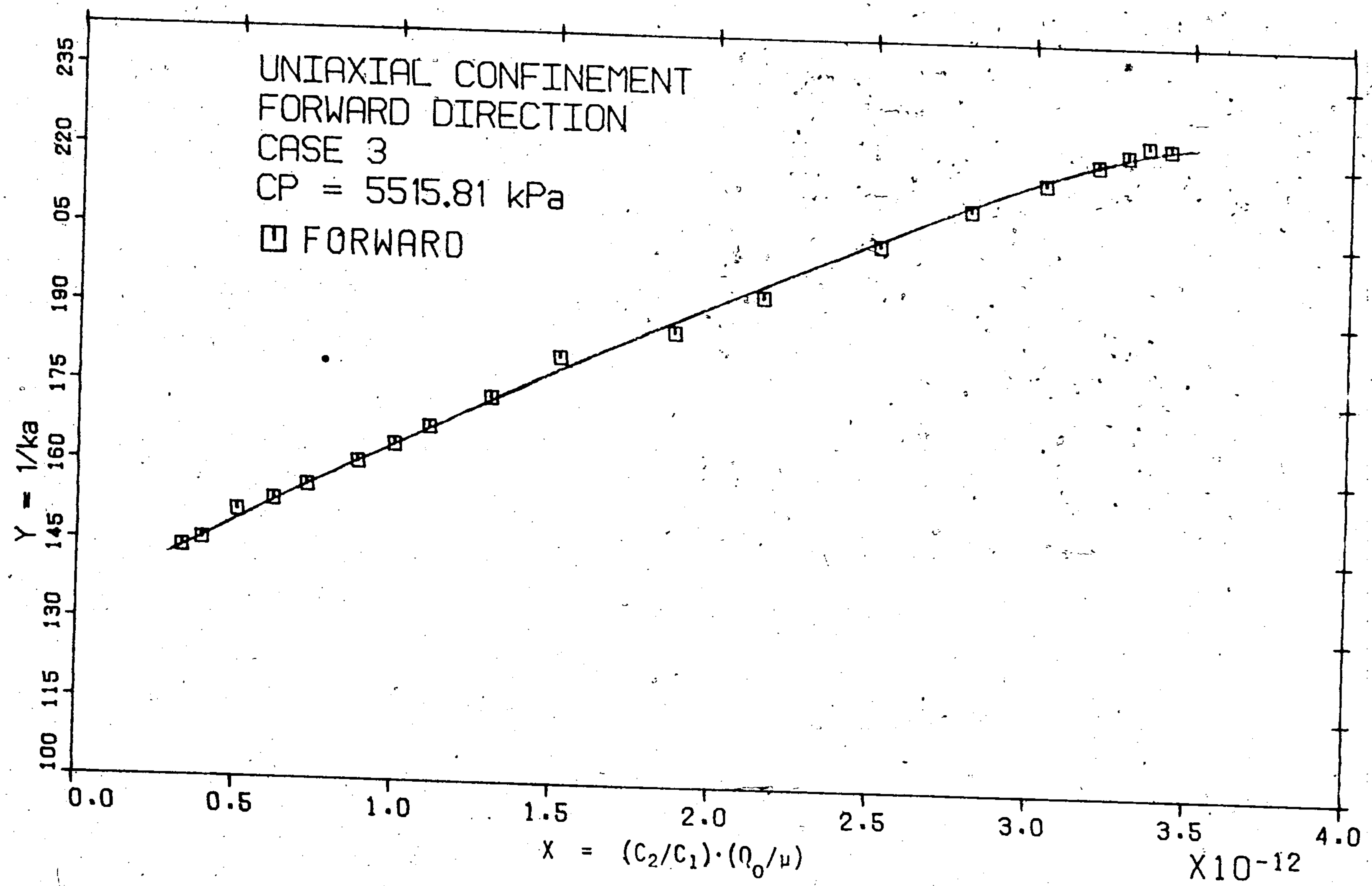

Figure 3-8: SENTURK'S DATA 3 VISCO-INERTIAL PLOT

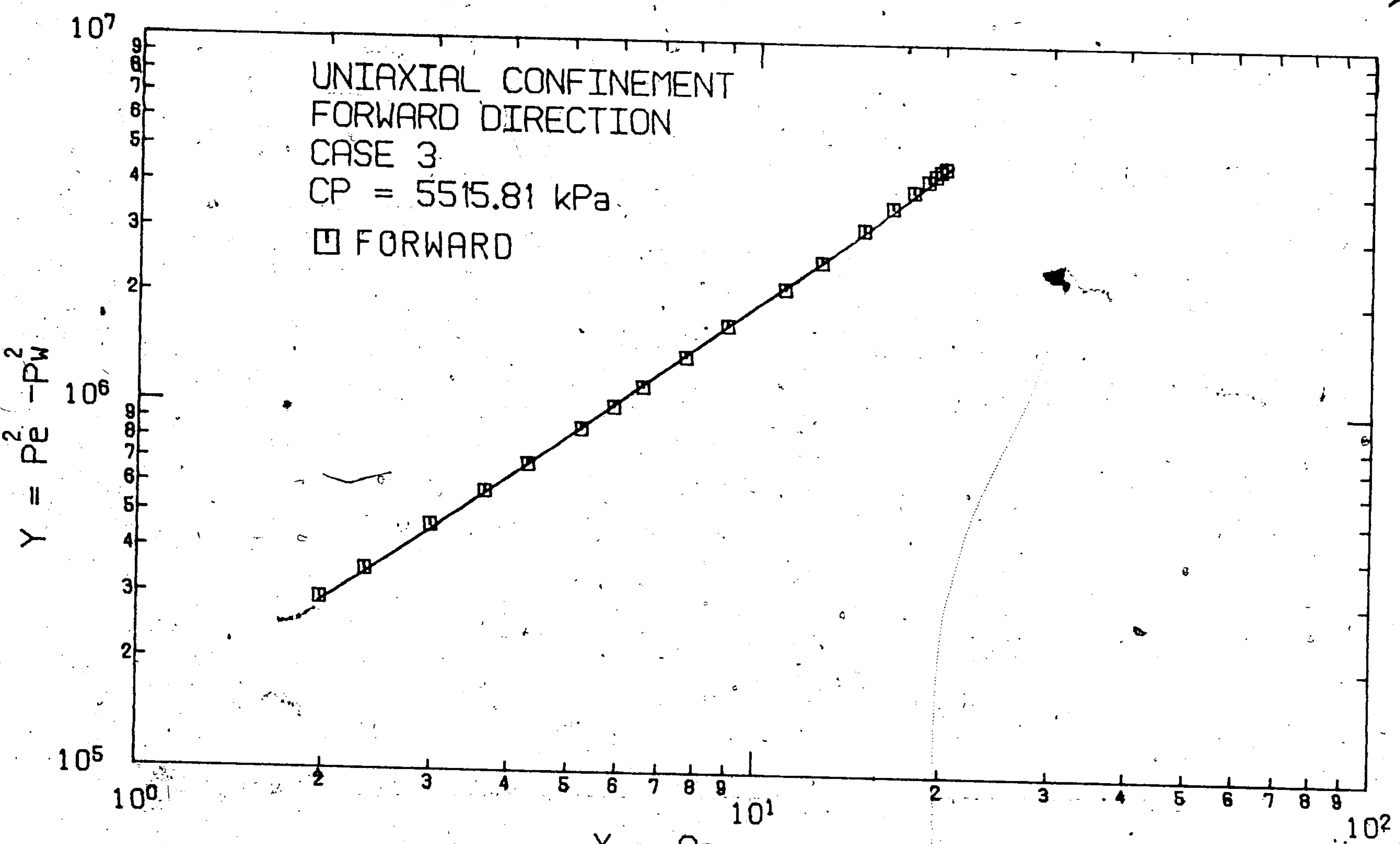

Figure 3-9: SENTURK'S DATA 3 BACK PRESSURE PLOT

TABLE 3-1: EFFECT OF FLOW METHODS ON FLOW PROFILES

PARAMETER	CASE 1		CASE 2		CASE 3		CASE 4	
Flow Method	Pw = Const Pe = Dec		Pw = Const Pe = Inc		Pe = Const Pw = Inc		Pe = Const Pw = Dec	
$Pe^2 - Pw^2$	Decrease		Increase		Decrease		Increase	
Qo	Decrease		Increase		Decrease		Increase	
Pm	Decrease		Increase		Increase		Decrease	
1/Pm	Increase		Decrease		Decrease		Increase	
	Using: Pm	Using: Qo	Using: Pm	Using: Qo	Using: Pm	Using: Qo	Using: Pm	Using: Qo
Ka	Inc	Inc	Dec	Dec	Dec	Inc	Inc	Dec
1/Ka	Dec	Dec	Inc	Inc	Inc	Dec	Dec	Inc
Slip	Inc	Inc	Dec	Dec	Dec	Inc	Inc	Dec
Inertia	Dec	Dec	Inc	Inc	Inc	Dec	Dec	Inc

where: Inc = Increase, Dec = Decrease, Const = Constant
Slip = Gas Slippage, Inertia = Inertial Effects

1. the flow method and the direction of flow influence the flow behavior.
2. abnormal behavior at higher flow rates may be due to
   a. normal behavior which depends on the flow method as depicted in Case 3.
   b. lower $(Pe^2 - Pw^2)$ at higher flow rates as in Cases 1 and 2 and depicted especially in the back-pressure plots.

The back-pressure flow relationship may be expressed as:

$$(Pe^2 - Pw^2) = 2Pm(Pe - Pw) \propto Qo \qquad (3.8)$$

This means that the flow rate is a function of both the mean pressure and the pressure drawdown. Keeping either of them constant, the variation of the other with respect to the flow rate can be analysed. Both pressure terms contribute to the magnitude of the flow rate, but the drawdown pressure, in addition, gives both direction and the driving force. If the drawdown pressure is greater than the mean pressure, increased compaction of the sample may result. If this condition continues without change, this may possibly lead to cracking or fracturing which in itself leads to increasing values of ka for increasing mean pressures.

Therefore, investigation of these problems may be carried out by

1. obtaining experimental data which cover both lower and higher flow rates and pressures, and by studying the significance of flow method and hysteresis on gas flow behavior,
2. reevaluating the confinement and fluid pressure relationship in terms of the stress-strain relationship generated during the flowing procedure under uniaxial confinement,
3. reassessing the existing visco-inertial model flow

equation. Since these problems have been noticed at higher flow rates and pressures, it becomes necessary to explore the possibility of using higher order equations.

4. STEADY STATE GAS FLOW MODEL AND PARAMETER ESTIMATION

The use of Forchheimer's quadratic equation, as discussed in the preceding pages, has facilitated the understanding of visco-inertial gas flow through porous media. It has been derived in Appendix A from consideration of both the Navier-Stokes equations of motion and dimensional analysis for laminar flow with negligible Reynolds stresses. For higher flow rates, the flow condition changes, and local irregularities become increasingly significant in the laminar mainstream such that Reynolds stresses begin to form.

As an aid to understanding the aspect of this study which involve higher flow rates and pressures, it has become necessary to derive the third order equation of Forchheimer as shown in Equation A-23 for 1-dimensional, linear, horizontal, incompressible fluid flow under the conditions of no-slip. The cubic term in this equation is regarded as a modification to Forchheimer's quadratic equation for data obtained at higher flow rates and pressures under the conditions of no-slip. It has been derived in Appendix A by considering both the kinetic energy equation of mean flow and dimensional analysis.

4.1 Derivation of a General Radial Gas Flow Equation

For 1-dimensional, horizontal, steady state, plane radial incompressible flow, Equation A-23 is written as

$$-\frac{dP}{dr} = \frac{\mu}{k} q + F_b \rho q^2 + \gamma \rho^2 q^3 \qquad (4.1)$$

where the linear distance x is replaced by the radial distance r. It is adapted to gas flow with the following basic assumptions:

1. Flow is steady, compressible and horizontal such that
   a. gravitational forces are neglected,
   b. density is not constant but depends on temperature and pressure as given by the equation of state for real gases

$$\rho = \frac{PM}{ZRT} = \frac{28.96GP}{ZRT} \qquad (4.2)$$

   c. the mean momentum of fluctuations is zero,
   d. Kinetic energy equation of mean flow is valid.
2. Slippage condition exists and the permeability term in Equation 4.1 is changed to its apparent value, Ka. Slippage effects are corrected by using the Klinkenberg equation (Equation 2.7).
3. Continuity equation for steady state condition is given as:

$$\rho_0 q_0 = \rho q = \text{Constant} \tag{4.3}$$

4. All flows are geometrically similar so that unique velocity and length scales can be obtained which satisfy them geometrically.
   a. The system is of plane radial geometry with uniform thickness.
   b. For 1-dimensional, horizontal cases, the flow rate per cross-sectional area at any radial distance, r, from a source or sink, is given as:

$$q = \frac{Q}{A} = \frac{Q}{2\pi rh} \tag{4.4}$$

5. Porous medium is both homogeneous and isotropic.
6. Both velocity and velocity fluctuation scales can be represented by a single unique velocity scale.
7. Viscosity, compressibility factor, and density are obtained at mean temperatures and pressures.
8. A single phase gas with constant composition saturates and flows through the porous medium.

Equation 4.1 can therefore be written as:

$$-\frac{dP}{dr} = \frac{\mu}{k_a}q + F_b\rho q^2 + \gamma\rho^2 q^3 \tag{4.5}$$

which, when multiplied across with the density term, yields

$$-\rho\frac{dP}{dr} = \frac{\mu}{k_a}(\rho q) + F_b(\rho q)^2 + \gamma(\rho q)^3 \tag{4.6}$$

By combining Equations 4.2 and 4.4 according to the continuity requirement of Equation 4.3, and substituting them into Equation 4.6, the following expression, after further simplification, is obtained:

$$-\frac{1}{2}\frac{dP^2}{dr} = \frac{\bar{\mu}\bar{T}\bar{Z}P_oQ_o}{2\pi k_a hT_o}\cdot\frac{1}{r} + \frac{28.96\,GP_o^2Q_o^2\bar{Z}\bar{T}F_b}{RT_o^2(2\pi h)^2r^2} + \frac{28.96^2G^2P_o^3Q_o^3\bar{Z}\bar{T}\gamma}{R^2T_o^3(2\pi h)^3r^3} \tag{4.7}$$

Since Pm is inversely proportional to Ka, and for any given set of boundary conditions Pm is known, Ka is also known and can be regarded as being constant. Hence, integrating between Pe and Pw, and re and rw, the following equation is obtained:

$$(P_e^2 - P_w^2) = \frac{\bar{\mu}\bar{T}\bar{Z}P_oQ_o}{\pi k_a hT_o}\ln\frac{r_e}{r_w} + \frac{28.96\,GP_o^2Q_o^2\bar{Z}\bar{T}F_b}{RT_o^2(2\pi)h^2}\left(\frac{1}{r_w} - \frac{1}{r_e}\right) + \frac{28.96^2G^2P_o^3Q_o^3\bar{Z}\bar{T}\gamma}{R^2T_o^3(4\pi^2)h^3}\left(\frac{1}{r_w^2} - \frac{1}{r_e^2}\right) \tag{4.8}$$

By convention, flow is taken as positive in the direction of increasing radius, and negative in the direction of decreasing radius. For production, flow is in the direction of decreasing radius such that $(Pe^2 - Pw^2)$ is always positive. Since production is being considered, it is convenient to reverse the convention so that flow is taken as positive. Therefore, Equation 4.8 becomes

$$P_e^2 - P_w^2 = \frac{\bar{\mu}\bar{Z}\bar{T}P_oQ_o}{\pi k_a h T_o} \ln\frac{r_e}{r_w} + \frac{28.96\,GP_o^2Q_o^2\bar{Z}\bar{T}F_b}{RT_o^2(2\pi)h^2}\left(\frac{1}{r_w} - \frac{1}{r_e}\right) + \frac{28.96^2G^2P_o^3Q_o^3\gamma ZT}{R^2T_o^3(4\pi^2)h^3}\left(\frac{1}{r_w^2} - \frac{1}{r_e^2}\right) \tag{4.9}$$

This conforms to the the convention commonly found in the literature. Equation 4.9 is valid in cgs units where

Pe, Pw, Po, are in atmospheres pressure,

ka, μ, are in darcy and centipoise respectively,

h, re, rw, are in cm,

Qo is in cm^3/sec. (at standard conditions),

To, T are in °K,

Fb is in $atm.sec^2/gm = cm^{-1}$,

γ is in $atm.cm^2.sec^3/gm^2 = cmsec/gm$,

R = Universal gas constant, in $atm.cm^3/gmmole$ °K.

In SI units, it becomes

$$P_e^2 - P_w^2 = 1.2955 \times 10^{-3}\,\frac{\bar{\mu}\bar{T}\bar{Z}Q_o}{k_a h} \ln\frac{r_e}{r_w} + 2.9229 \times 10^{-15}\,\frac{G\bar{Z}\bar{T}Q_o^2F_b}{h^2}\left(\frac{1}{r_w} - \frac{1}{r_e}\right) + 6.5946 \times 10^{-21}\,\frac{G^2\bar{Z}\bar{T}Q_o^3\gamma}{h^3}\left(\frac{1}{r_w^2} - \frac{1}{r_e^2}\right) \tag{4.10}$$

where

Pe, Pw, Po are in kPa, T, To are in °K,

μ is in μPa.s, K, Ka are in μm^2,

h, re, rw are in m, Qo is in m^3/day,

γ is in msec/kg, Fb is in m^{-1},

R is in kPa.m^3/kgmole °K.

With the following relations

$$C_1 = \frac{1.2955 \times 10^{-3}}{h} \ln \frac{r_e}{r_w} \tag{4.11a}$$

$$C_2 = 2.9229 \times 10^{-15} \frac{G}{h^2} \left(\frac{1}{r_w} - \frac{1}{r_e}\right) \tag{4.11b}$$

$$C_3 = 6.5946 \times 10^{-21} \frac{G^2}{h^3} \left(\frac{1}{r_w^2} - \frac{1}{r_e^2}\right) \tag{4.11c}$$

Equation 4.10 is rewritten as .

$$P_e^2 - P_w^2 = \frac{C_1 \bar{\mu} \bar{T} \bar{Z} Q_o}{k_a} + C_2 \bar{Z} \bar{T} Q_o^2 F_b + C_3 \bar{Z} \bar{T} Q_o^3 \gamma \tag{4.12}$$

Correcting for slippage by substituting for ka with the relation in Equation 2.7, Equation 4.12 becomes

$$P_e^2 - P_w^2 = \frac{C_1\bar{\mu}\bar{T}\bar{Z}Q_o}{k} - 2b(P_e - P_w) + C_2\bar{Z}\bar{T}Q_o^2F_b$$

$$+ \frac{C_2\bar{Z}\bar{T}Q_o}{P_m}(b\cdot F_b) + C_3\bar{Z}\bar{T}Q_o^3\gamma + \frac{C_3\bar{Z}\bar{T}Q_o^3}{P_m}(b\cdot\gamma) \qquad (4.13)$$

For simplicity, let

$$CC1 = C_1\bar{\mu}\bar{T}\bar{Z}Qo \qquad (4.14a)$$

$$CC2 = C_2\bar{Z}\bar{T}Qo^2 \qquad (4.14b)$$

$$CC3 = C_3\bar{Z}\bar{T}Qo^3 \qquad (4.14c)$$

$$PEW = 2(Pe-Pw) \qquad (4.14d)$$

$$Pm = (Pe+Pw)/2 \qquad (4.14e)$$

Therefore Equations 4.12 and 4.13 become respectively.

$$P_e^2 - P_w^2 = \frac{CC1}{k_a} + CC2\cdot F_b + CC3\cdot\gamma \qquad (4.15)$$

$$P_e^2 - P_w^2 = \frac{CC1}{k} - b\cdot PEW + CC2\cdot F_b + \frac{CC2}{P_m}\cdot(b\cdot F_b)$$

$$+ CC3\cdot\gamma + \frac{CC3}{P_m}\cdot(\gamma\cdot b) \qquad (4.16)$$

Using the quadratic form, Equation 4.15 reduces to

$$P_e^2 - P_w^2 = \frac{CC1}{k_a} + CC2\cdot F_b \qquad (4.17)$$

This is the SI version of Equation 2.29 of Tek et al for which slippage is not corrected. When corrected for slippage, it becomes

$$P_e^2 - P_w^2 = \frac{CC1}{k} - b \cdot PEW + CC2 \cdot F_b + \frac{CC2}{P_m}(b \cdot Fb) \qquad (4.18)$$

If the flow rate is such that the flow condition obeys Darcy's law, Equation 4.15 further reduces to

$$P_e^2 - P_w^2 \text{ [illegible]} \qquad (4.19)$$

Correcting for slippage using Equation 2.7, and rearranging, this equation becomes

$$k_a = \frac{CC1}{P_e^2 - P_w^2} = k\left(1 + \frac{b}{P_m}\right) \qquad (4.20)$$

4.2 Parameter Estimation

4.2.1 Graphical Parameter Estimation

A linear Klinkenberg plot of ka versus 1/Pm can be obtained using Equation 4.20. The intercept at infinite mean pressure yields the absolute gas permeability, k, while the slope yields the gas slippage coefficient, b, as a product of bk.

Equation 4.17 can be rearranged into

$$\frac{P_e^2 - P_w^2}{CC1} = \frac{1}{k_a} + \frac{CC2}{CC1} \cdot F_b \qquad (4.21)$$

while Equation 4.18 can be written in the form of

$$\frac{(P_e^2 - P_w^2) + b \cdot PEW}{CC1} = \frac{1}{k} + \frac{CC2}{CC1} \cdot F_b\left(1 + \frac{b}{P_m}\right) \qquad (4.22)$$

Both forms yield linear visco-inertial plots. The expression for the ordinate in the visco-inertial plot, using Equation 4.21, is its reciprocal for the Klinkenberg plot, using Equation 4.20. The intercept on the first plot using Equation 4.21 gives the reciprocal of the apparent gas permeability, ka, while the slope gives the inertial resistance coefficient,Fb. For the second plot, using Equation 4.22, the intercept yields the reciprocal of the absolute gas permeability,k, and the slope gives the inertial resistance coefficient,Fb, provided the slippage coefficient,b, is known from the Klinkenberg plot. Equations 4.21 and 4.22 are, respectively, the radial SI version of Equations 3.1 and 3.3, which are due to Kolada. The plots obtained from them are known, respectively, as the "conventional visco-inertial plot" and the "modified visco-inertial plot".

A back-pressure curve of $(Pe^2 - Pw^2)$ versus Q is plotted on log-log paper to delineate the plot points in the viscous region. The points that lie on the 45 degree line are taken to be in the viscous region. They are used in the Klinkenberg plot to obtain both the gas permeability, k, and the gas slippage coefficient, b.

The points on the linear profile of both the

Klinkenberg and the visco-inertial plots are used to find the best straight lines by the method of least squares. The parameter values obtained are checked with those obtained by graphical means.

4.2.2 Numerical Parameter Estimation

Numerical methods permit the use of both the quadratic and the cubic model flow equations in estimating the parameters simultaneously. The model equations are fitted to the experimental data, and plotted to check for the best fit.

4.2.3 Direct Multiple Linear Regression Method

Equation (4.15) is linear in its coefficients even though it is itself nonlinear. If the combined variables in Equation 4.16 can be represented by single variables, linearity in its coefficients may be achieved. In these forms, both equations can be adapted to a multiple linear regression technique for parameter estimation. The same case exists if Equation 4.16 is further simplified by neglecting the combined variables.

Linearity in the coefficients can similarly be achieved for the quadratic case when Equation 4.18 is used. By neglecting its combined variable, this equation is further simplified to the SI version of Equation 2.32 which is due to Piplapure.

4.2.4 Model Fitting

The cubic equation (Equation 4.15) can be rearranged in terms of ka, Fb, gamma, as

$$\frac{P_e^2 - P_w^2}{CC1} = \frac{1}{k_a} + \frac{CC2}{CC1} \cdot F_b + \frac{CC3}{CC1} \cdot \gamma \tag{4.23}$$

or, in terms of its polynomial in Qo, as

$$P_e^2 - P_w^2 = \left(\frac{C_1\bar{\mu}\bar{T}\bar{Z}}{k_a}\right) \cdot Q_o + (C_2\bar{Z}\bar{T}F_b) \cdot Q_o^2 + (C_3\bar{Z}\bar{T}\gamma) \cdot Q_o^3 \tag{4.24}$$

For the quadratic case, Equation 4.24 reduces to

$$P_e^2 - P_w^2 = \left(\frac{C_1\bar{\mu}\bar{T}\bar{Z}}{k_a}\right) \cdot Q_o + (C_2\bar{Z}\bar{T}F_b) \cdot Q_o^2 \tag{4.25}$$

while Equation 4.23 becomes Equation 4.21.

Fitted visco-inertial plots are made by plotting both the fitted values of the left-hand side of Equations 4.21 and 4.23, and experimental data, respectively on the ordinate against CC2/CC1 on the abscissa. The best fit, cubic or quadratic, is sought for the experimental data. Similarly, fitted back-pressure plots on log-log paper are made by plotting both the fitted values of the left-hand side of Equations 4.24 and 4.25, and experimental data, respectively on the ordinate against Qo. The best fit, beyond the linear section which obeys Darcy's law, is determined.

The formal adaptation of these model equations for computer application is given in Appendix B.

5. CONFINEMENT AND FLUID PRESSURE CONSIDERATIONS

Following the discussions in Chapter 3, a need arises for a re-evaluation of confinement and fluid pressure considerations with respect to the partial uniaxial confining pressure imposed on the core. The geometry of the core is cylindrical; therefore it suggests a thick-walled cylindrical model. If the core is assumed to possess elastic properties, analysis can be made using the theory of elasticity. This assumption, therefore, furnishes a good method for investigating the state of stress and strain (deformation) as gas flows into the well bore from the external boundary.

5.1 Stress-Strain Analysis

By definition (59), principal stresses at any point within a stressed body, are stresses which are normal to three mutually perpendicular planes in which there are no shearing stresses. Hence, the state of stress at any point within the core in the cell may be expressed, respectively, in terms of the principal stresses - axial, Sz, radial, Sr, and tangential, S+. The sum of the radial and tangential stresses gives the horizontal stresses. They can either be compressive or tensile. By convention, a negative sign denotes compressive stress, and a positive sign indicates tensile stress.

Similarly, principal strains have no shearing strains associated with them. Their extensions are in the directions of the principal stresses with which they are related according to the generalized Hooke's law(60)

$$\varepsilon_z = \frac{1}{E}(-\nu S_r - \nu S_t + S_z) \qquad (5.1)$$

$$\varepsilon_r = \frac{1}{E}(S_r - \nu S_t - \nu S_z) \qquad (5.2)$$

$$\varepsilon_t = \frac{1}{E}(-\nu S_r + S_t - \nu S_z) \qquad (5.3)$$

where E is the Young's modulus and the Poisson's ratio is given as

$$\nu = \left|\frac{\text{Lateral Strain}}{\text{Axial Strain}}\right| \qquad (5.4)$$

The strains are caused by uniaxial stress only and both the lateral and axial strains are of opposite sign for uniaxial stress. The ratio, which is an elastic constant, is usually a positive number which varies for different materials, according to Jaeger(61), in the range of 0.10 and 0.50. Assuming Poisson's relation, Jaeger established that this ratio simplifies to 0.25. Also assuming a solid, incompressible material, he established the ratio to be 0.5. Furthermore, the ratio for sedimentary materials(62) is found to lie between 0.115 and 0.300. Several investigators(63,64,65) have used 0.25, and for this work, the value of 0.25 is chosen as an approximation to the true value of the ratio.

For uniaxial confining stress, the principal axial strain is assumed to be zero and Equation 5.1 reduces to

$$S_z = \nu(S_r + S_t) \tag{5.5}$$

Substituting this into Equations 5.2 and 5.3, and solving for the radial and tangential stresses, the following expressions are obtained:

$$S_r = \frac{E}{(1+\nu)(1-2\nu)}[(1-\nu)\varepsilon_r + \nu\varepsilon_t] \tag{5.6a}$$

$$S_t = \frac{E}{(1+\nu)(1-2\nu)}[(1-\nu)\varepsilon_t + \nu\varepsilon_r] \tag{5.6b}$$

The strain-displacement relationships in cylindrical co-ordinates due only to the radial flow rate of displacement U, are given by

$$\varepsilon_r = \frac{(U + \frac{dU}{dr}dr) - U}{dr} = \frac{dU}{dr} \tag{5.7a}$$

$$\varepsilon_t = \frac{(r+U)d\theta - rd\theta}{rd\theta} = \frac{U}{r} \tag{5.7b}$$

Since flow is assumed to be radial in the direction of the principal radial stress, the additional portion of the tangential strain due to incremental tangential displacement is neglected.

Equations 5.7a and 5.7b are substituted into Equations 5.6a and 5.6b to obtain

$$S_r = \frac{E}{(1+\nu)(1-2\nu)} [(1-\nu) \frac{dU}{dr} + \nu \frac{U}{r}] \quad (5.8a)$$

$$S_t = \frac{E}{(1+\nu)(1-2\nu)} [(1-\nu) \frac{U}{r} + \nu \frac{dU}{dr}] \quad (5.8b)$$

If an infinitesimal element in static equilibrium within the core is considered, then by three dimensional force balance, the equation of equilibrium in radial direction only is given by

$$\frac{\partial S_r}{\partial r} + \frac{1}{r}\frac{\partial \tau_{r\theta}}{\partial \theta} + \frac{\partial \tau_{rz}}{\partial z} + \frac{1}{r}(S_r - S_t) + R = 0 \quad (5.9)$$

By assumption, shear stresses are zero. For a plane horizontal radial core, gravitational forces R are assumed zero. Therefore Equation 5.9 reduces to

$$\frac{\partial S_r}{\partial r} + \frac{1}{r}(S_r - S_t) = 0 \quad (5.10a)$$

From inspection, Equation 5.10a suggests that the radial stress is dependent only on the radius r. Therefore, it can be written as

$$\frac{dS_r}{dr} + \frac{1}{r}(S_r - S_t) = 0 \qquad (5.10b)$$

Substituting Equations 5.8a and 5.8b into Equation 5.10b and simplifying, yields the following second order differential equation:

$$\frac{d^2U}{dr^2} + \frac{1}{r}\frac{dU}{dr} - \frac{U}{r^2} = 0 \qquad (5.11)$$

By integrating this, the following general equation is obtained:

$$U = A_1 r + \frac{A_2}{r} \qquad (5.12)$$

Both the inner and the outer pressures are compressive on the radial core at their respective radii. Therefore the boundary conditions for the core are

$$\begin{aligned} r &= r_w & S_r &= -P_w \\ r &= r_e & S_r &= -P_e \end{aligned} \qquad (5.13)$$

Substituting Equations 5.12 and 5.13 into Equation 5.8a, and solving for the constants of integration, yields

$$A_1 = \frac{(1+\nu)(1-2\nu)}{E} \cdot \frac{P_w r_w^2 - P_e r_e^2}{r_e^2 - r_w^2} \qquad (5.14a)$$

$$A_2 = \frac{(1+\nu)}{E} \cdot \frac{r_e^2 r_w^2 (P_w - P_e)}{r_e^2 - r_w^2} \qquad (5.14b)$$

These equations, together with Equation 5.12, are substituted into Equations 5.8a and 5.8b to yield the general radial and tangential stresses in terms of the boundary conditions as follows:

$$S_r = \frac{P_w r_w^2 - P_e r_e^2}{r_e^2 - r_w^2} - \frac{(P_w - P_e)\, r_w^2 r_e^2}{(r_e^2 - r_w^2)\, r^2} \qquad (5.15a)$$

$$S_t = \frac{P_w r_w^2 - P_e r_e^2}{r_e^2 - r_w^2} + \frac{(P_w - P_e)\, r_w^2 r_e^2}{(r_e^2 - r_w^2)\, r^2} \qquad (5.15b)$$

From these equations, which are originally due to Lame(66), both the radial and the tangential stresses are compressive for cases where Pe is greater than or equal to Pw.

With these equations, the stresses at any radial point r are easily evaluated. This suggests that the externally applied stresses may be regarded as continuations of the internal stresses. For uniaxial confinement pressure condition, these equations are substituted into Equation 5.5 to get

$$S_z = 2\nu \left[\frac{P_w r_w^2 - P_e r_e^2}{r_e^2 - r_w^2} \right] \qquad (5.16)$$

The result from Brant's investigation(67) suggests that only 85% of the internal fluid pressures within the pores react against the imposed confining pressure. Fatt(68), added that this percentage is pressure dependent and does vary from rock to rock. Therefore with this correction, Equation 5.16 yields the following equation:

$$S_z = 1.7\nu \left[\frac{P_w r_w^2 - P_e r_e^2}{r_e^2 - r_w^2} \right] \tag{5.17}$$

and using, for a limiting case, 0.25 as the value of the Poisson's ratio, Equation 5.17 becomes

$$S_z = 0.425 \left[\frac{P_w r_w^2 - P_e r_e^2}{r_e^2 - r_w^2} \right] \tag{5.18}$$

6. EXPERIMENTAL EQUIPMENT AND PROCEDURE

6.1 Experimental Apparatus

The apparatus consists of a Boyles' law porosimeter (Figure 6-1) and a flow-test equipment (Figure 6-2). The Boyles' law porosimeter is used to measure the porosity of the core samples usually prior to starting the experimental runs. It consists of a vaccum pump, a constant volume bottle connected to a radial chamber, a gauge and a manometer. The flow test equipment is used to conduct the experimental runs. It consists of a radial cell, a hydraulic pump, a monitoring console for pressure and flow rate readings, and a copper constantan thermocouple.

Two radial cells, designed to house the core sample, are connected, respectively, to the flow-test equipment for uniaxial confinement (Figure 6-3), and for triaxial confinement (Figure 6.4). The experimental set-up, which contains the radial cell for uniaxial confinement, is similar to the set-up that Senturk used(69). This radial cell, together with the hydraulic pump, provides uniaxial loading by confining the core in the direction of its axial height. Similarly, the triaxial overburden radial cell, together with the hydraulic pump, is expected to provide a uniform confining pressure in both the horizontal and the normal directions. This radial cell is designed in such a way that gas enters into the core sample through a sintered screen which ensures a uniform radial flow. The rubber

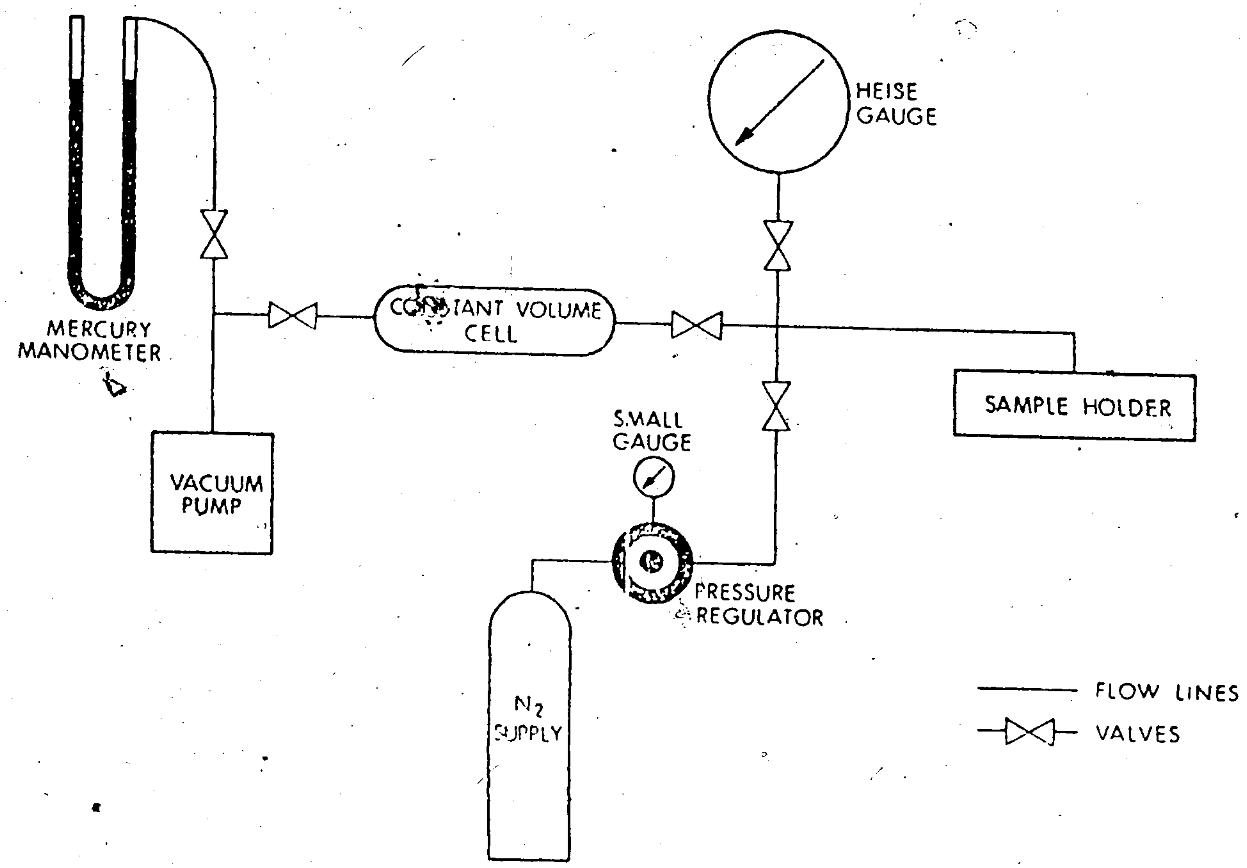

Figure 6-1 Boyles' Law Porosimeter (After Senturk(72))

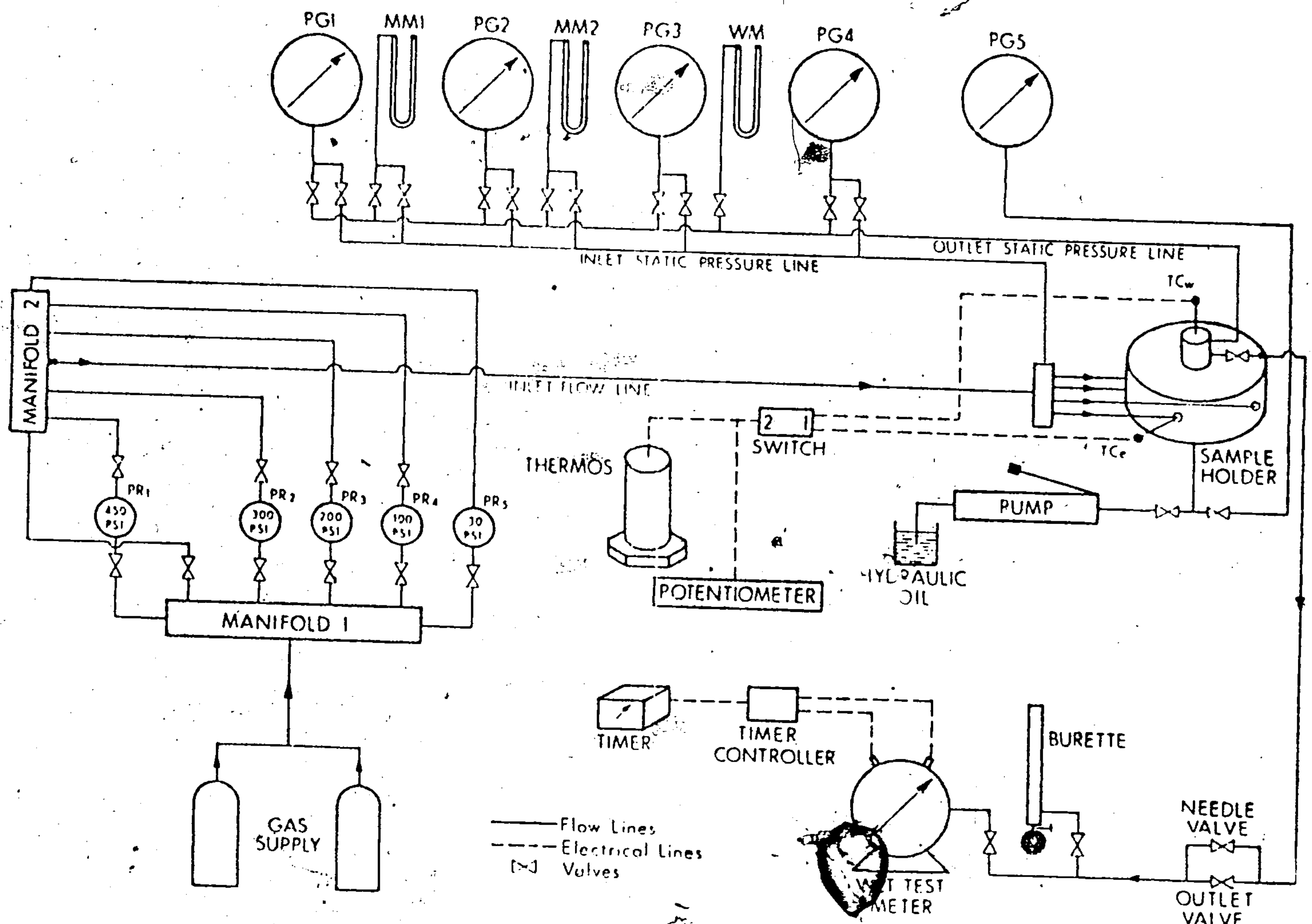

Figure 6-2 Flow-test Equipment (After Senturk (72))

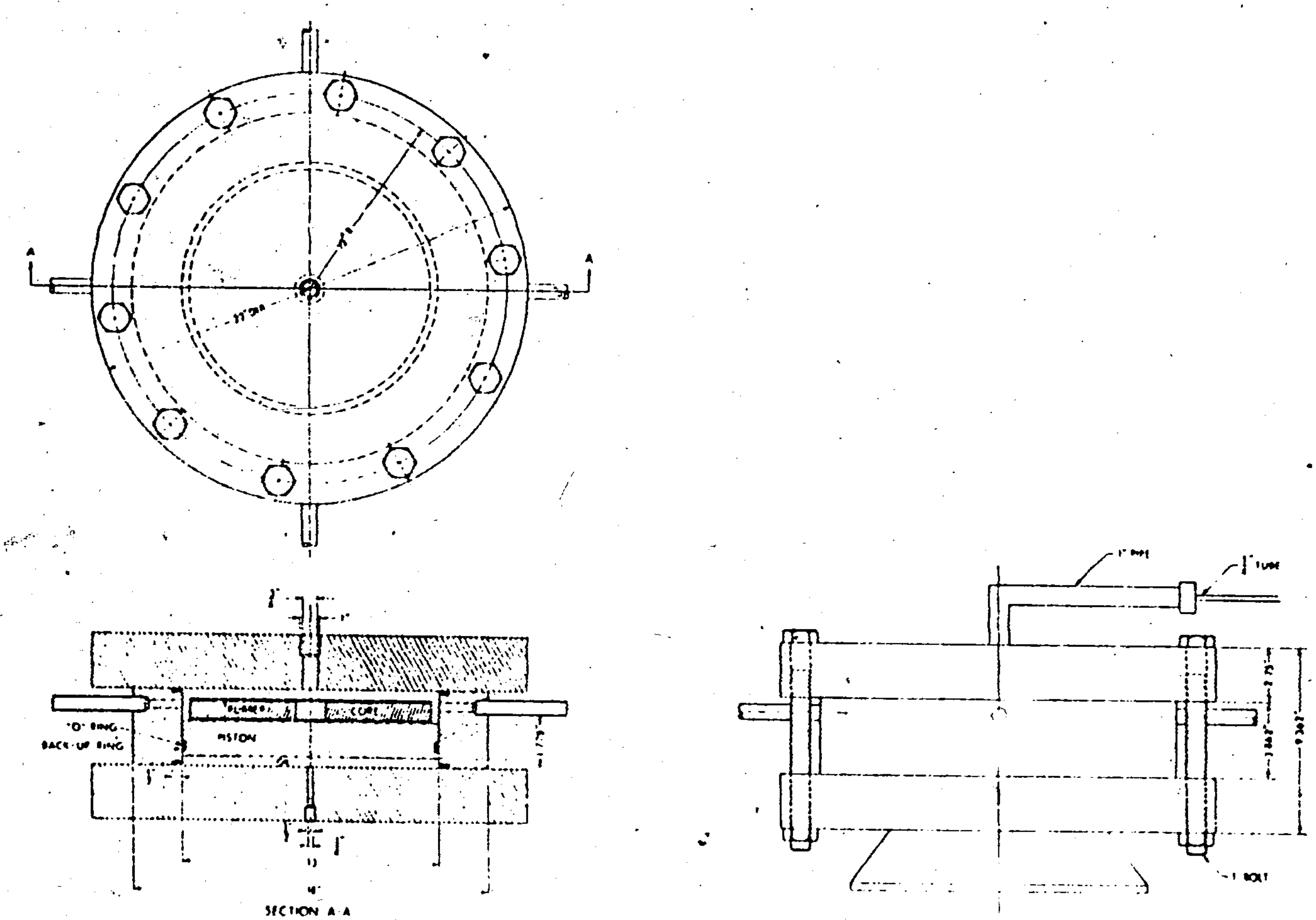

Figure 6-3 Radial Cell for Uniaxial Confinement (After Senturk (72))

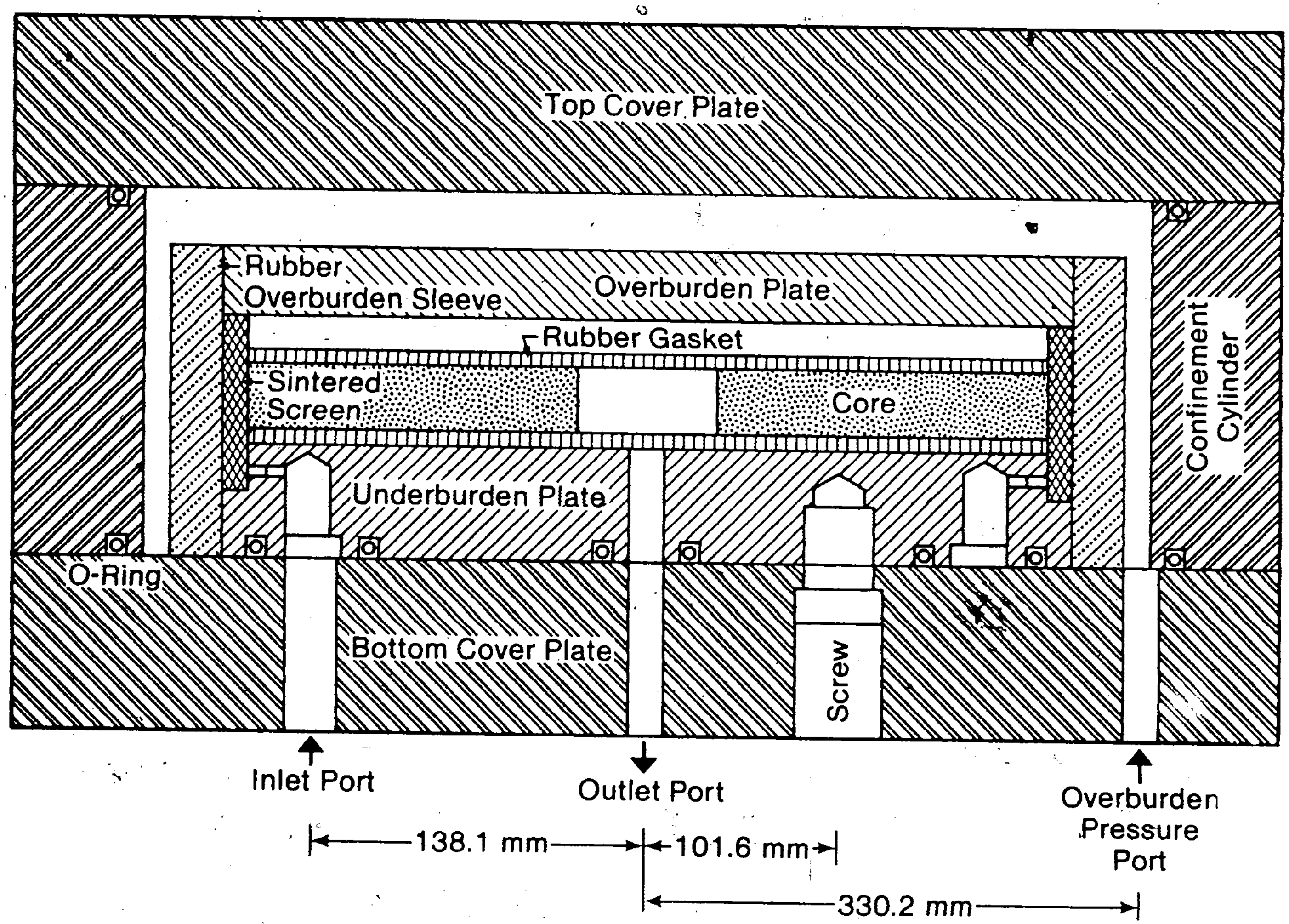

Figure 6-4. Radial Tri-axial Overburden Cell

overburden sleeve is wrapped tightly round the core sample, the sintered screen, and both the overburden and the underburden plates. This is then enclosed in the confinement cylinder. When pressurized by using the hydraulic pump, a uniform, all-sided (triaxial) confinement is expected on the core sample. However, the rubber overburden sleeve in this cell is loose, and to ensure a triaxial confinement, the sleeve was held tight with a wire. With either cell, varying confining pressures, CP, on the core can be provided as desired during the course of the runs.

6.2 Porosity Determination

Estimation of effective porosities can be made with the Boyles' law porosimeter which is operated by the gas expansion method. With this method, the stabilized pressure, P2, of the gas, which occupies the constant volume bottle of volume V2, is measured. By allowing the gas to expand through a connector valve into the radial chamber of volume V3, which contains solid aluminium blanks of volume V1, the new equalizing pressure, P3, is recorded. Since both volumes, V2 and V3, are constant, the equalizing pressure varies with the volume of the solid blanks in the radial chamber. Plotting P3 against V1, and P2/P3 against V1, (Figure 6-5), serves as a calibration for the porosimeter.

If the volume of the solid blanks represents the effective grain volume of a core sample, then, replacing the

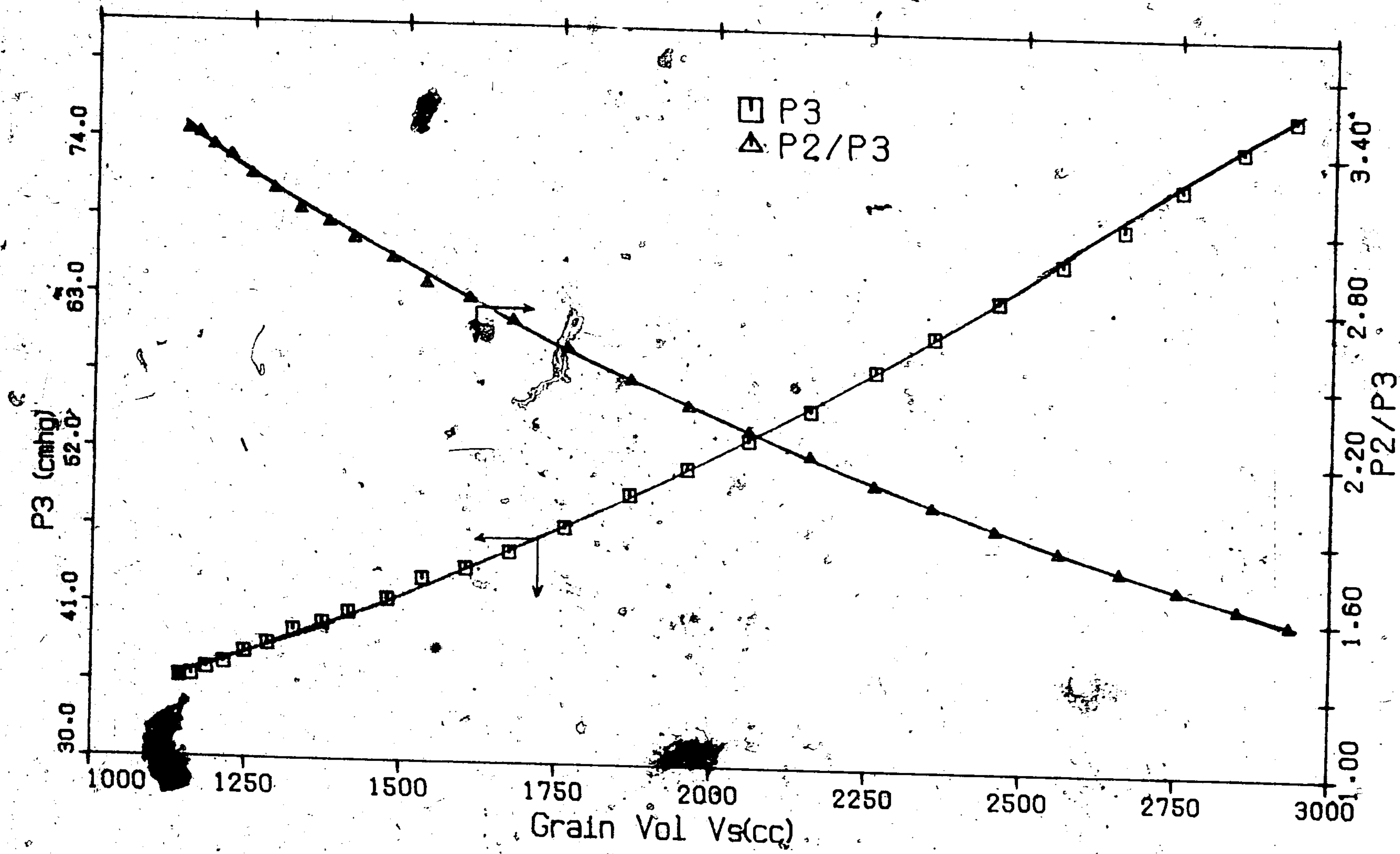

Figure 6-5 CALIBRATION OF BOYLES LAW POROSIMETER

blanks with a core sample, and repeating the experiment, its effective grain volume can be obtained from the plots. From the dimensions of the core samples, which were previously measured, the bulk volume is calculated, and porosity is determined from the following definition:

$$\phi = (\text{Pore volume}/\text{Bulk Volume}) \times 100\ \% \qquad (6.1)$$

6.3 Flow Test Methods

The four flow cases considered in Chapter 3 are rearranged to give:

- Flow Method 1, where both Pe and Pw increase (forward direction), or both decrease (reverse direction),
- Flow Method 2, where Pw is kept constant while Pe increases (forward direction), or while Pe decreases (reverse direction),
- Flow Method 3, where Pe is kept constant while Pw increases (forward direction), or while Pw decreases (reverse direction).

Keeping either Pw or Pe constant while the other is varied, results, by Equation 3.8, in larger drawdown pressures, which induce radial compaction. Also, by increasing or decreasing both Pw and Pe, higher mean pressures and lower drawdown pressures result. Therefore, the expected differences between Flow Method 1 and Flow Methods 2 and 3 may be given as:

a) The mean pressure is larger but the drawdown pressure is much less in Flow Method 1 than in Flow Methods 2 and 3.

b) Depending on the magnitude of Pw and Pe, $(Pe^2 - Pw^2)$ may increase more rapidly for increasing Qo in Flow Methods 2 and 3 than in Flow Method 1.

c) As flow progresses, the generated confinement pressure, by Equation 5.17, may increase more slowly in Flow Method 1 than in Flow Methods 2 and 3.

Conducting the experimental runs in both forward and reverse directions serves to check for hysteresis.

6.4 Experimentation

The core sample is mounted into the radial cell and the flow-test equipment is pressure-tested for leaks. Gas is passed into the core sample several hours prior to starting any experimental run. For each run, and for each step within a run, the inlet pressure, Pe, is pre-selected and measured, as gas passes through the inlet line to the outer periphery of the core. This is repeated for different pre-defined confining pressures, CP.

Using the timer, the flow rate is obtained as the ratio of one complete revolution of the wet-test meter dial to the time it takes to make a complete revolution. When this time is constant, the flow is assumed to be steady and all readings are taken at this condition. These include:

- the outlet pressure, Pw, at the inner periphery,
- the confining pressure, CP,

- the galvanometer readings, Tce and Tcw, for the inlet and outlet temperatures respectively,
- the flow temperature on top of the wet-test meter,
- the ambient conditions of room temperature and barometric pressure.

7. TREATMENT OF DATA

Readings and measurements are taken in English units. They are converted into the current SI units with standard reference condition of temperature and pressure being 288.150 °K and 101.325 kPa, respectively.

7.1 Temperature Conversion

The anticipated optimum temperature range, between 15°C and 30°C for corresponding millivolt (mV) readings, is obtained from conversion charts and curve fitted. The ensuing linear relation for the temperature range is

$$°C = (mV+0.021456)/0.040465$$

7.2 Physical and Fluid Properties

The physical properties of the core samples are summarized in Table 7.1.

Evaluation of the fluid properties - compressibility factor and gas viscosity - is made at arithmetic mean temperature and pressure, using nitrogen. The compressibility factors for nitrogen at given temperatures and pressures are determined from the curve-fitted data of Hilsenrath et al(70) using a Lagrangian interpolation technique. The viscosity of nitrogen is obtained from the

TABLE 7-1: PHYSICAL PROPERTIES OF THE CORE SAMPLES

Core sample	1C	4A	2
Inner Radius,m	0.00319	0.00820	0.00815
Outer Radius,m	0.15239	0.15256	0.15225
Height,m	0.02568	0.02600	0.02803
Porosity,fraction	0.10620	0.22714	0.23432

curve-fitted equation of Kestin and Wang(7.1):

$$\mu = 10^{5}\{0.1778\times10^{-3}[1+0.8958\times10^{-3}(P_{atm}-1) + 0.612\times10^{[illegible]}(P_{atm}-1)^{2} + 0.3977\times10^{-7}(P_{atm}-1)^{3}] + 0.455\times10^{-6}(T-[273.15+25])\} \quad \mu - Pa\cdot s \tag{7.2}$$

Both treatments for the compressibility factor and viscosity are given in computer subroutine LAGINI.

8. EXPERIMENTAL RESULTS AND DISCUSSION

Flow Method 1 has been used on Core Samples 1C and 4A for 24 experimental runs in both forward and reverse directions under uniaxial confinement. High flow rates and pressures were reached for various predefined confining pressures, CP. Runs 7, 8, and 9, were made on Core 4A for lower flow rates and pressures, using Flow Method 2. Core Sample 2 was obtained after the radial cell for uniaxial confinement was replaced with the triaxial overburden radial cell. Hence runs on Core 2 could not be made under uniaxial confinement. Instead, four runs were made on it under triaxial confinement, and by using both flow methods. The predefined confining pressure, CP, on Core 2, was kept constant at 4136.9 kPa.

8.1 Plot Profiles with Flow Method 1

Figures 8-1, 8-2, and 8-3 show, respectively, the Klinkenberg, visco-inertial, and back-pressure plots, for Core 1C, Run 7, in the forward direction. Linearity in the Klinkenberg plot exists at the lower ranges of flow rates and pressures, after which deviation starts in a downward manner. The visco-inertial plot has a surprising profile in which three stages are observed as $(Pe^2 - Pw^2)/CC1$, (which is $1/Ka$), increases for increasing flow rate, Qo. After the

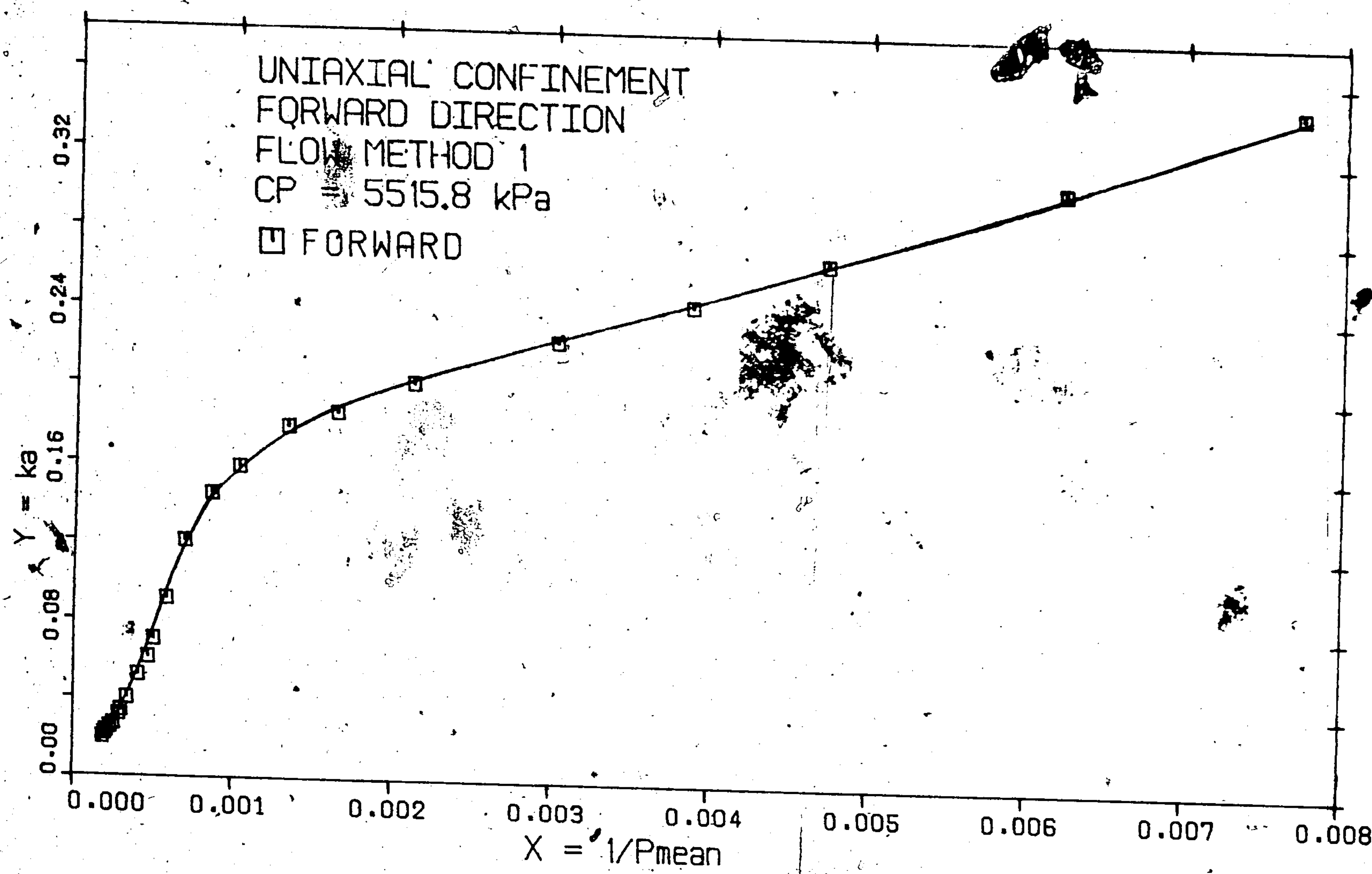

Fig.8-1: CORE 1C KLINKENBERG PLOT ~~RUN~~ 7

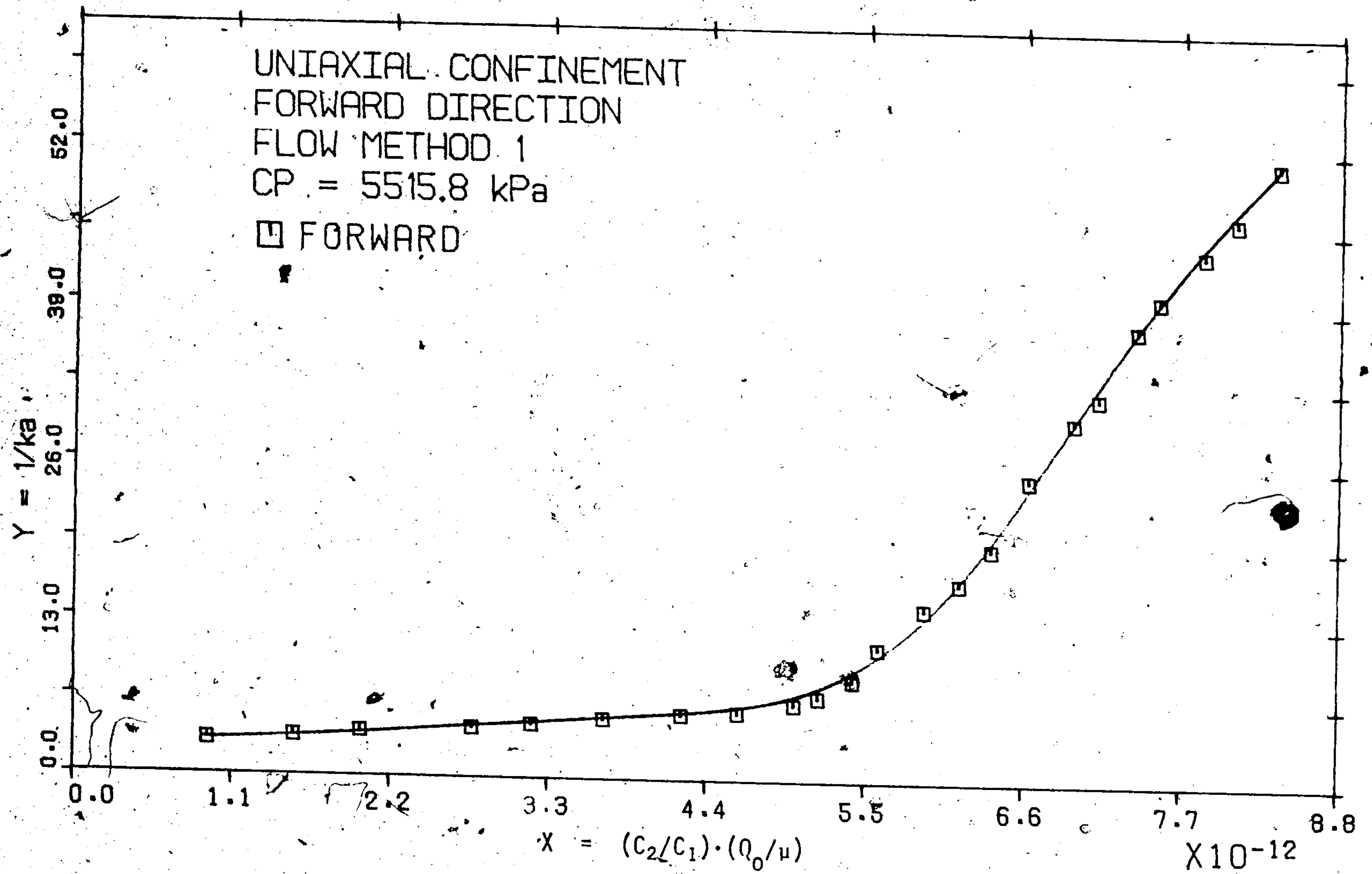

Fig.8-2: CORE 1C VISCO-INERTIAL PLOT RUN 7

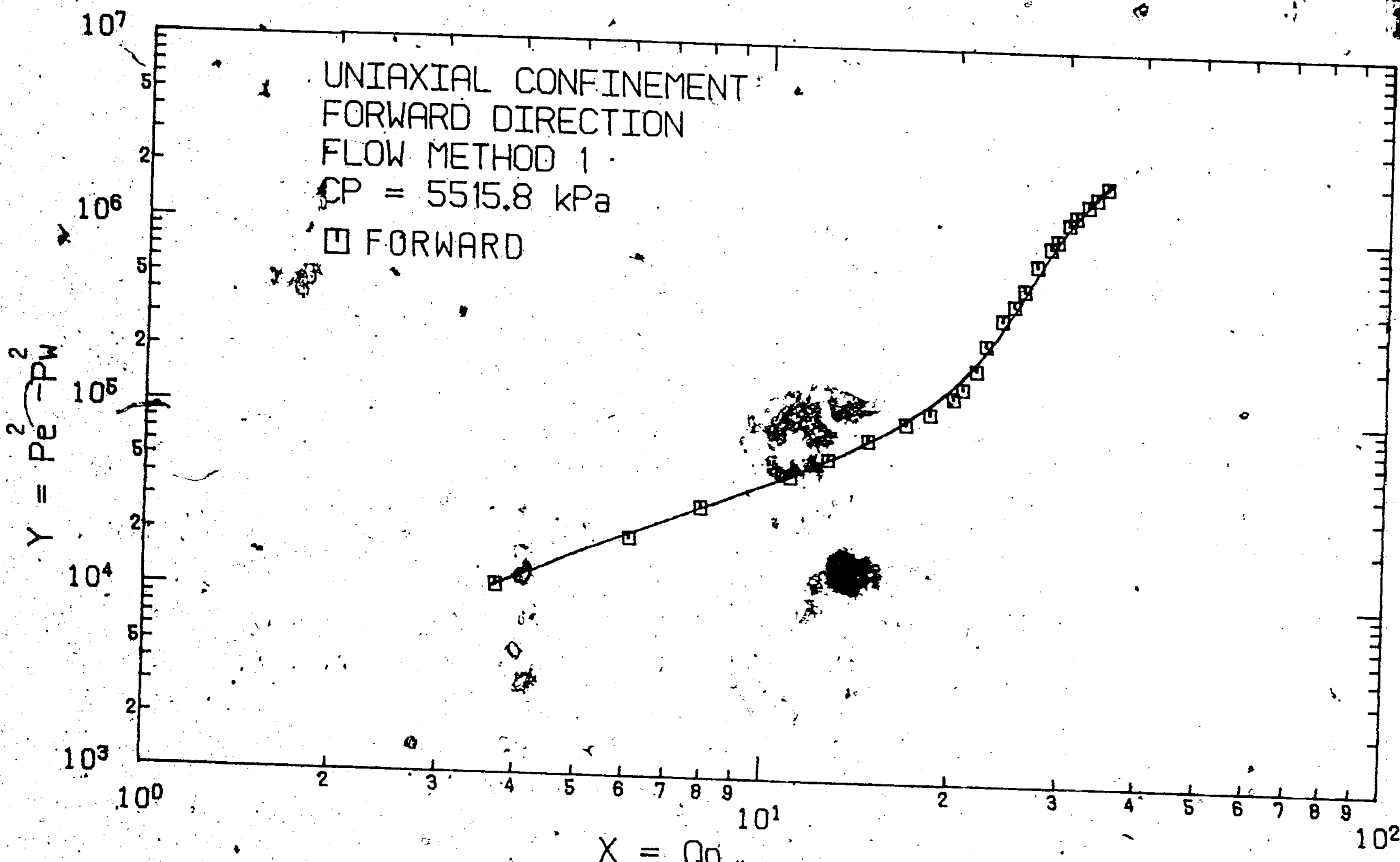

Fig.8-3: CORE 1C BACK PRESSURE PLOT RUN 7

first stage, 1/ka sharply increases with steeper slopes as Qo further increases. In the third stage, the steepness of the slope reduces as 1/ka continues to increase for further increases in Qo. The back-pressure plot on log-log paper shows three corresponding regions as $(Pe^2 - Pw^2)$ increases with increasing Qo. Its first region is linear with slope angle of 45° after which, the slope increases in its second stage, but decreases in the third stage. The general profile for these plots, therefore, is such that $(Pe^2 - Pw^2)$ increases, while ka decreases, with increasing Qo and Pm.

From the model Equation 4.21 and the literature, the visco-inertial plot is expected to slope down at lower flow rates and pressures, and become linear as flow rates and pressures increase. Accordingly, the back-pressure plot is expected to be linear with slope of 45° and increase in slope for higher Qo. By Flow Method 1 for the forward direction, both Pe and Pw increase for increasing Qo and, therefore, $(Pe^2 - Pw^2)$ increases with increasing Pm and increasing Qo. This is equivalent to Case 2 of Table 3.1. With analysis similar to that used for Case 2 in Chapter 3, ka is expected to decrease for decreasing 1/Pm, (Klinkenberg plot), and 1/ka is expected to increase with increasing Qo, (visco-inertial plot). These predicted profiles, arising from the flow method used, agree with observed experimental plot profiles.

The anomalies, observed in the later stages, and which involve the variation of $(Pe^2 - Pw^2)$ and ka with Qo, lead to the following observations:

a) Linearity of Model Equation (4.21) is obtained only in the first region with moderate flow rates and pressures. Beyond this, $(Pe^2 - Pw^2)$, increases rapidly with increasing Qo, as can be seen from the steepness of the slope.

b) In the third region, Qo appears to increase faster than it should be for increasing $(Pe^2 - Pw^2)$.

The first observation suggests a higher order model equation, while the second poses a problem similar to that observed from Figures 3.3 and 3.6, in which lower $(Pe^2 - Pw^2)$ values were obtained for increasing Qo.

8.2 Plot Profiles with Flow Method 2

Surprising profiles have been observed in Figures 8.4 to 8.9, which correspond, respectively, to the Klinkenberg, the visco-inertial and the back-pressure plots of Runs 8 and 9 using Core Sample 4A. In both the Klinkenberg and the visco-inertial plots, ka values are observed to decrease initially with increasing Pm and Qo, and then increase with increasing Pm and Qo. In the back-pressure plots, $(Pe^2 - Pw^2)$ increases with increasing Qo. The slope-angle is initially 45°, after which it decreases with increasing Qo. In this later region, the plots indicate lower $(Pe^2 - Pw^2)$ for increasing Qo. These profiles are similar to those of Figures 3.1 to 3.6, and, therefore, they pose similar problems.

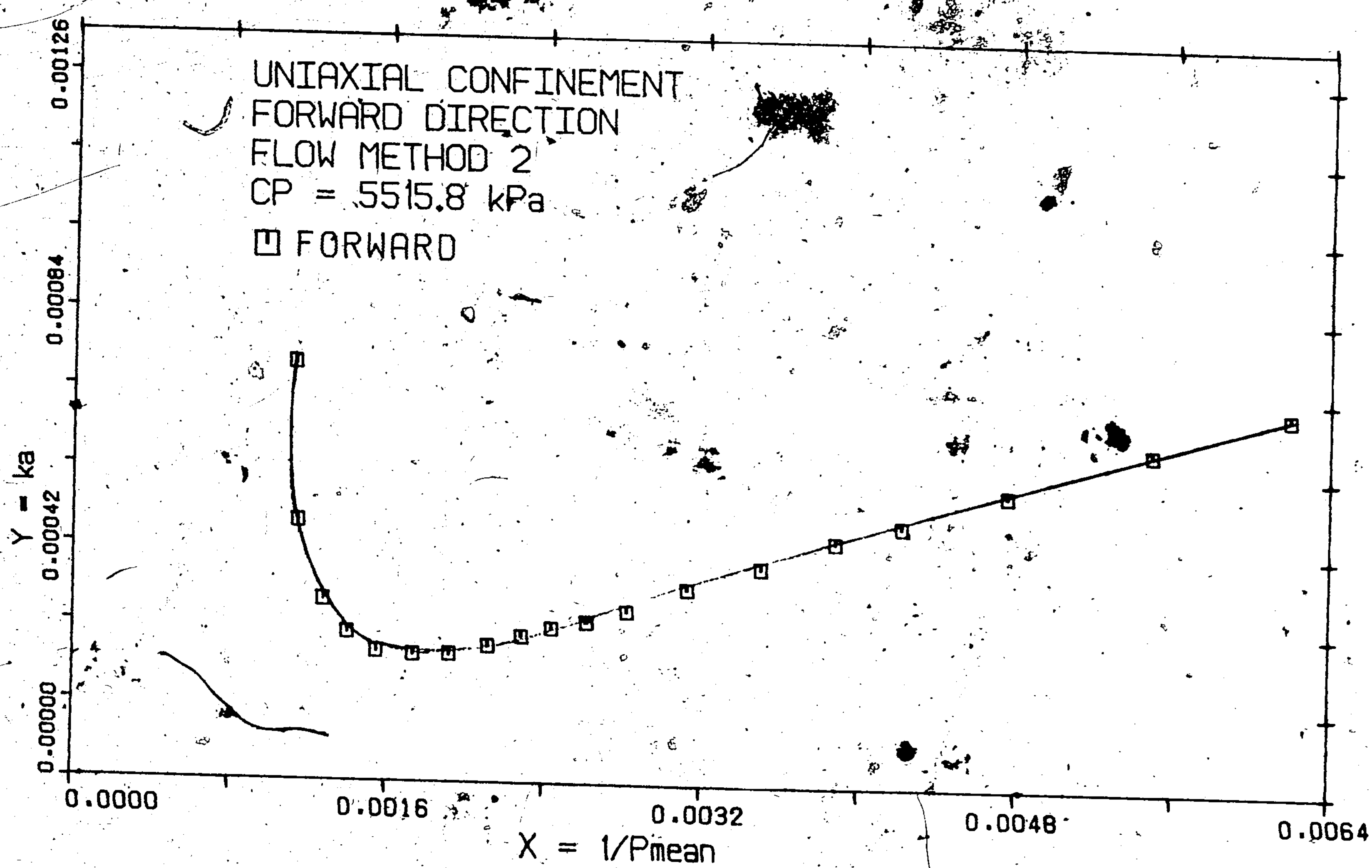

Fig.8-4: CORE 4A KLINKENBERG PLOT RUN 8

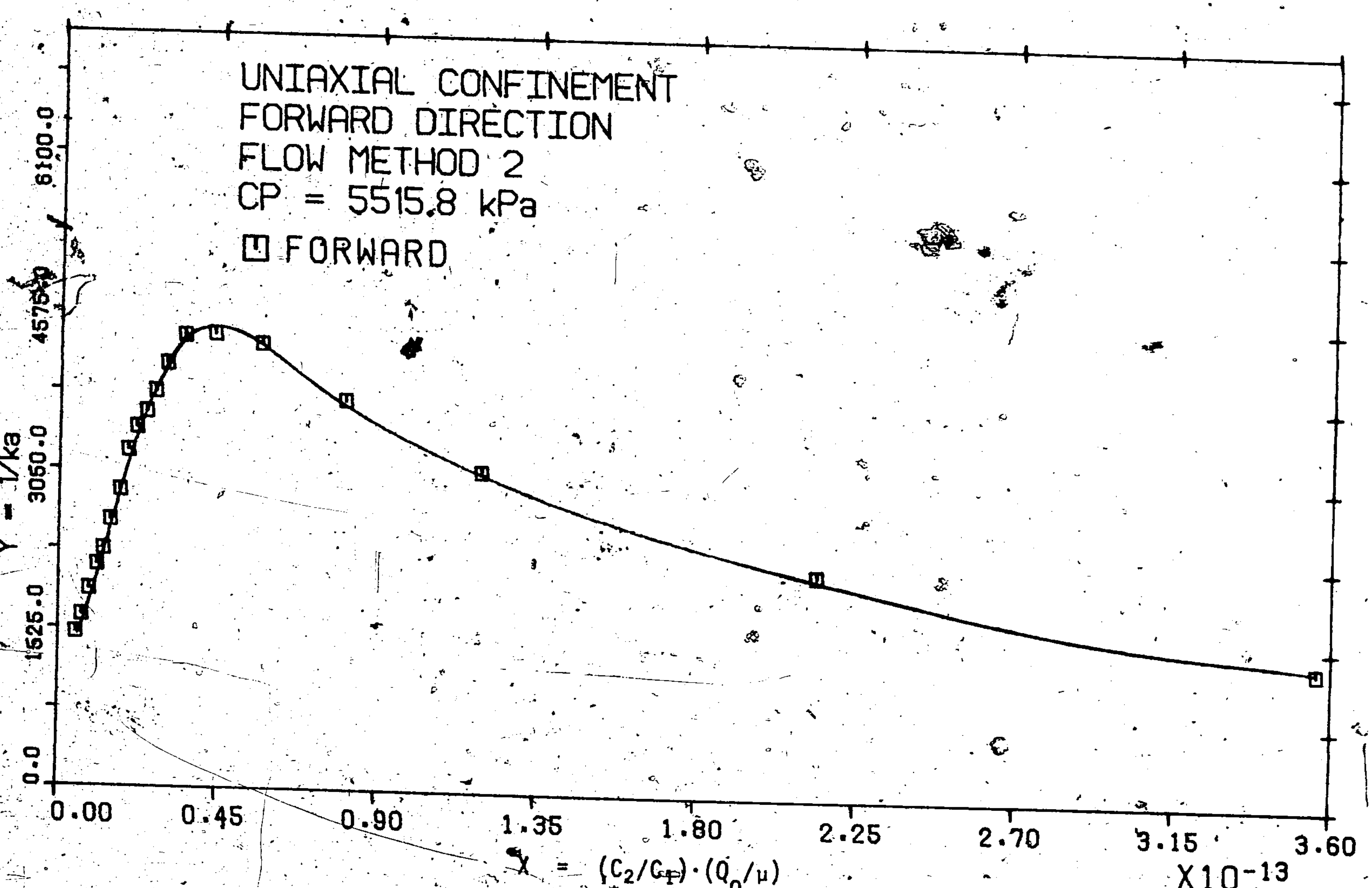

Fig.8-5: CORE 4A. VISCO-INERTIAL PLOT RUN 8

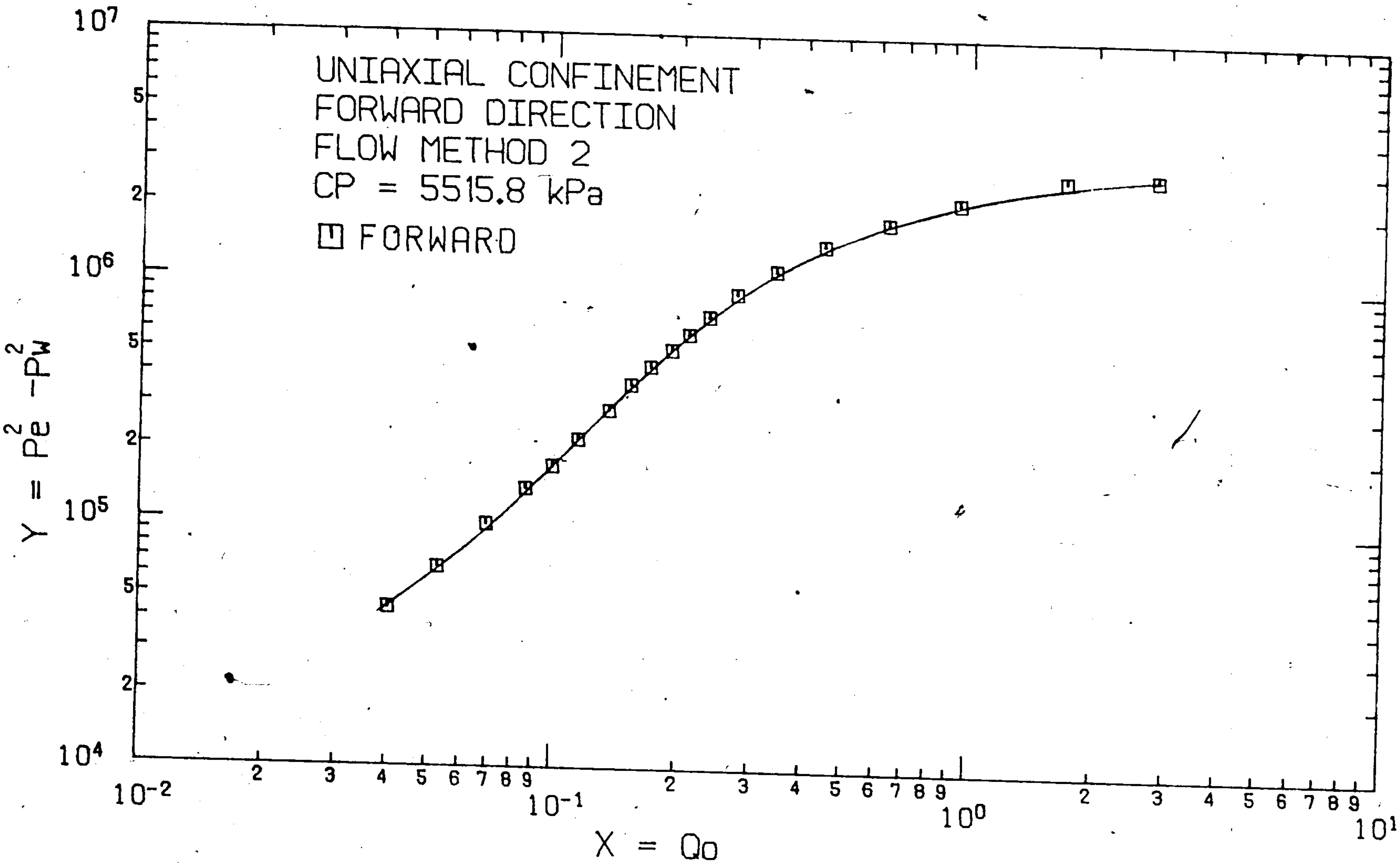

Fig.8-6: CORE 4A BACK PRESSURE PLOT RUN 8

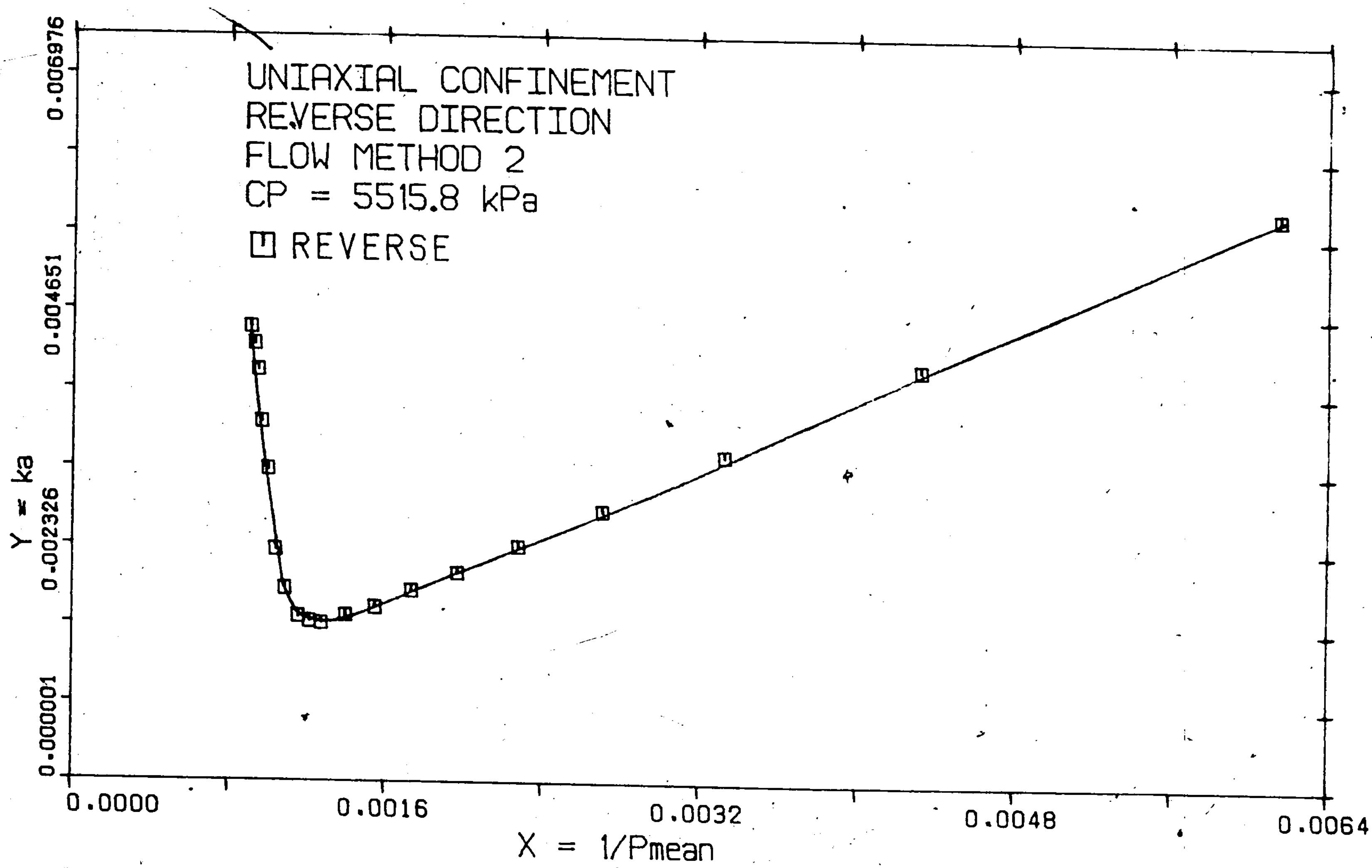

Fig.8-7: CORE 4A KLINKENBERG PLOT RUN 9

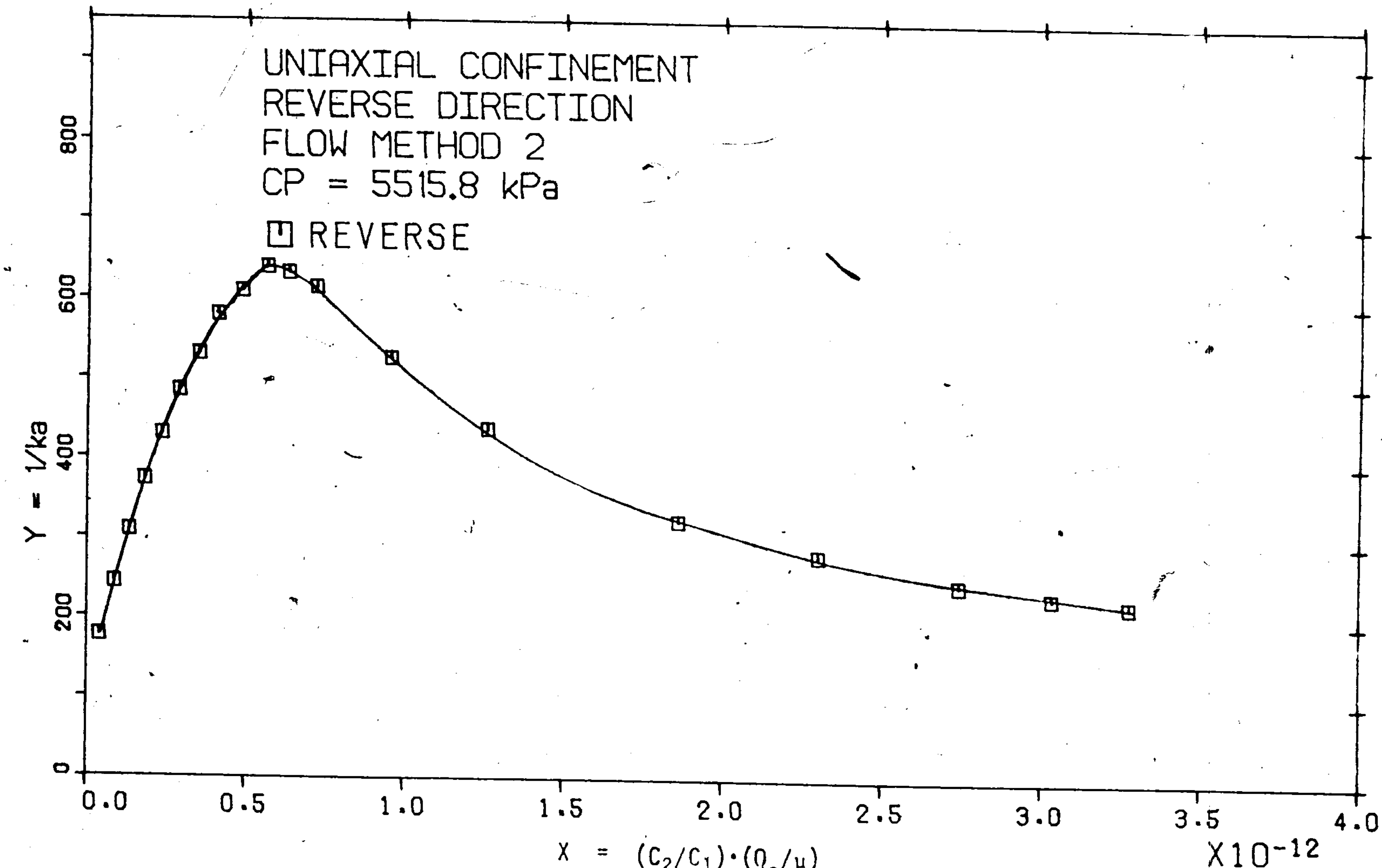

Fig.8-8: CORE 4A VISCO-INERTIAL PLOT RUN 9

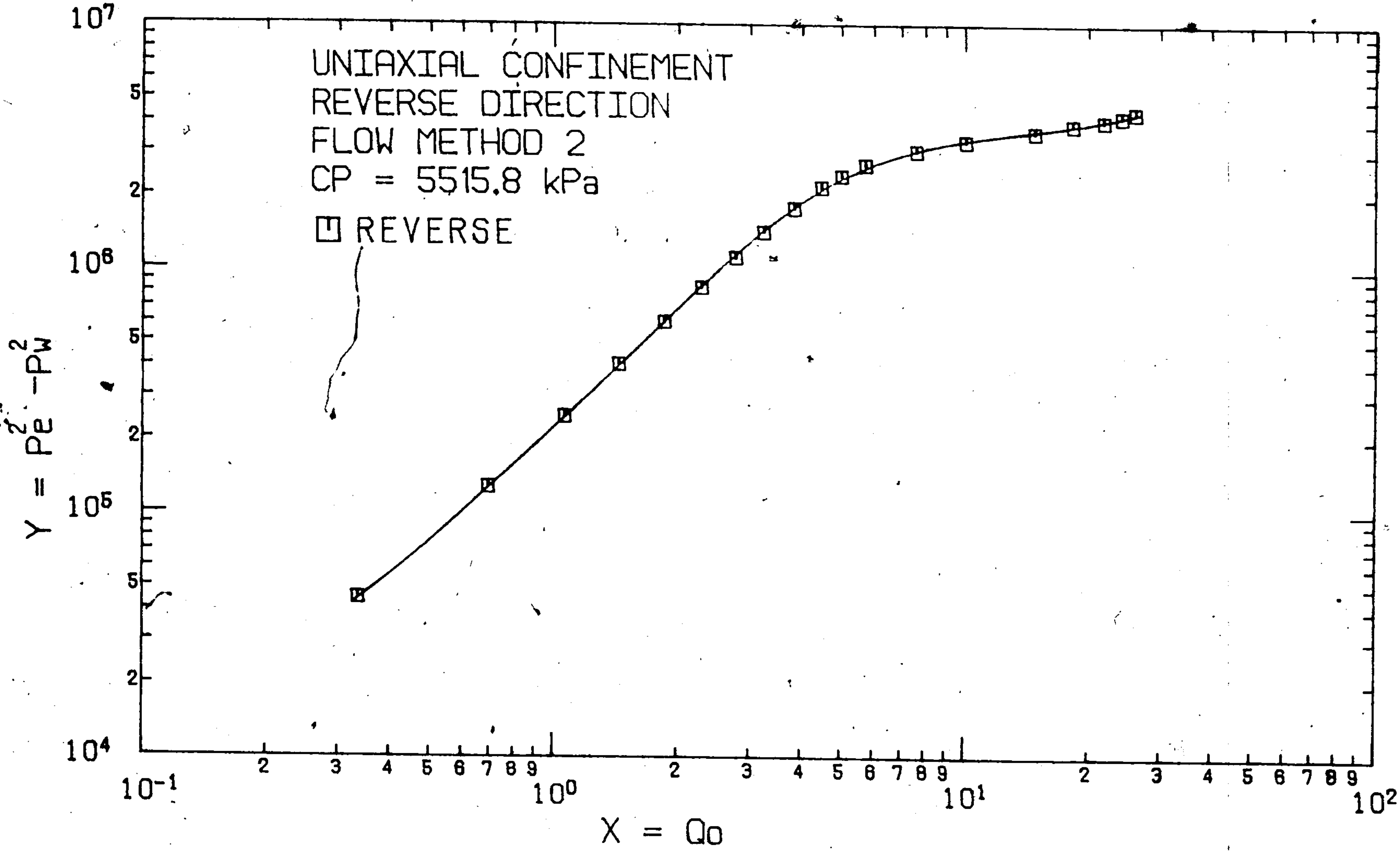

Fig.8-9: CORE 4A BACK PRESSURE PLOT RUN 9

In Run 8, Pw was kept constant at atmospheric pressure while Pe was increased. Run 9 is in the reverse direction as Pe decreased instead of being increased. The conditions for these runs are similar to Cases 2 and 1, respectively, in Table 3.1 of Chapter 3. If a similar analytical procedure is followed in both the Klinkenberg and the visco-inertial plots, ka is expected to decrease for Run 8, and to increase for Run 9, with respect to both Qo and Pm. Also, by using a similar analysis for the back-pressure plot, (Pe^2 - Pw^2) should increase with increasing Qo for Run 8, and decrease with decreasing Qo for Run 9. Generally, the plot profiles agree with predicted profiles at the earlier stage, but the prediction fails at the later stage where ka increases with increasing Qo and Pm.

8.3 Fitted Visco-Inertial and Back-Pressure Plots

In order to study further the observations obtained from the plot profiles, especially in the region of higher flow rates and pressures, fitted visco-inertial and back-pressure plots are made on the experimental data by using both cubic and quadratic model equations. The cubic equation, by having an additional term in gamma for increasing Qo, is regarded as a modification to the quadratic equation.

Both the model cubic equation (Equation 4.15) and the model quadratic equation (Equation 4.17) are adapted, respectively, to Equations 4.23 and 4.21, and are used to give fitted visco-inertial plots. Equations 4.23 and 4.21 are, respectively, quadratic and linear, and expressions on the left of these equations, which are the same for both equations, are used to calculate the experimental y values. Fitted y values are calculated, respectively, from Equations 4.23 and 4.21 by using a multiple linear regression fit. Both experimental and fitted y values are plotted on the same graph against CC2/CC1. For the fitted back-pressure plots, experimental data are, similarly, treated with Equations 4.24 and 4.25, which are, respectively, cubic and quadratic in Qo. Fitted y values are calculated by using a polynomial fit on cubic and quadratic model equations, and both experimental and fitted y values are plotted on the same log-log plot against Qo.

Figure 8-10, shows the fitted visco-inertial plot, for Core 1C Run 7 in the forward direction. Comparing the experimental data with the fitted plots obtained with both the cubic and the quadratic model flow equations, the experimental data have a closer fit with the cubic equation than with the quadratic equation. Specifically, the cubic fit is closer in the region of higher flow rates and pressures than in the region with lower flow rates and pressures.

The fitted back-pressure plots were generally poor. Erratic behavior was obtained on the fit with both model equations in the region of lower flow rates. Specifically, the quadratic equation yielded unreliable fitted values in

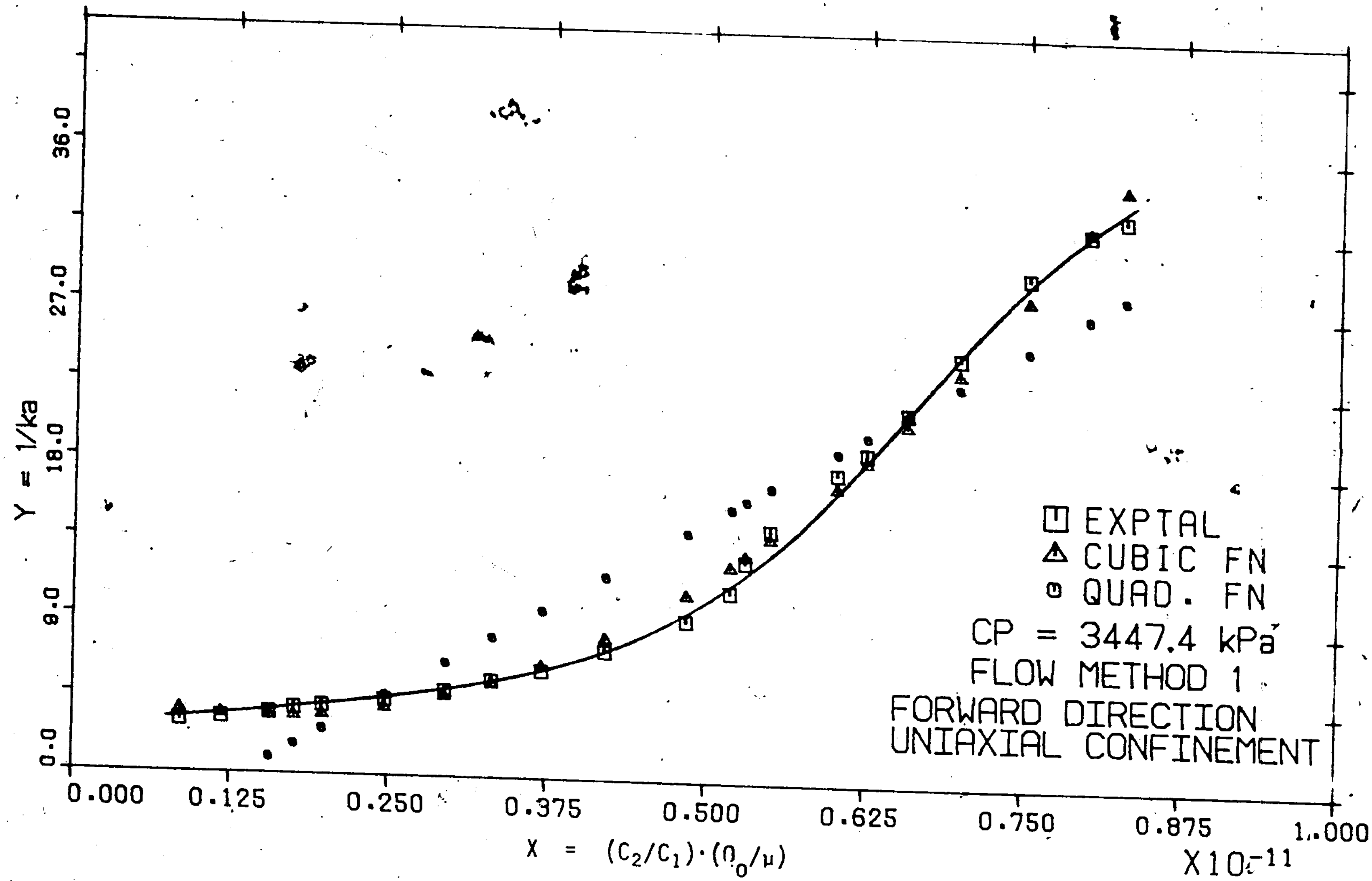

Figure 8-10 CORE 1C RUN 4 VISCO-INERTIAL FIT PLOT

the lower region. This made plotting in this section unreliable. Comparing the fits with the experimental data in the region of higher flow rates where both fits are reliable, the cubic equation gave a closer fit. Reasons for the poor fit in the region of lower flow rates could be attributed to the following:

a) This is the viscous region where, by Darcy's law, $(Pe^2 - Pw^2)$ has a linear relationship with Qo. Therefore using higher order equations to fit this linear section should not be expected to produce good results.

b) In the regression procedure, using Equations 4.24 and 4.25, known variable is Qo, while the rest of the experimentally determined variables, as well as the parameters, Ka, Fb, and gamma, which are yet to be estimated, are all lumped as the unknown variable. By having large unknowns in a system that is not very stable in its matrix formation, (problem of ill-conditioning, which is treated in Appendix B), erratic behavior could be the case. This is reflected in the determined values of the determinants, and the error sum of squares.

Figure 8.11, which is the fitted back-pressure plot plot for Core 1C, Run 3 in the forward direction, shows the experimental data and the fitted cubic equation. More plots are shown in Appendix C.

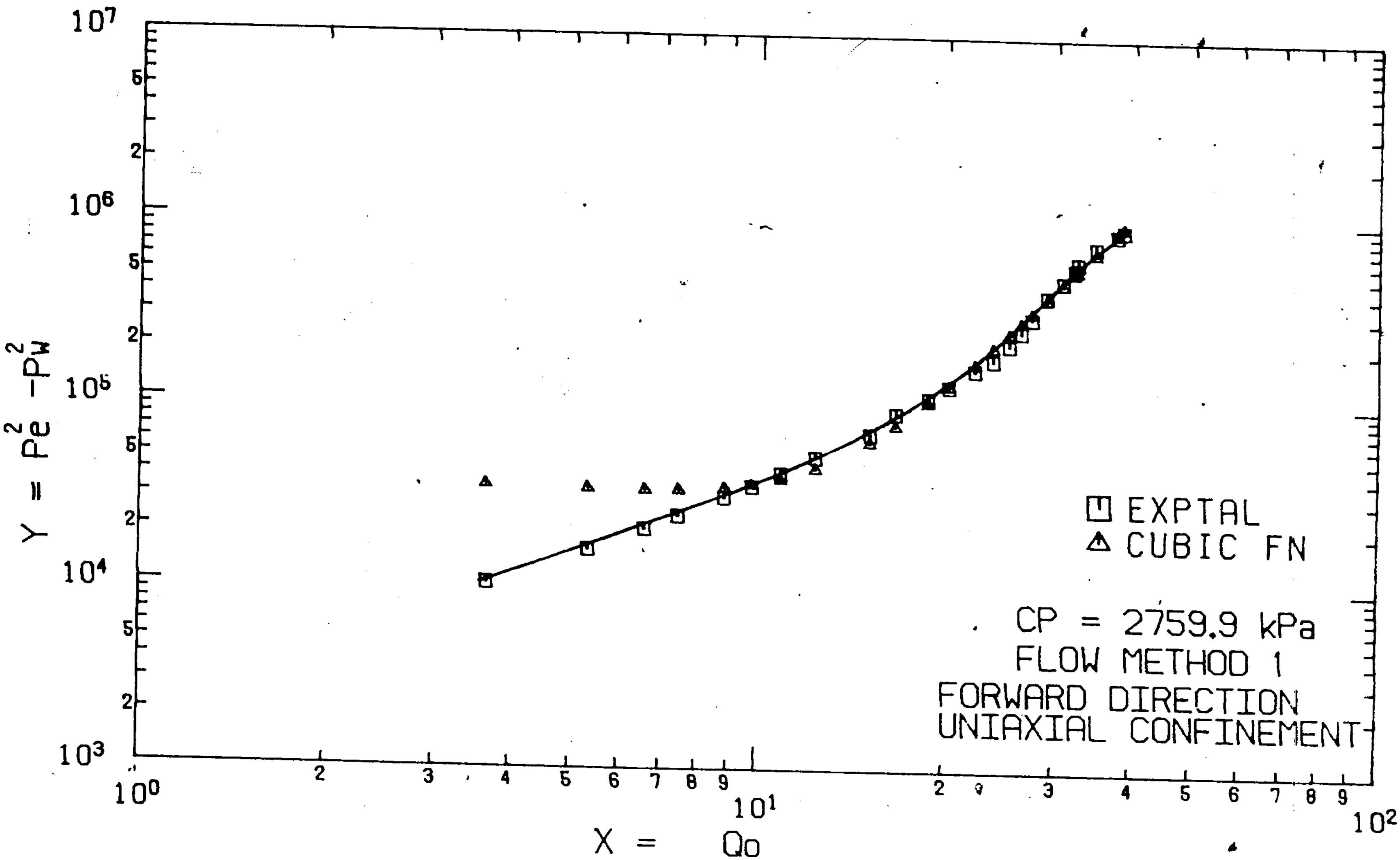

Figure 8-11 CORE 1C RUN 3 BACK PRESSURE FIT PLOT

8.4 Effect of Stress and Flow Methods on Plot Profiles

In the preceding sections, lower ($Pe^2 - Pw^2$) values were observed in the plot profiles for increasing Qo and ka. In this section, a possible explanation to this phenomenon is attempted by analysing the back-pressure flow relationship as given by Equation 3.8. By this equation, ($Pe^2 - Pw^2$) is proportional to Qo, and is a product of Pm and (Pe-Pw). While Pm provides magnitude, (Pe-Pw) provides both magnitude and direction, and therefore, these effects manifest themselves according to the respective magnitudes of Pe and Pw.

By Flow Method 1, Pm increases at a faster rate than (Pe-Pw), and by Flow Method 2, (Pe-Pw) increases at a faster rate than Pm. With increasing pressures, which corresponds to increasing Qo, the effect of Pm increases more for Flow Method 1, while the effect of (Pe-Pw) increases more for Flow Method 2. Both effects lead to increased stresses on the core material. The direct effect of obtaining large drawdown pressures may lead to radial compaction. For the same pressure conditions, such stress may be attained faster, and possibly be more acute, with Flow Method 2 than with Flow Method 1. Depending on the strength of the core samples, this stressed condition may generate cracks and fractures which in turn create increased permeability with resultant increases in Qo. Therefore, the overall effect is to cause increases in ka for increasing Qo and lower ($Pe^2 - Pw^2$). This predicted behavior is similar to what was observed at higher pressures while using Flow Method 1, and at moderate pressures while using Flow Method 2.

The anomalous behavior from these effects suggests a probable confinement pressure problem. Figure 8.12 of Core 1C Run 3, shows, for Flow Method 1, the variation of ka with generated confining pressure,CP, which was obtained from Equation 5.18. The plot shows a decreasing ka profile with increasing CP, which is similar to the findings of Fatt(72) and Senturk(73). Figure 8.13 shows, for Core 4A, Run 9, the variation of ka with CP using Flow Method 2. The value of ka decreases with generated CP after which ka increases for further increases in CP.

After Run 9 on Core 4A, the radial cell was dismantled and a crack was noticed on the core sample as shown in Plates 1 and 2 . No crack was noticed on Core 1C, and on Core 4A prior to making runs on it with Flow Method 2. It is significant to note that both the anomalous plot profile in Figure 8.13 and the crack were observed with respect to the use of Flow Method 2 in Run 9, Core 4A. It is, therefore, probable that the use of Flow Method 2 could be responsible for the crack.

8.5 Plot Profiles using a Tri-axial Radial Cell

Runs 1 and 2 were made using Flow Method 1 in forward and reverse directions, respectively. Run 3 in the forward direction, and Run 4 in the reverse direction, were similarly made using Flow Method 2. The plot profiles show

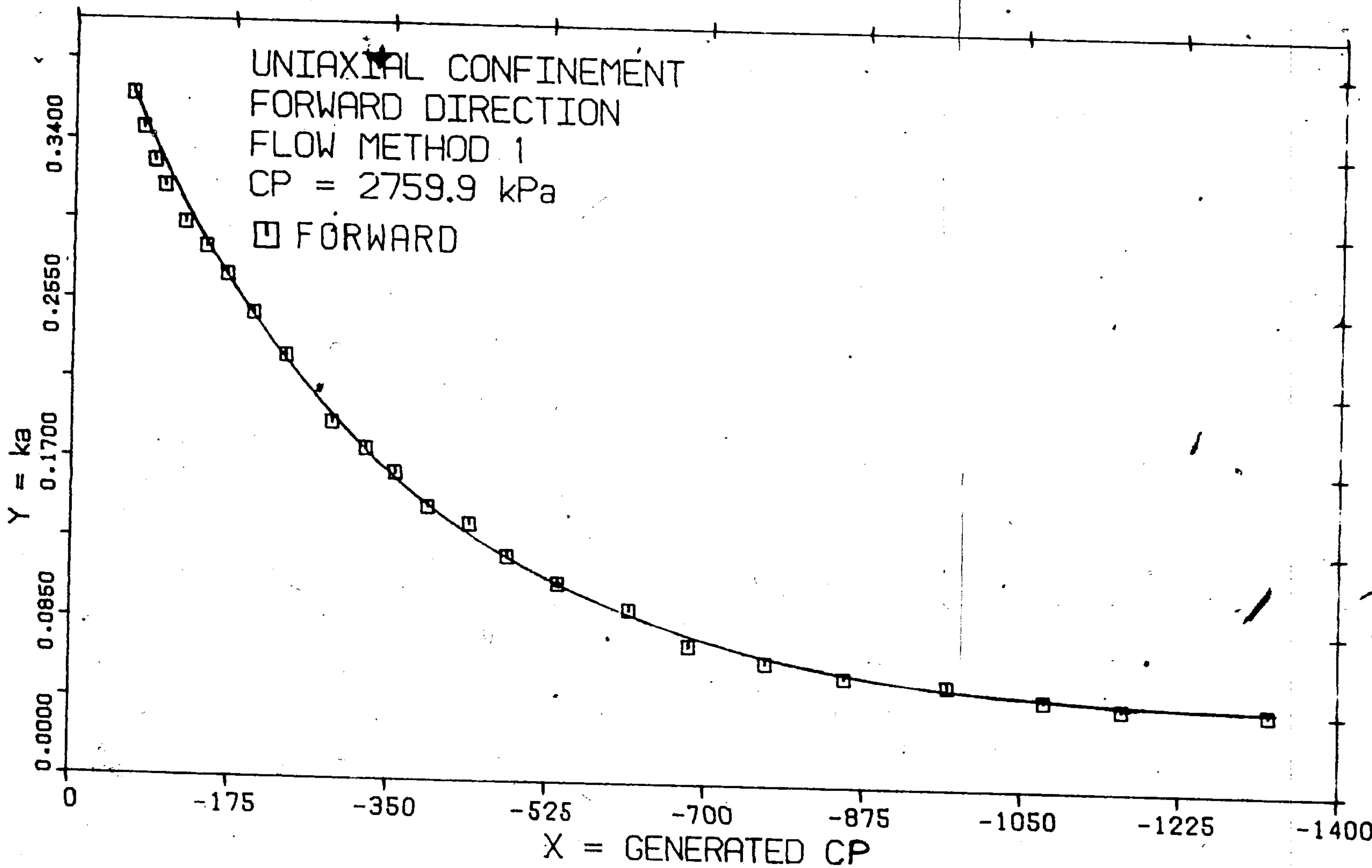

FIGURE 8-12: CORE 1C GENERATED CP VERSUS ka RUN 3

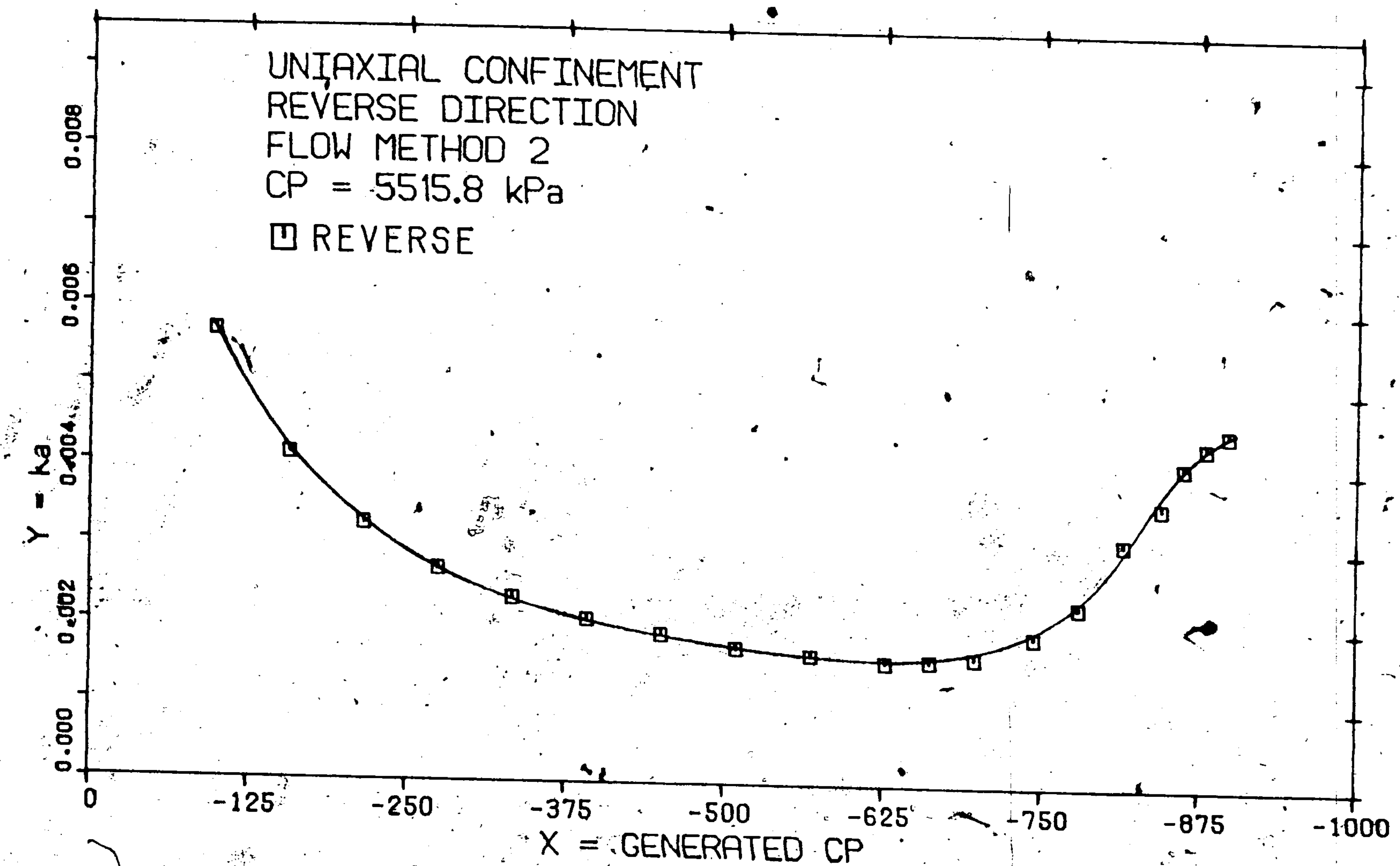

FIGURE 8-13: CORE 4A GENERATED CP WITH ka RUN 9

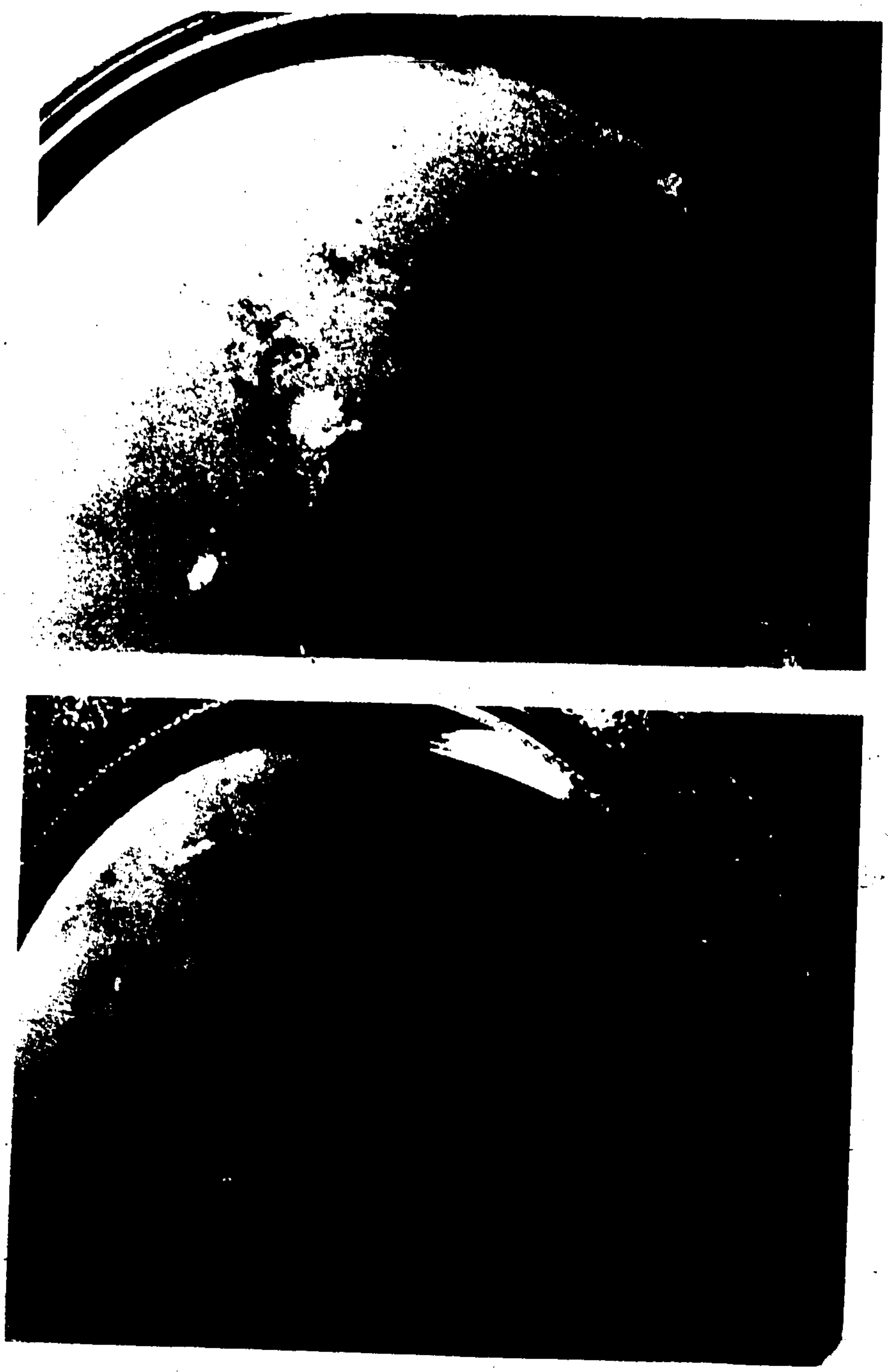

Plate 8:1 Photographs of Core 4A showing Fracture

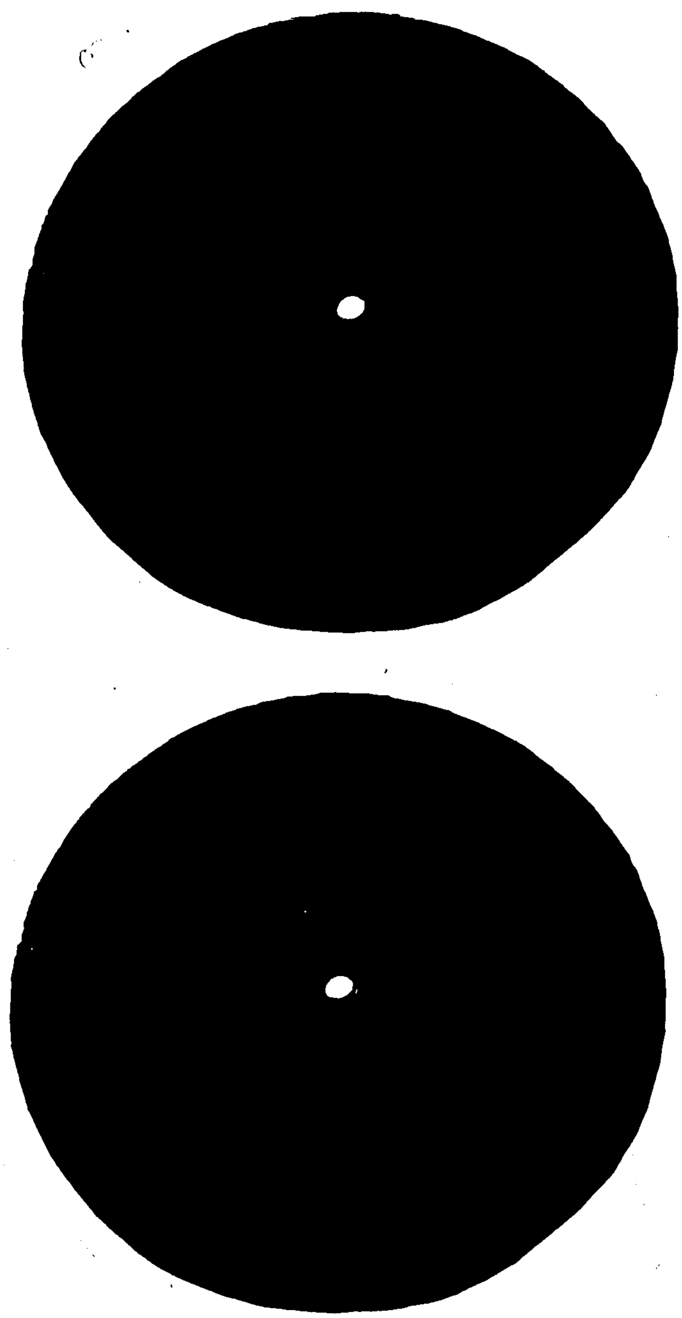

Plate 8:2 Photographs of Rubber Gaskets showing marks of fracturing of Core 4A

distinct differences between the flow methods used. Figures 8-14 and 8-15 show, respectively, the Klinkenberg and the visco-inertial plot profiles for Run 1 using Flow Method 1. They have anomalous behavior similar to that obtained previously with Flow Method 2, when a uniaxial radial cell was used. The cause of this is unknown, but it is suspected that, possibly, the loose rubber overburden sleeve could not give adequate confinement at higher pressures. Anomalous behavior started occurring between 2800.0 kPa and 2940.0 kPa. The predefined CP, which was kept constant at 4136.9 kPa, could possibly have been inadequate for complete confinement at higher fluid pressures, and as the fluid pressures approached its predefined value.

Figures 8-16 and 8-17 show respectively the Klinkenberg and visco-inertial plot profiles for Run 3, using Flow Method 2. The plots have expected profiles.

8.6 Parameter Estimation Results

8.6.1 Graphical and Linear Fit Methods

Estimated parameter values from both graphical and linear fit methods are summarized in Tables 8-1, 8-2, 8-3, 8-4. All runs are with Flow Method 1, except Run 7 on Core 4A, and Run 1SEN from Senturk's data(74), which are both with Flow Method 2.

The graphical method is limited in the choice of the best fit line. Proper delineation of viscous plot points from both Klinkenberg and back-pressure plots by visual

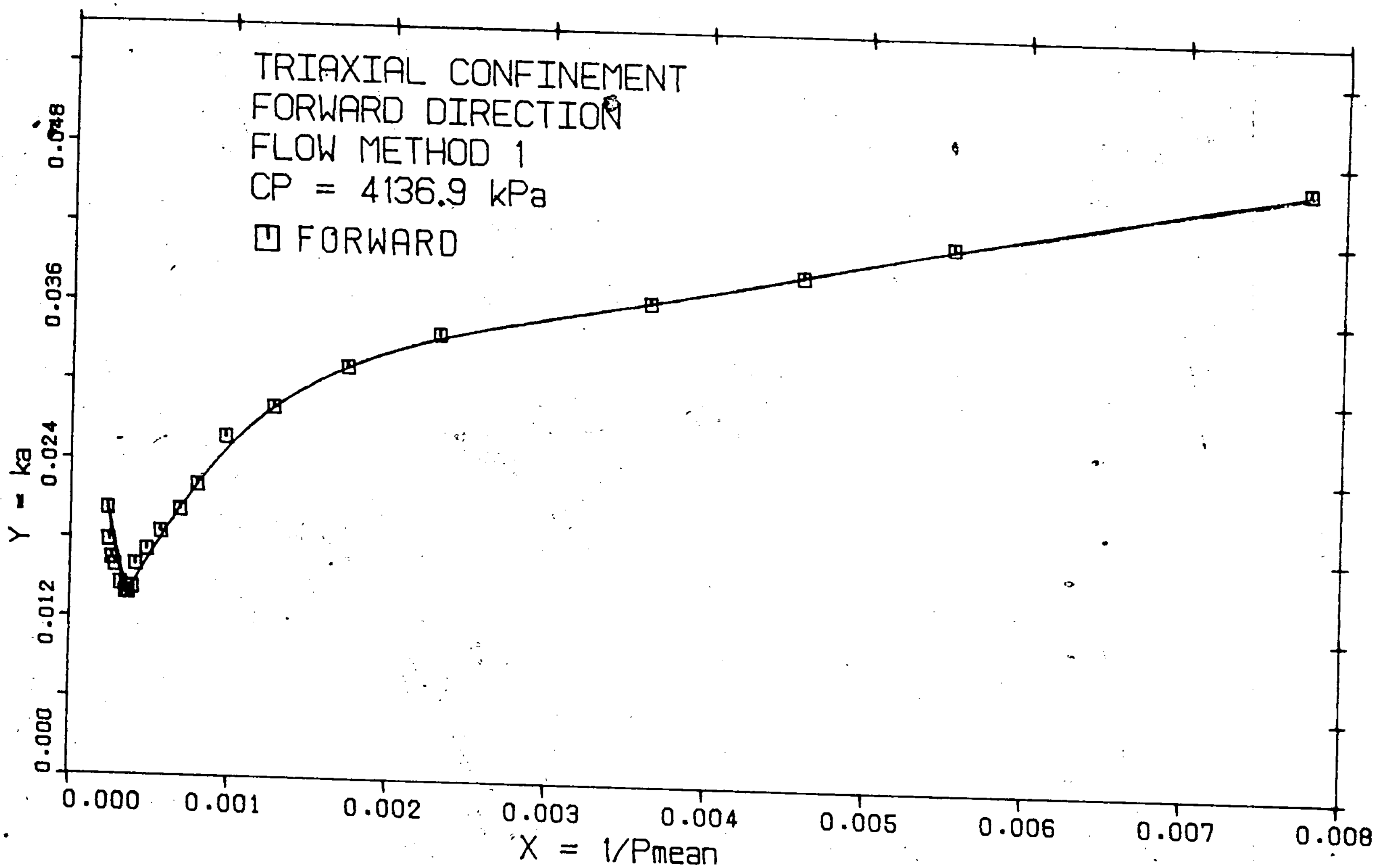

Figure 8-14: CORE 2 KLINKENBERG PLOT RUN 1

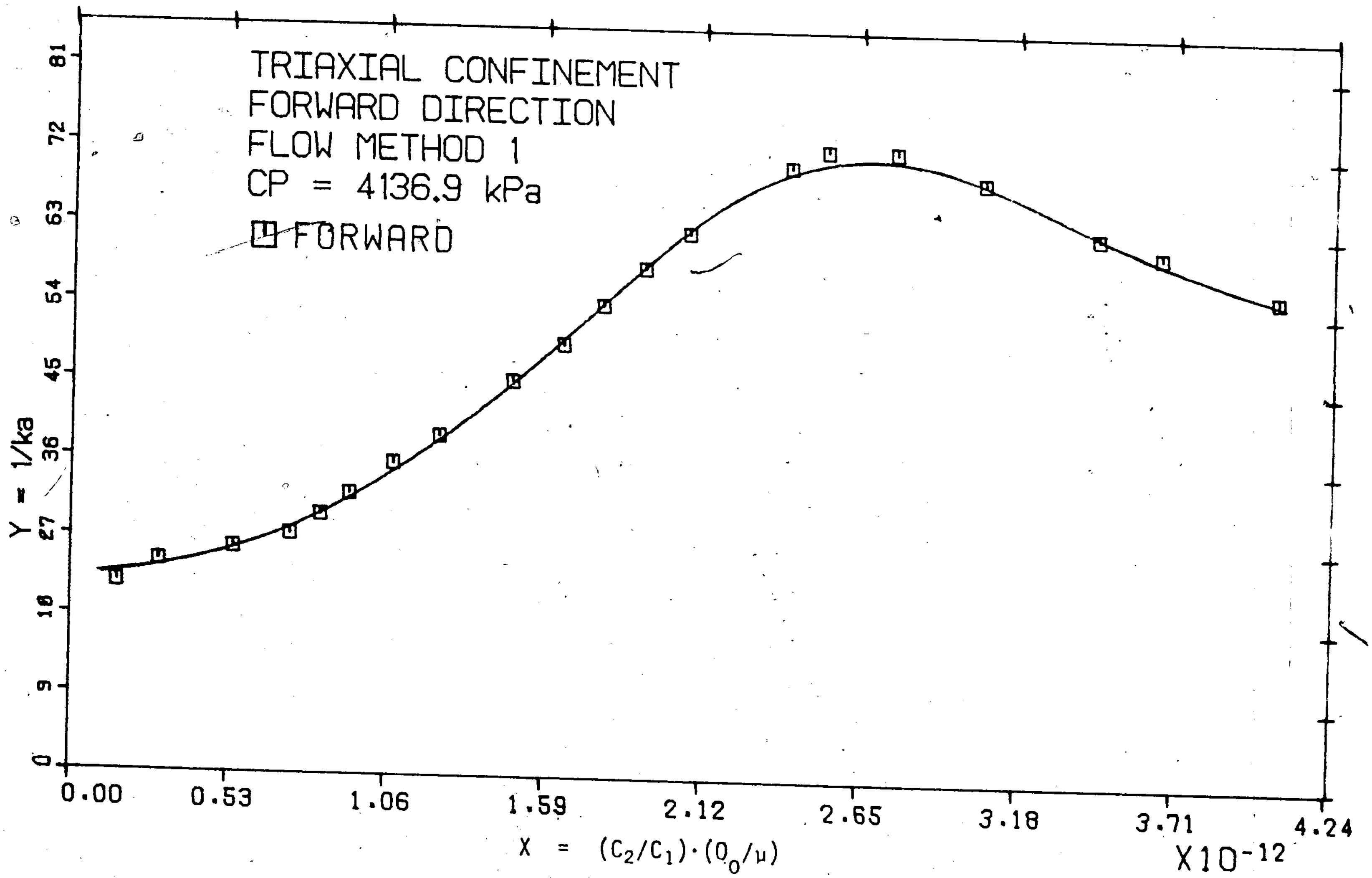

Figure 8-15: CORE 2 VISCO-INERTIAL PLOT RUN 1

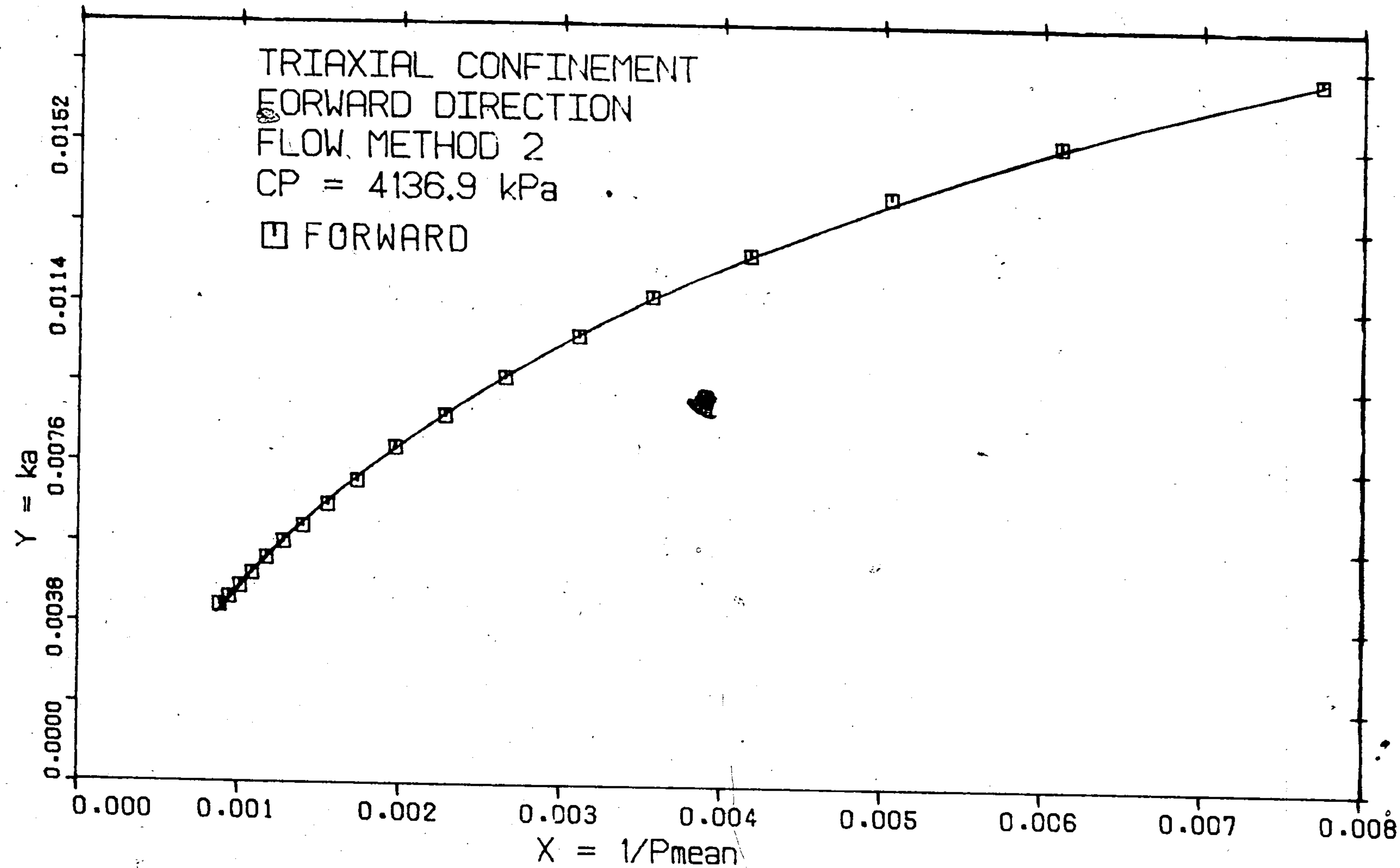

Figure 8-16: CORE 2 KLINKENBERG PLOT RUN 3

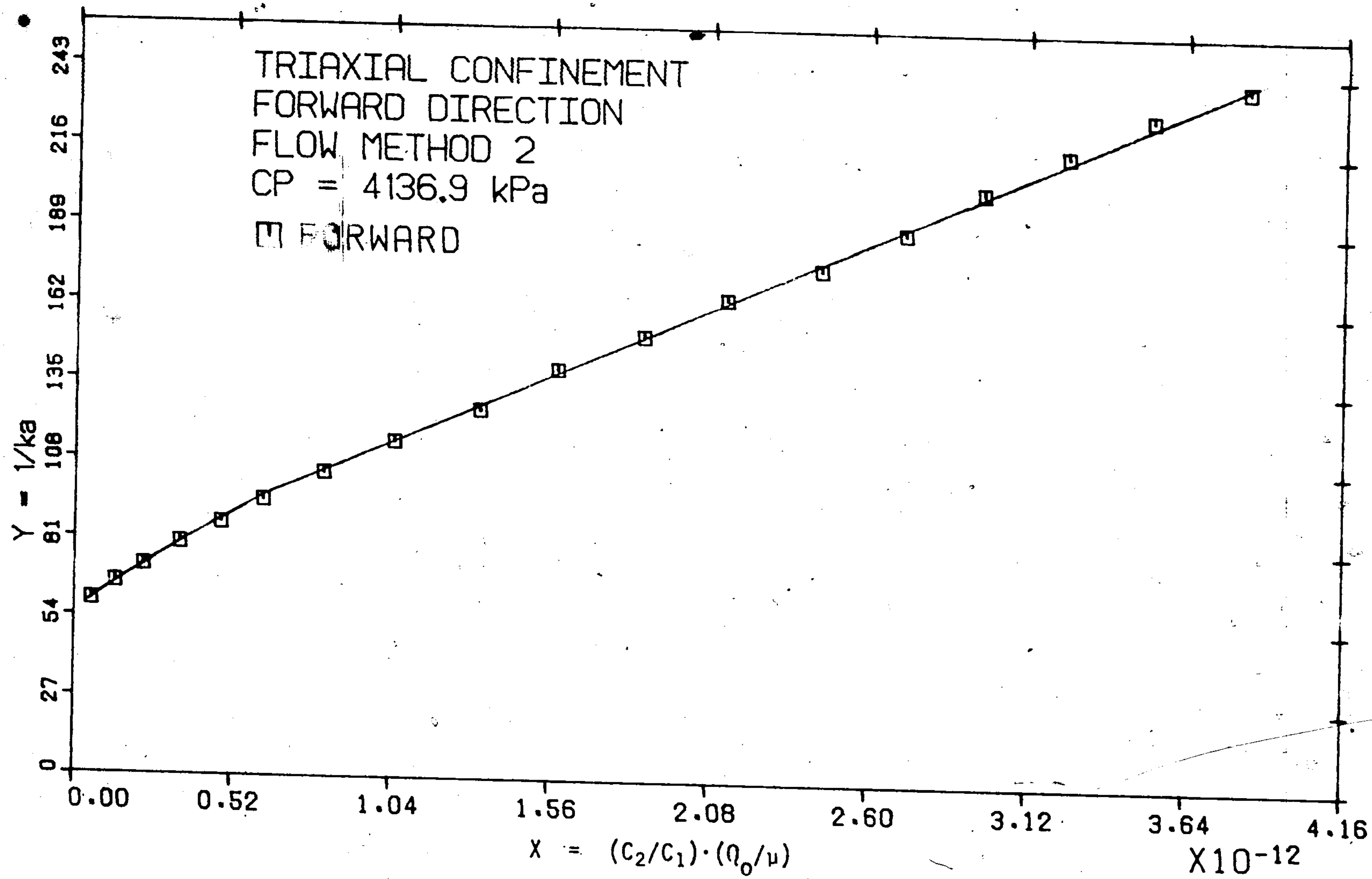

Figure 8-17: CORE 2 VISCO-INERTIAL PLOT RUN 3

TABLE 8-1: GRAPHICAL PARAMETER ESTIMATION FOR CORE 1C

FORWARD RUNS

Run NO	CP kPa	k μm^2	b KPa	kabs μm^2	Fb m^{-1} $x10^{12}$
2	NILL	0.1200	164.06	0.2983	0.7390
3	2759.9	0.2205	82.831	0.4444	0.4688
4	3447.4	0.1761	116.93	0.4460	0.8391
5	4136.9	0.2000	100.00	0.3729	0.3089
6	4826.3	0.1469	140.15	0.2798	0.4806
7	5515.8	0.1455	175.78	0.4522	0.7252

REVERSE RUNS

Run NO	CP kPa	k μm^2	b KPa	kabs μm^2	Fb m^{-1} $x10^{12}$
3	2759.9	0.1546	87.500	0.2764	0.3791
4	3447.4	0.1172	216.18	0.3148	0.9349
5	4136.9	0.1846	141.24	0.5152	0.4001
6	4826.3	0.1739	141.23	0.4928	0.5751
7	5515.8	0.1247	117.93	0.2698	0.8991

TABLE 8-2: GRAPHICAL PARAMETER ESTIMATION FOR CORE 4A

FORWARD RUNS

Run No	CP KPa	K µm²	b kPa	kabs µm²	Fb m⁻¹ x10¹²
1	NILL	0.1031	298.30	0.6267	2.1693
2	2759.9	0.2455	81.250	0.4134	0.4222
3	3447.4	0.1525	235.36	0.5812	0.9806
4	4136.9	0.1478	79.942	0.2576	1.0294
5	4826.3	0.1334	180.69	0.4231	1.2672
6	5515.8	0.1841	161.29	0.5000	1.0181

REVERSE RUNS

Run No	CP KPa	K µm²	b kPa	kabs µm²	Fb m⁻¹ x10¹²
1	NILL	0.1250	212.50	0.3626	0.9160
2	2759.9	0.1388	119.48	0.2471	0.8118
3	3447.4	0.1279	112.07	0.2491	1.2426
4	4136.9	0.1200	102.43	0.2394	1.4216
5	4826.3	0.1338	169.23	0.4681	1.7179
6	5515.8	0.1090	164.21	0.2787	2.3077
7	5515.8	0.0002	233.71	0.0003	11117.5
1SEN	4826.3	0.0086	24.713	0.0079	28.581

TABLE 8-3: PARAMETER ESTIMATION BY LINEAR FIT FOR CORE 1C
(Using Truncated Plot Points)

FORWARD RUNS

Run No	CP kPa	k μm^2	b kPa	kcor μm^2	kabs μm^2	Fb m^{-1} $\times 10^{12}$
2	NILL	0.1027	217.28	0.1036	0.3797	1.0991
3	2759.9	0.2257	79.622	0.2256	0.4502	0.5202
4	3447.4	0.1717	123.44	0.1726	0.4532	0.8627
5	4136.9	0.1926	110.77	0.1929	0.4040	0.3787
6	4826.3	0.1422	149.67	0.1425	0.3302	0.6233
7	5515.8	0.1454	176.94	0.1453	0.4537	0.7262

REVERSE RUNS

Run No	CP kPa	k μm^2	b kPa	kcor μm^2	kabs μm^2	Fb m^{-1} $\times 10^{12}$
2	NILL	0.0253	704.06	0.0261	0.0505	1.8252
3	2759.9	0.1547	88.223	0.1548	0.2751	0.3680
4	3447.4	0.1150	224.85	0.1167	0.4790	1.2504
5	4136.9	0.1872	154.62	0.1871	0.5139	0.3880
6	4826.3	0.1726	150.45	0.1725	0.4841	0.5690
7	5515.8	0.1171	143.20	0.1190	0.2777	0.9337

TABLE 8-4: PARAMETER ESTIMATION BY LINEAR FIT FOR CORE 4A
(Using Truncated Plot Points)

FORWARD RUNS

Run No	CP kPa	k μm^2	b kPa	kcor μm^2	kabs μm^2	Fb m^{-1} $\times 10^{12}$
1	NILL	0.1052	288.59	0.1052	0.6302	2.1869
2	2759.9	0.2290	97.792	0.2288	0.4550	0.5452
3	3447.4	0.1506	240.44	0.1518	0.6269	1.0731
4	4136.9	0.1457	81.112	0.1457	0.2610	1.0245
5	4826.3	0.1357	175.59	0.1356	0.4151	1.2334
6	5515.8	0.1513	232.52	0.1504	0.7720	1.5253

REVERSE RUNS

Run No	CP kPa	k μm^2	b kPa	kcor μm^2	kabs μm^2	Fb m^{-1} $\times 10^{12}$
1	NILL	0.1141	245.84	0.1120	0.5286	1.7325
2	2759.9	0.1338	131.23	0.1134	0.3232	1.4047
3	3447.4	0.1234	123.06	0.1235	0.3020	1.8584
4	4136.9	0.1191	102.87	0.1191	0.2411	1.4206
5	4826.3	0.1288	180.93	0.1297	0.5011	1.7708
6	5515.8	0.1096	161.29	0.1100	0.3562	2.0734
7	5515.8	0.0002	244.88	0.0002	0.0004	16593.
1SEN	4826.3	0.0055	102.28	0.0058	0.0098	36.042

inspection may not always be quite accurate. By linear fitting those points suspected to be in the viscous region, and checking for the value of the linear correlation coefficient, Raa, the best estimates of K and b, based on the method of least squares, are obtained. Similar treatment by linear fitting is carried out for the visco-inertial case.

The choice of b for the modified visco-inertial plot influences not only the value of the corrected K, Kcor, but also the value of the corrected Fb. Poor values of b, reflected in the Raa value being far from unity, gives poor values of the corrected parameters.

8.6.2 Numerical Methods

Simultaneous parameter estimation has been undertaken by using:

(a) the cubic equation (Equation 4.15),

(b) the slippage corrected versions of the cubic and quadratic equations (Equations 4.16 and 4.18),

(c) Case(b) when their combined variables are neglected.

They are summarized in Tables 8-5, 8-6, 8-7, 8-8. Application of these cases have been made on both complete and truncated plot points. Complete plot points represent all the plot points; they span both higher and lower flow rates and pressures. Truncated plot points are those plot points which were used for the linear fit parameter estimation. They represent plot points with lower flow rates

TABLE 8-5: NUMERICAL PARAMETER ESTIMATION FOR CORE 1C
(Using Complete Plot Points)

FORWARD RUNS

Run No	CP kPa	Ka µm²	Fb m⁻¹ x10¹²	Gamma msec/Kg x10¹⁶
2	NILL	0.3070	6.9138	0.7701
3	2759.9	0.2055	2.8954	0.5431
4	3447.4	0.2082	5.8621	0.9165
5	4136.9	0.1268	6.6411	1.1546
6	4826.3	0.0615	9.9375	2.1428
7	5515.8	0.0734	10.609	2.1489

REVERSE RUNS

Run No	CP kPa	Ka µm²	Fb m⁻¹ x10¹²	Gamma msec/Kg x10¹⁶
2	NILL	0.0600	3.1942	0.6476
3	2759.9	0.0100	4.8932	0.7332
4	3447.4	0.1086	5.5596	1.0283
5	4136.9	0.0954	7.4485	1.3169
6	4826.3	0.0643	11.038	2.2152
7	5515.8	0.0626	11.984	2.5433

TABLE 8-6: NUMERICAL PARAMETER ESTIMATION FOR CORE 4A (Using Complete Plot Points)

FORWARD RUNS

Run No	CP kPa	Ka μm^2	Fb m^{-1} $x10^{12}$	Gamma msec/kg $x10^{16}$
1	NILL	0.1046	17,890	6.5656
2	2759.9	0.1002	12.162	6.5956
3	3447.4	0.0702	23.051	13.151
4	4136.9	0.0705	22.392	12.030
5	4826.3	0.0550	23.510	11.878
6	5515.8	0.0501	32.302	14.168

REVERSE RUNS

Run No	CP kPa	Ka μm^2	Fb m^{-1} $x10^{12}$	Gamma msec/kg $x10^{16}$
1	NILL	0.1116	15.605	7.3886
2	2759.9	0.0944	11.700	5.8221
3	3447.4	0.0632	21.893	11.673
4	4136.9	0.0565	20.636	13.171
5	4826.3	0.0950	18.744	9.7133
6	5515.8	0.0658	21.609	10.651
7	5515.8	0.00044	33240.	76140.
1SEN	4826.3	0.0101	52.290	4.3530

TABLE 8-7: NUMERICAL PARAMETER ESTIMATION FOR CORE 1C (Using Truncated Plot Points)

FORWARD RUNS

Run No	CP kPa	k µm²	b kPa	kabs µm²	Fb m^{-1} x10^{12}	Gamma msec/kg x10^{16}
2	NILL	0.1106	140.51	0.2341	0.8016	0.3673
3	2759.9	0.1956	104.67	0.3853	0.3519	0.2091
4	3447.4	0.1725	112.75	0.4529	0.4256	0.1782
5	4136.9	0.1673	114.43	0.3741	0.1881	0.0438
6	4826.3	0.1563	126.39	0.3984	0.1014	0.1168
7	5515.8	0.1420	128.33	0.4298	0.1929	0.3864

REVERSE RUNS

Run No	CP kPa	k µm²	b kPa	kabs µm²	Fb m^{-1} x10^{12}	Gamma msec/kg x10^{16}
2	NILL	0.0356	307.95	0.0600	1.0936	0.6476
3	2759.9	0.0497	515.45	0.2478	0.1109	0.0502
4	3447.4	0.1382	176.49	0.9372	0.2850	0.0932
5	4136.9	0.1744	159.08	0.4273	0.0471	0.0802
6	4826.3	0.1954	123.03	0.4664	0.1023	0.0191
7	5515.8	0.1025	148.61	0.2444	0.4687	0.1212

TABLE 8-8: NUMERICAL PARAMETER ESTIMATION FOR CORE 4A
(Using Truncated Plot Points)

FORWARD RUNS

Run No	CP KPa	k µm²	b KPa	kabs µm²	Fb m^{-1} $x10^{12}$	Gamma msec/kg $x10^{16}$
1	NILL	0.1520	181.88	0.5950	0.8058	0.1127
2	2759.9	0.2014	134.03	0.4280	0.3183	0.1965
3	3447.4	0.1894	169.98	0.4334	0.3674	0.8987
4	4136.9	0.1469	106.58	0.2602	1.0016	1.8775
5	4826.3	0.1156	214.78	0.3723	0.6997	0.3803
6	5515.8	0.1123	273.19	0.3729	0.7998	1.3308

REVERSE RUNS

Run No	CP KPa	k µm²	b KPa	kabs µm²	Fb m^{-1} $x10^{12}$	Gamma msec/kg $x10^{16}$
1	NILL	0.0839	359.55	0.2400	3.0924	2.4012
2	2759.9	0.0994	183.96	0.2969	0.9571	0.8435
3	3447.4	0.1022	168.73	0.2335	0.6719	1.3693
4	4136.9	0.1184	104.29	0.2309	1.0616	0.2516
5	4826.3	0.1490	101.96	0.4098	0.6830	0.3795
6	5515.8	0.1120	156.41	0.1849	1.0176	3.1086
7	5515.8	0.0002	232.01	0.0004	15080.	76140.
1SEN	4826.3	0.0080	33.505	0.0101	35.673	4.3530

and pressures.

Case (c) has generally more stable matrices than case (b), and parameters estimated with it are closer to those obtained by linear fit. It has slightly larger values of the error sum of squares than Case (b). However, Case (b) shows greater signs of ill-conditioning than Case (c), and therefore produces less reliable results. Non-linear effect in the combined variables, inspite of the linearization of the coefficients, could probably be the cause. The quadratic case (Case (c)) is the same as Equation 2.32 due to Piplapure.

The numerical method, which depends mainly on the model equation, and the number of data points used, appear to be superior to the combined graphical and linear fit methods because :

(a) parameters can be estimated simultaneously,

(b) interactions between parameters can be monitored properly.

However, the graphical/linear fit method gives fundamental parameter estimations on which the validity of the numerical methods can be checked.

Table 8-9 gives a summary of the parameter estimation for Core 4A, Runs 8 and 9, and for Core 2, Runs 1 to 4. It is observed that values of the inertial resistance coefficient, Fb, from both methods of parameter estimation for Runs 8 and 9, are both large and negative. Possible causes for this could be attributed to similar causes of the

TABLE 8-9: PARAMETER ESTIMATION

For Core 4a Runs 8 and 9, Core 2 Runs 1 to 4

BY GRAPHICAL/LINEAR FIT METHOD

Flow Method	Run No	CP kPa	k μm²	b kPa	kcor μm²	kabs μm²	Fb m^{-1} $x10^{12}$
2	8#	5515.8	0.00023	242.28	0.00019	0.00032	-7614.7
2	9#	4826.3	0.00200	218.25	0.00140	0.00206	-111.80
1	1*	4136.9	0.01680	269.86	0.01814	0.03536	10.237
1	2*	4136.9	0.01470	100.58	0.01480	0.01910	4.2042
2	3*	4136.9	0.00347	567.41	0.00390	0.01600	46.969
2	4*	4136.9	0.00276	819.92	0.00280	0.01320	37.914

BY NUMERICAL METHOD

Flow Method	Run No	CP kPa	k μm²	b kPa	kabs μm²	Fb m^{-1} $x10^{12}$
2	8#	5515.8	0.00016	357.66	0.00038	-12470.
2	9#	4826.3	0.00078	801.79	0.00265	-299.97
1	1*	4136.9	0.01983	216.25	0.15130	4.4176
1	2*	4136.9	0.01500	94.666	0.02716	0.7191
2	3*	4136.9	0.01220	55.407	0.01669	44.367
2	4*	4136.9	0.00304	733.16	0.01906	53.958

where : # = core 4a - under uniaxial confinement

* = core 2 - under triaxial confinement

abnormal Klinkenberg and visco-inertial plot profiles obtained for these runs. Generally, there are noticeable differences between parameters obtained by the numerical method, and those obtained by the graphical/linear fit method. Specifically for core 2, parameter values obtained in the forward direction differ from those obtained in the reverse direction.

8.7 Analysis of the Estimated Parameters

Parameter values, ka, b, Fb, and gamma, have been estimated numerically from the truncated plot points, under uniaxial confinement pressure. The values for k and b, which are in the viscous region, are close to those obtained by both graphical and linear fit methods. The estimated Fb and gamma values obtained with complete plot points are higher than those obtained with truncated plot points. This suggests the possibility of gamma becoming significant in the lower region of flow as soon as the flow rate is large enough to induce fluctuations. Hence, the magnitude of the inertial term increases with increasing flow rates and pressures, and both gamma and Fb values begin to increase.

8.7.1 Gas Permeability in the Higher Flow Regime

It is observed from Tables 8-1 to 8-8, that the values of the apparent gas permeability,ka, obtained with the truncated plot points, are greater than those obtained with the complete plot points. In many cases, ka values obtained by using the complete plot points, are smaller than the absolute gas permeability,K, obtained from both graphical and linear fit methods with truncated plot points. It can be inferred from these observations that the apparent gas permeability,Ka, is higher at lower flow rates and pressures, (lower flow regime), and lower at higher flow rates and pressures (higher flow regime). In other words, since the flow regime depends on the magnitude of the flow rate, the apparent gas permeability,Ka, has an inverse relationship with Qo.

According to Equation 2.7, Ka is inversely proportional to the mean pressure,Pm, and it decreases for increasing pressure towards its limiting value,K, at infinite mean pressure. This also corresponds to an inverse relationship of Ka with Qo. Gas slippage decreases as Ka decreases, and with increasing pressures. From theory, the gas properties at higher pressures, approximate those of a liquid, and, therefore, the effect of gas slippage becomes minimal under this flow condition.

8.7.2 Observations on Inertial Resistance Coefficient and Gamma

From Tables 8-1 to 8-8, the values of both gamma and the inertial resistance coefficient,Fb, obtained with the complete plot points under uniaxial confinement are higher than those obtained with the truncated plot points. This suggests that these parameters have higher values when higher flow regimes are traversed, and lower values when lower flow regimes are traversed. This may seem anomalous at first since Fb, defined according to Equation A-22b, has a dimension of L^{-1}, and therefore is characteristic of the length scale in the porous media. Gamma, on the other hand, is defined according to Equation A-22c, and has a dimension of LTM^{-1}, which is the same as the reciprocal of viscosity.

When Darcy's law is obeyed at low flow rates, the inertial term is negligible. With increasing flow rate, deviation from Darcy's law is obtained, and a quadratic term is added to account for the increasing inertial term. As the flow rate further increases, with corresponding increases in the fluid pressure, the need for the cubic term becomes significant. It can then be inferred that generating both inertial and cubic terms beyond the flow regime in which Darcy's law is satisfied, is dependent on the flow regimes traversed as flow rates increase.

Similar observations have been recorded by several investigators. Irmay(75) remarked that the values of a and b in his Equation 2.22 differed as Re increased for higher flow rates. Using different gases with different viscosity values, Senturk(76) concluded that Fb could be a function of viscosity. Crafton's observations(77) are condensed in Equation 2.31.

8.7.3 Friction Factor - Reynolds Number Evaluation

From Equation A-12a, the Reynolds number, Re, is given as the ratio of the inertial to the viscous forces, and is given dimensionally as

$$R_e = \frac{L\rho q}{\mu} \tag{8.1}$$

Friction factor, f, is given as the ratio of the dissipative forces to the inertial forces(78). If Equations A-23 and A-23a are each divided by the inertial term, the following expressions are obtained:

$$\frac{-\frac{dP}{dx}}{F_b \rho q^2} = \frac{(\mu/k)q}{F_b \rho q^2} + 1 + \frac{\gamma \rho^2 q^3}{F_b \rho q^2} \tag{8.2}$$

$$\frac{-\frac{dP}{dx}}{F_b \rho q^2} = \frac{(\mu/k)q}{F_b \rho q^2} + 1 \tag{8.3}$$

Multiplying Equations 8.2 and 8.3 by 64 and simplifying, the following equations are obtained:

$$\frac{64(-\frac{dP}{dx})}{F_b \rho q^2} = \frac{64}{\frac{F_b \rho q k}{\mu}} + 64 + \frac{64 \gamma \rho q}{F_b} \tag{8.4}$$

$$\frac{64(-\frac{dP}{dx})}{F_b \rho q^2} = \frac{64}{\frac{F_b \rho q k}{\mu}} + 64 \tag{8.5}$$

For simplification, let

$$f = \frac{64(-\frac{dP}{dx})}{F_b \rho q^2} = \frac{\text{Dissipative Forces}}{\text{Inertial Forces}} \tag{8.6a}$$

$$R_e = \frac{F_b \rho q k}{\mu} = \frac{\text{Inertial Forces}}{\text{Viscous Forces}} \tag{8.6b}$$

$$T_f = 64\left(\frac{\gamma \rho q}{F_b}\right) \tag{8.6c}$$

Also, let Tf be regarded as the turbulence factor which measures the increasing significance of the cubic term beyond the inertial term. Therefore substituting Equations 8-6a, 8.6b, and 8.6c into Equations 8.4 and 8.5, the following expressions are obtained respectively as:

$$f = \frac{64}{P_e} + 64 + T_f \tag{8.7}$$

$$f = \frac{64}{R_e} + 64 \tag{8.8}$$

Equation 8.8 is similar to the friction factor expression used by Mackett(79) for Forchheimer's quadratic equation. It differs from Equation 8.7 by the term Tf which is zero or negligible for the quadratic case, and a positive quantity for the Forchheimer's cubic case.

A log-log plot of friction factor, f, against the Reynolds number, Re, should give, from Equations 8.7 and 8.8:

a) a linear viscous plot at low Re, represented by $f = 64/Re$,

b) a deviation from linear viscous region due to the increasing inertial effects which corresponds to increases in Re. This is represented by $f = 64$.

c) an indication of any possible flow effects due higher Re beyond the inertial region. This is represented by $f = Tf$.

Similarly, Equation 4.12 is divided by its inertial term, (the quadratic term), and then multiplied through by 64 to get the following expression:

$$\frac{64(P_e^2 - P_w^2)}{C_2\bar{Z}\bar{T}Q_oF_b} = \frac{64}{\frac{F_bQ_ok_a}{\mu}\cdot\frac{C_2}{C_1}} + 64 + \frac{64C_3}{C_2}\cdot\frac{\gamma Q_o}{F_b} \qquad (8.9)$$

The product of the absolute gas permeability, k, and the inertial resistance coefficient, Fb, gives the length scale for the Reynolds number. Using the apparent gas permeability, ka, instead of the absolute gas permeability, k, gives a larger value of the length scale due to the gas slippage effect. For the purposes of the Reynolds number evaluation, the absolute gas permeability, k, is used. Therefore, Equation 8.9 is reduced to Equation 8.7, where

$$f = \frac{64(P_e^2 - P_w^2)}{C_2\bar{Z}\bar{T}Q_o^2F_b} \qquad (8.9a)$$

$$R_e = \frac{F_bQ_ok_a}{\mu} \cdot \frac{C_2}{C_1} \qquad (8.9b)$$

$$T_f = \frac{64C_3}{C_2} \cdot \frac{\gamma Q_o}{F_b} \qquad (8.9c)$$

Figure 8-18 shows the log-log plot of friction factor, f, against Reynolds number, Re, for Core Sample 1C, Run 3, in which f decreases initially with increasing Re, and later increases with increasing Re. This is expected from Equation 8.7 and therefore the plot of f against Re suggests an existence of some term beyond the visco-inertial flow regime.

8.8 Effect of Confining Pressure and Hysteresis

The object of running the experiments in both the forward and the reverse directions is to check for hysteresis. The general plot profiles are the same for both directions, but the estimated parameter values, as well as their trend with confining pressures, are significantly different in many cases.

The first runs of Core amples 4A and 1C in both directions, did not have any predefined CP. Their estimated

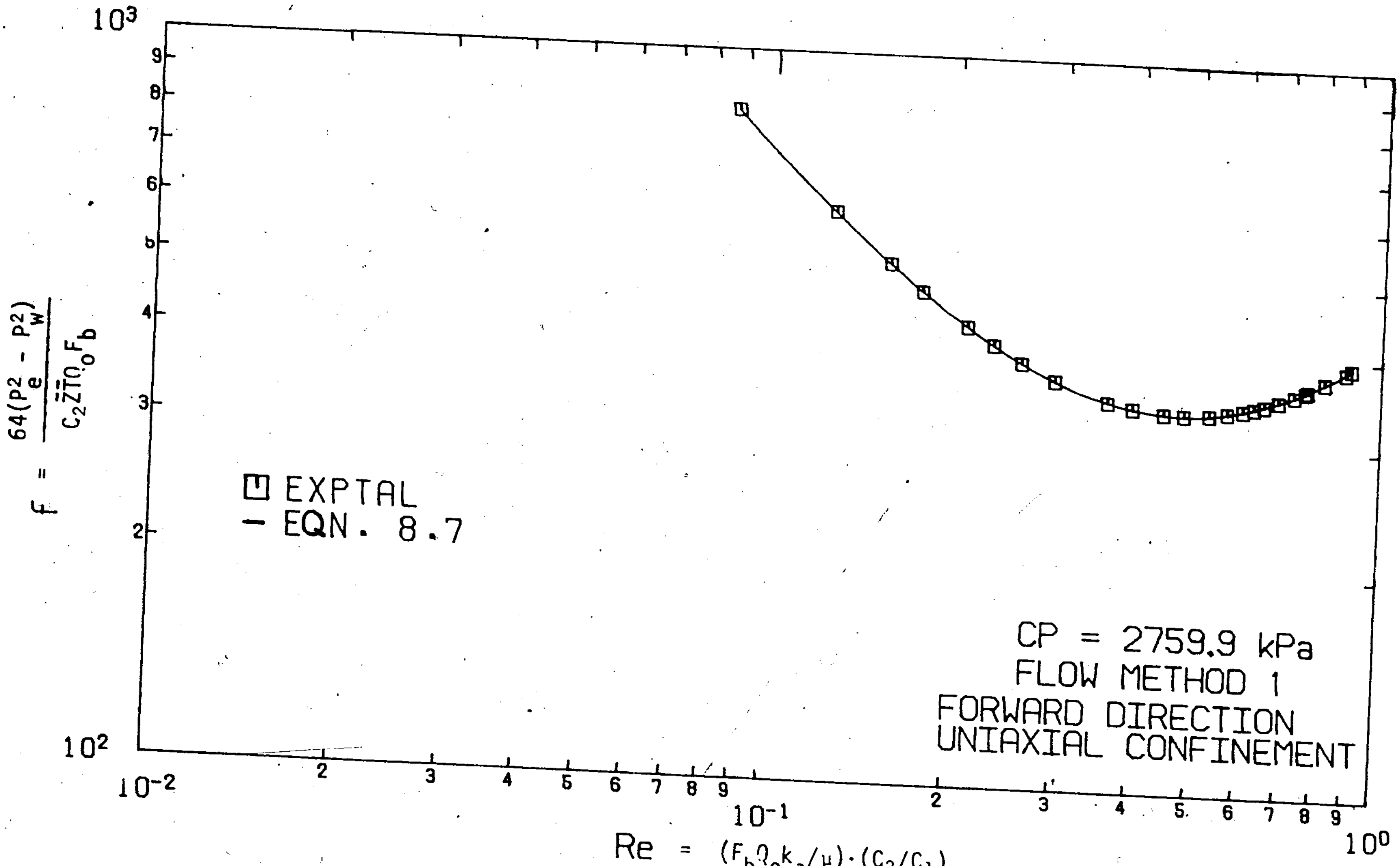

Figure 8-18 CORE 1C RUN 3 FRICTION FACTOR-RE PLOT

parameters are observed, from Tables 8-1 to 8-8, to be seemingly out of phase with those of the other runs. Though the parameter values are expected to show a continuous trend with increasing predefined CP, the parameter values of the first runs, in many cases, are larger than those of the second runs. From this observation, confinement pressure appears to exhibit a substantial effect on the flow behavior.

The following points are gathered from Figures 8-19 to 8-22, and from Tables 8-1 to 8-8, for Core 1C and Core 4A, using Flow Method 1:

1. Permeability,k, decreases in forward direction, but increases in reverse direction, with increasing confining pressure,CP. The values in the forward direction are higher than those obtained in the reverse direction.
2. Gas slippage coefficient,b, increases in the forward direction, but decreases in the reverse direction, with increasing CP.
3. Inertial coefficient,Fb, increases in both forward and reverse directions with CP.
4. Gamma increases in both forward and reverse directions with CP.

From Table 8-9, parameter values obtained in the forward direction for Core 2, under triaxial confinement, are significantly different from those obtained in the reverse direction.

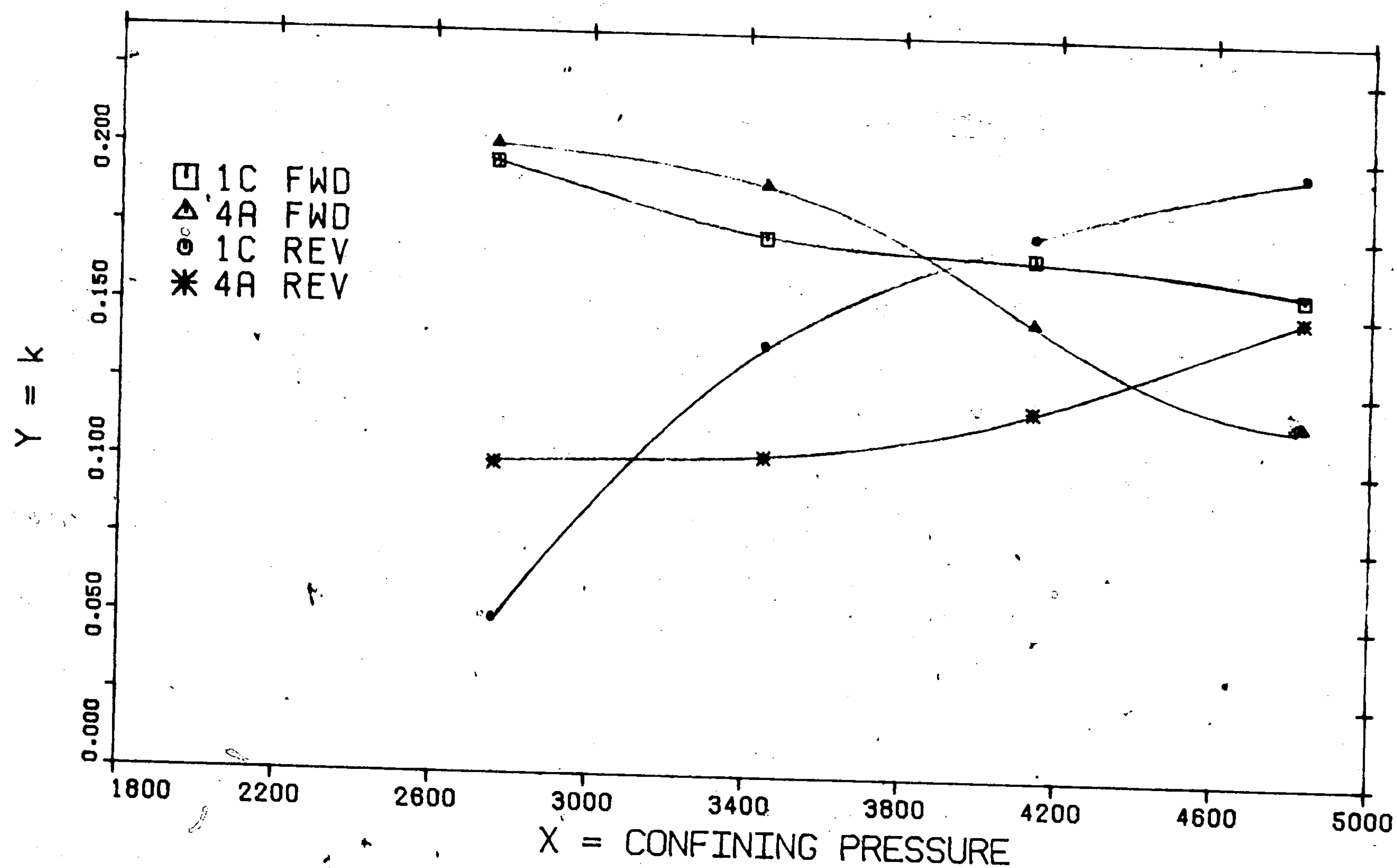

Figure 8-19 VARIATION OF k WITH CONFINING PRESSURE

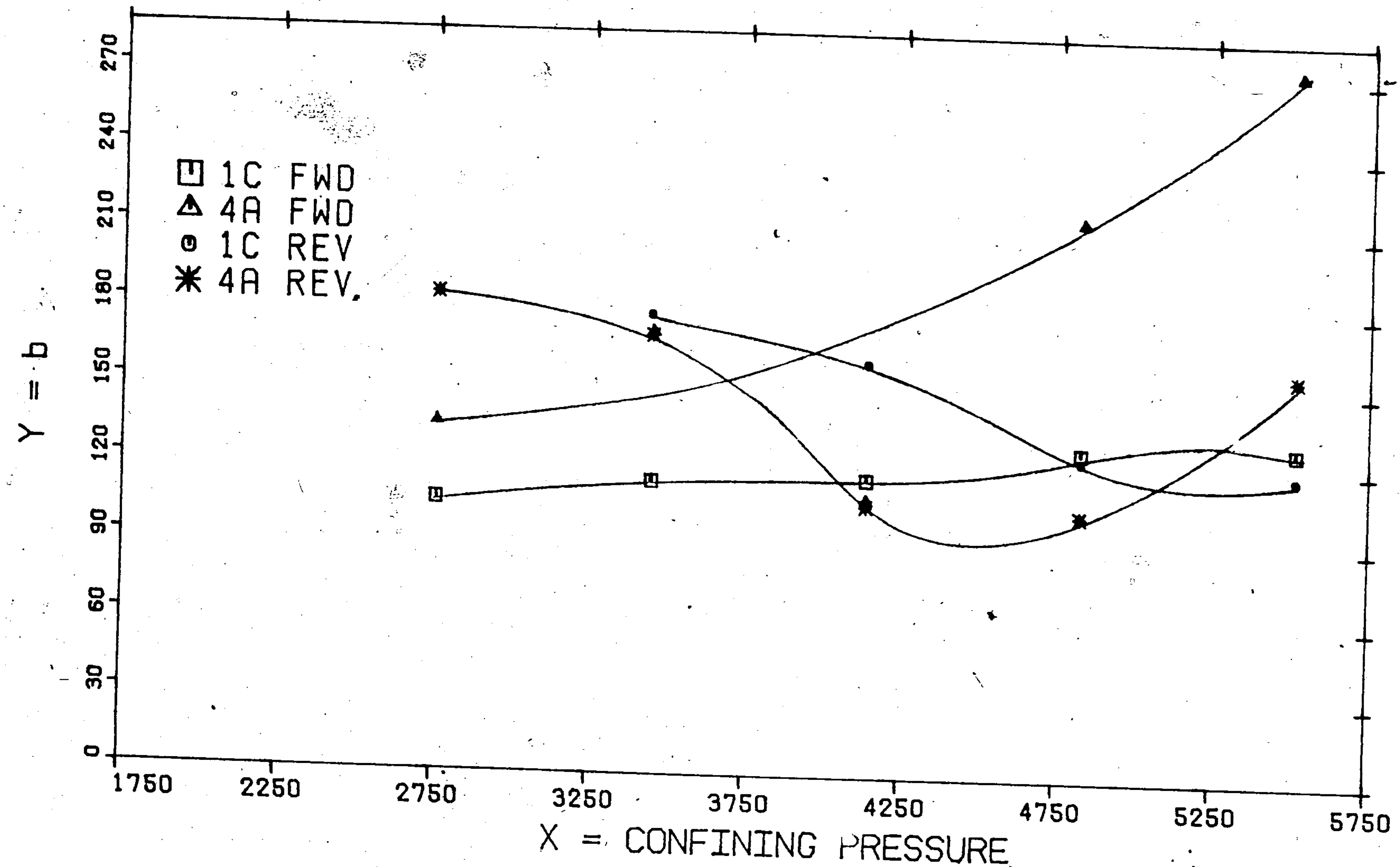

Figure 8-20 VARIATION OF b WITH CONFINING PRESSURE

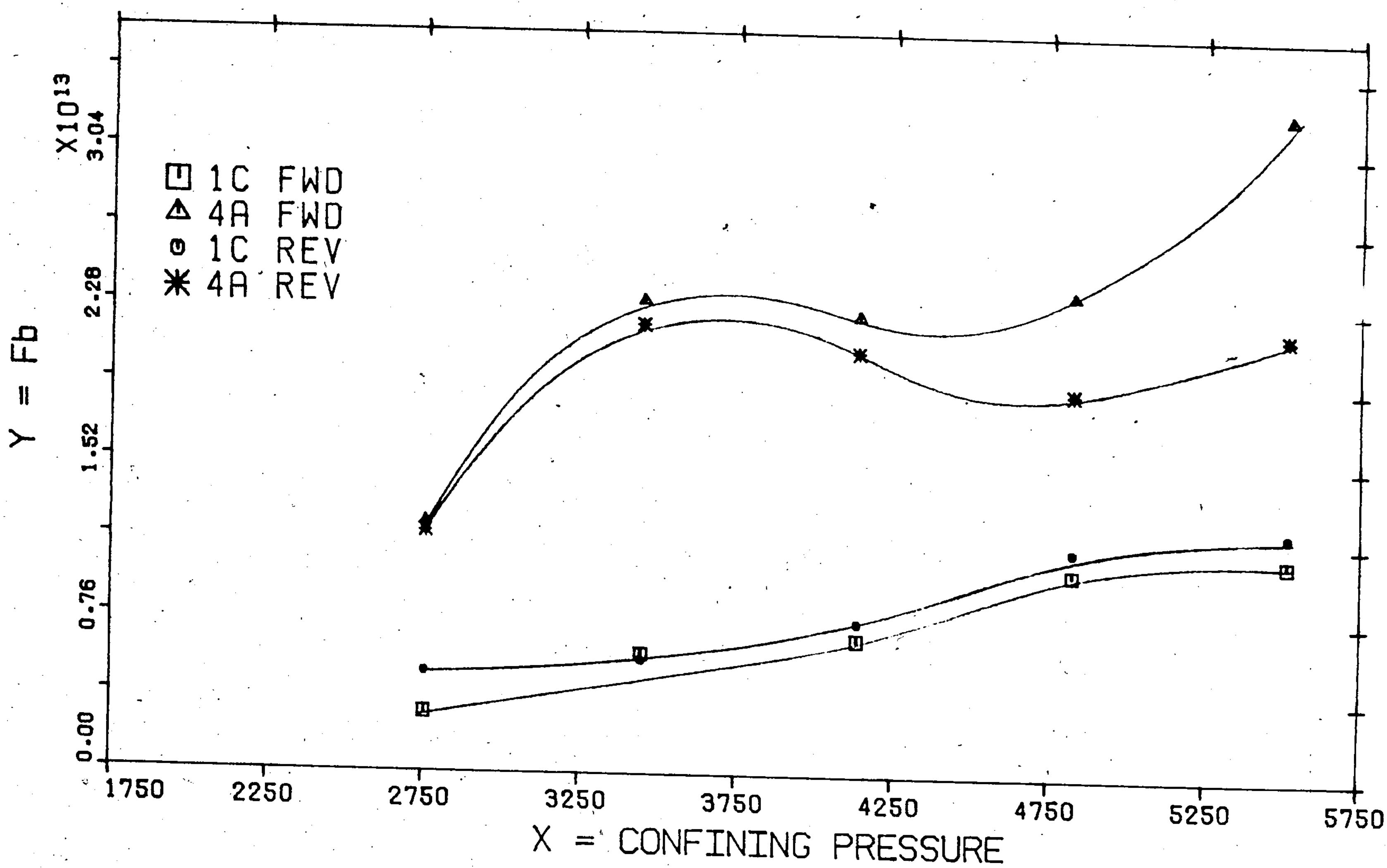

Figure 8-21 VARIATION OF Fb WITH CONFINING PRESSURE

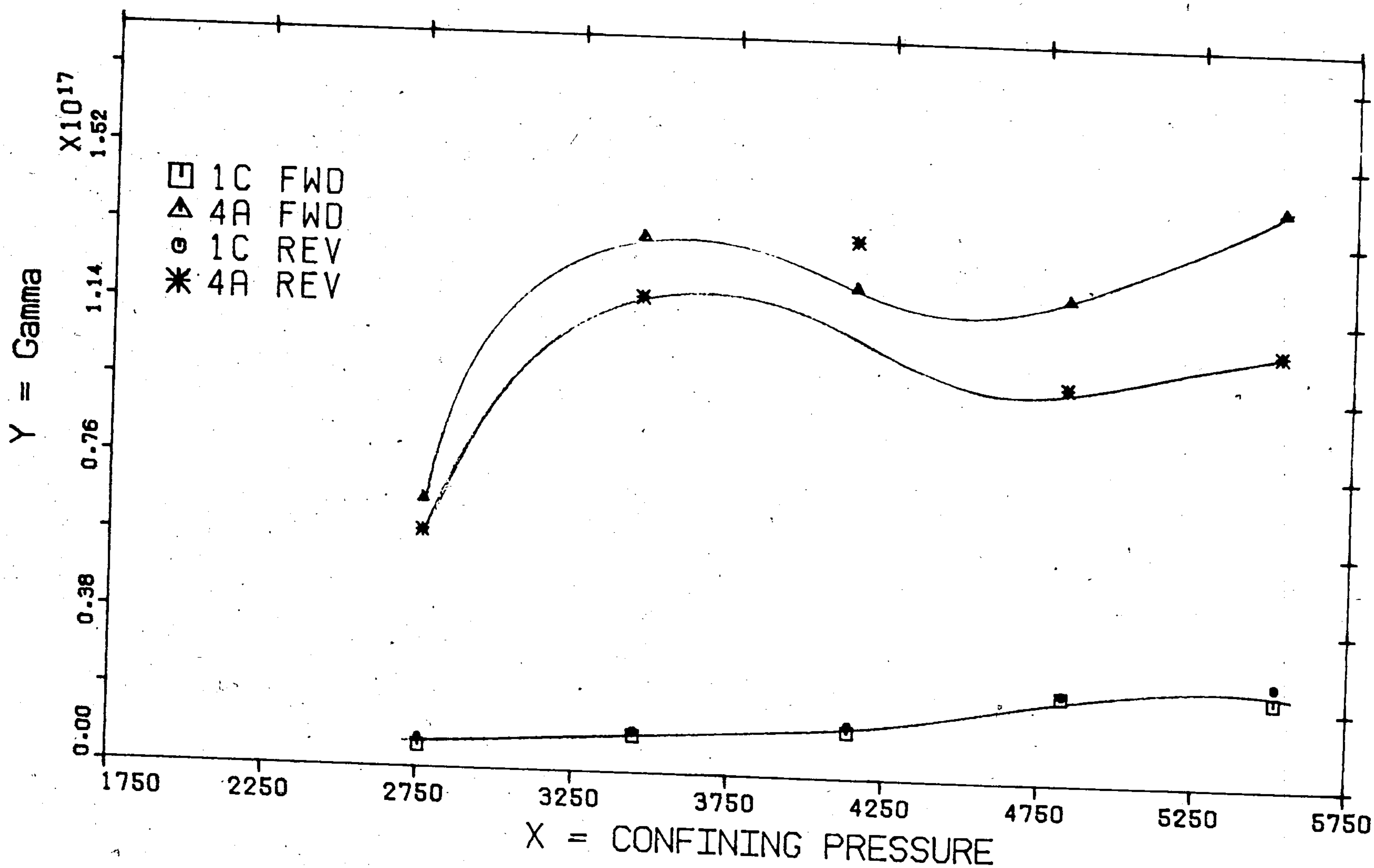

Figure 8-22 VARIATION OF GAMMA WITH CONFINING PRESSURE

The foregoing observations reflect a significant effect of hysteresis on the flow behavior especially on both permeability and gas slippage coefficient. Since confinement pressure affects compaction of the core sample, reorientation of the grains in the porous medium may take place, and could cause changes in permeability and porosity. Hence, conducting the flowing experiment in both forward and reverse directions could cause this change and, by deduction for gas flow, the gas slippage coefficient could also be affected.

8.9 Gamma Relationship with Other Parameters

From theory in Appendix A, and the parametric analysis in Section 8.7, gamma appears to have some relationship with the other parameters, and with viscosity. Hence, by dimensional analysis, and from Equations A-22c and A-22d, gamma can be related by:

$$\gamma = fn\,(\mu^c \phi^e k^d F_b^f b^g) \tag{8.10}$$

which reduces to:

$$\gamma = fn\,(\mu^c \phi^e k^d F_b^{2d}) \tag{8.11}$$

It is noticed that gas slippage coefficient, b, does not appear in Equation 8.11. This is not surprising because gamma manifests itself at higher flow rates and pressures, under which condition gas properties approximate to that of liquid.

Equation 8.11 can be represented in different forms, and used to fit the data from Tables 8-5 and 8-6 for a complete plot profile. The following forms are possible:

$$\gamma = a\mu^b(kF_b^2)^c \tag{8.12}$$

$$\gamma = a\mu^b k^c F_b^d \tag{8.13}$$

$$\gamma = a\mu^b k^c F_b^d \phi^e \tag{8.14}$$

$$\gamma = a\mu^b(kF_b^2)^c \phi^e \tag{8.15}$$

Table (8-10) gives a summary of the values of the coefficients, their accompanying error sum of squares and their standard deviations. The best fit is chosen therefrom.

Viscosity has been calculated at standard condition of pressure and temperature in order to obtain a reference viscosity value. Only nitrogen has been used.

The following observations are gathered from Table (8-10):

1. Fit 3 gives the best relationship of gamma with other parameters.

TABLE 8-10: VARIATION OF GAMMA WITH OTHER PARAMETERS

Fit	a	b	c	d	e	Xsqr	Stddev
1	1.5089 $\times 10^{-5}$	-0.8961	0.8961			0.3052	0.5403
2	1.8057 $\times 10^{-3}$	-1.6705	-0.4622	1.6705		0.2625	0.5006
3	4.7353 $\times 10^{9}$	-0.6980	-0.0527	0.6980	1.8014	0.0628	0.2446
4	6.5743 $\times 10^{7}$	-0.4257	0.4257		1.7594	0.1260	0.3468

2. The coefficient of the viscosity term, which is negative, bears a consistent relationship with that of the Fb term. This could depict a possible relationship between Fb and viscosity.
3. Porosity term exists and its coefficient is appreciable.
4. Gamma increases as Fb increases.
5. Both Fb and a constant quantity play a dominant role in the magnitude of gamma. This constant could be similar, or identical, to the dimensionless shape factor, C6, which was obtained in the derivation of gamma in Appendix A.
6. Both apparent gas permeability and viscosity have an inverse dependence on gamma.

Hence gamma is given from Fit 3 as

$$\gamma = 4.7353 \times 10^{9} \left(\frac{F_b}{\mu}\right)^{0.6980} \frac{\phi^{1.8014}}{k_a^{0.0527}} \tag{8.16}$$

At the flow condition under which gamma manifests itself, ka approximates to k, for decreasing gas slip. Hence, by replacing ka with k, Equation 8.16 becomes

$$\gamma = 4.7353 \times 10^{9} \left(\frac{F_b}{\mu}\right)^{0.6980} \frac{\phi^{1.8014}}{k^{0.0527}} \tag{8.17}$$

The variation of gamma, and fitted gamma, with apparent gas permeability, ka, is shown in Figure 8-23 on a log-log plot. The profile shows an inverse relationship of gamma with ka.

This analysis, together with the relationship obtained for gamma is limited in the sense that data for them came from very limited number of cores and for nitrogen only. The data used are comprised of both forward and reverse runs using Flow Method 1, and for different confining pressures. While this may not be conclusive, this analysis

1. shows an inverse relationship of gamma with permeability.
2. shows less dependence of gamma on gas slippage coefficient.
3. supplies a possible estimate of gamma in terms of the other parameters and viscosity.
4. shows some correspondence in the properties of gamma

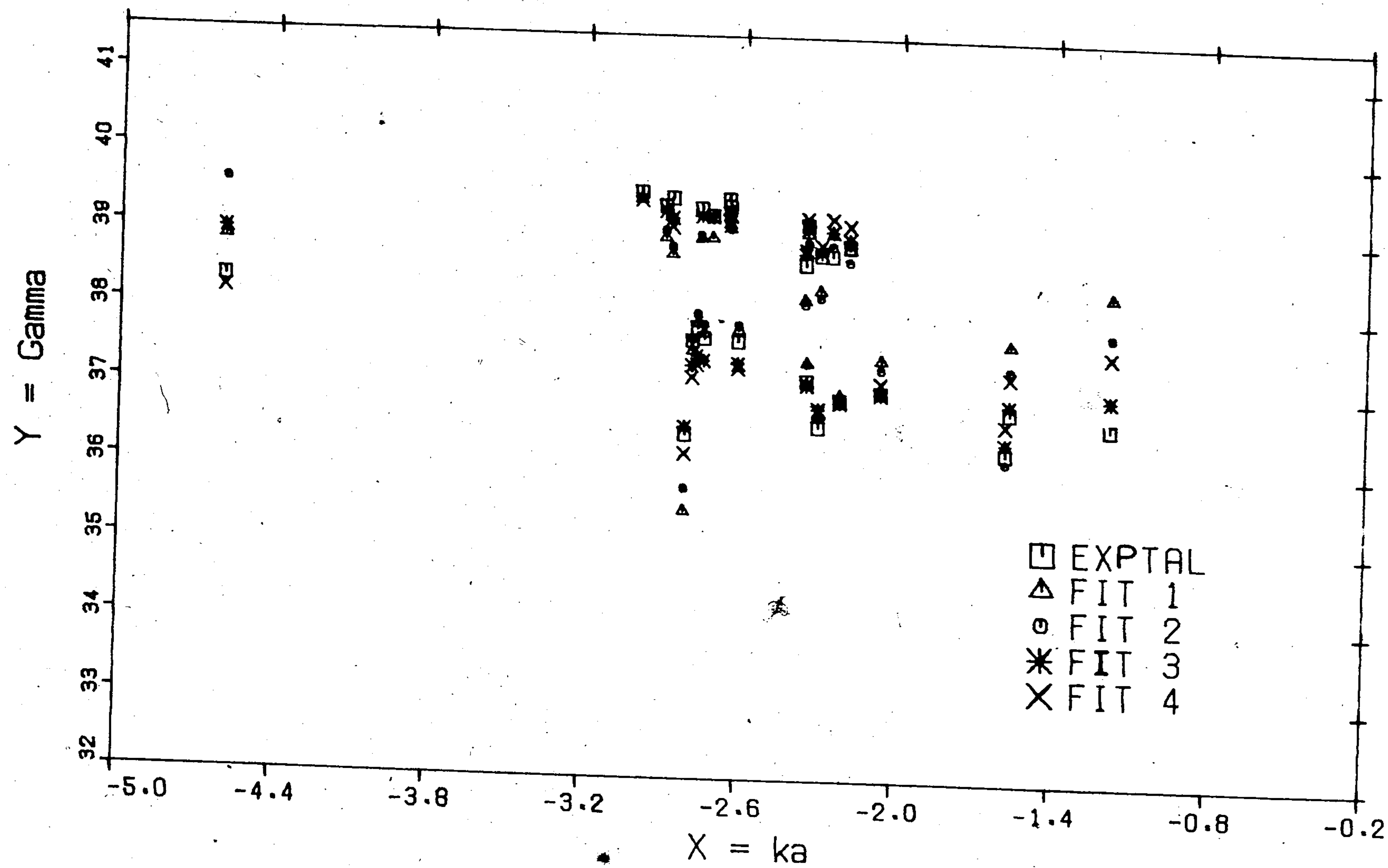

Figure 8-23 Variation of Gamma and Fitted Gamma with ka

between theory and experimental results.
Further investigation is needed to explain these findings.

8.10 Nomenclature for Gamma

The foregoing treatment has shown the possible existence of gamma. This parameter has been identified as being within the cubic term, which is beyond the visco-inertial region. The cubic term, as treated in this work, is synonymous with the turbulent term. Hence gamma should have the properties associated with the turbulent flow. Since gamma should be known with a name that reflects its characterics, it is suggested it be known as the 'turbulence resistance coefficient'.

9. CONCLUSION and RECOMMENDATIONS

9.1 CONCLUSIONS

There has been, generally, a good correspondence between theory and experimental results, especially in the properties of gamma - the flow parameter in the cubic term of the general cubic flow equation. Anomalous flow behavior was obtained when Flow Method 2 was used at lower pressures and on uniaxial radial confinement. Similar behavior was observed at considerably higher pressures when Flow Method 1 was used on triaxial radial confinement. It is believed that this behavior is dependent on the type of confinement and on the flow method used.

The following are the conclusions:

9.1.1 Flow Phenomena

1. A general cubic flow equation has been developed from consideration of kinetic energy equation of mean flow and dimensional relations. The physical basis of the cubic term in the model flow equation has been established by using the boundary layer theory to explain the flow phenomenon at higher flow rates and pressures through a porous path.
2. Gamma, the main parameter in this cubic term, is
   a. related to a characteristic dimensionless shape factor which is significant at higher flow rates.
   b. is inversely related to viscosity.

3. The flow model equation
   a. spans a wide range of flow rates,
   b. is regarded as a modification to Forchheimer's quadratic equation,
   c. has been modified, and corrected, for gas slippage effect.

9.1.2 Experimental Evidence

1. In comparison with the quadratic equation, and under uniaxial confinement, the cubic equation gave a better fit on the experimental data.
2. Both Fb and gamma have been observed to depend on the flow rate and the flow regime.
3. Gamma has less dependence on the slippage coeffient in the higher flow regime.
4. Gamma has an inverse relationship with permeability and viscosity.
5. The log-log plot of the friction factor against the Reynolds number suggests an existence of some term beyond the visco-inertial flow regime.
6. Relationship between gamma and other parameters has been obtained. Both Fb and a constant dimensionless quantity have a considerable effect on the magnitude of gamma.

9.1.3 The Flow Method

1. The flow method clearly has a very significant effect in the type of results obtained. The flow regime reached is

linked to the flow method used.

2. Flow Method 1 appears to be better suited for higher flow regimes, and Flow Method 2 seems more appropriate for lower regimes, especially for viscous and visco-inertial flow regimes.
3. Some relationship has been observed to exist between the horizontal stresses prevailing on the core material, and the flow method used. More pressure drawdown could be generated by using Flow Method 2 than by using Flow Method 1.

9.1.4 Confining Pressure and Hysteresis

1. The stress-strain analysis for uniaxial confining pressure has been used to describe the state of stress and strain on the core during the flowing process with success.
2. There is a noticeable difference between the parameter values obtained by imposing a predefined confining pressure,CP, and those obtained without any predefined CP.
3. Both the apparent and the absolute permeability, ka and k, are found to decrease with CP in the forward direction.
4. There is a noticeable increase of gamma and Fb with CP.
5. Gas slippage coefficient increases in the forward direction, but decreases in the reverse direction, with increasing CP. This may be due to compaction effect

which involves grain reorientation within the core material.

6. Hysteresis has been observed on the flowing experiments.

9.1.5 Plot Profiles and Parameter Estimation

1. The plot profiles seem to be comprised of points in the lower flow rates and pressures, and those in the higher flow rates and pressures.
2. A quadratic fit appears suitable for lower flow rates and pressures, while a cubic fit appears suitable for all the plot points, especially those which are obtained at higher flow rates and pressures.
3. The plot profiles obtained by using Flow Method 2 showed some anomalous behavior beyond the viscous region. This is believed to be due to the combined effect of confinement and flow method.
4. The estimated parameter values from all the estimation methods are generally close for the truncated plot points. The numerical method seems superior to the graphical and linear fit methods.
5. The choice of gas slippage coefficient, b, affects not only the corrected gas permeability value, on the graphical method of parameter estimation, but also the value of the corrected Fb so obtained. The use of the linear correlation coefficient has increased the accuracy of the estimated value of b.
6. Under triaxial confinement, anomalous plot profiles were

noticed at considerably higher pressures with Flow Method 1. Normal behavior, for lower flow rates and pressures, was obtained with Flow Method 2. It is believed that the loose rubber overburden sleeve could not effect complete confinement at higher pressures.

9.2 RECOMMENDATIONS

The recommendations and suggestions for further research are presented below:

1. More investigation is needed on the flow phenomena involving the higher flow rates and pressures so as to
   a. check the concept of a third order term in the flow equation,
   b. discretize the flow regimes encountered,
   c. examine the properties of gamma, and its relationship with other parameters.
   d. check the friction factor-Reynolds number criterion.
2. There is need for more investigation on the effect of hysteresis on flow behavior.
3. The flow methods have to be applied to more radial flow experiments to ascertain their particular roles in
   a. the flow regimes,
   b. confining pressure effects,
   c. possible hysteresis effect.

   Excessive drawdown pressures should not be used while using Flow Method 2.
4. The stress-strain analysis should be made prior to using

any type of radial cell.

5. Numerical methods involving iterative procedures should be explored in addition to those with direct procedures.
6. The loose rubber overburden sleeve, on the radial triaxial overburden cell, should be replaced by one which fits more closely.
7. Further investigation should be made with triaxial overburden radial cell in order to study, and compare, the observations obtained with uniaxial confinement radial cell.
8. The radial cell should be designed so that runs can be made using both uniaxial and triaxial confinement on the same core. This is expected to aid comparison between the two methods of confinement.
9. The use of the average pressures in radial systems should be explored in preference to the use of the mean pressure.

CITED REFERENCES

1. Piplapure, A.R., Steady Radial Gas Flow Through Porous Media , M.Sc. Thesis in Petroleum Engineering, University of Alberta, Edmonton (1970).
2. Senturk Y., Effect of Confinement Pressure On Visco-Inertial Flow Parameters In Porous Media, M.Sc. Thesis in Petroleum Engineering, University of Alberta, Edmonton (1975).
3. Hubbert, M.K., "Darcy's Law and the Field Equations of the Flow of Underground Fluids", Trans., A.I.M.E., vol 207, 222-239 (1956) p.222
4. Darcy, H., "Les Fontaines Publiques de la Ville de Dijon", Victor Dalmont, Paris(1856).
5. Hall, W.A., "An Analytical Derivation of the Darcy's Law", Trans. Amer. Geophysical Union, vol 37, 185-188, (1956), p.188
6. Hubbert, M.K., loc. cit.
7. Hubbert, M.K.: "The Theory of Ground-Water Motion", Jour. Geol., vol 48, p 785. (1940)
8. Irmay, S., "On the Theoretical Derivation of Darcy and Forchheimer Formulas", Trans. Amer. Geophysical Union, vol. 39, 702-706, (1958) p.705
9. Scheidegger, A.E., The Physics of Flow Through Porous Media , 3rd Ed., University of Toronto press (1974)
10. Klinkenberg, L.J., "The Permeability of Porous Media to Liquids and Gases", API, Drill. and Prod. Prac., p.200 (1941).

11. Calhoun, J.C.Jr., and Yuster, S.T., "A Study of The Flow of Homogeneous Fluids Through Ideal Porous Media", Drilling and Prod. Practice, p.335 (1946)

12. Yuster, S.T., "Homogeneous Permeability Determination", Drilling and Prod. Practice A.P.I., p.356 (1946)

13. Rose, W.A., "Permeability and Gas-Slippage Phenomena", Drill. and Prod. Pract, A.P.I., p.209 (1948)

14. Heid, J.G. McMahon, J.J. Nielsen, R.F. and Yuster, S.T.: "Study of The Permeability of Rocks to Homogeneous Fluids", Drill. and Prod. Pract., 230-246 (1950) p.238

15. Dranchuk, P.M., and Sadiq, S., "The Intepretation of Permeability Measurements", Jour. Can. Pet. Tech., p.130 (July-September, 1965)

16. Jones, S.C.: "A Rapid Accurate Unsteady-State Klinkenberg Permeameter", S.P.E.Jour., 383-397 (Oct.1972) p.390

17. Casse, F.J., and Ramey, H.J.Jr.: "The Effect of Temperature and Confining Pressure on Single-Phase Flow in Consolidated Rocks", Jour. Pet. Tech., 1051-1059 (Aug. 1979) p.1057

18. Al-Hussainy, R., Ramey, H.J.Jr., and Crawford, P.B., "The Flow of Real Gases Through Porous Media", Jour. Pet. Tech., , p.624 (May, 1966).

19. Mackett, R.A.: Viscous and Visco-Inertial Gas Flow in Limestone Cores, M.Sc. Thesis in Petroleum Engineering, University of Alberta, Edmonton, (November, 1966)

20. Fancher, G.H. and Lewis, J.A., "Flow of Simple Fluids

Through Porous Materials",Ind. Eng. Chem., vol 25, p.1139 (1933).

21. Elenbaas,J.R. and Katz,D.L.,"A Radial Turbulent Flow Formula",Trans., A.I.M.E., vol 174, p.25 (1948).

22. Cornell,D., and Katz,D.L.,"Pressure Gradients In Natural Gas Reservoirs",Trans., A.I.M.E., vol 195, p.61 (1953)

23. Hubbert,M.K.,op. cit. p.227.

24. Houpert,A.,"On The Flow of Gases in Porous Media",Revue de L'Institut Francais du Petrole, XIV(11), p.1468 (1959)

25. Wright,D.E.,"Non-linear Flow Through Granular Media", J. Hydraul. Div. Amer. Soc. Civ. Eng. Proceedings, vol. 94 (HY4), p.851 (1968).

26. Hubbert,M.K.,op. cit.p.230.

27. Linquist,E.:Proc. 1st Congr. Grands Barr. Stockholm, vol 5, 81, (1933) (As quoted by Reference 9)

28. King, G.:Z. Ver. deuts. Ing. 84, 85 (1940) (As quoted by Reference 9)

29. Collins,R.E.:Flow of Fluids Through Porous Materials, 3rd Ed., University of Toronto Press, (1974), p.51

30. Scheidegger,A.E., op. cit.pp.155-160.

31. Forchheimer,P.:"Wasserbewegung durch Boden",Z. Ver. Deutsch Ing., vol.45, 1782-1788, (1901)

32. Green,L.Jr. and Duwez,P.,"Fluid Flow Through Porous Metals", Trans. ASME J. Appl. Mech, vol 18, p.39, (1951)

33. Kolada,L.J.:Steady Linear Gas Flow Through Porous Media, M.Sc. Thesis in Petroleum Engineering, University of

Alberta, Edmonton, (1968)

34. Senturk,Y. op. cit. p.55.

35. Irmay,S. loc. cit.

36. Scheidegger,A.E., loc. cit.

37. Basak,P, and Soni,J.P.:"Critical Reappraisal of Forchheimer's Relation",Indian Geotech. Jour., vol 7, no 4, p.298 (Oct. 1977)

38. Firoozabadi,A.,Katz,D.L.,"An Analysis of High-Velocity Gas Flow Through Porous Media",Jour. Pet. Tech., 211-216, (Feb., 1979).

39. Elenbaas,J.R. and Katz,D.L., op. cit. p.35

40. Green,L.Jr. and Duwez,P., loc.cit.

41. Cornell,D. and Katz,D.L., op. cit. p.62

42. Tek,M.R., Coats,K.H., and Katz,D.L.:"The Effect of Turbulence on Flow of Natural Gas Through Porous Reservoirs",Jour. Pet. Tech., 799-806 (July, 1962) p.801

43. Crafton,J.W.:Investigations For Equations of Radial Turbulent Gas Flow, M.Eng. Thesis in Petroleum Engineering, University of Oklahoma, U.S.A. (1966)

44. Piplapure,A.R., loc. cit.

45. Cornell,D., and Katz,D.L., loc. cit.

46. Dranchuk,P.M. and Sadiq,S. loc. cit.

47. Hamilton,R.J.:A Study of Linear Steady State Gas Flow Through Consolidated Porous Media, M.Sc. Thesis in Petroleum Engineering, University of Alberta, (Feb.1963)

48. Sadiq,S.:The Inertial Resistance Coefficient and Other Reservior Rock Properties, M.Sc. Thesis in Petroleum

Engineering ,University of Alberta, Edmonton (Jan.1965)

49. Dranchuk,P.M. and Kolada,L.J.:"Interpretation of Steady Linear Visco-Inertial Gas Flow Data",J. Can. Pet. Tech., vol 7 no 1 36-40 (1968)

50. Piplapure,A.R., loc. cit.

51. Dranchuk,P.M. and Piplapure,A.R.:"Inertial and Slip Effects in Steady-State Radial Gas Flow Through Porous Media",Jour. Pet. Tech. A.I.M.E., 1155-1156 (Oct.1973).

52. Kolada,L.J.: op. cit. pp.18-19.

53. Cornell,D.:Flow of Gases Through Consolidated Porous Media, Ph.D. Thesis, University of Michigan, Ann Arbor, Michigan (1952).

54. Piplapure,A.R., op. cit. pp.42-44

55. Senturk,Y. op. cit. pp.66-67

56. Piplapure,A.R., op. cit. p. D-18

57. Senturk,Y. op. cit. p.221.

58. ibid. p.181

59. Seely,F.B. and Smith,J.O.:Advanced Mechanics of Materials , 2nd Ed. (1952) John Wiley & Sons Inc, New York, U.S.A.

60. Popov,E.P.:Mechanics of Materials, 2nd Ed. (1976) Prentice Hall Inc. New Jersey, U.S.A.

61. Jaeger,J.C.:Elasticity, Fracture and Flow, Science Paperback Reprint 1978, Chapman & Hall, London.

62. Birch,F.,Schairer,J.F.,Spicer,H.C.:Handbook of Physical Constants, Geological Society of America, Special Papers, vol 36, (Jan. 1942) p.76

63. Harrison,E., Kieschnick Jr,W.F. and McGuire,W.J.:"The Mechanics of Fracture Induction and Extension",Trans. A.I.M.E., vol 201, 252-263, (1954) p.255

64. Haimson,B.C. and Tharp,T.M.:"Stresses Around Boreholes in Bilinear Elastic Rock",Soc. Pet. Eng. Jour., 145-151, (April,1974) p.150

65. Scott,Jr.P.P.,Bearden W.G.,Howard G.C.:"Rock Rupture as Affected by Fluid Properties",Trans. A.I.M.E., vol 198, pp.111-124 (1953) p.114

66. Seely,F.B. and Smith,J.O., op. cit. p.296

67. Brant,H:"A Study of Speed of Sound in Porous Granular Media", Trans. ASME, J. Appl. Math. vol.77 pp.479-486 (1955)

68. Fatt.I.,"Pore Compressibilities of Sandstone Reservoir Rocks", Trans. A.I.M.E., vol 213 pp.362-364 (Mar.1958)

69. Senturk,Y. op. cit. pp. 30-32.

70. Hilsenrath,J. et al:Tables of Thermal Properties of Gases , Table 7-1, U.S. Dept. of Commerce, National Bureau of Standards, Circular no 564, (1955)

71. Kestin J. and Wang H.E.:"The Viscosity of Five Gases : A Re-evaluation", Trans. ASME, vol.80 pp.11-17, (Jan.1958)

72. Fatt,I.:"Reduction in Permeability with Overburden Pressure", Trans. A.I.M.E., vol.195, Technical Note, no 147, p 329, (1952)

73. Senturk,Y. op. cit. p.74.

74. ibid. p.161.

75. Irmay,S. loc.cit

76. Senturk,Y. op. cit. p.57.

77. Crafton,J.W.:loc. cit.

78. Green,L.Jr. and Duwez,P., loc.cit. p.40

79. Mackett,R.A.:op. cit. p.25.

80. Hughes,W.F. and Gaylord,E.W.:Basic Equations of Engineering Science, Schaum's Series, McGraw-Hill, New York, (1964) p.24.

81. Bird,R.B.,Stewart,W.E., and Lightfoot,E.N.:Transport Phenomena, John Wiley, N.Y. (1960) p.5.

82. Tennekes,H. and Lumley,J.L.:A First Course in Turbulence, M.I.T. Press, Cambridge, U.S.A. (1977) p.28.

83. Schlichting,H.:Boundary Layer Theory, McGraw-Hill N.Y. (1979) p.558.

84. Raudkivi,A.J. and Callender,R.A.:Advanced Fluid Mechanics-An Introduction, John Wiley & Sons N.Y. (1975) pp.142-144.

85. Schlichting,H. op.cit. p.13.

86. Hubbert,M.K. op. cit. pp.229-230

87. Monin,A.S. and Yaglom,A.M.:Statistical Fluid Mechanics: Mechanics of Turbulence vol.i, M.I.T. Press, Cambridge, U.S.A., (1971) pp.38-41.

88. Tennekes,H. and Lumley,J.L. op. cit. p.60.

89. Hubbert,M.K. op. cit. p.226.

90. Muskat,M.:Flow of Homogeneous Fluids Through Porous Media , (1st Ed.,2nd printing, 1946) J.W.Edwards,Inc. Ann Arbor, Michigan, U.S.A. p.57.

91. Schlichting,H. op.cit. pp 25-44.

92. Monin,A.S. and Yaglom,A.M. op. cit. p.43.

93. Bevington P.R.:Data Reduction and Error Analysis For the Physical Sciences, McGraw-Hill, New York (1969)

94. Draper N.R. and Smith H.:Applied Regression Analysis, John Wiley & Sons, New York (1967)

95. Forsythe G.E. and Moler C.B.:Computer Solution of Linear Algebraic Systems, Prentice-Hall Inc, Englewood Cliffs, N.J. (1967) pp.82-86.

96. Gerald C.F.:Applied Numerical Analysis, Addison-Wesley Publishing Co. Reading Mass. U.S.A. (1978) p.471

UNCITED BIBLIOGRAPHY

Blick, E.F., "Capillary-Orifice Model for High-Speed Flow Through Porous Media", Ind. and Eng. Chem., Process Design and Development, vol 5, no 1, 90-94 (Jan 1966)

Chwyl, E.: An Analysis of Transient Gas Flow Through Porous Media, M.Sc. Thesis in Petroleum Engineering, University of Alberta, Edmonton (1968)

Dake, L.P.: Fundamentals of Reservior Engineering, Elsevier Scientic Publishing Co. Amsterdam (1978).

Dranchuk, P.M.: Fluid Mechanics of Natural Gas Production, Graduate Lecture Notes, 1978, Department of Mineral Engineering, University of Alberta, Edmonton, Alberta.

Energy Resources Conservation Board (E.R.C.B.): GAS WELL TESTING, Theory and Practice, Alberta (1979 Metric ed.)

Flores, J.: Steady and Transient Radial Gas Flow, Ph.D. Thesis in Petroleum Engineering, University of Alberta, Edmonton (May, 1973).

Geertsma, J., "Estimating The Coefficient of Inertial Resistance in Fluid Flow Through Porous Media", Soc. Pet. Eng. Jour., vol, 14, 445-450 (October 1974)

Katz, D.L. et al: Handbook of Natural Gas Engineering, McGraw-Hill Book Co, New York, (1959).

McFarland, J.D.: Transition to Turbulence in Porous Media, M.Sc. Thesis in Petroleum Engineering, University of Alberta, Edmonton (Oct. 1974) p.54.

Muskat, M.: Physical Principles of Oil Production, McGraw-Hill Book Co., New York, (1949) Rajaratnam,N., and Parker,G.:Engineering Fluid Mechanics, Graduate Lecture Notes, 1979, Department of Civil Engineering, University of Alberta, Edmonton, Alberta.

Rowan,G., and Clegg,M.W.:"An Approximate Method for Non-Darcy [illegible] Gas Flow", Soc. Pet. Eng. Jour., 96-114, [illegible]

Tek,M.R., [illegible] of a Generalized Darcy Equation", Trans. A.I.M.E., vol. 210, 376-378 (1957)

Wilhelmi,B and Somerton,W.H.:"Simultaneous Measurement of Pore and Elastic Properties of Rocks Under Triaxial Stress Conditions", Soc. Pet. Eng. Jour., 283-294, (Sept.1967)

APPENDIX A

DERIVATION OF SECOND AND THIRD ORDER EQUATIONS OF FORCHHEIMER

A. APPENDIX A - DERIVATION OF SECOND AND THIRD ORDER EQUATIONS OF FORCHHEIMER

The general Navier-Stokes equations of motion of viscous fluid for incompressible fluid is given in cartesian tensor notation(79) as

$$\rho \frac{\partial u_j}{\partial t} + \partial u_i \frac{\partial u_j}{\partial x_i} = - \frac{\partial P}{\partial x_j} + \mu \frac{\partial^2 u_j}{\partial x_i \partial x_i} + \rho X_j \quad \text{(A-1)}$$

where Einstein summation convention is used for i,j = 1, 3, in horizontal and vertical directions respectively. The term, X, represents body or gravitational forces. Both density and viscosity are assumed to be constant.

For steady-state, horizontal flow Equations A-1 become

$$\rho u_i \frac{\partial u_j}{\partial x_i} = - \frac{\partial P}{\partial x_j} + \mu \frac{\partial^2 u_j}{\partial x_i \partial x_i} \quad \text{(A-2)}$$

These equations comprise of inertial term on the left, and differential pressure gradient and viscous terms on the right. For flow along a capillary tube, and assuming a no-slip condition at the fluid-solid interface, Newton's law of viscosity is given by

$$\tau = - \mu \frac{\partial u_j}{\partial x_i} \quad \text{(A-3)}$$

where the viscous momentum is in the direction of the negative velocity gradient(80).

Equations A-2 can be rearranged in the form of

$$-\frac{\partial P}{\partial x_j} = \rho U_i \frac{\partial u_j}{\partial x_i} + \mu \frac{\partial^2 u_j}{\partial x_i \partial x_i} \qquad \text{(A-4)}$$

Since the continuity equation for steady state, incompressible flow is given as

$$\frac{\partial u_i}{\partial x_i} = 0 \qquad \text{(A-4a)}$$

the following expansion can be made

$$\frac{\partial u_i u_j}{\partial x_j} = u_i \frac{\partial u_j}{\partial x_i} + u_j \frac{\partial u_i}{\partial x_i} \qquad \text{(A-4b)}$$

Subsequently Equations A-4 become

$$-\frac{\partial P}{\partial x_j} = \rho \frac{\partial u_i u_j}{\partial x_i} + u_j \frac{\partial^2 u_j}{\partial x_i \partial x_i} \qquad \text{(A-5)}$$

A.1 Reynolds Equations

As velocity increases, local irregularities in flow streamlines begin to form and manifest themselves as fluctuations. Within a critical velocity range, which is characteristic of the medium through which the fluid is flowing, the produced fluctuations may be negligible. With higher velocities, these may no longer be negligible and Navier-Stokes equations are rewritten to reflect this new condition.

Fluctuation may be defined(81,82) as the difference between the measured field values of the measurable quantity and their time-averaged values. Its presence manifests itself in an apparent increase in the viscosity of the fundamental flow. It can be related as:

Observed Value = Mean Value + Fluctuation

Specifically, for velocity components and pressure, the relations are:

$$u_i = \overline{u}_i + u_i' \qquad P = \overline{P} + p' \tag{A-6}$$

Time-averaged, or mean, values are taken at a fixed point in space over an interval of time such that steady state condition is achieved. By definition, this is represented as

$$\overline{u}_i = \lim_{T\to\infty} \frac{1}{T} \int_{t_o}^{t_o+T} u_i\,dt \tag{A-6a}$$

and by deduction, the mean of the fluctuations is zero:

$$\overline{u_i'} = \lim_{T\to\infty} \frac{1}{T} \int_{t_o}^{t_o+T} (u_i - \overline{u}_i)\,dt = 0 \tag{A-6b}$$

From the law of averages, the product of both the mean value and its generated fluctuations is zero. Consequently, the process of averaging products is related by

$$\overline{u_i u_j} = \overline{(\bar{u}_i + u'_i)(\bar{u}_j + u_j)} = \bar{u}_i \bar{u}_j + \overline{u'_i u'_j} \qquad \text{(A-6c)}$$

If $\overline{u'_i u'_j} = 0$, velocity fluctuations are not correlated and destructive combination takes place. This eventually brings fluctuations down to a minimum. If this term is non-zero, they are said to be correlated and will combine constructively to form an additional stress which acts against the smooth laminar flow of the mainstream. It is negative in sign.

Applying the averaging operation on Navier-Stokes Equations A-1, yields the Reynolds equations:

$$\rho \frac{\partial \bar{u}_j}{\partial x_i} + \rho \bar{u}_i \frac{\partial \bar{u}_j}{\partial x_i} = \frac{\partial \bar{P}}{\partial x_i} + \mu \frac{\partial^2 \bar{u}_j}{\partial x_i \partial x_i} + \rho X_j + \frac{\partial}{\partial x_i}\left(-\rho \overline{u'_i u'_j}\right) \qquad \text{(A-7)}$$

where $\tau_{ij} = -\overline{\rho u'_i u'_j}$

= Reynolds stress tensor due to increased fluctuations. It contains nine components in 3-dimensional cartesian coordinates as shown

$$\begin{vmatrix} \sigma_{xx} & \tau_{xy} & \tau_{xz} \\ \tau_{xy} & \sigma_{yy} & \tau_{yz} \\ \tau_{xz} & \tau_{yz} & \sigma_{zz} \end{vmatrix} = \begin{vmatrix} \rho\overline{u'^2_{xx}} & \rho\overline{u'_x u'_y} & \rho\overline{u'_x u'_y} \\ \rho\overline{u'_x u'_y} & \rho\overline{u'^2_{yy}} & \rho\overline{u'_y u'_z} \\ \rho\overline{u'_x u'_z} & \rho\overline{u'_y u'_z} & \rho\overline{u'^2_{zz}} \end{vmatrix} \qquad \text{(A-7a)}$$

The diagonal components are the normal stresses while the off-diagonal components are the shear stresses.

The addition of the Reynolds stresses on Reynolds equations differentiates them from the Navier-Stokes equations. For steady st.te horizontal flow they become

$$-\frac{\partial \bar{P}}{\partial x_j} = \mu \frac{\partial^2 \bar{u}_j}{\partial x_i \partial x_i} + \rho \bar{u}_i \frac{\partial \bar{u}_j}{\partial x_i} + \frac{\partial}{\partial x_i}\left(\rho \overline{u_i' u_j'}\right) \qquad \text{(A-8)}$$

A.2 Kinetic Energy of Mean Flow

Since the mean momentum of the fluctuations, by Equations A-6b is zero, the effect on mean flow of increasing velocity may best be treated as its effects on kinetic and turbulent energy equations(83).
Cross-multiplying the Reynolds equations with the mean veolcity yields

$$\frac{\partial}{\partial t}\left(\frac{\rho \bar{u}_j \bar{u}_j}{2}\right) + \bar{u}_i \frac{\partial}{\partial x_i}\left(\frac{\rho \bar{u}_j \bar{u}_j}{2}\right) = \rho \bar{u}_j X_j - \frac{\partial}{\partial x_j}(\bar{P}\bar{u}_j)$$
$$+ \mu \bar{u}_j \frac{\partial^2 \bar{u}_j}{\partial x_i \partial x_i} + \bar{u}_j \frac{\partial}{\partial x_i}\left(-\rho \overline{u_j' u_j'}\right) \qquad \text{(A-9)}$$

where, from continuity equations (A-4a), the following relationships have been obtained:

$$\frac{\partial}{\partial x_j}\left(\frac{\rho \bar{u}_i \bar{u}_i \bar{u}_j}{2}\right) = \bar{u}_i \frac{\partial}{\partial x_i}\left(\frac{\rho \bar{u}_i \bar{u}_i}{2}\right) + \left(\frac{\rho \bar{u}_i \bar{u}_i}{2}\right)\frac{\partial \bar{u}_i}{\partial x_i} = \bar{u}_i \frac{\partial}{\partial x_i}\left(\frac{\rho \bar{u}_i \bar{u}_i}{2}\right) \qquad \text{(A-9a)}$$

$$\frac{\partial}{\partial x_j}\left(\bar{P}\bar{u}_j\right) = \bar{u}_j \frac{\partial P}{\partial x_j} + \bar{P}\frac{\partial \bar{u}_j}{\partial x_j} = \bar{u}_j \frac{\partial \bar{P}}{\partial x_j} \qquad \text{(A-9b)}$$

For steady state, horizontal flow, Equations A-9 become

$$\frac{\partial}{\partial x_i}\left(\frac{\rho \bar{u}_i \bar{u}_j \bar{u}_j}{2}\right) = -\bar{u}_j \frac{\partial \bar{P}}{\partial x_j} + \mu \bar{u}_j \frac{\partial^2 \bar{u}_j}{\partial x_i \partial x_i} + \bar{u}_j \frac{\partial}{\partial x_i}\left(-\rho \overline{u_i' u_j'}\right) \qquad \text{(A-10)}$$

(i) (i) (ii) (iii)

where

(i) = Rate of change of kinetic energy + Rate at which work is done by the mean pressure;

(ii) = Rate at which work is done by viscous forces;
= Work done on mean flow by mean viscous stress;

(iii) = Rate at which work is done on mean flow by Reynolds stresses.

If Equation A-7 is cross-multiplied by Equation A-6, an equation for the total kinetic energy is obtained. The difference between this equation and Equation A-9 gives the turbulent kinetic energy equation:

$$\frac{\partial}{\partial t}\left(\frac{\rho \overline{u_i' u_j'}}{2}\right) + \bar{u}_i \frac{\partial}{\partial x_i}\left(\frac{\rho \overline{u_i' u_j'}}{2}\right) + \rho \overline{u_i' u_j'} \frac{\partial \bar{u}_j}{\partial x_i} + \frac{\partial}{\partial x_i}\left(\overline{u_i \frac{u_i' u_j'}{2}}\right) \qquad \text{(A-11)}$$

$$= -\frac{\partial}{\partial x_j}\left(\overline{P' u_j'}\right) + \mu \overline{u_j' \frac{\partial^2 u_j}{\partial x_i \partial x_i}}$$

It is assumed that, for the case of the porous medium, flow may not be high enough to necessitate the use of this equation. Rather an increase in velocity increases the chances of fluctuations becoming significant and resulting in large kinetic energy losses. Since measurable flow properties are usually taken at their mean values, the equation for the kinetic energy of mean flow may logically be very appropriate to use.

A.3 Dimensional Similarity Criteria

As defined by Schlichting(85), two flows about geometrically similar bodies are similar if the forces acting on a fluid particle bear a fixed ratio each time and at all geometrically similar points. Specifically for a steady, incompressible, horizontal flow, the condition of similar flow is satisfied only if at all corresponding points, a constant ratio of inertial to viscous forces exists. This criterion has been used by Hubbert(86) in his definition of Reynolds number for porous media.

By Monin and Yaglom(87), flows are geometrically similar if the properties of their boundaries are determined uniquely by the same length scale, and by some typical mean velocity. Let L and U be some typical mean length and velocity scales which respectively characterize such geometrically similar flows. Further let the length scale be taken generally as the distance along which the velocity scale U of the flow undergoes a perceptible change. Therefore the Reynolds number is given as

$$Re = UL\rho/\mu = \text{Inertial term/viscous term}$$
$$= \text{dimensionless} \tag{A-12a}$$

Combining dimensionally both the viscosity coefficient μ and the density ρ with U and L, therefore, the following relations are obtained:

$$\rho \frac{\partial \bar{u}_i \bar{u}_j}{\partial x_i} \sim \frac{\rho U^2}{L} = \text{Const} \cdot \frac{\rho U^2}{L} \tag{A-12}$$

$$\mu \frac{\partial^2 \bar{u}_j}{\partial x_i \partial x_i} \sim \frac{\mu U}{L^2} = \text{Const} \cdot \frac{\mu U}{L^2} \tag{A-13}$$

$$\frac{\partial}{\partial x_i} (-\rho \overline{u_i' u_j'}) \sim -\frac{\rho U'^2}{L} = -\text{Const} \cdot \frac{\rho U'^2}{L} \tag{A-14}$$

$$\frac{\partial}{\partial x_i} \left(\frac{\rho \bar{u}_i \bar{u}_i \bar{u}_j}{2} \right) \sim \frac{\rho U^3}{2L} = \text{Const} \cdot \frac{\rho U^3}{2L} \tag{A-15}$$

$$\mu \bar{u}_j \frac{\partial^2 u_i}{\partial x_i \partial x_i} \sim \frac{\mu U^2}{L^2} = \text{Const} \cdot \frac{\mu U^2}{L^2} \tag{A-16}$$

$$\bar{u}_j \frac{\partial}{\partial x_i} \left(- \rho \overline{u_i' u_j'} \right) \sim -\frac{\rho U'^2 U}{L} = -\text{Const} \cdot \frac{\rho U'^2 U}{L} \tag{A-17}$$

where U' is due to fluctuation, for i = j.

Using these relations, Equations A-5, A-8, A-10 become for steady state, 1-dimensional, horizontal flow:

$$- \frac{dP}{dx} = \frac{C_1 \mu U}{L^2} + \frac{C_2 \rho U^2}{L} \qquad \text{(A-18)}$$

$$- \frac{dP}{dx} = \frac{C_1 \mu U}{L^2} + \frac{C_2 \rho U^2}{L} + \frac{C_3 \rho U'^2}{L} \qquad \text{(A-19)}$$

$$- U \frac{dP}{dx} = \frac{C_4 \mu U^2}{L^2} + \frac{C_5 \rho U^3}{L} + \frac{C_6 \rho U'^2 U}{LU} \qquad \text{(A-20)}$$

Equation A-19 is similar to Equation 2.30 which Crafton obtained by using the force momentum balance. But Equation A-20 underlines the use of kinetic energy considerations in explaining the flow conditions. Both equations contain the Reynolds stresses and have the same closure problem.

Explanation of flow phenomena as velocity increases may not be very effective if the force momentum balance for mean steady flow is used(87). By Equation A-6b, the mean of the produced fluctuation is zero, therefore, its mean force momentum is zero. This poses a serious setback for Equation A-19.

Two possible expressions may be obtained when Equation A-20 is divided by U. The first expression reverts to the Reynolds equation and is identical to Equation A-19. The second is:

$$-\frac{dP}{dx} = \frac{C_4\mu U}{L^2} + \frac{C_5\rho U^2}{L} + \frac{C_6\rho U'^2 U}{UL} \qquad \text{(A-21)}$$

Where the first two terms on the right are identical to the first two terms on the right of Equations A-18 and A-19. Therefore their constant coefficients C1 and C4, and C2 and C5, are respectively equal. The constant coefficient, C6, of Equation A-21, is different from C3 of Equation A-19. The coefficients of the terms on the right hand side of Equations A-18, A-19, and A-21 are constants since both viscosity, density and length are assumed constant.

Close resemblances are noticed between Equations A-18 and 2.17, and between Equations A-21 and 2.24. This suggests that Equations A-18 and A-21 are similar, respectively, to the second and third order equations of Forchheimer. The velocity scales in the third term on the right of Equation A-21 have been obtained as a combination of velocity fluctuation and mean velocity. Equation A-21 is made up of the differential pressure gradient on the left, and the viscous, the inertial, and the cubic term on the right.

If M, L, T, are denoted as dimensions of mass, length and time, both the differential pressure gradient and viscosity are represented dimensionally as $[ML^{-2}T^{-2}]$ and $[ML^{-1}T^{-1}]$ respectively. The inertial resistance coefficient in the inertial term has a dimension of $[L^{-1}]$. The permeability expression in the viscous term, has a dimension $[L^2]$, and can be expressed as

$$k = Nd^2 \tag{A-21a}$$

where N is a shape factor(88)

If these dimensional relations are applied on Equation A-21, an equation of the form of:

$$-\frac{dP}{dx} = \frac{\mu}{k} U + \beta\rho U^2 + \gamma\rho^2 U'^2 U \tag{A-22}$$

is obtained where

$$k = L^2/C4 = [L^2] \text{ by dimension} \tag{A-22a}$$

$$\beta = C5/L = Fb = [L^{-1}] = \text{ by dimension} \tag{A-22b}$$

$$\gamma = C6/(UL\rho) = \text{Gamma} = [LTM^{-1}] \text{ by dimension} \tag{A-22c}$$

$UL\rho = [ML^{-1}T^{-1}]$ = dimension of viscosity

This implies that:

C6 = dimensionless.

$$\gamma\mu = (C6*u)/(UL\rho) = C6/Re = \text{dimensionless} \tag{A-22d}$$

Comparing Equations A-21a and A-22a, it follows that

1/C4 = N = a shape factor for k

Similarly coefficients C5 and C6 could be shape factors for Fb, and gamma respectively.

The foregoing relations imply the following properties of gamma:

1. It is related to turbulent viscosity or shear resistance.
2. It acts in opposite sense to flow due to Reynolds stresses.
3. It is related to a dimensionless shape factor C6 which is significant at higher flow rates.
4. It is a flow functional parameter.

By inspection of Equation A-22 and from Equation A-6, both U' and U have the same order of magnitude at higher flow rates corresponding to higher Reynolds numbers. Let them be represented by the same velocity scale q such that q is free to assume values of velocity for increasing flow rates, and for different flow situations. The scale q, therefore, becomes a measurable quantity, and Equation A-22 can be written as:

$$-\frac{dP}{dx} = \frac{\mu}{k}q + F_b\rho q^2 + \gamma\rho^2 q^3 \qquad \text{(A-23)}$$

while quadratic Equation A-18 can similarly be written as

$$-\frac{dP}{dx} = \frac{\mu}{k}q + F_b\rho q^2 \qquad \text{(A-23a)}$$

Equation A-23 is identical to the relationship given as Equation 2.25 by Firoozabadi and Katz.

A.4 Significance of the Cubic Term

The foregoing equations depict the dominance of the cubic term at higher flow rates when fluctuations U′ combine with the mean velocity U in the ratio of 2:1. Gamma has the dimensions of LTM^{-1} which is also the dimensions of the reciprocal of viscosity. From these dimensions, the inverse dependence of gamma on the shear resistance to flow, (viscosity), is suggested. Hence from Equation A-23, the differential pressure gradient increases, for increasing flow rates, and as shear resistance decreases for increasing values of gamma. These can be related for each increasing value of the flow rate as:

$$\frac{dP}{dx} \propto \frac{1}{\mu} \propto \gamma \qquad \text{(A-24)}$$

Muskat(89) described this condition as being physically unreasonable.

From boundary layer theory(90), and by the condition of no slip at the boundary, fluid flow is characterized by very high resistance to flow at the boundary (no slip condition), and a much lesser resistance at the centre (potential flow condition). The boundary layer is closest to the fluid-solid interface, and at the boundary, the flow rate is zero by no-slip condition. The nominal boundary layer thickness,d, is the normal distance from the fluid-solid interface at which the velocity is 99% of the free stream velocity in the approximately potential flow region.

For a small cross-sectional area available to flow, as in Figure A-1, the effective available cross-sectional area, situated at the centre, is quite small. Resistance to flow induces a creeping flow condition in the centre. With higher flow rates, corresponding to a large differential pressure gradient, the flow encounters more resistance as the boundary layer is permeated. Subsequently, by overcoming this resistance, the boundary layer thickness decreases and the cross-sectional area open to the flow increases. The viscosity value within the increased cross-sectional area, open to flow, is lower than its original value before the boundary layer was decreased.

Therefore, with increasing flow rates,

1. differential pressure gradient increases,
2. boundary layer thickness decreases,
3. cross-sectional area open to flow increases,
4. resistance to flow in the increased cross-sectional area decreases as the boundary layer growth is reduced in the flow direction.

If A′ is this new cross-sectional area, these can jointly be related as

$$\frac{dP}{dx} \propto \frac{1}{\mu} \propto A' \qquad \text{(A-25)}$$

Equations A-24 and A-25, which are similar in expression, suggest that gamma is related to A′ and that as gamma increases for increasing kinetic energy of flow, both

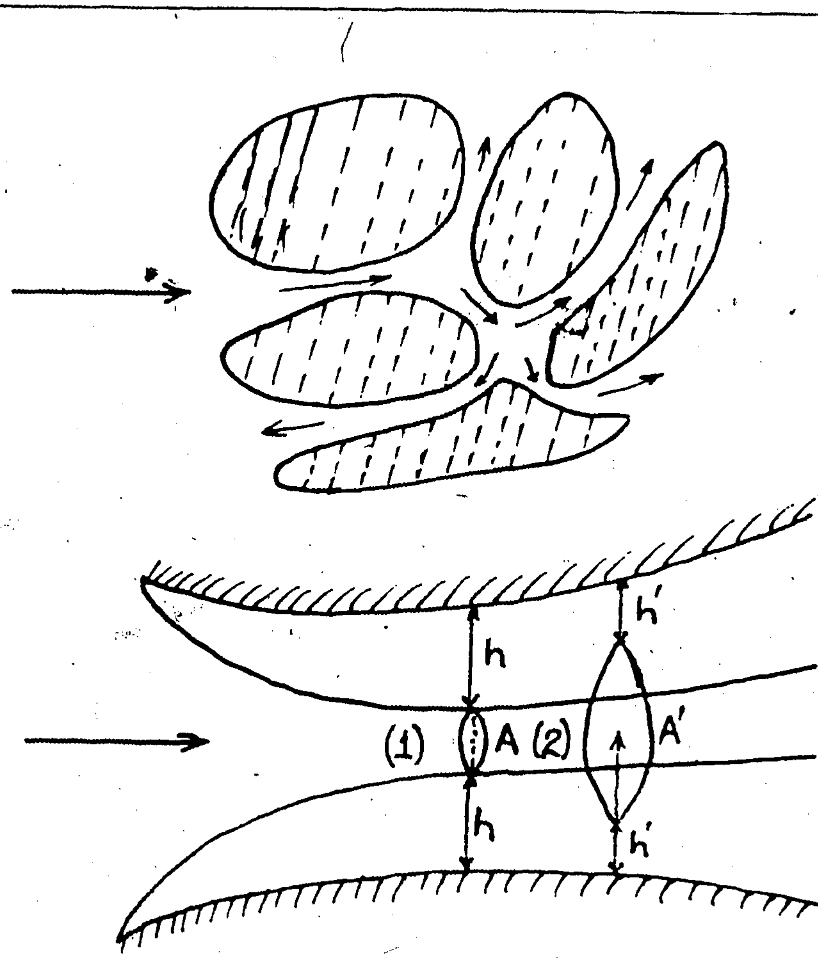

where:

(1)..h = initial boundary layer thickness at lower flow rates.

..A = initial cross-sectional area open to flow at lower flow rates.

(2)..h' = reduced boundary layer thickness at higher flow rates.

..A' = increased cross-sectional area open to flow at higher flow rates.

Figure A-1: Schematic Flow Through Porous Media the boundary layer thickness, and the resistance to flow, closest to the centre, decrease. For lower flow rates with negligible kinetic energy of flow, the cubic term is not necessary.

By Schlicting, the ratio of the boundary layer thickness to the length scale of the path varies inversely with the square root of the Reynolds number. Similarly, the total drag coefficient, D, or the skin frictional coefficient(91), varies inversely with the square root of the Reynolds number. Combining these relations, results in:

$$\frac{d}{L} \sim \frac{1}{\sqrt{R_e}} \sim D = \frac{\tau_0}{\rho U^2} = \sqrt{\frac{\mu}{\rho UL}} \qquad \text{(A-26)}$$

which in rewritten form can be expressed as:

$$D^2 = \frac{\mu}{LU\rho} = \frac{C}{R_e} = \text{dimensionless} \qquad \text{(A-27)}$$

Equation A-27 is similar to Equation A-22c and combining both equations, gives

$$\gamma\mu = \frac{\mu}{LU\rho} = \frac{C_6}{R_e} = D^2 = \text{dimensonless} \qquad \text{(A-28)}$$

From this expression, gamma depends directly on the square of the skin frictional coefficient, and inversely on both viscosity and the Reynolds number. The dimensionless shape factor C6 is related to the square of the skin frictional coefficient, D.

These factors, including gamma, operate at higher flow rates, and with higher Reynolds number, within the boundary layer.

APPENDIX B

ADAPTATION OF MODEL EQUATIONS TO COMPUTER APPLICATIONS

B. APPENDIX B - ADAPTATION OF MODEL EQUATIONS TO COMPUTER APPLICATION

B.1 Equations for Parameter Estimation

Equation 4.15 gives a general cubic flow equation in terms of ka, Fb, and gamma. In its rearranged form, as in Equation 4.23, it is:

$$\frac{P_e^2 - P_w^2}{CC1} = \frac{1}{k_a} + \frac{CC2}{CC1} \cdot F_b + \frac{CC3}{CC1} \cdot \gamma \qquad \text{(B-1)}$$

This equation is linear in its coefficients. Designating the desired parameters as coefficients, a multiple linear regression technique for estimating the parameters can be developed. Subsequently, Equation B-1 is put in the following form:

$$Y = W_0 + W_1 X_1 + W_2 X_2 \qquad \text{(B-2)}$$

where

Y = (Pe² - Pw²)/CC1	Wo = 1/ka
X1 = CC2/CC1	W1 = Fb
X2 = CC3/CC1	W2 = gamma

Equation 4.16, rearranged below,

$$\frac{P_e^2 - P_w^2}{CC1} = \frac{1}{k} - \frac{PEW}{CC1} \cdot b + \frac{CC2}{CC1} \cdot F_b + \frac{CC2}{CC1 \times P_m} (b \cdot F_b) + \frac{CC3}{CC1} \cdot \gamma + \frac{CC3}{CC1 \times P_m} \cdot (\gamma \cdot b) \qquad \text{(B-3)}$$

can similarly be treated if its combined parameters are represented by single variables. In this condition, Equation B-3 reduces to

$$Y = W_0 + W_1X_1 + W_2X_2 + W_3X_3 + W_4X_4 + W_5X_5 \qquad \text{(B-4)}$$

wher

Y = (Pe² - Pw²)/CC1	Wo = 1/k
X1 = -PEW/CC1	W1 = b
X2 = CC2/CC1	W2 = Fb
X3 = CC2/(CC1*Pm)	W3 = b*Fb
X4 = CC3/CC1	W4 = gamma
X5 = CC3/(CC1*Pm)	W5 = gamma*b

For the quadratic case, Equations B-1 and B-3 reduce to

$$\frac{P_e^2 - P_w^2}{CC1} = \frac{1}{k_a} + \frac{CC2}{CC1} \cdot F_b \qquad \text{(B-5)}$$

$$\frac{P_e^2 - P_w^2}{CC1} = \frac{1}{k} - \frac{PEW}{CC1} \cdot b + \frac{CC2}{CC1} \cdot F_b + \frac{CC2}{CC1 \times P_m} \cdot (b \cdot F_b) \qquad \text{(B-6)}$$

which are equivalent to Equations 4.21 and 4.22. By similarly linearizing their coefficients, the following forms are obtained:

$$Y = W_0 + W_1X_1 \qquad \text{(B-7)}$$

$$Y = W_0 + W_1X_1 + W_2X_2 + W_3X_3 \qquad (B-8)$$

They follow directly the form of Equations B-2 and B-4.

B.2 Equations for Model Fitting The Data

Equation (4.22), reproduced below,

$$(P_e^2 - P_w^2) = \left(\frac{C_1\bar{\mu}\bar{T}\bar{Z}}{k_a}\right)\cdot Q_o + (C_2\bar{Z}\bar{T}F_b)\cdot Q_o^2 + (C_3\bar{Z}\bar{T}\gamma)\cdot Q_o^3 \qquad (B-9)$$

is a polynomial in Qo which can be expressed as

$$Y = W_1X_1 + W_2X_2 + W_3X_3 \qquad (B-10)$$

where

$Y = Pe^2 - Pw^2$

$W1 = (C_1\bar{\mu}\bar{T}\bar{Z})/k_a$ $\qquad X1 = Qo$

$W2 = C_2\bar{Z}\bar{T}F_b$ $\qquad X2 = Qo^2$

$W3 = C_3\bar{Z}\bar{T}\gamma$ $\qquad X3 = Qo^3$

For the quadratic case, Equations B-9 and B-10, respectively, reduce to

$$(P_e^2 - P_w^2) = \left(\frac{C_1\bar{\mu}\bar{T}\bar{Z}}{k_a}\right)\cdot Q_o + (C_2\bar{Z}\bar{T}F_b)\cdot Q_o^2 \qquad (B-11)$$

$$Y = W_1X_1 + W_2X_2 \tag{B-12}$$

B.3 Multiple Linear Regression

The foregoing equations have the following general form which is linear in the coefficients:

$$Y_i = W_o + W_1X_{i1} + W_2X_{i2} + \cdots W_nX_{in} + e_i \tag{B-13}$$

or, in condensed form:

$$Y_i = W_o + \sum_{j=1}^{n} W_jX_{ij} + e_i \tag{B-13a}$$

for i = 1, N, j = 1, n, and e is the error.

By method of least squares(92,93), the sum of error squares with respect to each of the parameters should be a minimum such that

$$\frac{\partial(\sum_{i=0}^{n} e_i^2)}{\partial W_j} = 0 \tag{B-14}$$

Solution of this equation for the best estimates of Wj, and rearranging, results in normal equations of order n:

$$\Sigma(X_{ik} - \overline{X}_k)(Y_i - \overline{Y}) \quad \sum_{i=1}^{n} \left[\left\{ \Sigma(X_{ik} - \overline{X})(X_{ij} - \overline{X}_j) \right\} \cdot W_j \right] \qquad \text{(B-15)}$$

where k = 1, n, and y, x, are respectively arithmetic means of Y and X. The value of Wo is determined as

$$W_0 = \overline{Y} - \sum_{j=1}^{n} W_j \overline{X} \qquad \text{(B-16)}$$

If in matrix form:

E(I) = Y - Ymean

D(I,J) = X(I,J) - Xmean(J)

DT(J,I) = D(I,J) = X(I,K) - Xmean(K) = D transpose

Equation B-15 becomes

DT(J,I)* E(I) = DT(J,I)*D(I,J)*W(J) (B-18)

Furthermore, if

B(J) = DT(J,I)*E(I)

A(J,J) = DT(J,I)*D(I,J)

then

B(J) = A(J,J)*W(J) (B-19)

and

W(J) = B(J)/A(J,J) (B-20)

The value of Wo is calculated from Equation B-16.

The foregoing proceedure is general for both parameter estimation and model fitting by polynomial fit.

B.3.1 The Problem of Ill-Conditioned Matrices

The solution of Equation B-19 is possible only if the generated symmetrical matrix A(J,J) is non-singular and has an inverse. Ill-conditioning is a common problem encountered in this type of generated matrix. The determinant is very small and, depending on the number of parameters to be estimated, can be almost zero. This is a characteristic of Hilbert matrices found generally in physical systems(95). Some suggested techniques aimed at minimizing such ill-conditioning are:

1. Run the program in double precision.
2. Ensure that the equations of D, and its transpose, are correct.
3. As much as possible, perform divisions last. Minimize truncations of significant decimal figures.
4. In matrix inversion, apply pivotal row interchange.
5. If possible, restrict the number of parameters to a minimum(96).

It was noticed that neglecting the combined variables enhanced the stability of the matrix system in terms of ill-conditioning.

B.4 Linear Fit For Graphical Parameter Estimation

A linear fit is performed for the plot points in the linear sections of both the Klinkenberg and the visco-inertial plots, by the method of least squares. The degree of linear fit is measured by the linear correlation coefficient, Raa:

$$R_{aa} = \frac{N\Sigma X_i Y_i - \Sigma X_i \Sigma Y_i}{[N\Sigma X^2 - (\Sigma X_i)^2]^{\frac{1}{2}}[N\Sigma Y_i^2 - (\Sigma Y_i)^2]^{\frac{1}{2}}} \qquad \text{(B-21)}$$

This linear fit does not require matrix formation.

APPENDIX C

GRAPHICAL RESULTS

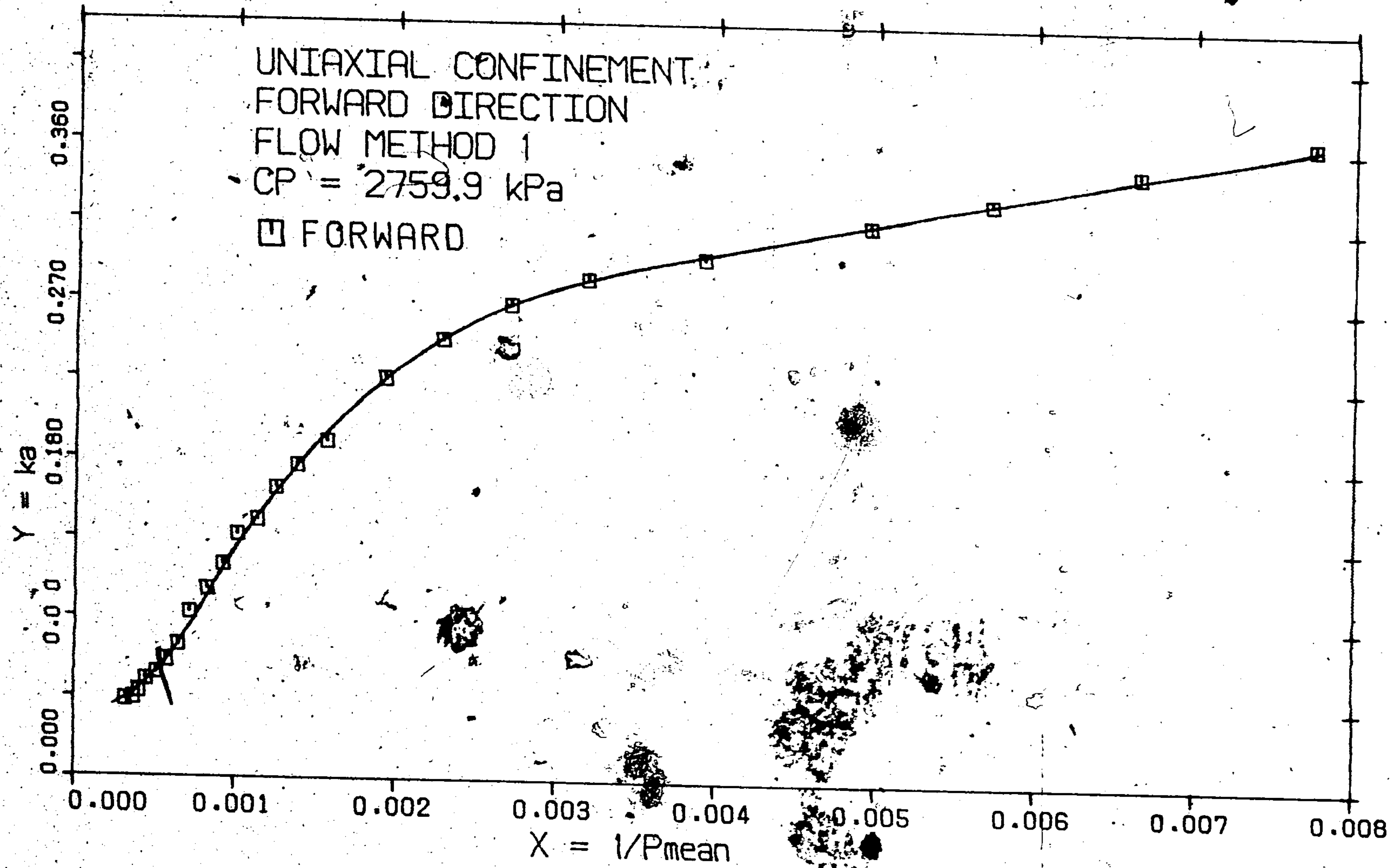

FIGURE C-1: CORE 1C KLINKENBERG PLOT RUN 3

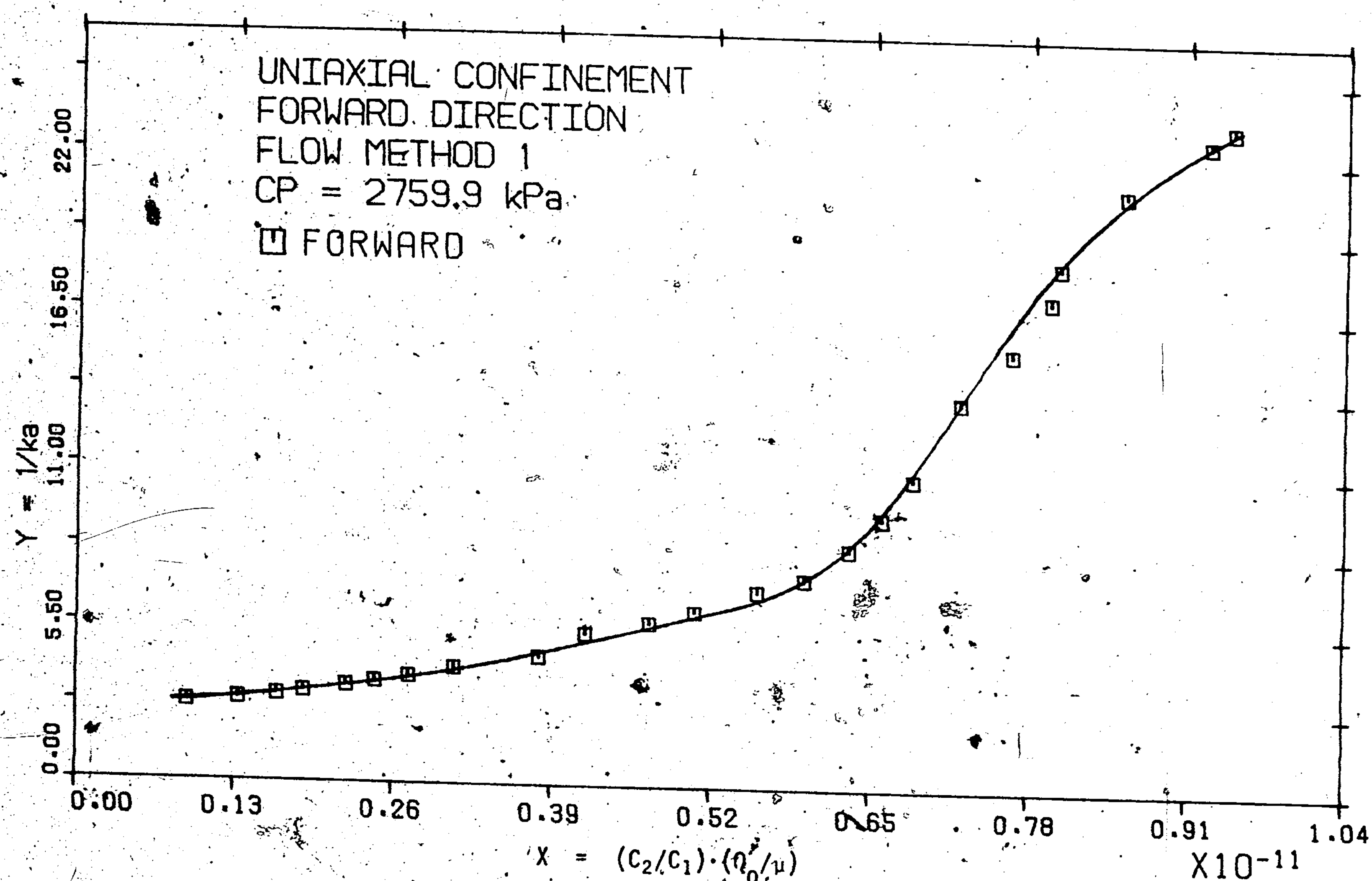

Figure C-2: CORE 1C VISCO-INERTIAL PLOT RUN 3

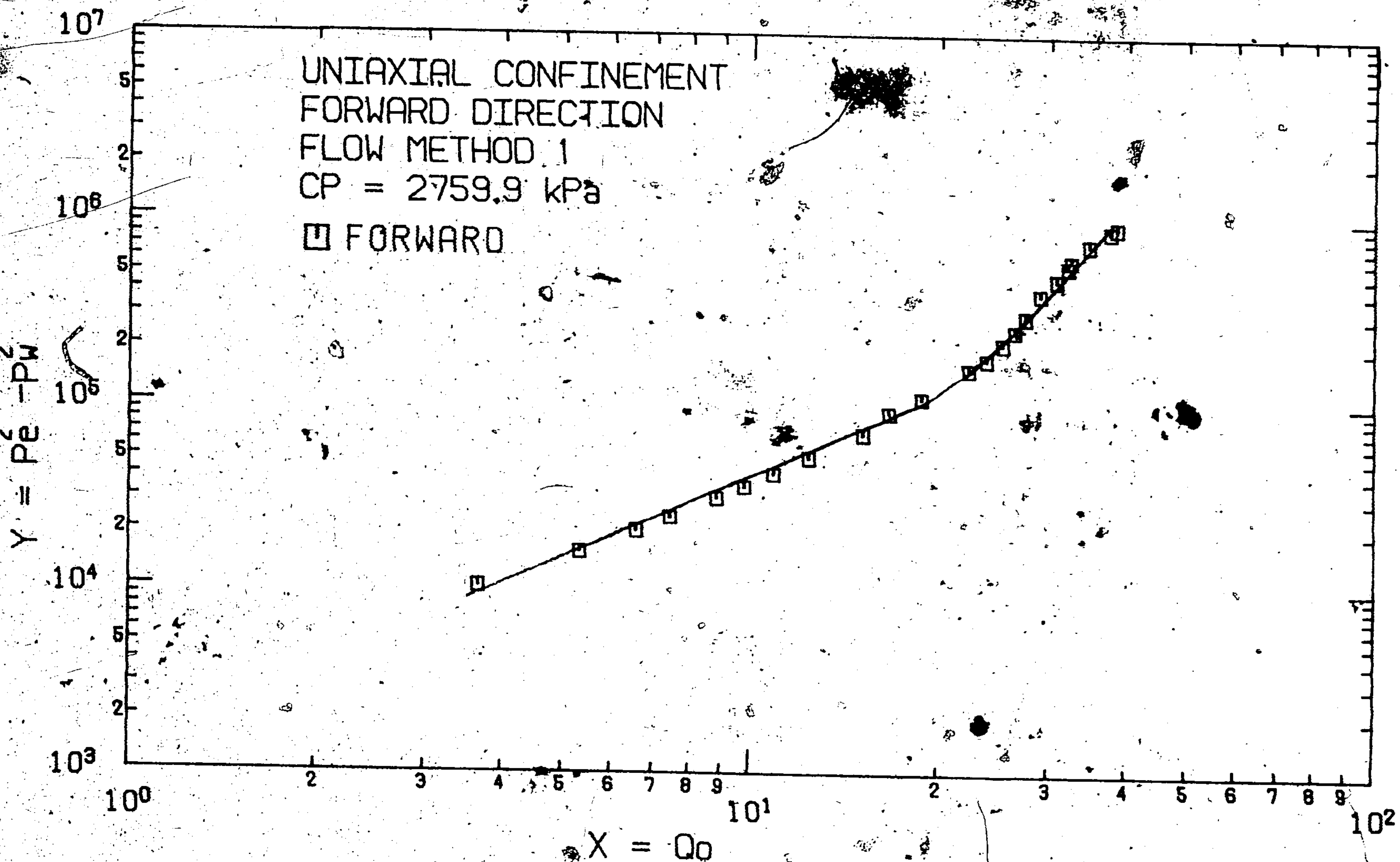

Figure C-3: CORE 1C BACK PRESSURE PLOT RUN 3

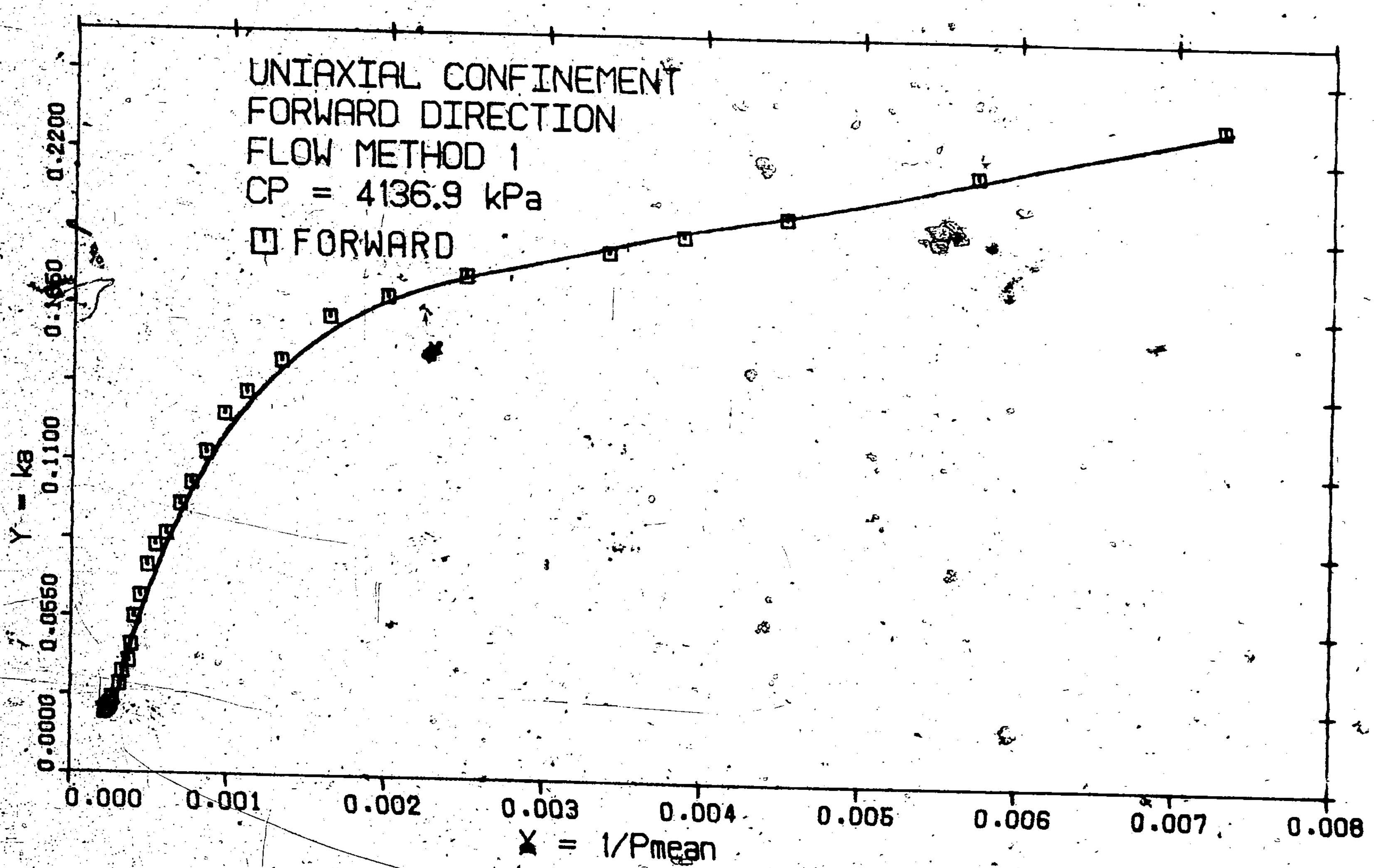

FIGURE C-4 CORE 4A KLINKENBERG PLOT RUN 4

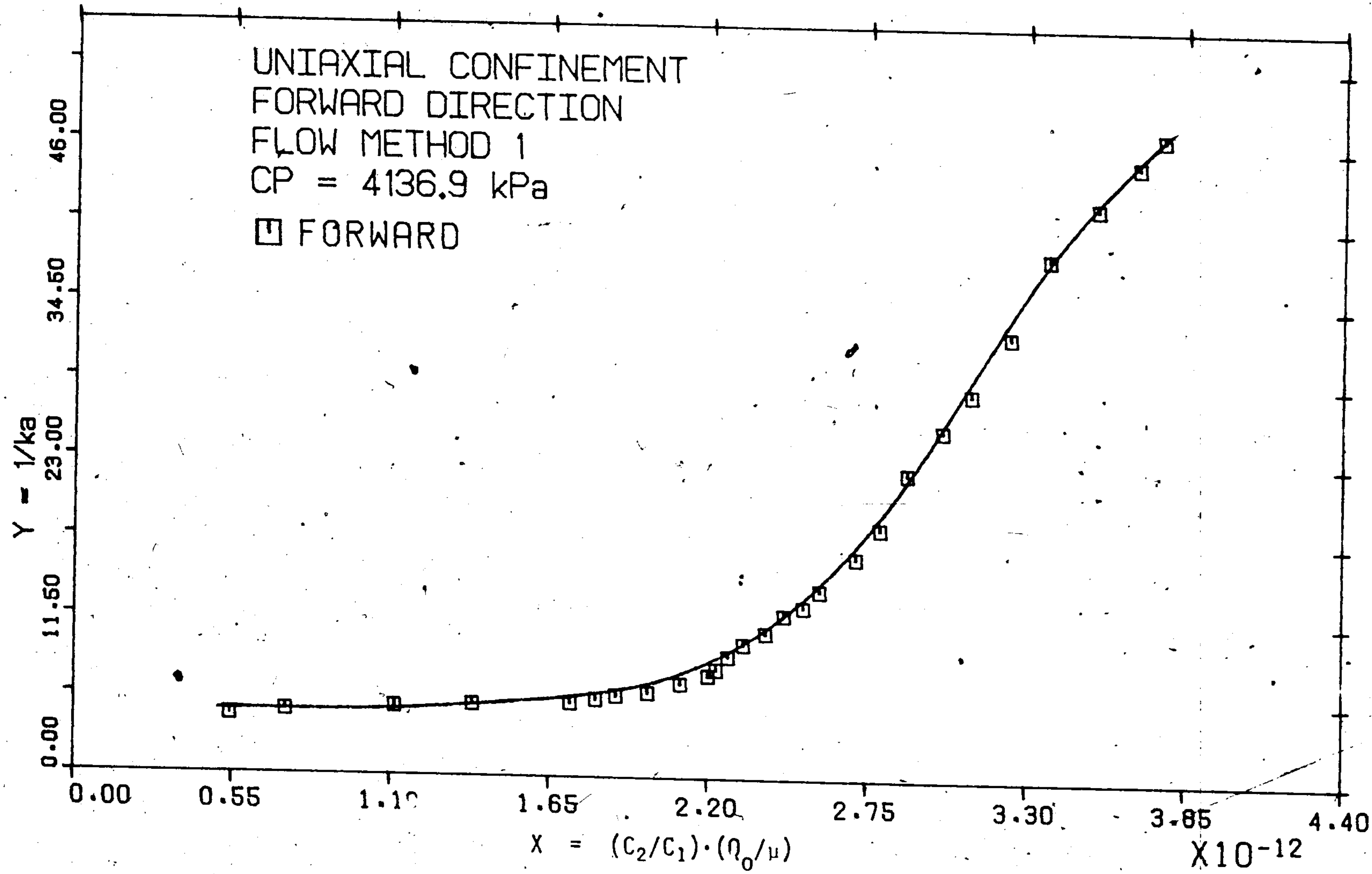

Figure C-5 CORE 4A VISCO-INERTIAL PLOT RUN 4

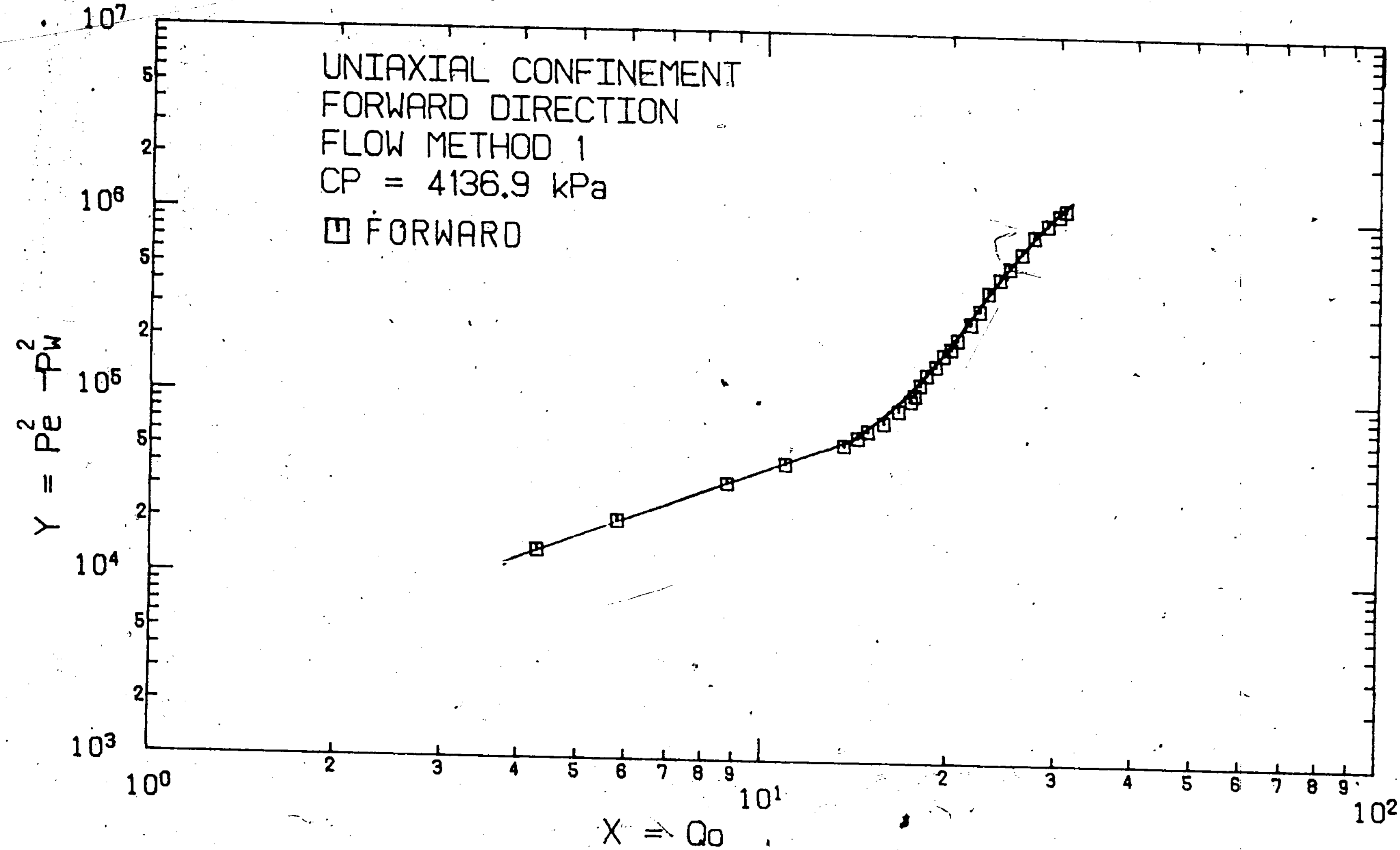

Figure C-6 CORE 4A BACK PRESSURE PLOT RUN 4

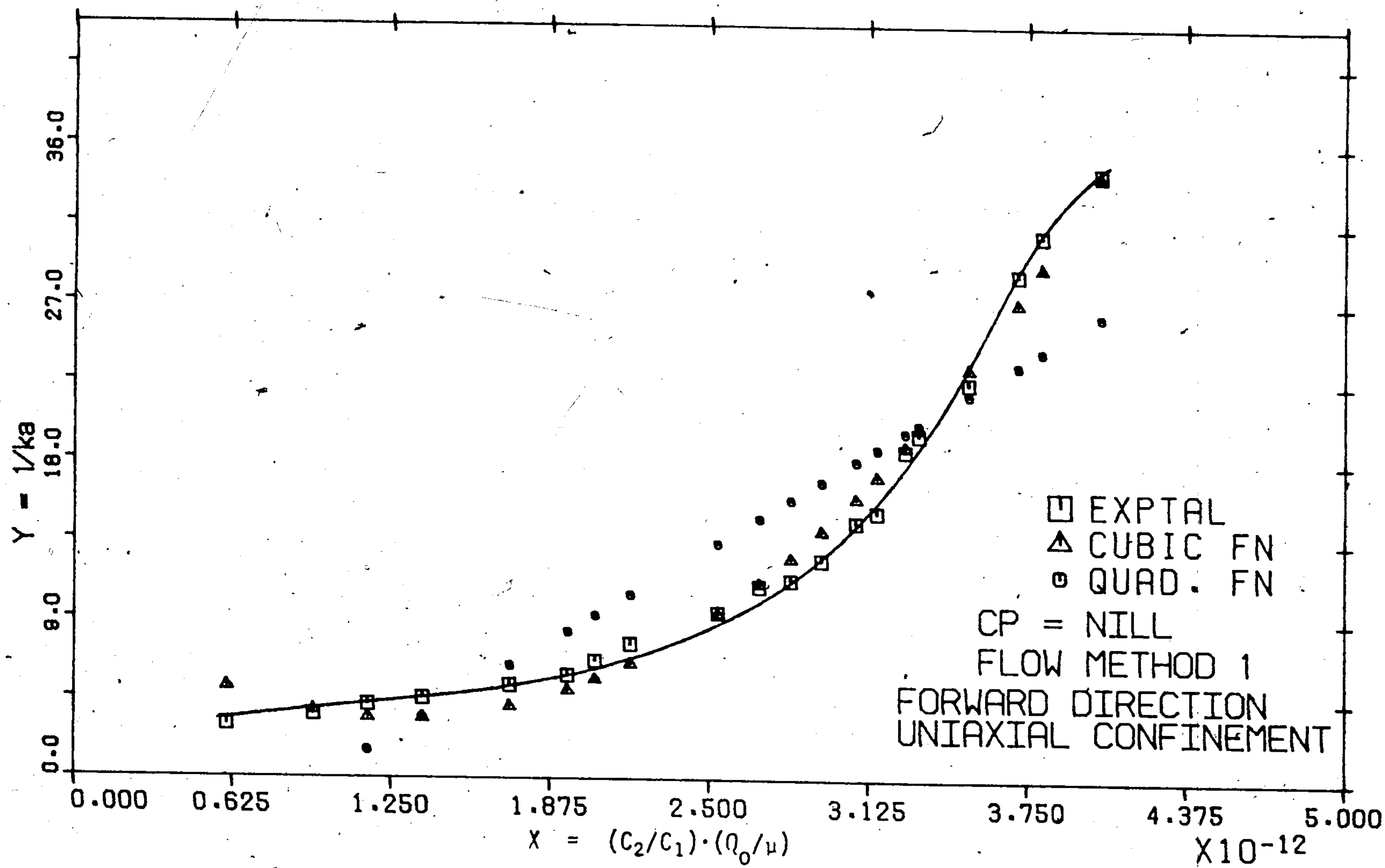

Figure C-7 CORE 4A RUN 1 VISCO-INERTIAL FIT PLOT

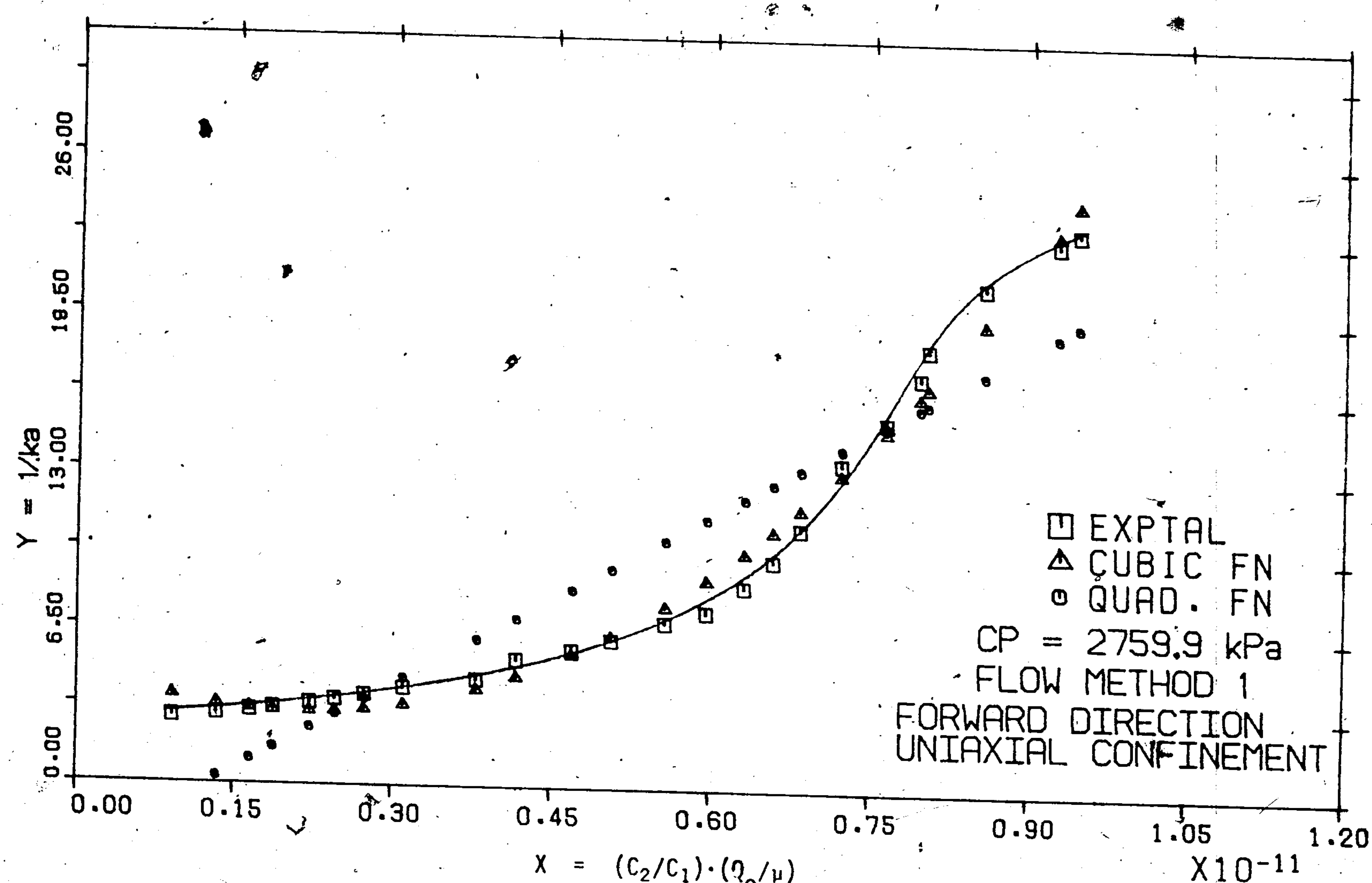

Figure C-8 CORE 1C RUN 3 VISCO-INERTIAL FIT PLOT

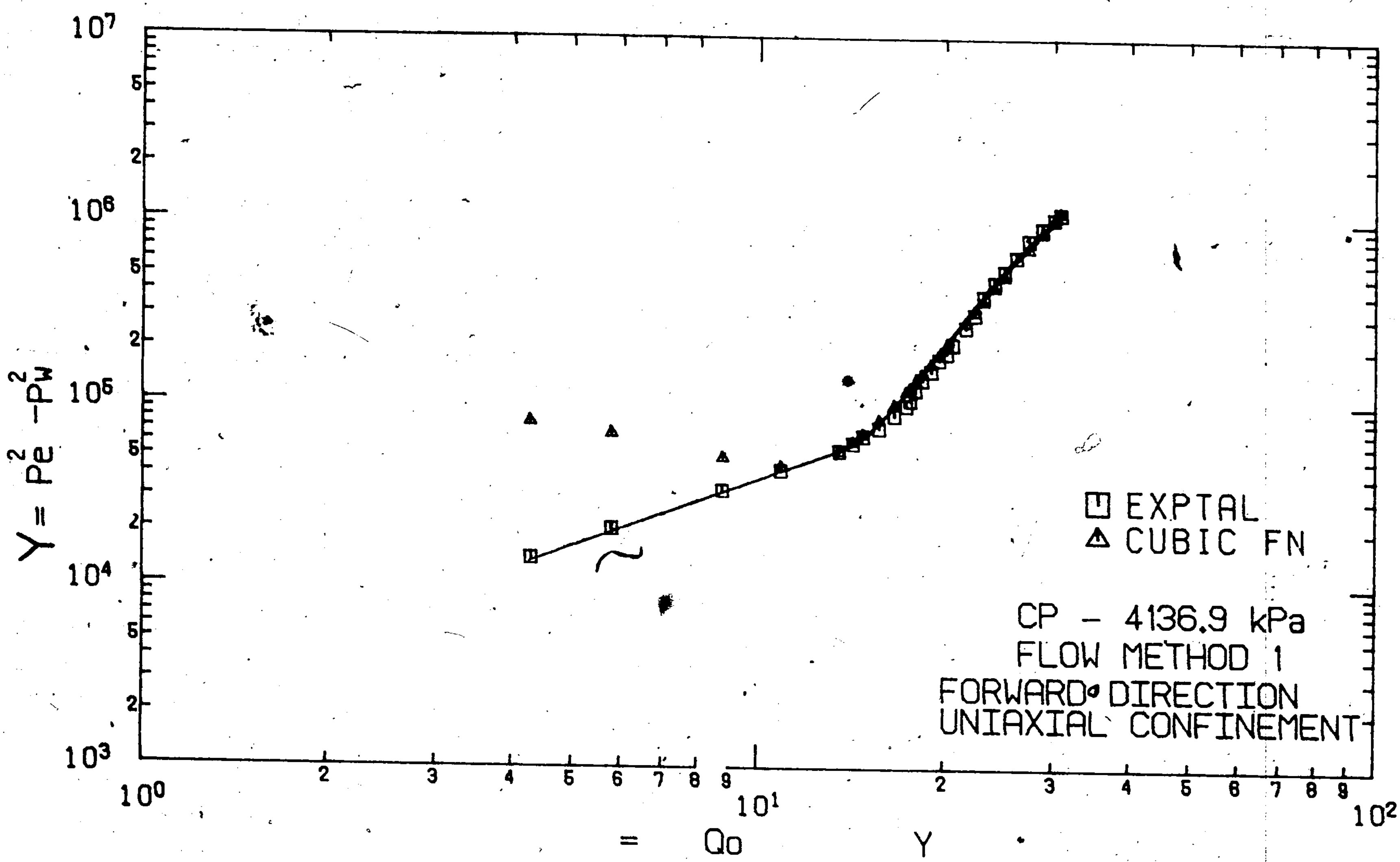

Figure C-9 CORE 4A RUN 4 BACK PRESSURE FIT PLOTX

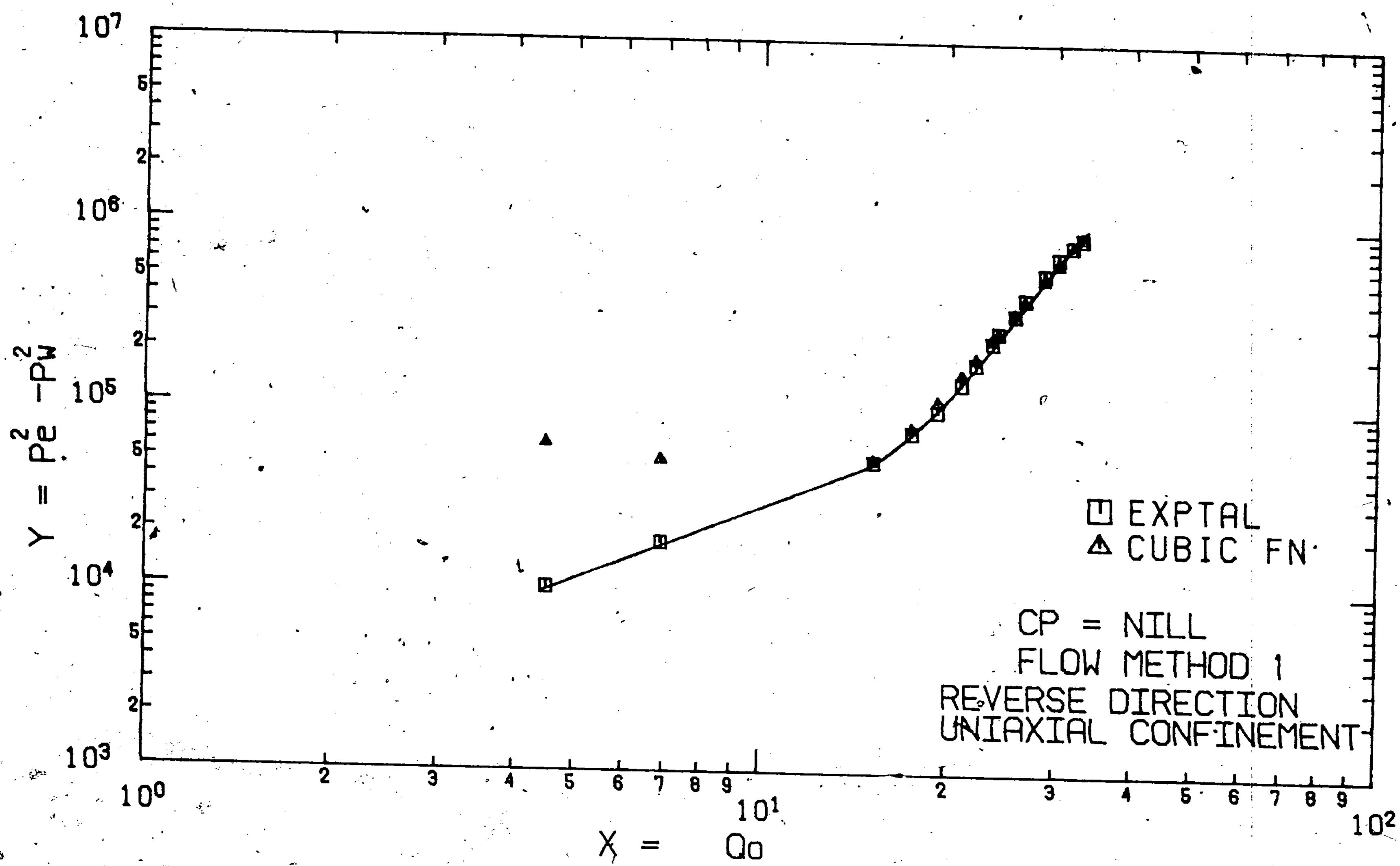

Figure C-10 CORE 4A RUN 1 BACK PRESSURE FIT PLOT

APPENDIX D

COMPUTER PROGRAM AND DATA LISTINGS

D. APPENDIX D - COMPUTER PROGRAM AND DATA LISTINGS

D.1 PROGRAM LISTINGS

```
C                              LIN
C.
CCCCCCCCCCCCCCCCCCCCCCCCCCCCCCCCCCCCCCCCCCCCCCCCCCCCCCCCCC
C
C      THIS PROGRAM PLOTS GRAPHS WITH A LINEAR LEAST SQUARE
C      FIT
C
C      Uses Applot**plotlib on Object File
C
C      Subroutines: LAGINT, LINXY, GRAPH, BOX
C
CCCCCCCCCCCCCCCCCCCCCCCCCCCCCCCCCCCCCCCCCCCCCCCCCCCCCCCCCC
C
C      EM=MOLECULAR WEIGHT
C      TR,PR,DR=REDUCED TEMPERATURE,PRESSURE, AND DENSITY
C      RESPECTIVELY
C      VIS=VISCOSITY IN MICRO-PA.S
C      GG=GAS GRAVITY
       IMPLICIT REAL*8(A-H,O-Z)
       REAL*4 DIRECT
       REAL*8 DLOG
       DIMENSION PE(60),PW(60),TE(60),TW(60),PM(60),W(60),
      ¢VIS(60),ZA(60),PB(60),CP(60),TS(60),QO(60),PEW(60),
      ¢CC1(60),CC2(60),CC3(60),PD(60),X(60),RD(60),AX(60),
      ¢T[illegible](60),TCW(60),E(60,100),ER(60),Y(60),AY(60),
      ¢BX(60),BY(60),CX(60),CY(60),DX(60),DY(60),EX(60),
      ¢EY(60),FX(60),FY(60),V(60),ZX(60),ZY(60),DIRECT(5),
      ¢EW(60),DMP(60)
       DATA TC,EM,PC,SIG/1.262D+02,2.8013D+01,3.35D+01,
      ¢3.798D+00/
       GG=EM/2.896D+01
       PCA=PC*(1.01325D+02)
       READ(5,1) NUM,NO,DIRECT,IFLAG
       READ(5,90) RE,RW,H,POR
       READ(5,3) NDJ
       READ(5,4) R,BZ
C
       IF(IFLAG.NE.(100))  GO TO 65
       RE=RE*3.048D-01
       RW=RW*3.048D-01
       H=H*3.048D-01
       GO TO 65
   65  WRITE(6,2) NUM,NO,DIRECT
       WRITE(6,89) RE,RW,H,POR
       C1=((1.2954909D-03)*DLOG(RE/RW))/H
       C2=((2.9228842D-15)*GG*(1/RW-1/RE))/H*H
```

```
    1 FORMAT(A4,A4,5A4,I3)
   90 FORMAT(4F10.7)
    3 FORMAT(2I3)
    2 FORMAT(/4X,'CORE SAMPLE NO ',A4,2X,'RUN ',A4,2X,5A4)
   89 FORMAT(4X,'RE=',F10.7,2X,'RW=',F10.7,2X,'H=',F10.7,
     ¢2X,'POROSITY=',F10.7)
    4 FORMAT(2F10.6)
      IF(IFLAG.EQ.(100)) GO TO 67
C
      READ(5,6)(PE(I),PW(I),CP(I),PB(I),TCE(I),TCW(I),
     ¢TS(I),I=1,NDJ)
    6 FORMAT(7F11.4)
      WRITE(6,7)
    7 FORMAT(/14X,'PE',12X,'PW',12X,'CP',12X,'PB',11X,
     ¢'TCE',12X,'TCW',12X,'TS',/13X,'(PSI)',9X,'(PSI)',9X,
     ¢'(PSI)',9X,'(CMHG)',7X,'(MVOLT)',8X,'(MVOLT)',8X,
     ¢'(SEC)'/)
      WRITE(6,8)(PE(I),PW(I),CP(I),PB(I),TCE(I),TCW(I),
     ¢TS(I),I=1,NDJ)
    8 FORMAT(6X,7E14.5)
C
      DO 9 I=1,NDJ
      PB(I)=PB(I)*1.33322D+00
      PE(I)=PB(I)+PE(I)*6.894757D+00
      PW(I)=PB(I)+PW(I)*6.894757D+00
      CP(I)=PB(I)+CP(I)*6.894757D+00
      TE(I)=((TCE(I)+2.145588250D-02)/4.046470588D-02)
     ¢+273.15
      TW(I)=((TCW(I)+2.145588250D-02)/4.046470588D-02)
     ¢+273.15
      W(I)=(TE(I)+TW(I))/2.
      QO(I)=(6.116438868D+02)/TS(I)
    9 CONTINUE
      GO TO 71
C
   67 READ(5,69) (PE(I),PW(I),W(I),QO(I),CP(I),I=1,NDJ)
   69 FORMAT(5F12.8)
      DO 68 I=1,NDJ
      PE(I)=PE(I)*6.894757D+00
      PW(I)=PW(I)*6.894757D+00
      W(I)=((W(I)-3.2D+01)/1.8D+00)+2.7315D+02
      QO(I)=QO(I)*2.86364D+01
      CP(I)=CP(I)*6.894757D+00
   68 CONTINUE
C
   71 DO 70 I=1,NDJ
      PM(I)=(PE(I)+PW(I))/2.
      P=PM(I)
      PR=P/PCA
      T=W(I)
      TR=T/TC
C
      CALL LAGINT(P,T,TR,PR,Z,DR,VS)
      ZA(I)=Z
```

```
      RD(I)=DR
      VIS(I)=VS
C
      PEW(I)=2.*(PE(I)-PW(I))
      CC1(I)=C1*ZA(I)*VIS(I)*T*QO(I)
      CC2(I)=C2*ZA(I)*T*QO(I)**2.
      CC3(I)=CC2(I)/PM(I)
   70 CONTINUE
      READ(5,18) EK1,BET1,BETA1,GAMA1
      READ(5,19) EKC,BETAC,GAMAC
   18 FORMAT(4E20.5)
   19 FORMAT(3E20.5)
      WRITE(6,10)
   10 FORMAT(/11X,'PEW',11X,'CC1',9X,'CC2',9X,'CC3')
      WRITE(6,11) (PEW(I),CC1(I),CC2(I),CC3(I),I=1,NDJ)
   11 FORMAT(4X,4E13.5)
C
      DO 77 I=1,NDJ
      CY(I)=(PM(I)*PEW(I))
      CX(I)=(QO(I))
      EW(I)=(PE(I)-PW(I))
      DMP(I)=EW(I)/PM(I)
   77 CONTINUE
      WRITE(6,78)
   78 FORMAT(/8X,'EVALUATING BACK PRESSURE PLOT VALUES',
     ¢//13X,'Y=(PE2-PW2)',8X,'X=(QO)',14X,'PM',14X,'PE-PW',
     ¢11X,'(PE-PW)/PM')
      WRITE(6,51) (CY(I),CX(I),PM(I),EW(I),DMP(I),I=1,NDJ)
   51 FORMAT(6X,5G18.5)
C
      ICOUNT=1
      DO 53 I=1,NDJ
      Y(I)=(PE(I)*PE(I)-PW(I)*PW(I))/CC1(I)
      X(I)=(CC2(I))/CC1(I)
   53 CONTINUE
C
   57 CALL LINXY(X,Y,NDJ,A,BETA,SIGMAA,SIGBET,RAA,VAR)
C
      IF(ICOUNT-2) 58,59,60
   58 EK=1.0/A
      WRITE(6,54)
   54 FORMAT(/8X,'EVALUATING VISCO-INERTIAL PLOT VALUES',
     ¢//11X,'Y=(PE2-PW2)/CC1',6X,'X=CC2/CC1')
      WRITE(6,55) (Y(I),X(I),I=1,NDJ)
      WRITE(6,52) EK,BETA,SIGMAA,SIGBET,VAR,RAA
   52 FORMAT(/6X,'KABS=',G12.5,5X,'BETA=',G12.5,/6X,
     ¢'SIGMAK=',G12.5,2X,'SIGMABETA=',E12.5,/6X,'VARIANCE='
     ¢,G12.5,1X,'LIN.CORR.=',G12.5)
   55 FORMAT(6X,2G18.5)
      DO 101 I=1,NDJ
      AX(I)=X(I)
      AY(I)=Y(I)
  101 CONTINUE
C
```

```
      DO 56 I=1,NDJ
      Y(I)=CC1(I)/(PE(I)*PE(I)-PW(I)*PW(I))
      X(I)=1.0/PM(I)
   56 CONTINUE
   74 ICOUNT=ICOUNT+1
      GO TO 57
C
   59 EK=A
      BK=BETA
      B=BETA/A
      WRITE(6,62)
   62 FORMAT(//8X,'EVALUATING KLINKENBERG PLOT VALUES',
     ¢//11X,'Y=CC1/(PE2-PW2)',7X,'X=1/PM').
      WRITE(6,63) (Y(I),X(I),I=1,NDJ)
      WRITE(6,61) EK,B,SIGMAA,SIGBET,VAR,RAA
   61 FORMAT(/6X,'K=',G12.5,10X,'B=',G12.5,/6X,'SIGMAK=',
     ¢G12.5,4X,'SIGMAB*K=',G12.5,/6X,'VARIANCE=',G12.5,
     ¢1X,'LIN.CORR.=',G12.5)
   63 FORMAT(6X,2G18.5)
      DO 100 I=1,NDJ
      BX(I)=X(I)
      BY(I)=Y(I)
  100 CONTINUE
C
      DO 73 I=1,NDJ
      Y(I)=(PEW(I)/CC1(I))*(PM(I)+B)
      X(I)=(CC2(I)/CC1(I))*(1.0+B/PM(I))
   73 CONTINUE
      GO TO 74
C
   60 EK=1.0/A
      WRITE(6,12)
   12 FORMAT(/8X,'EVALUATING MODIFIED VISCO-INERTIAL PLOT
     ¢VALUES',//11X,'Y=(PEW/CC1)*(PM+B)',6X,'X=(CC2/CC1)*
     ¢(1+B/PM)')
      WRITE(6,13) (Y(I),X(I),I=1,NDJ)
      WRITE(6,14) EK,BETA,SIGMAA,SIGBET,VAR,RAA,B
   14 FORMAT(/6X,'KCOR=',G12.5,5X,'BETA=',G12.5,/6X,
     ¢'SIGMAK=',G12.5,2X,'SIGMABETA=',E12.5,/6X,
     ¢'VARIANCE=',G12.5,1X,'LIN.CORR.=',G12.5,/6X,'B=',
     ¢G12.5)
   13 FORMAT(6X,2G18.5).
C     DO 102 I=1,NDJ
C     DX(I)=X(I)
C     DY(I)=Y(I)
C 102 CONTINUE
C
      DO 114 I=1,NDJ
      EY(I)=CP(I)
      EX(I)=(1.70)*(PW(I)*RW*RW-PE(I)*RE*RE)/(RE*RE-RW*RW)
      V(I)=EY(I)/EX(I)
  114 CONTINUE
      WRITE(6,115)
  115 FORMAT(/8X,'EFFECT OF CP ON HORIZONTAL STRESSES',
```

```
     ¢//11X,'Y=CP APPLIED',6X,'X=HOR.STRESSES',6X,'V=RATIO')
      WRITE(6,33) (EY(I),EX(I),V(I),I=1,NDJ)
   33 FORMAT(6X,3G18.5)
C
      DO 202 I=1,NDJ
      FX(I)=0.25*EX(I)
      FY(I)=BY(I)
  202 CONTINUE
      WRITE(6,113)
  113 FORMAT(/8X,'EVALUATING CP AND Kabs PLOT VALUES',
     ¢//14X,'Y=Kabs',8X,'X=GENERATED CP')
      WRITE(6,116) (FY(I),FX(I),I=1,NDJ)
  116 FORMAT(6X,2G18.5)
C
C     WRITE(6,38)
      WRITE(6,36)
   36 FORMAT(/14X,'PE',12X,'PW',12X,'RD',10X,'VIS',12X,
     ¢'T',13X,'ZA',13X,'QO',/13X,'(KPA)',9X,'(KPA)',19X,
     ¢'(MICRO-PA.S)',5X,'(DEG K)',20X,'(CU M/D)'/)
      WRITE(6,37)(PE(I),PW(I),RD(I),VIS(I),W(I),ZA(I),QO(I)
     ¢,I=1,NDJ)
C     WRITE(6,38)
   37 FORMAT(6X,7E14.5)
C
      CALL GRAPH(AX,AY,BX,BY,CX,CY,DX,DY,EX,EY,FX,FY,NDJ,
     ¢IFLAG,DIRECT)
C
C  38 FORMAT(///)
      STOP
      END
C
C
C
C
      SUBROUTINE GRAPH(AX,AY,BX,BY,CX,CY,DX,DY,EX,EY,FX,FY,
     ¢NDJ,IFLAG,DIRECT)
      IMPLICIT REAL*8(A-H,O-Z)
      REAL*4 X,Y,ALPHA,XLEG,YLEG,CPHOR1,CPHOR2,DIRECT,CPTYPE
      DIMENSION X(60),Y(60),ALPHA(20),AX(60),AY(60),BX(60),
     ¢BY(60),CX(60),CY(60),DX(60),DY(60),EX(60),EY(60),
     ¢FX(60),FY(60),ZX(60),ZY(60),CPTIT(2),DIRECT(5),
     ¢XLEG(7),YLEG(7),CPHOR1(12),CPHOR2(12),TYPE(2),
     ¢CPTYPE(5)
      XSIZE=8.0
      YSIZE=4.75
C
      READ(5,4) CPTIT
   91 READ(5,4) TYPE
      READ(5,31) CPTYPE
      WRITE(6,4) TYPE
      WRITE(6,31) CPTYPE
   31 FORMAT(5A4)
C
      X0=-1.5
```

```
      Y0=-2.25
      X1=X0+11.0
      Y1=Y0+8.5
C
      ICOUNT=1
      KA=1
      KB=1
      KC=1
      ND=NDJ
      DO 333 I=1,NDJ
      X(I)=AX(I)
      Y(I)=AY(I)
  333 CONTINUE
C
   40 READ(7,50) HA,HB,VA,VB,PAGE
   50 FORMAT(4E20.4,A4)
      READ(7,1) ALPHA
    1 FORMAT(20A4)
      IF(ICOUNT-4) 21,81,21
   81 READ(7,2) CPHOR1
      READ(7,2) CPHOR2
      READ(7,3) XLEG
      READ(7,3) YLEG
    2 FORMAT(12A4)
    3 FORMAT(7A4)
    4 FORMAT(2A8)
C
   21 NF=1
      CALL CGPEP1(7.0,7.0)
      CALL CGPL(X,Y,X,ND,NF,KA,KB,KC,0,HA,HB,8.0,VA,VB,
     ¢4.75,ALPHA,+6)
      CALL CGPEP5(-7.0,-0.35,DIRECT,8,0.15,0.0)
C
      CALL PLOT(8.0,4.75,3)
      CALL PLOT(8.0,4.5,2)
      CALL PLOT(0.0,0.0,3)
C
      CALL PSYM(1.1,3.65,0.15,TYPE,0.0,16)
      CALL PSYM(1.1,3.90,0.15,CPTIT,0.0,16)
      CALL PSYM(1.1,4.15,0.15,DIRECT,0.0,16)
      CALL PSYM(1.1,4.40,0.15,CPTYPE,0.0,16)
      IF(ICOUNT-4) 82,83,82
   83 CALL PSYM(2.75,-0.5,0.15,XLEG,0.0,28)
      CALL PSYM(-0.5,0.5,0.15,YLEG,90.0,28)
      CALL PSYM(2.,-0.9,0.15,CPHOR1,0.0,48)
      CALL PSYM(0.5,-1.2,0.15,CPHOR2,0.0,48)
   82 CALL BOX(X0,Y0,X1,Y1,PAGE)
      IF(ICOUNT-4) 58,60,57
   58 IF(ICOUNT-3) 56,59,60
   56 IF(ICOUNT-2) 53,54,59
C
   53 DO 103 I=1,NDJ
      X(I)=BX(I)
      Y(I)=BY(I)
```

```
  103 CONTINUE
   41 ICOUNT=ICOUNT+1
      GO TO 40
C
   54 DO 104 I=1,NDJ
      X(I)=CX(I)
      Y(I)=CY(I)
  104 CONTINUE
      KA=2
      KB=2
      GO TO 41
C
C  55 DO 105 I=1,NDJ
C     X(I)=DX(I)
C     Y(I)=DY(I)
C 105 CONTINUE
C     KA=1
C     KB=1
C     GO TO 41
C
   59 DO 115 I=1,NDJ
      X(I)=EX(I)
      Y(I)=EY(I)/EX(I)
  115 CONTINUE
      KA=1
      KB=1
      GO TO 41
C
   60 DO 116 I=1,NDJ
      X(I)=FX(I)
      Y(I)=FY(I)
  116 CONTINUE
      KA=1
      KB=1
      GO TO 41
C
   57 NF=0
      CALL CGPL(X,Y,X,ND,NF,KA,KB,KC,0,HA,HB,8.0,VA,VB,
     ¢4.75,ALPHA,+6)
      RETURN
      END
C
C
C
      SUBROUTINE BOX(X0,Y0,X1,Y1,PAGE)
      CALL PLOT(X0,Y0,3)
      CALL PLOT(X0,Y1,2)
      CALL PLOT(X1,Y1,2)
      CALL PLOT(X1,Y0,2)
      CALL PLOT(X0,Y0,2)
      CALL PSYM(8.9,-0.85,0.15,PAGE,270.0,4)
   20 RETURN
      END
C
```

```
C
C
      SUBROUTINE LINXY(X,Y,NDJ,A,BETA,SIGMAA,SIGBET,RAA,VAR)
      IMPLICIT REAL*8(A-H,O-Z)
      DIMENSION X(160),Y(160)
      SUM=0.0
      SUMX=0.0
      SUMY=0.0
      SUMX2=0.0
      SUMXY=0.0
      SUMY2=0.0
C
      DO 50 I=1,NDJ
      WET=1.0
      SUM=SUM+WET
      SUMX=SUMX+WET*X(I)
      SUMY=SUMY+WET*Y(I)
      SUMX2=SUMX2+WET*X(I)*X(I)
      SUMXY=SUMXY+WET*X(I)*Y(I)
      SUMY2=SUMY2+WET*Y(I)*Y(I)
   50 CONTINUE
C
      DELTA=SUM*SUMX2-SUMX*SUMX
      A=(SUMX2*SUMY-SUMX*SUMXY)/DELTA
      BETA=(SUMXY*SUM-SUMX*SUMY)/DELTA
      CJ=NDJ-2
      S1=SUMY2+A*A*SUM+BETA*BETA*SUMX2
      S2=A*SUMY+BETA*SUMXY-A*BETA*SUMX
      VAR=(S1-2*S2)/CJ
      SIGMAA=DSQRT(VAR*SUMX2/DELTA)
      SIGBET=DSQRT(VAR*SUM/DELTA)
      DEN=DSQRT(DELTA*(SUM*SUMY2-SUMY*SUMY))
      RAA=(SUM*SUMXY-SUMX*SUMY)/DEN
      RETURN
      END
C
C
C
      SUBROUTINE LAGINT(P,T,TR,PR,Z,DR,VS)
C
C     This subroutine performs Lagrangian Interpolation
C     within a set of (TF,ZF) pairs to give the Z value
C     corresponding to any TF. The degree of the
C     interpolating polynomial is one less than the number
C     of points supplied.
C     TF = Temperatures in deg. Kelvin
C     T  = Desired Temperature in deg. Kelvin
C     ZF = Compressibility factor, dimensionless
C     Z  = Desired Compressibility factor.
C     PA = Desired Pressure in Atmospheric Pressure
C     P  = Desired Pressure in kPa
C     DR = Reduced density
C     VS = Viscosity in micro-Pascal.seconds
C
```

```
      IMPLICIT REAL*8(A-H,O-Z)
      DIMENSION TF(3),ZF(3)
      DATA TF/2.90D+02,3.00D+02,3.10D+02/
      ZC=0.290
      N=3
      PA=P/1.01325D+02
      ZF(1)=0.99999064D+00-0.26875701D-03*PA+0.20388746D-05
     ¢*PA*PA+0.50842660D-08*PA*PA*PA
      ZF(2)=1.00000000D+00-0.18372581D-03*PA+0.21148108D-05
     ¢*PA*PA+0.26213210D-08*PA*PA*PA
      ZF(3)=0.99999132D+00-0.10218783D-03*PA+0.18772473D-05
     ¢*PA*PA+0.25452826D-08*PA*PA*PA
      Z=0.0
      DO 20 I=1,N
      TERM=ZF(I)
      DO 10 J=1,N
      IF(I.EQ.J) GO TO 10
      ZF(I)=ZF(I)*(T-TF(J))/(TF(I)-TF(J))
   10 CONTINUE
      Z=Z+ZF(I)
   20 CONTINUE
      VS=1.0D+05*(0.1778D-03*(1.+0.8958D-03*(PA-1.)
     ¢+0.612D-06*(PA-1.)*(PA-1.)+0.3997D-07*(PA-1.)*(PA-1.)
     ¢*(PA-1.))+0.455D-06*(T-(273.16+25)))
      DR=ZC*PR/(Z*TR)
      RETURN
      END
```

```
C                                   RENO
C
CCCCCCCCCCCCCCCCCCCCCCCCCCCCCCCCCCCCCCCCCCCCCCCCCCCCCCCCCCCCCC
C
C      THIS PROGRAM PERFORMS A MULTIPLE LINEAR REGRESSION
C      FIT USING LEAST SQUARES FOR NUMERICAL PARAMETER
C      ESTIMATION.
C
C      THE MODEL EQUATIONS ARE TRUNCATED, FOR THIS PROGRAM,
C      BY NEGLECTING THEIR COMBINED VARIABLES.
C
C      Subroutines: LAGINT, MFIT, MTIV
C
CCCCCCCCCCCCCCCCCCCCCCCCCCCCCCCCCCCCCCCCCCCCCCCCCCCCCCCCCCCCCC
C
C      EM=MOLECULAR WEIGHT
C      TR,PR,DR=REDUCED TEMPERATURE,PRESSURE, AND DENSITY
     ¢RESPECTIVELY
C      VIS=VISCOSITY IN MICRO-PA.S
C      GG=GAS GRAVITY
       IMPLICIT REAL*8(A-H,O-Z)
       REAL *4 DIRECT
       REAL *8 DLOG,DABS
       DIMENSION PE(60),PW(60),TE(60),TW(60),PM(60),W(60),
     ¢VIS(60),ZA(60),PB(60),CP(60),TS(60),QO(60),PEW(60),
     ¢YF(60),CC1(60),CC2(60),CC3(60),XMEAN(60),X(60,5),C(5),
     ¢TCE(60),TCW(60),E(60),A(5,5),B(5),ER(60),DIRECT(5),
     ¢ERR(60),DP(60),CC4(60),CC5(60),REY(60),RD(60),Y(60)
       DATA TC,EM,PC,SIG/1.262D+02,2.8013D+01,3.35D+01,
     ¢3.798D+00/
       GG=EM/2.896D+01
       PCA=PC*(1.01325D+02)
       READ(5,1) NUM,NO,DIRECT,IFLAG
       READ(5,90) RE,RW,H,POR
       READ(5,3) NDJ
       READ(5,4) R
C
       IF(IFLAG.NE.(100))  GO TO 81
       RE=RE*3.048D-01
       RW=RW*3.048D-01
       H=H*3.048D-01
       GO TO 81
   81  WRITE(6,2) NUM,NO,DIRECT
       WRITE(6,89) RE,RW,H,POR
C      WRITE(6,5) R
       C1=((1.2954909D-03)*DLOG(RE/RW))/H
       C2=((2.9228842D-15)*GG*(1/RW-1/RE))/H*H
       C3=(6.5946061D-21)*GG*GG*(1/(RW*RW)-1/(RE*RE))/H*H*H
    1  FORMAT(A4,A4,5A4,I3)
   90  FORMAT(4F10.7)
    3  FORMAT(I2)
    2  FORMAT(/4X,'CORE SAMPLE NO ',A4,2X,'RUN ',A4,2X,5A4)
```

```
  89 FORMAT(4X,'RE=',F10.7,2X,'RW=',F10.7,2X,'H=',F10.7,
    ¢2X,'POROSITY=',F10.7)
   4 FORMAT(F10.6)
   5 FORMAT(4X,'R=',F10.6)
     IF(IFLAG.EQ.(100)) GO TO 67
C
     READ(5,6)(PE(I),PW(I),CP(I),PB(I),TCE(I),TCW(I),TS(I)
    ¢,I=1,NDJ)
   6 FORMAT(7F11.4)
C    WRITE(6,7)
   7 FORMAT('1',14X,'PE',12X,'PW',12X,'CP',12X,'PB',11X,
    ¢'TCE',12X,'TCW',12X,'TS',/13X,'(PSI)',9X,'(PSI)',9X,
    ¢'(PSI)',9X,'(CMHG)',7X,'(MVOLT)',8X,'(MVOLT)',8X,
    ¢'(SEC)'/)
C    WRITE(6,8)(PE(I),PW(I),CP(I),PB(I),TCE(I),TCW(I),TS(I)
C   ¢,I=1,NDJ)
   8 FORMAT(6X,7E14.4)
C
     DO 9 I=1,NDJ
     PB(I)=PB(I)*1.33322D+00
     PE(I)=PB(I)+PE(I)*6.894757D+00
     PW(I)=PB(I)+PW(I)*6.894757D+00
     CP(I)=PB(I)+CP(I)*6.894757D+00
     TE(I)=((TCE(I)+2.145588250D-02)/4.046470588D-02)
    ¢+273.15
     TW(I)=((TCW(I)+2.145588250D-02)/4.046470588D-02)
    ¢+273.15
     W(I)=(TE(I)+TW(I))/2.
     QO(I)=(6.116438868D+02)/TS(I)
   9 CONTINUE
     GO TO 82
C
  67 READ(5,86) (PE(I),PW(I),W(I),QO(I),CP(I),I=1,NDJ)
  86 FORMAT(5F12.8)
     DO 68 I=1,NDJ
     PE(I)=PE(I)*6.894757D+00
     PW(I)=PW(I)*6.894757D+00
     W(I)=((W(I)-3.2D+01)/1.8D+00)+2.7315D+02
     QO(I)=QO(I)*2.86364D+01
     CP(I)=CP(I)*6.894757D+00
  68 CONTINUE
C
  82 DO 84 I=1,NDJ
     PM(I)=(PE(I)+PW(I))/2.
     P=PM(I)
     PR=P/PCA
     T=W(I)
     TR=T/TC
C
     CALL LAGINT(P,T,TR,PR,Z,DR,VS)
     ZA(I)=Z
     RD(I)=DR
     VIS(I)=VS
C
```

```
      PEW(I)=2.*(PE(I)-PW(I))
      CC1(I)=C1*ZA(I)*VIS(I)*T*QO(I)
      CC2(I)=C2*ZA(I)*T*QO(I)*QO(I)
      CC3(I)=CC2(I)/PM(I)
      CC4(I)=C3*ZA(I)*T*QO(I)*QO(I)*QO(I)
      CC5(I)=CC4(I)/PM(I)
   84 CONTINUE
C     WRITE(6,38)
      M=1
      ICOUNT=1
C     WRITE(6,43)
   43 FORMAT(/6X,'Y',13X,'X1',14X,'X2',11X,'X3')
      DO 52 I=1,NDJ
      Y(I)=(PE(I)*PE(I)-PW(I)*PW(I))/(CC1(I))
      X(I,1)=(-PEW(I)/CC1(I))
      X(I,2)=CC2(I)/(CC1(I))
   52 CONTINUE
C
      READ(5,18) EK1,BE1,BETA1,GAMA1
      READ(5,19) EKC,BETAC,GAMAC
   18 FORMAT(4E20.5)
   19 FORMAT(3E20.5)
C
      N=2
   63 NU=NDJ-N
      FNU=NU
C
      CALL MFIT(X,Y,NDJ,N,CO,C,A,DET,YF,XSQR)
C
      WRITE(6,151) DET,(C(J),J=1,N)
  151 FORMAT(6E20.5)
C
      IF(ICOUNT-3) 73,95,95
   73 IF(ICOUNT-2) 65,66,95
   65 EK=1.0/CO
      BE=C(1)
      BETA=C(2)
      WRITE(6,59) EK,BE,BETA,XSQR
   59 FORMAT(/8X,'K=',G12.5,9X,'BE=',G13.5,8X,'BETA=',
     ¢G12.5,10X,'XSQR=',G12.5)
      GO TO 70
C
   66 EKA=1.0/CO
      BETA=C(1)
      GAMA=C(2)
      WRITE(6,71) EKA,BETA,GAMA,XSQR
   71 FORMAT(/9X,'KABS=',G12.5,6X,'BETA=',G13.5,8X,'GAMA=',
     ¢G12.5,/6X,'XSQR=',G12.5)
      GO TO 70
C
   95 EK=1/CO
      BE=C(1)
      BETA=C(2)
      GAMA=C(3)
```

```
      WRITE(6,96) EK,BE,BETA,GAMA,XSQR
   96 FORMAT(/11X,'K=',G12.5,18X,'BE=',G12.5,12X,'BETA=',
     ¢G12.5,/8X,'GAMA=',G12.5,14X,'XSQR=',G12.5)
C
   70 WRITE(6,54)
   54 FORMAT(/16X,'LIN.CORR.COEF')
      DO 58 J=1,N
   58 WRITE(6,55) (A(J,JJ),JJ=1,N)
   55 FORMAT(4X,5E14.5)
C
C     POR=((1.0665790D+06)*(DABS(EK)**(-1.12))/BETA)**
     ¢(1./1.67)
      WRITE(6,40) DET,POR
   40 FORMAT(12X,'DETERMINANT=',E14.5/4X,'FRACTIONAL
     ¢POROSITY=',E14.5)
      SSQ=0.0
      DO 69 I=1,NDJ
      ER(I)=(Y(I)-YF(I))
      ERR(I)=(ER(I)/Y(I))
      SSQ=SSQ+(ER(I)*ER(I))
   69 CONTINUE
      WRITE(6,41)
   41 FORMAT(/9X,'Y OBSERVED',6X,'Y CALC',8X,'REL.ERR')
      WRITE(6,42) (Y(I),YF(I),ERR(I),I=1,NDJ)
   42 FORMAT(6X,3E14.5)
C
      S=(SSQ/(NDJ-N))**0.5
      WRITE(6,85) SSQ,S
   85 FORMAT(/4X,'SSQ=',E11.4,9X,'STD.DEV.=',E11.4/)
C
      IF(ICOUNT-2) 60,94,64
C
   60 N=2
      DO 62 I=1,NDJ
      Y(I)=(PE(I)*PE(I)-PW(I)*PW(I))/CC1(I)
      X(I,1)=CC2(I)/CC1(I)
      X(I,2)=CC4(I)/CC1(I)
   62 CONTINUE
      ICOUNT=ICOUNT+1
      GO TO 63
C
   94 N=3
      DO 99 I=1,NDJ
      Y(I)=(PE(I)*PE(I)-PW(I)*PW(I))/CC1(I)
      X(I,1)=-PEW(I)/CC1(I)
      X(I,2)=CC2(I)/CC1(I)
      X(I,3)=CC4(I)/CC1(I)
   99 CONTINUE
      ICOUNT=ICOUNT+1
      GO TO 63
C
C     WRITE(6,38)
   64 WRITE(6,36)
   36 FORMAT(/14X,'PE',12X,'PW',12X,'RD',10X,'VIS',12X,
```

```
     ¢'T',13X,'ZA',13X,'QO',/13X,'(KPA)',9X,'(KPA)',19X,
     ¢'(MICRO-PA.S)',5X,'(DEG K)',20X,'(CU M/D)'/)
      WRITE(6,37)(PE(I),PW(I),RD(I),VIS(I),W(I),ZA(I),QO(I)
     ¢,I=1,NDJ
C     WRITE(6,38)
   37 FORMAT(6X,7E14.4)
C  38 FORMAT(///)
      STOP
      END
C
C
C
      SUBROUTINE MFIT(X,Y,NDJ,N,CO,C,A,DET,YF,XSQR)
      IMPLICIT REAL*8(A-H,O-Z)
      REAL*8 DLOG,DABS
      DIMENSION A(5,5),E(60),D(60,5),DT(5,60),
     ¢X(60,5),Y(60),YF(60),XMEAN(60),C(5),B(5)
C
      FNDJ=NDJ
      SUM=FNDJ
      YMEAN=0.0
      DO 28 J=1,N
      XMEAN(J)=0.0
   28 CONTINUE
C
C  ACCUMULATE SUMS
C
      DO 50 I=1,NDJ
      YMEAN=YMEAN+Y(I)
      DO 44 J=1,N
   44 XMEAN(J)=XMEAN(J)+X(I,J)
   50 CONTINUE
      YMEAN=YMEAN/SUM
      DO 53 J=1,N
   53 XMEAN(J)=XMEAN(J)/SUM
C
C     ACCUMULATE MATRICES B AND A
C
      DO 67 I=1,NDJ
      E(I)=Y(I)-YMEAN
      DO 67 J=1,N
      D(I,J)=X(I,J)-XMEAN(J)
   67 CONTINUE
C
      DO 20 I=1,NDJ
      DO 20 J=1,N
      DT(J,I)=D(I,J)
   20 CONTINUE
      DO 22 J=1,N
      DO 22 K=1,N
      A(J,K)=0.0
      B(J)=0.0
      DO 22 I=1,NDJ
      A(J,K)=A(J,K)+DT(J,I)*D(I,K)
```

```
      B(J)=B(J)+DT(J,I)*E(I)
   22 CONTINUE
C
C     INVERT SYMMETRIC MATRIX
C
      CALL MTINV(A,N,DET)
C
C     IF(DET) 101,91,101
C  91 C0=0.0
C     XSQR=0.0
C     GO TO 150
C
C     CALCULATE COEFFICIENTS
C
  101 C0=YMEAN
      XSQ=0.0
      DO 17 I=1,NDJ
   17 YF(I)=0.0
      DO 108 J=1,N
      C(J)=0.0
      DO 104 K=1,N
  104 C(J)=C(J)+A(J,K)*B(K)
      C0=C0-C(J)*XMEAN(J)
      DO 108 I=1,NDJ
  108 YF(I)=YF(I)+X(I,J)*C(J)
      FREEN=NDJ-N-1
      DO 113 I=1,NDJ
      YF(I)=YF(I)+C0
  113 XSQ=XSQ+(Y(I)-YF(I))*(Y(I)-YF(I))
      XSQR=XSQ/FREEN
C 150 RETURN
      RETURN
      END
C
C
C
C
      SUBROUTINE MTINV(A,N,DET)
      IMPLICIT REAL*8(A-H,O-Z)
      DIMENSION A(5,5),IK(5),JK(5)
C
C     This subroutine inverts asymmetric matrix and
C     calculates its determinant.
C
      DET=1.0
      DO 91 K=1,N
C
      T=0.0
   21 DO 30 I=K,N
      DO 30 J=K,N
      IF(DABS(T)-DABS(A(I,J))) 24,24,30
   24 T=A(I,J)
      IK(K)=I
      JK(K)=J
```

```
   30 CONTINUE
C
      IF(T)41,32,41
   32 DET=0.0
      GO TO 98
   41 I=IK(K)
      IF(I-K)21,51,43
   43 DO 50 J=1,N
      SAVE=A(K,J)
      A(K,J)=A(I,J)
   50 A(I,J)=-SAVE
   51 J=JK(K)
      IF(J-K) 21,61,53
   53 DO 73 I=1,N
      SAVE=A(I,K)
      A(I,K)=A(I,J)
   73 A(I,J)=-SAVE
C
   61 DO 70 I=1,N
      IF(I-K) 63,70,63
   63 A(I,K)=-A(I,K)/T
   70 CONTINUE
      DO 80 I=1,N
      DO 80 J=1,N
      IF(I-K) 74,80,74
   74 IF(J-K) 75,80,75
   75 A(I,J)=A(I,J)+A(I,K)*A(K,J)
   80 CONTINUE
      DO 90 J=1,N
      IF(J-K) 83,90,83
   83 A(K,J)=A(K,J)/T
   90 CONTINUE
      A(K,K)=1.0/T
   91 DET=DET*T
C
      DO 97 L=1,N
      K=N-L+1
      J=IK(K)
      IF(J-K) 94,94,92
   92 DO 93 I=1,N
      SAVE=A(I,K)
      A(I,K)=-A(I,J)
   93 A(I,J)=SAVE
   94 I=JK(K)
      IF(I-K) 97,97,95
   95 DO 96 J=1,N
      SAVE=A(K,J)
      A(K,J)=-A(K,J)
   96 A(I,J)=SAVE
   97 CONTINUE
   98 RETURN
      END
```

```
C                               POLY
C
CCCCCCCCCCCCCCCCCCCCCCCCCCCCCCCCCCCCCCCCCCCCCCCCCCCCCCCCCCCCC
C
C      THIS PROGRAM PERFORMS A MULTIPLE LINEAR REGRESSION
C      CURVE FIT USING LEAST SQUARES, TO DETERMINE THE BEST
C      FIT.
C
C      Uses : Applot+*Plotlib on object file
C
C      Subroutines: LAGINT, MFIT, XPLOT, BOX, MTINV
C
CCCCCCCCCCCCCCCCCCCCCCCCCCCCCCCCCCCCCCCCCCCCCCCCCCCCCCCCCCCCC
C
C      EM=MOLECULAR WEIGHT
C      TR,PR,DR=REDUCED TEMPERATURE,PRESSURE, AND DENSITY
C      RESPECTIVELY
C      VIS=VISCOSITY IN MICRO-PA.S
C      GG=GAS GRAVITY
       IMPLICIT REAL*8(A-H,O-Z)
       REAL *4 DIRECT
       REAL *8 DLOG,DABS
       DIMENSION PE(60),PW(60),TE(60),TW(60),PM(60),W(60),
      ¢VIS(60),ZA(60),PB(60),CP(60),TS(60),QO(60),PEW(60),
      ¢YF(60),CC1(60),CC2(60),CC3(60),XMEAN(60),X(60,5),
      ¢TCE(60),TCW(60),E(60),A(5,5),B(5),ER(60),HY(60),
      ¢ERR(60),DP(60),CC4(60),CC5(60),AX(60),AY(60),BY(60),
      ¢CX(60),DY(60),EY(60),GY(60),FRC(60),RET(60),FRCM(60),
      ¢FRTM(60),SFT(60),SFC(60),DIRECT(5),RD(60),Y(60),C(5)
       DATA TC,EM,PC,SIG/1.262D+02,2.8013D+01,3.35D+01,
      ¢3.798D+00/
       GG=EM/2.896D+01
       PCA=PC*(1.01325D+02)
       READ(5,1) NUM,NO,DIRECT,IFLAG
       READ(5,90) RE,RW,H,POR
       READ(5,3) NDJ
       READ(5,4) R
C
       IF(IFLAG.NE.(100))  GO TO 81
       RE=RE*3.048D-01
       RW=RW*3.048D-01
       H=H*3.048D-01
       GO TO 81
   81  WRITE(6,2) NUM,NO,DIRECT
       WRITE(6,89) RE,RW,H,POR
C      WRITE(6,5) R
       C1=((1.29549O9D-03)*DLOG(RE/RW))/H
       C2=((2.9228842D-15)*GG*(1/RW-1/RE))/H*H
       C3=(6.5946061D-21)*GG*GG*(1/(RW*RW)-1/(RE*RE))/H*H*H
    1  FORMAT(A4,A4,5A4,I3)
   90  FORMAT(4F10.7)
    3  FORMAT(I3)
    2  FORMAT(/4X,'CORE SAMPLE NO ',A4,2X,'RUN ',A4,2X,5A4)
   89  FORMAT(4X,'RE=',F10.7,2X,'RW=',F10.7,2X,'H=',F10.7,
```

```
     ¢2X,'POROSITY=',F10.7)
    4 FORMAT(F10.6)
    5 FORMAT(4X,'R=',F10.6)
      IF(IFLAG.EQ.(100)) GO TO 67
C
      READ(5,6)(PE(I),PW(I),CP(I),PB(I),TCE(I),TCW(I),TS(I)
     ¢,I=1,NDJ)
    6 FORMAT(7F11.4)
C     WRITE(6,7)
    7 FORMAT('1',14X,'PE',12X,'PW',12X,'CP',12X,'PB',11X,
     ¢'TCE',12X,'TCW',12X,'TS',/13X,'(PSI)',9X,'(PSI)',9X,
     ¢'(PSI)',9X,(CMHG)',7X,'(MVOLT)',8X,'(MVOLT)',8X,
     ¢'(SEC)'/)
C     WRITE(6,8)(PE(I),PW(I),CP(I),PB(I),TCE(I),TCW(I),TS(I)
C    ¢,I=1,NDJ)
    8 FORMAT(6X,7E14.4)
C
      DO 9 I=1,NDJ
      PB(I)=PB(I)*1.33322D+00
      PE(I)=PB(I)+PE(I)*6.894757D+00
      PW(I)=PB(I)+PW(I)*6.894757D+00
      CP(I)=PB(I)+CP(I)*6.894757D+00
      TE(I)=((TCE(I)+2.145588250D-02)/4.046470588D-02)
     ¢+273.15
      TW(I)=((TCW(I)+2.145588250D-02)/4.046470588D-02)
     ¢+273.15
      W(I)=(TE(I)+TW(I))/2.
      QO(I)=(6.116438868D+02)/TS(I)
    9 CONTINUE
      GO TO 82
C
   67 READ(5,86) (PE(I),PW(I),W(I),QO(I),CP(I),I=1,NDJ)
   86 FORMAT(5F12.8)
      DO 68 I=1,NDJ
      PE(I)=PE(I)*6.894757D+00
      PW(I)=PW(I)*6.894757D+00
      W(I)=((W(I)-3.2D+01)/1.8D+00)+2.7315D+02
      QO(I)=QO(I)*2.86364D+01
      CP(I)=CP(I)*6.894757D+00
   68 CONTINUE
C
   82 DO 84 I=1,NDJ
      PM(I)=(PE(I)+PW(I))/2.
      P=PM(I)
      PR=P/PCA
      T=W(I)
      TR=T/TC
C
      CALL LAGINT(P,T,TR,PR,Z,DR,VS)
      ZA(I)=Z
      RD(I)=DR
      VIS(I)=VS
C
      PEW(I)=2.*(PE(I)-PW(I))
```

```
      CC1(I)=C1*ZA(I)*VIS(I)*T*QO(I)
      CC2(I)=C2*ZA(I)*T*QO(I)*QO(I)
      CC4(I)=CC2(I)/PM(I)
      CC3(I)=C3*ZA(I)*T*QO(I)*QO(I)*QO(I)
      CC5(I)=CC3(I)/PM(I)
   84 CONTINUE
C     WRITE(6,38)
      READ(5,18) EK1,BE1,BETA1,GAMA1
      READ(5,19) EKC,BETAC,GAMAC
   18 FORMAT(4E20.5)
   19 FORMAT(3E20.5)
      ICOUNT=1
C
      N=3
      CO=0.0
      DO 52 I=1,NDJ
      Y(I)=(PE(I)*PE(I)-PW(I)*PW(I))
      X(I,1)=QO(I)
      X(I,2)=QO(I)*QO(I)
      X(I,3)=QO(I)*QO(I)*QO(I)
   12 FORMAT(4G14.5)
   52 CONTINUE
   63 NU=NDJ-N
      FNU=NU
C
      CALL MFIT(X,Y,NDJ,N,CO,C,A,DET,YF,XSQR)
C
C     WRITE(6,151) DET,(C(J),J=1,N)
C 151 FORMAT(6E20.5)
C
      IF(ICOUNT-2) 66,97,105
C
   66 DO 15 I=1,NDJ
      CX(I)=QO(I)
      DY(I)=Y(I)
      EY(I)=YF(I)
   15 CONTINUE
      WRITE(6,111)
  111 FORMAT(/4X,'Back Pressure Cubic Fit')
      WRITE(6,59) C(1),C(2),C(3),XSQR,DET
   59 FORMAT(/8X,'C(1)=',G12.5,9X,'C(2)=',G13.5,8X,'C(3)=',
     ¢G12.5,10X,'XSQR=',G12.5,4X,'DETERMINANT=',G12.5)
      GO TO 70
C
   97 EK=1.0/CO
      BETA=C(1)
      GAMA=C(2)
      DO 10 I=1,NDJ
      AX(I)=X(I,1)
      AY(I)=Y(I)
      BY(I)=YF(I)
   10 CONTINUE
      WRITE(6,60)
   60 FORMAT(/4X,'Visco-Inertial Cubic Fit')
```

```
C     WRITE(6,71) EK,BETA,GAMA,XSQR,DET
   71 FORMAT(/9X,'KABS=',G12.5,6X,'BETA=',G13.5,8X,'GAMA=',
     ¢G12.5,/6X,'XSQR=',G12.5,4X,'DETERMINANT=',G12.5)
      GO TO 70
C
  105 EK=1.0/C0
      BETA=C(1)
      DO 106 I=1,NDJ
      HY(I)=YF(I)
  106 CONTINUE
      WRITE(6,104)
  104 FORMAT(/4X,'Visco-Inertial Quadratic Fit')
      WRITE(6,107) EK,BETA,XSQR,DET
  107 FORMAT(/9X,'KABS=',G12.5,6X,'BETA=',G13.5,8X,'XSQR=',
     ¢G12.5,4X,'DETERMINANT=',G12.5)
C
   70 WRITE(6,54)
   54 FORMAT(/16X,'LIN.CORR.COEF')
      DO 58 J=1,N
   58 WRITE(6,55) (A(J,JJ),JJ=1,N)
   55 FORMAT(4X,5E14.5)
C
      SSQ=0.0
      DO 69 I=1,NDJ
      ER(I)=(Y(I)-YF(I))
      ERR(I)=(ER(I)/Y(I))
      SSQ=SSQ+(ER(I)*ER(I))
C
C     EVALUATION OF REYNOLDS NUMBERS AND FRICTION FACTORS
C
C     EK1, BETA1, GAMA1 are parameters obtained with the
C     truncated plot points.
C     EKC, BETAC, GAMAC are parameters obtained with the
C     complete plot points.
C
      REC(I)=(CC2(I)*EKC*BETAC)/CC1(I)
      RET(I)=(CC2(I)*EK1*BETA1)/CC1(I)
      SFC(I)=(CC3(I)*GAMAC)/(CC2(I)*BETAC)
      SFT(I)=(CC3(I)*GAMA1)/(CC2(I)*BETA1)
      FRC(I)=64.0*(PE(I)*PE(I)-PW(I)*PW(I))/(CC2(I)*BETAC))
      FRT(I)=64.0*(PE(I)*PE(I)-PW(I)*PW(I))/(CC2(I)*BETA1))
      FRCM(I)=64.0(1.0/REC(I)+1.0+SFC(I))
      FRTM(I)=64.0(1.0/RET(I)+1.0+SFT(I))
   69 CONTINUE
C     WRITE(6,46)
   46 FORMAT(/6X,'PARAMETERS FOR REYNOLDS NO AND FRICTION
     ¢FACTOR')
C     WRITE(6,44) EK1,BE1,BETA1
   44 FORMAT(4X,'K=',E11.4,5X,'B=',E11.4,5X,'BETA=',E11.4)
C     WRITE(6,41)
   41 FORMAT(/9X,'X(I,1)',6X,'Y OBSERVED',6X,'Y CALC',8X,
     ¢'REL.ERR',9X,'REY',6X,'FR.FACTOR')
C     WRITE(6,42) (X(I,1),Y(I),YF(I),ERR(I),REB(I),FRB(I)
     ¢,I=1,NDJ)
```

```
   42 FORMAT(6X,6E14.5)
C
      S=(SSQ/(NDJ-N))**0.5
C     WRITE(6,85) SSQ,S
   85 FORMAT(/4X,'SSQ=',E11.4,9X,'STD.DEV.=',E11.4/)
C
      IF(ICOUNT-2) 64,102,23
C
   64 N=2
      DO 62 I=1,NDJ
      Y(I)=(PE(I)*PE(I)-PW(I)*PW(I))/CC1(I)
      X(I,1)=CC2(I)/CC1(I)
      X(I,2)=CC3(I)/CC1(I)
   62 CONTINUE
      ICOUNT=ICOUNT+1
      GO TO 63
C
  102 N=1
      DO 103 I=1,NDJ
      Y(I)=(PE(I)*PE(I)-PW(I)*PW(I))/CC1(I)
      X(I,1)=CC2(I)/CC1(I)
  103 CONTINUE
      ICOUNT=ICOUNT+1
      GO TO 63
C
   23 WRITE(6,414)
  414 FORMAT(/2X,'REC',3X,'FRT',5X,'RET',7X,'FRT',6X,
     ¢'FRCM',6X,'FRTM',4X,'SFC',4X,'SFT')
      WRITE(6,424)(REC(I),FRC(I),RET(I),FRT(I),FRCM(I),
     ¢FRTM(I),SFC(I),SFT(I),I=1,NDJ)
  424 FORMAT(F6.3,F7.2,F8.3,3F10.2,2F7.3)
C
C     WRITE(6,38)
C     WRITE(6,36)
   36 FORMAT(/14X,'PE',12X,'PW',12X,'RD',10X,'VIS',12X,
     ¢'T',13X,'ZA',13X,'QO',/13X,'(KPA)',9X,'(KPA)',19X,
     ¢'(MICRO-PA.S)',5X,'(DEG K)',20X,'(CU M/D)'/)
C     WRITE(6,37)(PE(I),PW(I),RD(I),VIS(I),W(I),ZA(I),QO(I)
C    ¢,I=1,NDJ)
C     WRITE(6,38)
   37 FORMAT(6X,7E14.4)
C  38 FORMAT(///)
C
      CALL XPLOT(AX,AY,BY,CX,DY,EY,GY,HY,REC,FRC,RET,FRT,
     ¢NDJ,IFLAG,DIRECT,FRCM,FRTM)
C
      STOP
      END
C
C
C
      SUBROUTINE XPLOT(AX,AY,BY,CX,DY,EY,GY,HY,REC,FRC,RET,
     ¢FRT,NDJ,IFLAG,DIRECT,FRCM,FRTM)
      IMPLICIT REAL*8(A-H,O-Z)
```

```
      REAL*4 X,Y,ALPHA,DIRECT,CPTYPE
      DIMENSION AX(60),BY(60),AY(60),ALPHA(20),X(60),Y(60),
     ¢CX(60),DY(60),EY(60),GY(60),REB(60),FRB(60),HY(60),
     ¢RET(60),FRT(60),REG(60),FRG(60),CPTIT(2),DIRECT(5),
     ¢TYPE(2),CPTYPE(5)
      REAL *8 TITLE(9)/'EXPTAL  ','CUBIC FN','QUAD. FN',
     ¢'EXPTAL  ','CUBIC FN','EXPTAL ','EQN. 8.7',
     ¢,'EXPTAL  ','EQN. 8.7'/
      XSIZE=8.0
      YSIZE=4.75
      ND=NDJ
      KA=1
      KB=1
      KC=1
      READ(5,4) CPTIT
      WRITE(6,4) CPTIT
      READ(5,4) TYPE
      WRITE(6,4) TYPE
      READ(5.31) CPTYPE
      WRITE(6,31) CPTYPE
    4 FORMAT(2A8)
   31 FORMAT(5A4)
  555 FORMAT(I3)
C
   80 X0=-1.5
      Y0=-2.25
      X1=X0+11.0
      Y1=Y0+8.5
C
      DO 19 I=1,NDJ
      X(I)=AX(I)
   19 Y(I)=AY(I)
      N=1
   67 READ(7,21) HA,HB,VA,VB,PAGE
   21 FORMAT(4E20.4,A4)
      READ(7,20) ALPHA
   20 FORMAT(20A4
      NF=1
      CALL CGPEP1(7.0,7.0)
   17 CALL CGPL(X,Y,X,ND,NF,KA,KB,KC,0,HA,HB,8.0,VA,VB,
     ¢4.75,ALPHA,+6)
      IF(N.EQ.6.OR.N.EQ.7.OR.N.EQ.8.OR.N.EQ.9) GO TO 121
      GO TO 122
  122 CALL CGPEP5(-2.00,-2.00,TITLE(N),8,0.15,0.0)
      GO TO 177
  121 CALL CGPEP5(-7.50,-2.00,TITLE(N),8,0.15,0.0)
C
  177 CALL PLOT(8.0,4.75,3)
      CALL PLOT(8.0,4.5,2)
      CALL PLOT(0.0,0.0,3)
C
      IF(N.EQ.3.OR.N.EQ.5.OR.N.EQ.7.OR.N.EQ.9) GO TO 98
      GO TO 97
   98 CALL PSYM(5.70,0.95,0.15,CPTIT,0.0,16)
```

```
      CALL PSYM(5.70,0.70,0.15,TYPE,0.0,16)
      CALL PSYM(5.20,0.45,0.15,DIRECT,0.0,20)
      CALL PSYM(5.20,0.25,0.15,CPTYPE,0.0,20)
      CALL BOX(X0,Y0,X1,Y1,PAGE)
C
   97 IF(N-8) 45,139,6
   45 IF(N-7) 42,115,139
   42 IF(N-6) 41,8,115
   41 IF(N-5) 411,5,8
  411 IF(N-4) 23,9,5
   23 IF(N-3) 22,10,9
   22 IF(N-2) 12,11,10
C
   12 NF=3
      KC=1
      DO 18 I=1,NDJ
      X(I)=AX(I)
   18 Y(I)=BY(I)
   15 N=N+1
      IF(N.EQ.4) GO TO 67
      IF(N.EQ.6) GO TO 67
      IF(N.EQ.8) GO TO 67
      GO TO 17
C
   11 NF=130
      KC=1
      DO 30 I=1,NDJ
      X(I)=AX(I)
   30 Y(I)=HY(I)
      GO TO 15
C
   10 KA=2
      KB=2
      DO 16 I=1,NDJ
      X(I)=CX(I)
   16 Y(I)=DY(I)
      GO TO 15
C
    9 DO 14 I=1,NDJ
      X(I)=CX(I)
   14 Y(I)=DABS(EY(I))
      NF=3
      KC=1
      GO TO 15
C
    5 DO 44 I=1,NDJ
      X(I)=RET(I)
   44 Y(I)=FRT(I)
      GO TO 15
C
    8 DO 13 I=1,NDJ
      X(I)=RET(I)
   13 Y(I)=FRTM(I)
      NF=15
```

```
      KC=5
      GO TO 15
C
  115 DO 144 1,1,NDJ
      X(I)=REC(I)
  144 Y(I)=FRC(I)
      GO TO 15
C
  139 DO 138 I=1,NDJ
      X(I)=REC(I)
  138 Y(I)=FRCM(I)
      NF=3
      KC=5
      GO TO 15
C
    6 NF=0
      CALL CGPL(X,Y,X,ND,NF,KA,KB,KC,0,HA,HB,8.0,VA,VB,
     ¢4.75,ALPHA,+6)
      RETURN
      END
```

D.2 EXPERIMENTAL DATA LISTINGS

CORE SAMPLE NO 1C RUN 2 FORWARD DIRECTION
RE=0.15239 RW=0.00319 H=0.02568 POROSITY=0.10620

PE (PSI)	PW (PSI)	CP (PSI)	PB (CMHG)	TCE (MV)	TCW (MV)	TS (SEC)
12.000	3.2000	3.00	69.350	0.8650	0.8660	139.82
16.000	5.3000	5.00	69.350	0.8690	0.8700	107.90
20.000	9.1000	9.00	69.350	0.8760	0.8760	98.050
26.000	12.400	12.50	69.350	0.8870	0.8850	72.150
40.400	25.000	25.00	69.350	0.8900	0.8910	51.400
60.400	45.100	45.00	69.350	0.9000	0.8970	40.470
80.000	64.700	64.00	69.350	0.8990	0.9010	36.130
98.000	83.000	83.00	69.350	0.9000	0.8980	34.800
132.40	115.20	115.00	69.330	0.9060	0.9040	30.000
160.00	143.20	143.00	69.320	0.9090	0.9070	29.600
194.40	176.80	176.00	69.320	0.9140	0.9120	28.300
240.00	222.40	222.00	69.320	0.9150	0.9110	27.560
280.40	262.80	263.00	69.290	0.9090	0.9100	26.210
310.40	293.20	293.00	69.290	0.9200	0.9200	25.780
344.00	325.20	325.00	69.290	0.9230	0.9220	24.470
376.40	356.80	356.00	69.290	0.9250	0.9200	23.140
404.00	380.00	380.00	69.290	0.9250	0.9230	20.890
490.00	462.00	462.00	69.290	0.9290	0.9300	18.000
572.00	544.00	544.00	69.290	0.9230	0.9200	16.560

PE (KPA)	PW (KPA)	RD	VIS (U-PAS)	T (DEG K)	ZA	QO (M3/D)
175.20	114.52	0.005	17.646	295.07	0.9997	4.375
202.77	129.00	0.006	17.654	295.17	0.9996	5.669
230.35	155.20	0.007	17.666	295.33	0.9996	6.238
271.72	177.95	0.008	17.682	295.58	0.9995	8.477
371.01	264.83	0.012	17.702	295.69	0.9993	11.90
508.90	403.41	0.017	17.732	295.88	0.9991	15.11
644.04	538.55	0.022	17.756	295.92	0.9988	16.93
768.14	664.72	0.026	17.774	295.90	0.9986	17.58
1005.3	886.71	0.035	17.818	296.05	0.9982	20.39
1195.6	1079.7	0.042	17.852	296.12	0.9978	20.66
1432.8	1311.4	0.050	17.896	296.24	0.9975	21.61
1747.2	1625.8	0.062	17.947	296.24	0.9970	22.19
2025.7	1904.3	0.072	17.990	296.16	0.9966	23.34
2232.5	2113.9	0.079	18.037	296.42	0.9964	23.73
2464.2	2334.6	0.088	18.079	296.48	0.9962	25.00
2687.6	2552.4	0.096	18.117	296.48	0.9960	26.43
2877.9	2712.4	0.102	18.150	296.51	0.9958	29.28
3470.8	3277.8	0.123	18.261	296.65	0.9954	33.98
4036.2	3843.1	0.144	18.360	296.45	0.9951	36.94

CORE SAMPLE NO 1C RUN 2 REVERSE DIRECTION
RE=0.15239 RW=0.00319 H=0.02568 POROSITY=0.01620

PE (PSI)	PW (PSI)	CP (PSI)	PB (CMHG)	TCE (MV)	TCW (MV)	TS (SEC)
525.00	500.60	500.00	69.300	0.9210	0.9250	18.110
470.00	448.50	446.00	69.300	0.9230	0.9230	21.450
406.00	386.10	383.00	69.300	0.9170	0.9200	25.730
312.00	291.40	289.00	69.300	0.9190	0.9240	30.000
228.00	208.60	204.00	69.300	0.9190	0.9220	40.420
139.20	122.80	115.00	69.300	0.9200	0.9240	65.100

PE (KPA)	PW (KPA)	RD	VIS (U-PAS)	T (DEG K)	ZA	QO (M3/D)
3712.1	3543.9	0.133	18.302	296.49	0.9952	33.77
3332.9	3184.7	0.119	18.232	296.49	0.9954	28.51
2891.7	2754.5	0.103	18.148	296.38	0.9958	23.77
2243.6	2101.5	0.079	18.039	296.45	0.9964	20.39
1664.4	1530.6	0.058	17.941	296.43	0.9972	15.13
1052.1	939.07	0.036	17.845	296.47	0.9981	9.395

CORE SAMPLE NO 1C RUN 3 FORWARD DIRECTION
RE=0.15239 RW=0.00319 H=0.02568 POROSITY=0.10620

PE (PSI)	PW (PSI)	CP (PSI)	PB (CMHG)	TCE (MV)	TCW (MV)	TS (SEC)
8.0000	2.3000	400.00	70.280	0.8540	0.8540	167.70
12.000	4.5000	400.00	70.280	0.8550	0.8600	115.10
16.000	7.6000	400.00	70.280	0.8570	0.8600	93.150
20.000	11.400	400.00	70.280	0.8570	0.8650	82.300
27.800	19.200	400.00	70.280	0.8560	0.8640	69.300
36.000	27.900	400.00	70.280	0.8550	0.8640	62.600
44.000	35.900	400.00	70.280	0.8540	0.8630	56.200
54.000	45.600	400.00	70.280	0.8510	0.8640	49.500
66.400	56.900	400.00	70.400	0.8410	0.8540	40.500
84.000	73.900	400.00	70.400	0.8400	0.8510	36.810
96.800	86.000	400.00	70.400	0.8400	0.8560	32.700
108.00	96.600	400.00	70.400	0.8400	0.8590	30.280
120.40	107.60	400.00	70.400	0.8380	0.8570	27.500
136.00	123.00	400.00	70.400	0.8350	0.8550	25.700
150.40	136.00	400.00	70.400	0.8370	0.8550	24.220
169.40	154.20	400.00	70.400	0.8380	0.8550	23.200
196.40	180.70	400.00	70.400	0.8350	0.8560	22.300
219.20	200.40	400.00	70.400	0.8350	0.8550	21.100
248.00	228.00	400.00	70.400	0.8350	0.8550	19.900
278.00	257.00	400.00	70.400	0.8350	0.8550	19.080
316.80	296.80	400.00	70.540	0.8450	0.8550	18.850
353.20	331.20	400.00	70.540	0.8400	0.8570	17.640
382.80	358.80	400.00	70.540	0.8400	0.8580	16.290
438.00	416.00	416.00	70.540	0.8360	0.8560	15.900

PE (KPA)	PW (KPA)	RD	VIS (U-PAS)	T (DEG K)	ZA	QO (M3/D)
148.86	109.56	0.005	17.631	294.78	0.9997	3.647
176.44	124.73	0.006	17.638	294.87	0.9997	5.314
204.01	146.10	0.006	17.643	294.90	0.9996	6.566
231.59	172.30	0.007	17.650	294.96	0.9996	7.432
285.37	226.08	0.009	17.657	294.93	0.9994	8.826
341.91	286.06	0.011	17.666	294.92	0.9993	9.771
397.07	341.22	0.014	17.674	294.90	0.9992	10.88
466.02	408.10	0.016	17.683	294.87	0.9991	12.36
551.67	486.17	0.019	17.685	294.62	0.9989	15.10
673.02	603.38	0.023	17.702	294.57	0.9986	16.62
761.27	686.81	0.027	17.718	294.64	0.9985	18.70
838.49	759.89	0.029	17.732	294.67	0.9983	20.20
923.99	835.73	0.032	17.742	294.62	0.9982	22.24
1031.5	941.91	0.036	17.757	294.56	0.9980	23.80
1130.8	1031.5	0.040	17.773	294.59	0.9978	25.25
1261.8	1157.0	0.044	17.794	294.60	0.9976	26.36
1448.0	1339.7	0.051	17.823	294.57	0.9973	27.43
1605.2	1475.6	0.057	17.847	294.56	0.9970	28.99
1803.8	1665.9	0.064	17.879	294.56	0.9967	30.74
2010.6	1865.8	0.071	17.913	294.56	0.9964	32.06
2278.3	2140.4	0.081	17.964	294.69	0.9961	32.45
2529.3	2377.6	0.090	18.005	294.65	0.9957	34.67
2733.4	2567.9	0.097	18.040	294.66	0.9955	37.55
3113.9	2962.3	0.112	18.106	294.59	0.9951	38.47

CORE SAMPLE NO 1C   RUN 3   REVERSE DIRECTION
RE=0.15239 RW=0.00319 H=0.02568 POROSITY=0.10620

PE (PSI)	PW (PSI)	CP (PSI)	PB (CMHG)	TCE (MV)	TCW (MV)	TS (SEC)
438.00	416.00	416.00	70.540	0.8360	0.8560	15.900
412.00	391.70	400.00	70.540	0.8340	0.8550	16.700
382.00	362.50	400.00	70.720	0.7860	0.7970	17.400
350.00	332.00	400.00	70.720	0.7880	0.8010	18.300
280.40	263.10	400.00	70.580	0.8330	0.8440	19.400
260.00	245.10	400.00	70.540	0.8320	0.8450	20.600
220.00	205.20	400.00	70.540	0.8330	0.8450	21.200
180.00	166.40	400.00	70.540	0.8300	0.8450	22.470
140.00	126.60	400.00	70.560	0.8310	0.8410	25.300
104.00	89.800	400.00	70.560	0.8300	[illegible]	26.200
76.400	61.000	400.00	70.560	0.8340	0.8450	29.100
58.000	41.000	400.00	70.560	0.8300	0.8430	32.300
38.000	20.000	400.00	70.560	0.8250	0.8400	42.000
20.000	6.4000	400.00	70.560	0.8350	0.8410	78.200

PE (KPA)	PW (KPA)	RD	VIS (U-PAS)	T (DEG K)	ZA	QO (M3/D)
3113.9	2962.3	0.112	18.106	294.59	0.9951	38.47
2934.7	2794.7	0.105	18.073	294.55	0.9953	36.63
2728.1	2593.6	0.098	17.977	293.24	0.9952	35.15
2507.5	2383.3	0.090	17.943	293.31	0.9955	33.42
2027.4	1908.1	0.072	17.911	294.40	0.9963	31.53
1886.7	1784.0	0.067	17.888	294.40	0.9965	29.69
1610.9	1508.8	0.057	17.843	294.41	0.9970	28.85
1335.1	1241.3	0.047	17.797	294.38	0.9974	27.22
1059.3	966.95	0.037	17.751	294.34	0.9979	24.18
811.13	713.22	0.028	17.710	294.33	0.9984	23.35
620.83	514.65	0.021	17.684	294.43	0.9988	21.02
493.97	376.76	0.016	17.659	294.35	0.9990	18.94
356.07	231.97	0.011	17.633	294.25	0.9993	14.56
231.97	138.20	0.007	17.622	294.39	0.9996	7.822

CORE SAMPLE NO 1C RUN 4 FORWARD DIRECTION
RE=0.15239 RW=0.00319 H=0.02568 POROSITY=0.10620

PE (PSI)	PW (PSI)	CP (PSI)	PB (CMHG)	TCE (MV)	TCW (MV)	TS (SEC)
8.0000	2.1000	500.00	69.680	0.9100	0.9100	179.40
12.000	4.6000	500.00	69.680	0.9100	0.9130	129.80
18.000	9.4000	500.00	69.680	0.9100	0.9150	98.200
24.000	15.400	500.00	69.680	0.9120	0.9160	87.300
30.000	21.400	500.00	69.680	0.9100	0.9150	77.450
40.000	30.600	500.00	69.680	0.9100	0.9150	62.000
60.000	51.000	500.00	69.680	0.9100	0.9160	52.000
78.000	68.900	500.00	69.680	0.9080	0.9190	46.200
99.600	90.500	500.00	69.680	0.9080	0.9180	41.250
128.00	118.20	500.00	69.680	0.9080	0.9200	36.300
160.00	148.50	500.00	69.680	0.9050	0.9200	31.450
190.00	177.60	500.00	69.600	0.9080	0.9170	29.300
229.40	217.10	500.00	69.600	0.9080	0.9150	28.600
260.40	247.40	500.00	69.600	0.9080	0.9180	27.530
296.00	280.40	500.00	69.600	0.9070	0.9200	25.100
334.40	319.00	500.00	69.600	0.9070	0.9210	24.100
360.20	343.20	500.00	69.600	0.9050	0.9200	22.900
397.00	378.00	500.00	69.600	0.9050	0.9200	21.500
445.00	423.00	500.00	69.600	0.9040	0.9200	19.900
456.00	431.00	500.00	69.600	0.9030	0.9200	18.700
462.00	436.00	500.00	69.860	0.8610	0.8670	18.100

PE (KPA)	PW (KPA)	RD	VIS (U-PAS)	T (DEG K)	ZA	QO (M3/D)
148.06	107.38	0.005	17.694	296.17	0.9997	3.409
175.64	124.61	0.005	17.699	296.21	0.9997	4.712
217.00	157.71	0.007	17.706	296.23	0.9996	6.229
258.37	199.08	0.008	17.714	296.27	0.9995	7.006
299.74	240.45	0.010	17.719	296.23	0.9994	7.897
368.69	303.88	0.012	17.729	296.23	0.9993	9.865
506.58	444.53	0.017	17.752	296.24	0.9990	11.76
630.69	567.95	0.022	17.772	296.26	0.9988	13.24
779.62	716.87	0.027	17.795	296.24	0.9985	14.83
975.43	907.86	0.034	17.827	296.27	0.9982	16.85
1196.1	1116.8	0.042	17.860	296.23	0.9978	19.45
1402.8	1317.3	0.050	17.893	296.23	0.9975	20.88
1674.4	1589.6	0.060	17.937	296.21	0.9971	21.39
1888.2	1798.6	0.067	17.973	296.24	0.9968	22.22
2133.6	2026.1	0.076	18.014	296.26	0.9965	24.37
2398.4	2292.2	0.086	18.060	296.27	0.9962	25.38
2576.3	2459.1	0.092	18.088	296.23	0.9960	26.71
2830.0	2699.0	0.101	18.131	296.23	0.9958	28.45
3161.0	3009.3	0.113	18.188	296.22	0.9955	30.74
3236.8	3064.4	0.115	18.200	296.21	0.9954	32.71
3278.5	3099.3	0.117	18.153	295.03	0.9951	33.79

CORE SAMPLE NO 1C RUN 4 REVERSE DIRECTION
RE=0.15239 RW=0.00319 H=0.02568 POROSITY=0.0

PE (PSI)	PW (PSI)	CP (PSI)	PB (CMHG)	TCE (MV)	TCW (MV)	TS (SEC)
536.00	511.00	513.00	69.840	0.8680	0.8750	17.000
498.00	477.00	500.00	69.840	0.8660	0.8760	18.400
469.00	451.00	500.00	69.840	0.8690	0.8780	19.700
446.00	433.60	500.00	69.840	0.8730	0.8820	21.300
408.00	397.30	500.00	69.840	0.8710	0.8780	22.400
307.00	296.00	500.00	69.840	0.8670	0.8790	23.500
290.00	281.00	500.00	69.850	0.8660	0.8810	25.600
259.00	250.50	500.00	69.850	0.8650	0.8800	27.350
218.00	209.60	500.00	69.860	0.8640	0.8750	29.700
168.00	158.80	500.00	69.870	0.8660	0.8750	31.900
130.00	120.60	500.00	69.870	0.8630	0.8760	36.100
98.000	88.300	500.00	69.870	0.8650	0.8760	42.300
76.200	65.900	500.00	69.870	0.8640	0.8740	46.900
55.000	44.500	500.00	69.920	0.8660	0.8750	55.600
40.000	30.000	500.00	69.920	0.8650	0.8750	70.400
25.000	14.500	500.00	69.920	0.8650	0.8760	82.300
16.000	6.3000	500.00	69.920	0.8670	0.8780	102.50
12.000	3.9000	500.00	69.920	0.8700	0.8760	129.80

PE (KPA)	PW (KPA)	RD	VIS (U-PAS)	T (DEG K)	ZA	QO (M3/D)
3788.7	3616.3	0.136	18.258	295.22	0.9948	35.98
3526.7	3381.9	0.127	18.210	295.21	0.9950	33.24
3326.8	3202.6	0.120	18.178	295.27	0.9951	31.05
3168.2	3082.7	0.115	18.157	295.37	0.9952	28.72
2906.2	2832.4	0.105	18.107	295.29	0.9955	27.31
2209.8	2134.0	0.080	17.984	295.25	0.9962	26.03
2092.6	2030.6	0.076	17.966	295.27	0.9964	23.89
1878.9	1820.3	0.068	17.929	295.24	0.9966	22.36
1596.2	1538.3	0.057	17.879	295.17	0.9970	20.59
1251.5	1188.0	0.045	17.823	295.19	0.9976	19.17
989.47	924.66	0.035	17.780	295.17	0.9981	16.94
768.84	701.96	0.027	17.745	295.19	0.9985	14.46
618.53	547.52	0.021	17.719	295.16	0.9988	13.04
472.43	400.04	0.016	17.698	295.19	0.9991	11.00
369.01	300.06	0.012	17.681	295.18	0.9993	8.688
265.59	193.19	0.008	17.665	295.19	0.9995	7.432
203.53	136.66	0.006	17.658	295.24	0.9996	5.967
175.96	120.11	0.005	17.655	295.25	0.9997	4.712

CORE SAMPLE NO 1C , RUN 5 FORWARD DIRECTION
RE=0.15239 RW=0.00319 H=0.02568 POROSITY=0.10620

PE (PSI)	PW (PSI)	CP (PSI)	PB (CMHG)	TCE (MV)	TCW (MV)	TS (SEC)
7.0000	2.0000	600.00	70.330	0.8840	0.8840	199.70
10.000	3.3000	600.00	70.330	0.8880	0.8860	140.80
16.000	7.6000	600.00	70.330	0.8880	0.8880	97.400
21.900	10.500	600.00	70.330	0.8800	0.8930	64.700
29.600	16.000	600.00	70.330	0.8930	0.8950	47.400
40.400	27.500	600.00	70.330	0.8950	0.8990	40.950
60.000	47.800	600.00	70.330	0.8950	0.9000	33.000
80.000	69.000	600.00	70.330	0.9000	0.9030	31.000
99.800	90.100	600.00	70.330	0.9030	0.9030	30.500
132.00	123.60	600.00	70.330	0.9040	0.9040	29.900
160.00	151.80	600.00	70.280	0.9050	0.9090	28.980
187.80	179.80	600.00	70.280	0.9070	0.9100	27.600
210.40	201.60	600.00	70.280	0.9070	0.9080	26.300
240.00	231.00	600.00	70.280	0.9100	0.9100	25.140
270.00	260.40	600.00	70.280	0.9100	0.9140	24.100
299.60	288.20	600.00	70.280	0.9080	0.9130	23.150
350.00	338.30	600.00	70.280	0.8950	0.9080	22.200
402.00	390.00	600.00	70.280	0.8960	0.9100	21.300
455.00	441.00	600.00	70.280	0.8980	0.9100	20.400
508.00	492.00	600.00	70.280	0.9000	0.9100	19.400
542.00	524.00	600.00	70.280	0.8950	0.9100	18.760
584.00	563.00	600.00	70.280	0.8960	0.9100	17.320
600.00	578.00	600.00	70.280	0.8940	0.9070	16.800
632.00	609.00	610.00	70.280	0.9000	0.9080	16.250

PE (KPA)	PW (KPA)	RD	VIS (U-PAS)	T (DEG K)	ZA	QO (M3/D)
142.03	107.55	0.005	17.664	295.53	0.9997	3.063
162.71	116.52	0.005	17.670	295.60	0.9997	4.344
204.08	146.17	0.006	17.676	295.63	0.9996	6.280
244.76	166.16	0.007	17.679	295.59	0.9996	9.454
297.85	204.08	0.009	17.695	295.77	0.9995	12.90
372.31	283.37	0.012	17.710	295.85	0.9993	14.94
507.45	423.33	0.017	17.733	295.86	0.9990	18.53
645.35	569.50	0.022	17.760	295.96	0.9988	19.73
781.86	714.98	0.027	17.784	296.00	0.9985	20.05
1003.9	945.96	0.036	17.821	296.02	0.9981	20.46
1196.9	1140.3	0.043	17.856	296.09	0.9978	21.11
1388.5	1333.4	0.050	17.889	296.13	0.9975	22.16
1544.4	1483.7	0.055	17.913	296.11	0.9972	23.26
1748.4	1686.4	0.063	17.949	296.17	0.9970	24.33
1955.3	1889.1	0.070	17.986	296.22	0.9967	25.38
2159.4	2080.8	0.077	18.017	296.18	0.9964	26.42
2506.9	2426.2	0.090	18.067	295.96	0.9960	27.55
2865.4	2782.7	0.103	18.131	296.00	0.9957	28.72
3230.8	3134.3	0.116	18.197	296.02	0.9954	29.98
3596.2	3485.9	0.130	18.265	296.05	0.9952	31.53
3830.7	3706.6	0.138	18.305	295.98	0.9950	32.60
4120.2	3975.4	0.148	18.360	296.00	0.9949	35.31
4230.6	4078.9	0.152	18.379	295.93	0.9949	36.41
4451.2	4292.6	0.160	18.426	296.02	0.9948	37.64

CORE SAMPLE NO 1C RUN 5 REVERSE DIRECTION
RE=0.15239 RW=0.00319 H=0.02568 POROSITY=0.10620

PE (PSI)	PW (PSI)	CP (PSI)	PB (CMHG)	TCE (MV)	TCW (MV)	TS (SEC)
632.00	609.00	610.00	70.280	0.9000	0.9080	16.250
617.00	597.00	600.00	70.630	0.8920	0.8830	17.200
594.00	575.00	600.00	70.630	0.8700	0.8810	17.700
547.00	531.00	600.00	70.650	0.8630	0.8800	18.600
487.00	474.00	600.00	70.650	0.8600	0.8760	19.800
408.00	396.00	600.00	70.650	0.8600	0.8790	20.500
327.00	316.60	600.00	70.650	0.8600	0.8750	21.700
219.00	210.00	600.00	70.670	0.8620	0.8760	23.500
144.00	135.60	600.00	70.670	0.8610	0.8750	25.600
58.000	45.200	600.00	70.670	0.8600	0.8730	31.000
43.200	29.600	600.00	70.670	0.8650	0.8760	35.780
28.800	13.700	600.00	70.670	0.8680	0.8750	40.200
20.000	7.2000	600.00	70.670	0.8660	0.8750	55.000
12.000	3.7000	600.00	70.670	0.8690	0.8730	95.200
8.0000	2.0000	600.00	70.670	0.8670	0.8720	142.10

PE (KPA)	PW (KPA)	RD	VIS (U-PAS)	T (DEG K)	ZA	QO (M3/D)
4451.2	4292.6	0.160	18.426	296.02	0.9948	37.64
4348.2	4210.3	0.157	18.389	295.61	0.9947	35.56
4189.7	4058.7	0.151	18.345	295.32	0.9947	34.56
3865.6	3755.3	0.140	18.279	295.22	0.9948	32.88
3451.9	3362.3	0.125	18.198	295.13	0.9950	30.89
2907.3	2824.5	0.105	18.101	295.17	0.9954	29.84
2348.8	2277.1	0.085	18.002	295.12	0.9960	28.19
1604.2	1542.1	0.058	17.879	295.16	0.9970	26.03
1087.1	1029.1	0.039	17.794	295.13	0.9979	23.89
494.11	405.86	0.016	17.695	295.09	0.9990	19.73
392.07	298.30	0.013	17.683	295.19	0.9993	17.09
292.79	188.68	0.009	17.668	295.22	0.9995	15.22
232.11	143.86	0.007	17.659	295.19	0.9996	11.12
176.96	119.73	0.005	17.653	295.21	0.9997	6.425
149.38	108.01	0.005	17.648	295.17	0.9997	4.304

CORE SAMPLE NO 1C . RUN 6 FORWARD DIRECTION
RE=0.15239 RW=0.00319 H=0.02568 POROSITY=0.10620

PE (PSI)	PW (PSI)	CP (PSI)	PB (CMHG)	TCE (MV)	TCW (MV)	TS (SEC)
8.0000	2.2000	700.00	70.380	0.8130	0.8070	193.80
14.000	6.3000	700.00	70.380	0.8210	0.8100	130.60
20.000	10.600	700.00	70.380	0.8250	0.8160	96.300
25.000	15.300	700.00	70.380	0.8270	0.8200	85.200
32.200	22.100	700.00	70.380	0.8310	0.8230	72.900
40.200	28.900	700.00	70.380	0.8330	0.8250	57.400
48.600	36.900	700.00	70.380	0.8350	0.8300	49.500
60.000	48.000	700.00	70.380	0.8360	0.8310	42.700
72.000	60.600	700.00	70.380	0.8390	0.8350	39.150
84.000	72.000	700.00	70.380	0.8400	0.8350	33.730
96.000	84.500	700.00	70.380	0.8390	0.8350	32.500
110.40	99.550	700.00	70.380	0.8350	0.8350	31.200
124.00	113.60	700.00	70.380	0.8380	0.8350	30.700
140.00	129.60	700.00	70.380	0.8350	0.8350	28.030
160.00	150.00	700.00	70.380	0.8340	0.8360	27.500
180.00	169.60	700.00	70.380	0.8340	0.8370	26.550
198.40	188.20	700.00	70.380	0.8320	0.8360	26.200
220.40	210.00	700.00	70.380	0.8340	0.8390	25.600
244.00	234.10	700.00	70.380	0.8330	0.8390	25.050
266.00	254.40	700.00	70.380	0.8330	0.8380	23.700
290.00	277.50	700.00	70.380	0.8340	0.8380	23.350
320.40	307.00	700.00	70.380	0.8300	0.8400	23.100
360.00	347.00	700.00	70.380	0.8300	0.8400	22.600
390.00	375.00	700.00	70.380	0.8330	0.8400	21.900
440.00	423.00	700.00	70.480	0.8490	0.8550	21.300
469.00	450.00	700.00	70.480	0.8460	0.8530	20.900
524.00	504.00	700.00	70.480	0.8480	0.8540	20.380
573.00	552.10	700.00	70.480	0.8450	0.8550	19.900
636.00	616.20	700.00	70.480	0.8450	0.8550	19.550
680.00	659.60	700.00	70.580	0.8450	0.8580	19.100
711.00	688.00	700.00	70.580	0.8450	0.8580	18.150
756.00	732.00	733.00	70.580	0.8500	0.8560	17.400

PE (KPA)	PW (KPA)	RD	VIS (U-PAS)	T (DEG K)	ZA	QO (M3/D)
148.99	109.00	0.005	17.581	293.70	0.9997	3.156
190.36	137.27	0.006	17.593	293.83	0.9996	4.683
231.73	166.92	0.007	17.604	293.96	0.9995	6.351
266.20	199.32	0.009	17.613	294.03	0.9995	7.179
315.84	246.21	0.010	17.624	294.12	0.9994	8.390
371.00	293.09	0.012	17.635	294.17	0.9993	10.66
428.92	348.25	0.014	17.648	294.25	0.9991	12.36
507.52	424.78	0.017	17.661	294.28	0.9990	14.32
590.25	511.65	0.020	17.678	294.36	0.9988	15.62
672.99	590.25	0.023	17.692	294.38	0.9986	18.13
755.73	676.44	0.026	17.705	294.36	0.9985	18.82
855.01	780.21	0.030	17.718	294.32	0.9983	19.60
948.78	877.08	0.034	17.735	294.35	0.9981	19.92
1059.1	987.39	0.038	17.751	294.32	0.9979	21.82
1197.0	1128.0	0.043	17.774	294.32	0.9976	22.24
1334.9	1263.2	0.048	17.797	294.33	0.9974	23.04
1461.8	1391.4	0.052	17.816	294.29	0.9972	23.35
1613.4	1541.7	0.058	17.843	294.35	0.9969	23.89
1776.2	1707.9	0.064	17.870	294.34	0.9967	24.42
1927.8	1847.9	0.069	17.894	294.33	0.9964	25.81
2093.3	2007.1	0.075	17.922	294.34	0.9962	26.19
2302.9	2210.5	0.083	17.956	294.32	0.9959	26.48
2575.9	2486.3	0.093	18.003	294.32	0.9956	27.06
2782.8	2679.4	0.101	18.040	294.35	0.9954	27.93
3127.7	3010.4	0.113	18.118	294.74	0.9951	28.72
3327.6	3196.6	0.120	18.150	294.67	0.9950	29.27
3706.8	3568.9	0.134	18.222	294.71	0.9947	30.01
4044.7	3900.6	0.146	18.286	294.69	0.9945	30.74
4479.0	4342.5	0.162	18.374	294.69	0.9944	31.29
4782.5	4641.9	0.173	18.438	294.72	0.9943	32.02
4996.3	4837.7	0.181	18.481	294.72	0.9943	33.70
5306.5	5141.1	0.192	18.550	294.76	0.9944	35.15

CORE SAMPLE NO 1C RUN 6 REVERSE DIRECTION
RE=0.15239 RW=0.00319 H=0.02568 POROSITY=0.10620

PE (PSI)	PW (PSI)	CP (PSI)	PB (CMHG)	TCE (MV)	TCW (MV)	TS (SEC)
756.00	732.00	733.00	70.580	0.8500	0.8560	17.400
707.00	684.00	700.00	70.580	0.8430	0.8540	18.250
665.00	643.00	700.00	70.580	0.8390	0.8520	18.850
633.00	613.00	700.00	70.580	0.8380	0.8490	19.400
587.00	570.00	700.00	70.580	0.8390	0.8500	20.000
492.00	477.00	700.00	70.000	0.8490	0.8510	21.250
455.00	441.00	700.00	70.000	0.8490	0.8510	21.800
396.00	382.00	700.00	69.940	0.8430	0.8500	22.550
354.00	341.00	700.00	69.940	0.8440	0.8460	23.100
275.00	261.40	700.00	69.940	0.8400	0.8450	23.800
257.00	245.00	700.00	69.940	0.8400	0.8410	24.400
232.00	221.00	700.00	69.940	0.8380	0.8380	25.300
201.00	192.00	700.00	69.940	0.8340	0.8380	26.500
159.00	150.00	700.00	69.940	0.8340	0.8370	27.300
111.00	101.00	700.00	69.940	0.8350	0.8390	29.100
80.400	70.200	700.00	69.940	0.8310	0.8370	33.650
60.400	49.790	700.00	69.940	0.8290	0.8360	39.320
48.200	36.400	700.00	69.870	0.8260	0.8360	40.700
20.400	9.5000	700.00	69.870	0.8280	0.8320	69.400
8.0000	2.0000	700.00	69.870	0.8310	0.8350	155.10

PE (KPA)	PW (KPA)	RD	VIS (U-PAS)	T (DEG K)	ZA	QO (M3/D)
5306.5	5141.1	0.192	18.550	294.76	0.9944	35.15
4968.7	4810.1	0.180	18.472	294.65	0.9943	33.51
4679.1	4527.4	0.169	18.408	294.57	0.9943	32.45
4458.5	4320.6	0.162	18.362	294.53	0.9943	31.53
4141.3	4024.1	0.150	18.302	294.55	0.9944	30.58
3485.5	3382.1	0.126	18.183	294.69	0.9948	28.78
3230.4	3133.9	0.117	18.136	294.69	0.9950	28.06
2823.6	2727.0	0.102	18.059	294.60	0.9954	27.12
2534.0	2444.4	0.092	18.007	294.56	0.9957	26.48
1989.3	1895.5	0.071	17.911	294.50	0.9964	25.70
1865.2	1782.5	0.067	17.889	294.45	0.9966	25.07
1692.8	1617.0	0.061	17.858	294.39	0.9968	24.18
1479.1	1417.0	0.053	17.821	294.34	0.9971	23.08
1189.5	1127.5	0.043	17.774	294.33	0.9976	22.40
858.56	789.62	0.030	17.722	294.36	0.9983	21.02
647.58	577.26	0.022	17.685	294.29	0.9987	18.18
509.69	436.54	0.017	17.661	294.25	0.9990	15.56
425.48	344.12	0.014	17.645	294.22	0.9991	15.03
233.81	158.65	0.007	17.614	294.19	0.9996	8.813
148.31	106.94	0.005	17.607	294.27	0.9997	3.944

CORE SAMPLE NO 1C RUN 7 FORWARD DIRECTION
RE=0.15239 RW=0.00319 H=0.02568 POROSITY=0.10620

PE (PSI)	PW (PSI)	CP (PSI)	PB (CMHG)	TCE (MV)	TCW (MV)	TS (SEC)
8.0000	2.0000	800.00	71.280	0.7710	0.7740	165.30
14.000	5.0000	800.00	71.280	0.7780	0.7810	101.00
22.000	11.800	800.00	71.280	0.7800	0.7840	77.600
30.000	17.300	800.00	71.280	0.7830	0.7850	55.850
40.400	28.000	800.00	71.280	0.7860	0.7880	48.550
60.200	49.000	800.00	71.280	0.7870	0.7870	41.900
80.000	69.200	800.00	71.280	0.7900	0.7870	36.500
100.00	90.000	800.00	71.280	0.7900	0.7900	33.370
132.00	122.50	800.00	71.280	0.7950	0.7950	30.680
159.80	150.80	800.00	71.280	0.7980	0.7950	29.630
200.00	190.80	800.00	71.280	0.7980	0.7950	28.250
240.40	229.80	800.00	71.280	0.8000	0.7960	27.300
280.40	267.80	800.00	71.280	0.8000	0.7950	25.750
300.40	286.20	800.00	71.280	0.8000	0.7950	24.700
348.00	333.00	800.00	69.850	0.7800	0.7800	23.800
420.00	403.00	800.00	69.800	0.7850	0.7850	22.750
474.00	455.00	800.00	69.800	0.7890	0.7860	21.650
495.00	475.00	800.00	69.800	0.7930	0.7900	21.100
557.00	535.00	800.00	69.800	0.7950	0.7940	20.250
612.00	590.00	800.00	69.800	0.8000	0.7960	19.750
675.00	652.00	800.00	69.800	0.8050	0.7990	18.870
711.00	687.00	800.00	69.800	0.8050	0.7990	18.300
754.00	728.00	800.00	69.800	0.8090	0.8010	17.600

PE (KPA)	PW (KPA)	RD	VIS (U-PAS)	T (DEG K)	ZA	QO (M3/D)
150.19	108.82	0.005	17.539	292.77	0.9997	3.700
191.56	129.51	0.006	17.552	292.94	0.9996	6.056
246.72	176.39	0.008	17.563	293.01	0.9995	7.882
301.87	214.31	0.010	17.572	293.06	0.9994	10.95
373.58	288.09	0.012	17.587	293.13	0.9992	12.60
510.10	432.88	0.017	17.609	293.13	0.9989	14.60
646.61	572.15	0.022	17.633	293.17	0.9986	16.76
784.51	715.56	0.028	17.657	293.20	0.9983	18.33
1005.1	939.64	0.036	17.698	293.33	0.9979	19.94
1196.8	1134.8	0.043	17.731	293.36	0.9975	20.64
1474.0	1410.6	0.053	17.776	293.36	0.9970	21.65
1752.5	1679.4	0.063	17.823	293.40	0.9966	22.40
2028.3	1941.4	0.073	17.867	293.39	0.9961	23.75
2166.2	2068.3	0.078	17.890	293.39	0.9959	24.76
2492.5	2389.1	0.090	17.926	292.96	0.9954	25.70
2988.9	2871.6	0.108	18.017	293.08	0.9948	26.89
3361.2	3230.2	0.122	18.087	293.14	0.9945	28.25
3506.0	3368.1	0.127	18.118	293.24	0.9944	28.99
3933.4	3781.8	0.143	18.201	293.31	0.9941	30.20
4312.7	4161.0	0.157	18.280	293.40	0.9939	30.97
4747.0	4588.4	0.173	18.373	293.50	0.9938	32.41
4995.2	4829.8	0.182	18.425	293.50	0.9938	33.42
5291.7	5112.4	0.192	18.491	293.57	0.9939	34.75

CORE SAMPLE NO 1C RUN 7 REVERSE DIRECTION
RE=0.15239 RW=0.00319 H=0.02568 POROSITY=0.10620

PE (PSI)	PW (PSI)	CP (PSI)	PB (CMHG)	TCE (MV)	TCW (MV)	TS (SEC)
799.00	772.50	800.00	69.980	0.8310	0.8270	17.000
776.00	752.50	800.00	69.980	0.8350	0.8270	18.000
745.00	727.00	800.00	69.980	0.8380	0.8320	19.450
694.00	678.50	800.00	69.980	0.8400	0.8350	20.400
604.00	590.00	800.00	70.000	0.8420	0.8350	21.400
526.00	514.00	800.00	70.000	0.8420	0.8350	22.500
464.00	453.00	800.00	70.000	0.84	0.8350	23.300
396.00	386.00	800.00	69.910	0.8200	0.8200	24.100
339.00	330.00	800.00	69.910	0.8220	0.8200	25.100
245.00	235.00	800.00	69.910	0.8250	0.8240	26.400
228.00	218.00	800.00	69.910	0.8270	0.8240	27.700
206.00	196.00	800.00	69.910	0.8300	0.8250	28.700
165.00	154.50	800.00	69.930	0.8330	0.8250	30.700
140.00	130.00	800.00	69.930	0.8330	0.8230	34.800
94.800	83.800	800.00	69.930	0.8350	0.8210	40.600
54.400	42.000	800.00	69.930	0.8320	0.8210	52.000
32.400	20.400	800.00	69.930	0.8350	0.8230	75.700
19.000	9.7000	800.00	69.930	0.8350	0.8250	123.00
14.000	5.2000	800.00	69.930	0.8340	0.8260	145.20

PE (KPA)	PW (KPA)	RD	VIS (U-PAS)	T (DEG.K)	ZA	QO (M3/D)
5602.2	5419.5	0.203	18.588	294.17	0.9942	35.98
5448.6	5281.6	0.198	18.556	294.22	0.9942	33.98
5229.9	5105.8	0.190	18.518	294.32	0.9942	31.45
4878.3	4771.4	0.178	18.446	294.38	0.9942	29.98
4257.8	4161.2	0.155	18.320	294.40	0.9943	28.58
3720.0	3637.2	0.135	18.217	294.41	0.9946	27.18
3292.5	3216.7	0.120	18.138	294.43	0.9949	26.25
2823.5	2754.6	0.103	18.032	293.94	0.9952	25.38
2430.5	2368.5	0.088	17.964	293.97	0.9957	24.37
1782.4	1713.5	0.064	17.858	294.06	0.9966	23.17
1665.2	1596.3	0.060	17.840	294.08	0.9968	22.08
1513.5	1444.6	0.054	17.817	294.13	0.9971	21.31
1230.9	1158.5	0.044	17.772	294.17	0.9976	19.92
1058.5	989.55	0.038	17.744	294.14	0.9979	17.58
746.86	671.01	0.026	17.693	294.14	0.9985	15.07
468.31	382.81	0.016	17.647	294.11	0.9991	11.76
316.62	233.89	0.010	17.626	294.17	0.9994	8.080
224.23	160.11	0.007	17.614	294.19	0.9996	4.973
189.76	129.08	0.006	17.609	294.19	0.9996	4.212

CORE SAMPLE NO 4A RUN 1 FORWARD DIRECTION
RE=0.15256 RW=0.00820 H=0.02600 POROSITY=0.22714

PE (PSI)	PW (PSI)	CP (PSI)	PB (CMHG)	TCE (MV)	TCW (MV)	TS (SEC)
8.0000	2.0000	4.00	70.170	0.7460	0.7450	129.60
16.000	7.8000	8.00	70.170	0.7510	0.7500	82.700
24.000	15.000	15.00	70.170	0.7550	0.7510	67.450
30.000	20.000	21.00	70.170	0.7570	0.7550	56.830
44.200	33.500	33.00	70.170	0.7580	0.7550	45.450
60.000	49.700	50.00	70.170	0.7600	0.7590	40.100
80.000	70.400	71.00	70.170	0.7630	0.7600	37.930
100.00	90.400	90.00	70.170	0.7650	0.7610	35.480
150.20	140.80	139.00	70.160	0.7700	0.7660	30.600
166.00	155.40	155.00	70.160	0.7700	0.7680	28.700
192.00	182.00	182.00	70.160	0.7700	0.7670	27.400
232.20	222.60	223.00	70.160	0.7710	0.7700	26.200
260.00	249.40	250.00	7[illegible]160	0.7720	0.7720	25.000
296.00	286.00	287.00	[illegible]	0.7730	0.7700	24.300
346.00	335.00	335.00	[illegible]	0.7610	0.7550	23.430
410.00	400.00	400.00	70.160	0.7660	0.7590	22.950
458.00	447.00	446.00	70.160	0.7670	0.7620	21.600
508.00	494.50	495.00	70.160	0.7690	0.7650	20.400
562.00	548.40	547.00	70.160	0.7700	0.7650	19.820
609.00	594.00	593.00	70.160	0.7730	0.7680	18.600

PE (KPA)	PW (KPA)	RD	VIS (U-PAS)	T (DEG K)	ZA	QO (M3/D)
148.71	107.34	0.005	17.509	292.10	0.9997	4.719
203.87	147.33	0.006	17.522	292.23	0.9996	7.396
259.03	196.97	0.008	17.533	292.29	0.9994	9.068
300.39	231.45	0.010	17.542	292.36	0.9994	10.76
398.30	324.53	0.013	17.558	292.38	0.9991	13.46
507.24	436.22	0.017	17.579	292.45	0.9989	15.25
645.13	578.94	0.023	17.603	292.50	0.9986	16.13
783.03	716.84	0.028	17.627	292.54	0.9983	17.24
1129.1	1064.3	0.041	17.688	292.66	0.9976	19.99
1238.1	1165.0	0.044	17.706	292.68	0.9974	21.31
1417.3	1348.4	0.051	17.735	292.67	0.9970	22.32
1694.5	1628.3	0.061	17.783	292.72	0.9966	23.35
1886.2	1813.1	0.068	17.816	292.76	0.9962	24.47
2134.4	2065.4	0.078	17.858	292.75	0.9959	25.17
2479.1	2403.3	0.090	17.901	292.41	0.9953	26.11
2920.4	2851.4	0.107	17.984	292.52	0.9948	26.65
3251.3	3175.5	0.119	18.046	292.57	0.9944	28.32
3596.1	3503.0	0.132	18.111	292.63	0.9941	29.98
3968.4	3874.6	0.145	18.183	292.65	0.9939	30.86
4292.4	4189.0	0.157	18.250	292.72	0.9937	32.88

CORE SAMPLE NO 4A RUN 1 REVERSE DIRECTION
RE=0.15256 RW=0.00820 H=0.02600 POROSITY=0.0

PE (PSI)	PW (PSI)	CP (PSI)	PB (CMHG)	TCE (MV)	TCW (MV)	TS (SEC)
609.00	594.00	593.00	70.160	0.7730	0.7680	18.600
552.00	537.00	535.00	70.160	0.7700	0.7670	19.300
496.00	481.70	479.00	70.160	0.7700	0.7660	20.340
442.00	429.00	423.00	69.750	0.7710	0.7710	21.400
380.00	369.00	364.00	69.750	0.7680	0.7700	23.000
352.00	342.30	336.00	69.750	0.7670	0.7700	23.900
312.00	303.30	296.00	69.750	0.7670	0.7700	25.400
264.00	255.00	249.00	69.720	0.7700	0.7720	26.000
200.00	191.00	184.00	69.720	0.7650	0.7680	27.600
152.00	143.00	130.00	69.720	0.7660	0.7640	29.100
98.000	88.400	88.00	69.720	0.7670	0.7680	31.800
58.200	46.400	43.00	69.700	0.7660	0.7700	35.020
32.600	19.000	17.00	69.700	0.7660	0.7700	40.400
14.200	6.2000	9.00	69.700	0.7650	0.7700	89.100
8.0000	2.3000	7.00	69.700	0.7650	0.7700	136.60

PE (KPA)	PW (KPA)	RD	VIS (U-PAS)	T (DEG K)	ZA	QO (M3/D)
4292.4	4189.0	0.157	18.250	292.72	0.9937	32.88
3899.4	3796.0	0.143	18.170	292.67	0.9939	31.69
3513.3	3414.7	0.128	18.096	292.66	0.9942	30.07
3140.5	3050.8	0.115	18.032	292.73	0.9946	28.58
2713.0	2637.2	0.099	17.954	292.68	0.9950	26.59
2519.9	2453.1	0.092	17.921	292.67	0.9953	25.59
2244.2	2184.2	0.082	17.874	292.67	0.9957	24.08
1913.2	1851.1	0.070	17.820	292.73	0.9962	23.52
1471.9	1409.9	0.053	17.742	292.62	0.9969	22.16
1141.0	1078.9	0.041	17.687	292.59	0.9976	21.02
768.64	702.45	0.027	17.629	292.65	0.9983	19.23
494.20	412.84	0.017	17.585	292.66	0.9989	17.47
317.69	223.93	0.010	17.556	292.66	0.9994	15.14
190.83	135.67	0.006	17.539	292.65	0.9996	6.865
148.08	108.78	0.005	17.533	292.65	0.9997	4.478

CORE SAMPLE NO 4A RUN 2 FORWARD DIRECTION
RE=0.15256 RW=0.00820 H=0.02600 POROSITY=0.22600

PE (PSI)	PW (PSI)	CP (PSI)	PB (CMHG)	TCE (MV)	TCW (MV)	TS (SEC)
8.0000	2.0000	400.00	70.270	0.7950	0.7920	131.45
12.000	4.7000	400.00	70.280	0.7950	0.7950	96.750
18.000	8.7000	400.00	70.280	0.7960	0.7990	66.330
24.000	13.100	400.00	70.280	0.7960	0.8010	50.120
30.000	17.800	400.00	70.280	0.7960	0.8020	39.870
40.200	28.400	400.00	70.280	0.7960	0.8050	34.500
54.200	43.800	400.00	70.280	0.7940	0.8050	32.000
70.000	60.400	400.00	70.280	0.7940	0.8060	30.640
90.000	81.000	400.00	70.280	0.7940	0.8060	29.700
108.20	99.300	400.00	70.280	0.7930	0.8050	28.350
138.20	129.40	400.00	70.260	0.7940	0.8050	27.200
160.00	151.00	400.00	70.280	0.7910	0.8040	26.260
186.60	176.40	400.00	70.280	0.7920	0.8040	25.100
210.80	199.40	400.00	70.280	0.7900	0.8040	24.300
238.00	226.70	400.00	70.280	0.7900	0.8050	23.700
265.00	251.00	400.00	70.470	0.7520	0.7520	22.300
298.00	282.00	400.00	70.470	0.7570	0.7570	21.200
325.00	307.00	400.00	70.470	0.7600	0.7600	20.130
372.00	353.00	400.00	70.470	0.7600	0.7630	19.[illegible]00
406.00	385.40	400.00	70.470	0.7630	0.7650	[illegible].110
435.00	413.00	413.00	70.470	0.7660	0.7660	17.130

PE (KPA)	PW (KPA)	RD	VIS (U-PAS)	T (DEG K)	ZA	QO (M3/D)
148.84	107.47	0.005	17.563	293.29	0.9997	4.653
176.44	126.10	0.006	17.568	293.33	0.9996	6.322
217.80	153.68	0.007	17.576	293.39	0.9996	9.221
259.17	184.02	0.008	17.583	293.41	0.9995	12.20
300.54	216.43	0.010	17.589	293.43	0.9994	15.34
370.87	289.51	0.012	17.602	293.46	0.9992	17.73
467.39	395.69	0.016	17.617	293.44	0.9990	19.11
576.33	510.14	0.020	17.635	293.45	0.9988	19.96
714.23	652.17	0.025	17.658	293.45	0.9985	20.59
839.71	778.35	0.030	17.677	293.43	0.99[illegible]2	21.57
1046.5	985.85	0.037	17.710	293.44	0.9978	22.49
1196.9	1134.8	0.043	17.732	293.39	0.9975	23.29
1380.3	1309.9	0.050	17.762	293.40	0.[illegible]72	24.37
1547.1	1468.5	0.056	17.787	293.38	0.[illegible]969	25.17
1734.7	1656.7	0.063	17.819	293.39	0.9966	25.81
1921.1	1824.5	0.069	17.797	292.26	0.9961	27.43
2148.6	2038.3	0.078	17.840	292.39	0.9958	28.85
2334.7	2210.6	0.084	17.874	292.46	0.9955	30.38
2658.8	2527.8	0.096	17.931	292.50	0.9951	31.86
2893.2	2751.2	0.105	17.975	292.56	0.9948	33.77
3093.2	2941.5	0.112	18.012	292.61	0.9946	35.71

CORE SAMPLE NO 4A RUN 2 REVERSE DIRECTION
RE=0.15256 RW=0.00820 H=0.02600 POROSITY=0.0

PE (PSI)	PW (PSI)	CP (PSI)	PB (CMHG)	TCE (MV)	TCW (MV)	TS (SEC)
435.00	413.00	413.00	70.470	0.7660	0.7660	17.130
400.00	379.30	400.00	70.470	0.7650	0.7670	18.200
386.00	367.40	400.00	70.470	0.7650	0.7700	19.000
350.00	333.80	400.00	70.470	0.7650	0.7710	20.200
320.00	308.40	400.00	70.540	0.7660	0.7710	21.750
291.00	281.60	400.00	70.540	0.7670	0.7720	23.330
260.00	251.60	400.00	70.540	0.7680	0.7730	24.700
237.00	229.00	400.00	70.540	0.7700	0.7730	25.300
180.00	171.40	400.00	70.520	0.7690	0.7750	27.100
168.00	159.50	400.00	70.520	0.7700	0.7750	28.350
146.00	137.90	400.00	70.520	0.7720	0.7760	30.400
125.00	117.00	400.00	70.520	0.7720	0.7760	32.250
105.60	97.300	400.00	70.770	0.7400	0.7400	33.320
96.000	87.500	400.00	70.770	0.7530	0.7560	34.400
70.800	60.800	400.00	70.770	0.7560	0.7560	35.700
46.000	34.400	400.00	70.770	0.7600	0.7610	41.700
30.200	21.100	400.00	70.770	0.7610	0.7640	67.200
10.800	3.2000	400.00	70.770	0.7680	0.7670	119.80

PE (KPA)	PW (KPA)	RD	VIS (U-PAS)	T (DEG K)	ZA	QO (M3/D)
3093.2	2941.5	112	18.012	292.61	0.9946	35.71
2851.9	2709.1	0.[illegible]03	17.969	292.61	0.9949	33.61
2755.3	2627.1	0.100	17.955	292.65	0.9950	32.19
2507.1	2395.4	0.091	17.914	292.66	0.9953	30.28
2300.4	2220.4	0.084	17.881	292.67	0.9956	28.12
2100.4	2035.6	0.076	17.850	292.70	0.9959	26.22
1886.7	1828.8	0.069	17.816	292.72	0.9962	24.76
1728.1	1672.9	0.063	17.791	292.75	0.9965	24.18
1335.1	1275.8	0.048	17.726	292.76	0.9972	22.57
1252.3	1193.7	0.045	17.713	292.77	0.9974	21.57
1100.7	1044.8	0.040	17.691	292.81	0.9976	20.12
955.86	900.71	0.034	17.668	292.81	0.9979	18.97
822.44	765.21	0.029	17.608	291.97	0.9982	18.36
756.25	697.64	0.027	17.613	292.33	0.9983	17.78
582.50	513.55	0.020	17.587	292.36	0.9987	17.13
411.51	331.53	0.014	17.564	292.47	0.9991	14.67
302.57	239.83	0.010	17.550	292.52	0.9993	9.102
168.82	116.42	0.005	17.536	292.65	0.9997	5.106

CORE SAMPLE NO 4A   RUN 3   FORWARD DIRECTION
RE=0.15256 RW=0.00820 H=0.02600 POROSITY=0.0

PE (PSI)	PW (PSI)	CP (PSI)	PB (CMHG)	TCE (MV)	TCW (MV)	TS (SEC)
8.0000	2.0000	500.00	70.270	0.7950	0.7920	155.60
14.000	4.6000	500.00	70.270	0.8040	0.8000	88.500
22.000	9.5000	500.00	70.270	0.8050	0.8050	57.500
28.000	14.400	500.00	70.270	0.8100	0.8070	48.300
38.200	24.800	500.00	70.270	0.8100	0.8100	41.300
50.000	38.400	500.00	70.270	0.8110	0.8110	40.300
64.000	53.500	500.00	70.270	0.8140	0.8140	39.270
80.000	70.500	500.00	70.270	0.8140	0.8160	38.000
98.000	89.000	500.00	70.270	0.8130	0.8160	37.350
120.00	111.60	500.00	70.270	0.8100	0.8140	36.800
140.00	130.90	500.00	70.270	0.8080	0.8100	35.000
169.20	160.00	500.00	70.340	0.8050	0.8100	34.000
194.20	185.40	500.00	70.340	0.8010	0.8100	33.530
224.40	215.40	500.00	70.340	0.8000	0.8070	32.650
257.60	248.70	500.00	70.340	0.7980	0.8070	31.500
282.40	273.00	500.00	70.340	0.7950	0.8060	30.800
316.00	306.00	500.00	70.340	0.7950	0.8060	29.530
360.40	350.00	500.00	70.340	0.7980	0.8050	28.600
412.00	400.00	500.00	70.380	0.8100	0.8070	27.230
455.00	441.00	500.00	70.380	0.8110	0.8060	25.700
504.00	489.50	500.00	70.380	0.8150	0.8060	24.450
534.00	519.00	517.00	70.380	0.8110	0.8060	23.550

PE (KPA)	PW (KPA)	RD	VIS (U-PAS)	T (DEG K)	ZA	QO (M3/D)
148.84	107.47	0.005	17.563	293.29	0.9997	3.931
190.21	125.40	0.006	17.577	293.50	0.9996	6.911
245.37	159.19	0.007	17.587	293.57	0.9995	10.64
286.74	192.97	0.009	17.597	293.66	0.9994	12.66
357.07	264.68	0.011	17.610	293.70	0.9993	14.81
438.42	358.44	0.015	17.625	293.72	0.9991	15.18
534.95	462.55	0.018	17.644	293.80	0.9989	15.58
645.27	579.77	0.023	17.663	293.82	0.9986	16.10
769.37	707.32	0.027	17.683	293.81	0.9984	16.38
921.06	863.14	0.033	17.705	293.75	0.9981	16.62
1059.0	996.21	0.038	17.723	293.67	0.9978	17.48
1260.4	1196.9	0.045	17.754	293.64	0.9974	17.99
1432.7	1372.1	0.052	17.780	293.59	0.9971	18.24
1641.0	1578.9	0.059	17.812	293.54	0.9968	18.73
1869.9	1808.5	0.068	17.848	293.51	0.9964	19.42
2040.9	1976.0	0.074	17.875	293.46	0.9961	19.86
2272.5	2203.6	0.083	17.914	293.46	0.9958	20.71
2578.6	2506.9	0.094	17.967	293.49	0.9954	21.39
2934.5	2851.7	0.107	18.037	293.66	0.9950	22.46
3230.9	3134.4	0.117	18.090	293.66	0.9947	23.80
3568.8	3468.8	0.130	18.154	293.71	0.9945	25.02
3775.6	3672.2	0.138	18.191	293.66	0.9943	25.97

CORE SAMPLE NO 4A RUN 3 REVERSE DIRECTION
RE=0.15256 RW=0.00820 H=0.02600 POROSITY=0.0

PE (PSI)	PW (PSI)	CP (PSI)	PB (CMHG)	TCE (MV)	TCW (MV)	TS (SEC)
534.00	519.00	517.00	70.380	0.8110	0.8060	23.550
488.00	472.90	500.00	69.950	0.8440	0.8330	24.400
427.00	412.50	500.00	69.950	0.8530	0.8400	25.600
372.00	357.40	500.00	69.950	0.8600	0.8550	26.400
315.00	299.90	500.00	69.950	0.8570	0.8570	27.300
263.00	249.10	500.00	69.950	0.8570	0.8600	28.200
236.00	222.30	500.00	69.800	0.8590	0.8600	29.000
188.00	176.80	500.00	69.800	0.8600	0.8600	30.500
138.00	129.00	500.00	69.800	0.8600	0.8600	32.900
104.00	95.800	500.00	69.800	0.8600	0.8620	39.100
61.600	52.000	500.00	69.800	0.8600	0.8630	44.730
40.000	28.700	500.00	69.800	0.8600	0.8640	52.200
24.200	14.200	500.00	69.800	0.8610	0.8610	78.650
10.000	3.2000	500.00	69.800	0.8630	0.8630	154.05

PE (KPA)	PW (KPA)	RD	VIS (U-PAS)	T (DEG K)	ZA	QO (M3/D)
3775.6	3672.2	0.138	18.191	293.66	0.9943	25.97
3457.9	3353.8	0.125	18.165	294.40	0.9948	25.07
3037.3	2937.3	0.110	18.097	294.60	0.9952	23.89
2658.1	2557.4	0.096	18.042	294.87	0.9956	23.17
2265.1	2161.0	0.081	17.973	294.86	0.9961	22.40
1906.6	1810.7	0.068	17.915	294.90	0.9966	21.69
1720.2	1625.8	0.061	17.885	294.92	0.9969	21.09
1389.3	1312.1	0.050	17.833	294.93	0.9974	20.05
1044.5	982.48	0.037	17.778	294.93	0.9979	18.59
810.11	753.58	0.029	17.742	294.96	0.9984	15.64
517.78	451.59	0.018	17.695	294.97	0.9990	13.67
368.85	290.94	0.012	17.671	294.98	0.9993	11.72
259.91	190.96	0.008	17.654	294.96	0.9995	7.777
162.01	115.12	0.005	17.642	295.01	0.9997	3.970

CORE SAMPLE NO 4A RUN 4 FORWARD DIRECTION
RE=0.15256 RW=0.00820 H=0.02600 POROSITY=0.0

PE (PSI)	PW (PSI)	CP (PSI)	PB (CMHG)	TCE (MV)	TCW (MV)	TS (SEC)
10.000	2.7000	600.00	70.000	0.7770	0.7770	143.00
16.000	7.6000	600.00	70.000	0.7780	0.7780	105.75
24.000	13.200	600.00	70.000	0.7780	0.7790	69.980
30.000	18.100	600.00	70.000	0.7750	0.7760	56.300
36.000	22.600	600.00	70.000	0.7740	0.7760	45.270
50.200	39.300	600.00	70.000	0.7740	0.7760	43.000
64.000	54.500	600.00	69.940	0.7740	0.7760	41.380
80.000	71.400	600.00	69.940	0.7750	0.7760	39.020
100.20	92.000	600.00	69.940	0.7740	0.7760	36.900
121.40	113.60	600.00	69.940	0.7740	0.7760	35.250
140.60	133.30	600.00	70.140	0.7600	0.7670	34.800
160.00	152.60	600.00	70.170	0.7630	0.7700	34.100
180.20	172.70	600.00	70.170	0.7640	0.7730	33.300
200.00	192.40	600.00	70.200	0.7640	0.7750	32.190
230.00	222.30	600.00	70.200	0.7660	0.7750	31.300
260.40	253.00	600.00	70.250	0.7650	0.7800	30.400
290.00	282.50	600.00	70.250	0.7650	0.7750	29.700
320.60	312.20	600.00	70.300	0.7550	0.7560	28.300
352.00	343.00	600.00	70.300	0.7550	0.7610	27.400
367.60	356.70	600.00	70.300	0.7520	0.7570	26.500
383.80	371.30	600.00	70.300	0.7570	0.7630	25.400
432.00	419.20	600.00	70.300	0.7600	0.7650	24.500
457.00	442.40	600.00	70.300	0.7570	0.7650	23.450
528.00	512.30	600.00	70.300	0.7600	0.7650	22.400
562.00	544.90	600.00	70.300	0.7600	0.7660	21.300
602.00	584.00	600.00	70.300	0.7700	0.7740	20.400
645.00	627.00	627.00	71.100	0.7500	0.7560	19.900

PE (KPA)	PW (KPA)	RD	VIS (U-PAS)	T (DEG K)	ZA	QO (M3/D)
162.27	111.94	0.005	17.545	292.88	0.9997	4.277
203.64	145.73	0.006	17.553	292.91	0.9996	5.784
258.80	184.34	0.008	17.560	292.92	0.9995	8.740
300.17	218.12	0.010	17.563	292.84	0.9994	10.86
341.54	249.15	0.011	17.568	292.83	0.9993	13.51
439.44	364.29	0.015	17.585	292.83	0.9991	14.22
534.51	469.01	0.018	17.601	292.83	0.9988	14.78
644.83	585.53	0.023	17.619	292.84	0.9986	15.68
784.10	727.56	0.028	17.641	292.83	0.9983	16.58
930.27	876.49	0.033	17.665	292.83	0.9980	17.35
1062.9	1012.6	0.038	17.673	292.55	0.9977	17.58
1196.7	1145.7	0.043	17.698	292.62	0.9974	17.94
1336.0	1284.3	0.048	17.723	292.67	0.9972	18.37
1472.5	1420.1	0.053	17.746	292.70	0.9969	19.00
1679.4	1626.3	0.061	17.782	292.72	0.9966	19.54
1889.1	1838.0	0.069	17.819	292.77	0.9962	20.12
2093.1	2041.4	0.076	17.850	292.71	0.9959	20.59
2304.2	2246.3	0.084	17.869	292.35	0.9955	21.61
2520.7	2458.6	0.092	17.909	292.41	0.9952	22.32
2628.2	2553.1	0.096	17.923	292.33	0.9951	23.08
2739.9	2653.7	0.100	17.948	292.46	0.9950	24.08
3072.3	2984.0	0.112	18.010	292.52	0.9946	24.97
3244.6	3144.0	0.118	18.038	292.49	0.9944	26.08
3734.2	3625.9	0.136	18.131	292.52	0.9940	27.31
3968.6	3850.7	0.145	18.176	292.54	0.9938	28.72
4244.4	4120.3	0.155	18.240	292.76	0.9937	29.98
4541.9	4417.8	0.166	18.279	292.29	0.9934	30.74

CORE SAMPLE NO 4A RUN 4 REVERSE DIRECTION
RE=0.15256 RW=0.00820 H=0.02600 POROSITY=0.0

PE (PSI)	PW (PSI)	CP (PSI)	PB (CMHG)	TCE (MV)	TCW (MV)	TS (SEC)
645.00	627.00	627.00	71.100	0.7500	0.7560	19.900
597.00	579.20	600.00	71.100	0.7570	0.7600	20.600
557.00	540.00	600.00	71.130	0.7590	0.7600	21.400
519.00	505.10	600.00	71.220	0.7720	0.7770	22.700
453.00	440.00	600.00	71.220	0.7750	0.7800	23.920
414.00	403.00	600.00	71.270	0.7860	0.7900	24.980
338.00	326.30	600.00	71.270	0.7860	0.7900	25.800
297.00	287.00	600.00	71.270	0.7850	0.7900	26.900
256.80	247.00	600.00	71.270	0.7850	0.7900	27.900
218.00	208.00	600.00	71.270	0.7860	0.7900	28.450
170.00	160.20	600.00	71.270	0.7880	0.7880	29.780
140.00	130.22	600.00	71.270	0.7880	0.7880	31.400
110.00	100.20	600.00	71.270	0.7880	0.7920	33.930
79.800	68.400	600.00	71.270	0.7880	0.7920	36.150
59.600	47.300	600.00	71.270	0.7880	0.7930	40.280
39.800	27.000	600.00	71.270	0.7890	0.7920	50.900
20.000	8.0000	600.00	71.270	0.7890	0.7890	78.900
12.000	4.1000	600.00	71.270	0.7890	0.7890	139.70

PE (KPA)	PW (KPA)	RD	VIS (U-PAS)	T (DEG K)	ZA	QO (M3/D)
4541.9	4417.8	0.166	18.279	292.29	0.9934	30.74
4211.0	4088.2	0.154	18.218	292.42	0.9936	29.69
3935.2	3818.0	0.144	18.165	292.45	0.9938	28.58
3673.3	3577.5	0.134	18.134	292.82	0.9941	26.94
3218.3	3128.6	0.117	18.053	292.89	0.9945	25.57
2949.4	2873.6	0.108	18.017	293.15	0.9949	24.49
2425.4	2344.8	0.088	17.925	293.15	0.9955	23.71
2142.8	2073.8	0.078	17.877	293.14	0.9959	22.74
1865.6	1798.0	0.068	17.830	293.14	0.9963	21.92
1598.1	1529.1	0.058	17.786	293.15	0.9968	21.50
1267.1	1199.6	0.045	17.733	293.15	0.9974	20.54
1060.3	992.85	0.038	17.699	293.15	0.9978	19.48
853.44	785.87	0.030	17.668	293.20	0.9982	18.03
645.22	566.62	0.022	17.634	293.20	0.9986	16.92
505.95	421.14	0.017	17.612	293.22	0.9989	15.18
369.43	281.18	0.012	17.590	293.22	0.9992	12.02
232.91	150.18	0.007	17.568	293.18	0.9995	7.752
177.76	123.29	0.006	17.561	293.18	0.9996	4.378

CORE SAMPLE NO 4A RUN 5 FORWARD DIRECTION
RE=0.15256 RW=0.00820 H=0.02600 POROSITY=0.22714

PE (PSI)	PW (PSI)	CP (PSI)	PB (CMHG)	TCE (MV)	TCW (MV)	TS (SEC)
8.0000	2.2000	700.00	70.800	0.7700	0.7680	138.20
12.000	4.2000	700.00	70.800	0.7800	0.7770	96.330
19.400	9.6000	700.00	70.800	0.7890	0.7890	67.330
26.000	14.400	700.00	70.840	0.7840	0.7840	51.500
32.400	20.200	700.00	70.840	0.7830	0.7870	44.230
40.000	28.320	700.00	70.840	0.7850	0.7850	41.900
54.000	43.500	700.00	70.840	0.7850	0.7860	38.150
70.000	60.000	700.00	70.840	0.7850	0.7890	34.180
90.000	81.000	700.00	70.840	0.7850	0.7880	31.900
108.00	99.000	700.00	70.880	0.7850	0.7890	29.700
126.40	117.80	700.00	70.910	0.7840	0.7880	28.000
142.00	133.40	700.00	70.910	0.7820	0.7850	27.200
160.00	150.60	700.00	70.910	0.7830	0.7890	26.430
180.00	170.60	700.00	70.910	0.7840	0.7900	26.000
199.60	189.20	700.00	70.910	0.7740	0.7800	25.400
224.40	214.20	700.00	70.950	0.7800	0.7850	24.900
250.00	236.20	700.00	70.950	0.7780	0.7850	24.050
272.00	257.80	700.00	70.950	0.7780	0.7850	23.700
300.00	284.00	700.00	70.950	0.7760	0.7850	22.900
334.60	319.00	700.00	69.640	0.7720	0.7800	22.620
386.20	371.50	700.00	69.640	0.7720	0.7800	22.200
433.00	418.40	700.00	69.640	0.7750	0.7800	21.700
488.00	473.30	700.00	69.640	0.7700	0.7760	21.230
522.00	507.30	700.00	69.590	0.7690	0.7750	20.880
571.00	556.50	700.00	69.590	0.7690	0.7750	20.500
604.00	589.00	700.00	69.590	0.7660	0.7770	20.100
662.00	647.00	700.00	69.590	0.7750	0.7850	19.500
710.00	694.10	700.00	69.570	0.7740	0.7850	18.800
745.00	728.00	728.00	69.600	0.7780	0.7870	18.270

PE (KPA)	PW (KPA)	RD	VIS (U-PAS)	T (DEG K)	ZA	QO (M3/D)
149.55	109.56	0.005	17.535	292.68	0.9997	4.426
177.13	123.35	0.006	17.549	292.92	0.9996	6.349
228.15	160.58	0.007	17.568	293.18	0.9995	9.084
273.71	193.73	0.009	17.569	293.06	0.9994	11.88
317.84	233.72	0.010	17.576	293.08	0.9994	13.83
370.24	289.70	0.012	17.585	293.08	0.9992	14.60
466.76	394.37	0.016	17.601	293.09	0.9990	16.03
577.08	508.13	0.020	17.621	293.13	0.9988	17.89
714.97	652.92	0.025	17.643	293.12	0.9985	19.17
839.13	777.08	0.030	17.663	293.13	0.9982	20.59
966.04	906.74	0.035	17.682	293.10	0.9979	21.84
1073.6	1014.3	0.038	17.697	293.04	0.9977	22.49
1197.7	1132.9	0.043	17.719	293.10	0.9975	23.14
1335.6	1270.8	0.048	17.743	293.13	0.9972	23.52
1470.7	1399.0	0.053	17.753	292.88	0.9970	24.08
1641.8	1571.4	0.059	17.787	293.02	0.9967	24.56
1818.3	1723.1	0.065	17.813	292.99	0.9964	25.43
1970.0	1872.1	0.071	17.839	292.99	0.9962	25.81
2163.0	2052.7	0.078	17.869	292.97	0.9959	26.71
2399.8	2292.3	0.087	17.905	292.86	0.9955	27.04
2755.6	2654.2	0.100	17.967	292.86	0.9950	27.55
3078.3	2977.6	0.112	18.027	292.89	0.9947	28.19
3457.5	3356.1	0.126	18.091	292.78	0.9943	28.81
3691.8	3590.5	0.135	18.134	292.76	0.9941	29.29
4029.7	3929.7	0.147	18.200	292.76	0.9939	29.84
4257.2	4153.8	0.156	18.244	292.75	0.9937	30.43
4657.1	4553.7	0.171	18.335	292.96	0.9937	31.37
4988.0	4878.4	0.183	18.404	292.94	0.9936	32.53
5229.4	5112.2	0.191	18.459	293.02	0.9936	33.48

CORE SAMPLE NO 4A RUN 5 REVERSE DIRECTION
RE=0.15256 RW=0.00820 H=0.02600 POROSITY=0.22714

PE (PSI)	PW (PSI)	CP (PSI)	PB (CMHG)	TCE (MV)	TCW (MV)	TS (SEC)
745.00	728.00	728.00	69.600	0.7780	0.7870	18.270
703.00	687.40	700.00	69.500	0.7800	0.7850	19.500
667.00	652.00	700.00	69.500	0.7790	0.7850	20.200
632.00	618.00	700.00	69.500	0.7750	0.7850	21.000
612.00	598.70	700.00	69.500	0.7750	0.7850	21.600
551.00	537.00	700.00	69.500	0.7720	0.7810	22.000
506.00	492.90	700.00	69.500	0.7720	0.7820	22.950
464.00	451.60	700.00	69.730	0.7780	0.7850	23.800
423.00	410.60	700.00	69.730	0.7790	0.7860	24.300
368.00	355.00	700.00	69.760	0.7810	0.7870	25.100
342.00	329.80	700.00	69.800	0.7820	0.7900	25.950
289.00	276.60	700.00	69.800	0.7850	0.7900	26.500
250.00	238.80	700.00	69.850	0.7870	0.7940	27.370
228.00	218.30	700.00	69.850	0.7860	0.7930	28.500
180.00	170.20	700.00	69.850	0.7850	0.7920	29.250
152.00	143.40	700.00	69.910	0.7860	0.7950	30.600
120.00	111.40	700.00	69.910	0.7870	0.7940	32.000
91.800	83.000	700.00	69.910	0.7890	0.7950	33.900
67.600	57.400	700.00	69.910	0.7900	0.7950	36.150
49.800	38.300	700.00	70.000	0.7900	0.7950	38.930
36.000	25.500	700.00	70.000	0.7900	0.7950	49.900
26.200	15.500	700.00	70.000	0.7900	0.7950	57.700
16.000	5.9000	700.00	70.000	0.7920	0.7950	73.630
10.000	2.6000	700.00	70.000	0.7930	0.7950	109.85

PE (KPA)	PW (KPA)	RD	VIS (U-PAS)	T (DEG K)	ZA	QO (M3/D)
5229.4	5112.2	0.191	18.459	293.02	0.9936	33.48
4939.7	4832.1	0.181	18.397	293.02	0.9936	31.37
4691.5	4588.0	0.172	18.345	293.01	0.9937	30.28
4450.1	4353.6	0.163	18.293	292.96	0.9937	29.13
4312.3	4220.5	0.158	18.266	292.96	0.9938	28.32
3891.7	3795.1	0.142	18.178	292.87	0.9940	27.80
3581.4	3491.1	0.131	18.120	292.88	0.9942	26.65
3292.1	3206.6	0.120	18.072	292.99	0.9945	25.70
3009.4	2924.0	0.110	18.021	293.02	0.9948	25.17
2630.3	2540.6	0.096	17.955	293.06	0.9952	24.37
2451.1	2366.9	0.089	17.927	293.10	0.9955	23.57
2085.6	2000.1	0.075	17.866	293.14	0.9960	23.08
1816.8	1739.6	0.066	17.825	293.22	0.9964	22.35
1665.1	1598.3	0.060	17.799	293.19	0.9967	21.46
1334.2	1266.6	0.048	17.744	293.17	0.9973	20.91
1141.2	1081.9	0.041	17.716	293.22	0.9976	19.99
920.58	861.28	0.033	17.680	293.22	0.9980	19.11
726.14	665.47	0.026	17.651	293.25	0.9984	18.04
559.29	488.96	0.019	17.624	293.27	0.9988	16.92
436.68	357.39	0.015	17.604	293.27	0.9991	15.71
341.54	269.14	0.011	17.589	293.27	0.9993	12.26
273.97	200.19	0.009	17.579	293.27	0.9994	10.60
203.64	134.00	0.006	17.569	293.29	0.9996	8.307
162.27	111.25	0.005	17.565	293.30	0.9997	5.568

CORE SAMPLE NO 4A RUN 6 FORWARD DIRECTION
RE=0.15256 RW=0.00820 H=0.02600 POROSITY=0.22714

PE (PSI)	PW (PSI)	CP (PSI)	PB (CMHG)	TCE (MV)	TCW (MV)	TS (SEC)
8.5000	2.0000	800.00	71.050	0.7770	0.7730	150.15
15.000	5.4000	800.00	71.050	0.7800	0.7770	90.400
20.000	9.2000	800.00	71.050	0.7850	0.7800	70.100
26.000	14.800	800.00	71.050	0.7860	0.7840	59.300
33.000	21.400	800.00	71.050	0.7860	0.7840	50.200
43.000	30.800	800.00	71.050	0.7870	0.7840	41.700
52.000	40.500	800.00	71.050	0.7870	0.7890	38.600
62.000	50.800	800.00	71.050	0.7900	0.7900	35.900
74.200	63.600	800.00	71.050	0.7950	0.7930	34.800
90.000	80.000	800.00	71.050	0.7940	0.7940	33.400
100.00	90.000	800.00	71.050	0.7950	0.7950	32.150
120.40	111.00	800.00	71.050	0.7960	0.7960	31.000
140.00	130.00	800.00	71.050	0.7950	0.7990	29.200
170.00	160.70	800.00	71.050	0.7950	0.7990	28.650
200.00	190.50	800.00	71.050	0.7930	0.7990	27.770
230.00	220.30	800.00	70.980	0.8000	0.8000	26.900
260.00	250.00	800.00	70.940	0.8000	0.8000	26.200
289.60	278.90	800.00	70.940	0.8010	0.8050	25.600
329.60	318.00	800.00	70.940	0.8010	0.8030	25.000
364.80	352.10	800.00	70.940	0.8000	0.8050	24.400
416.00	402.80	800.00	70.940	0.7990	0.8050	23.700
464.00	450.80	800.00	70.940	0.8000	0.8050	23.300
520.00	507.50	800.00	70.940	0.8000	0.8030	22.900
569.00	555.20	800.00	70.480	0.8150	0.8200	22.200
615.00	601.40	800.00	70.480	0.8150	0.8200	21.750
669.00	654.70	800.00	70.440	0.8150	0.8190	21.200
725.00	711.10	800.00	70.430	0.8100	0.8200	20.800
767.00	752.00	800.00	70.430	0.8100	0.8200	20.100
807.00	792.00	800.00	70.430	0.8100	0.8200	19.750
836.00	819.00	820.00	70.430	0.8140	0.8210	18.800

PE (KPA)	PW (KPA)	RD	VIS (U-PAS)	T (DEG K)	ZA	QO (M3/D)
153.33	108.51	0.005	17.542	292.83	0.9997	4.074
198.15	131.96	0.006	17.552	292.92	0.9996	6.766
232.62	158.16	0.007	17.561	293.02	0.9995	8.725
273.99	196.77	0.009	17.570	293.08	0.9994	10.31
322.25	242.27	0.010	17.577	293.08	0.9993	12.18
391.20	307.08	0.013	17.588	293.09	0.9992	14.67
453.25	373.96	0.015	17.601	293.15	0.9990	15.85
522.20	444.98	0.018	17.615	293.20	0.9989	17.04
606.32	533.23	0.021	17.633	293.30	0.9987	17.58
715.25	646.31	0.025	17.651	293.30	0.9985	18.31
784.20	715.25	0.028	17.663	293.33	0.9983	19.02
924.85	860.04	0.033	17.687	293.35	0.9980	19.73
1060.0	991.04	0.038	17.709	293.38	0.9978	20.95
1266.8	1202.7	0.045	17.743	293.38	0.9974	21.35
1473.7	1408.2	0.053	17.775	293.35	0.9970	22.03
1680.4	1613.5	0.061	17.814	293.45	0.9967	22.74
1887.2	1818.3	0.068	17.848	293.45	0.9964	23.35
2091.3	2017.5	0.076	17.885	293.52	0.9961	23.89
2367.1	2287.1	0.086	17.931	293.50	0.9957	24.47
2609.8	2522.2	0.095	17.973	293.51	0.9954	25.07
2962.8	2871.8	0.108	18.034	293.50	0.9950	25.81
3293.7	3202.7	0.120	18.095	293.51	0.9946	26.25
3679.9	3593.7	0.134	18.167	293.49	0.9943	26.71
4017.1	3921.9	0.146	18.249	293.88	0.9942	27.55
4334.2	4240.5	0.158	18.312	293.88	0.9941	28.12
4706.5	4607.9	0.172	18.388	293.87	0.9940	28.85
5092.6	4996.8	0.186	18.468	293.82	0.9939	29.41
5382.2	5278.8	0.197	18.531	293.82	0.9940	30.43
5658.0	5554.5	0.207	18.594	293.82	0.9940	30.97
5857.9	5740.7	0.214	18.642	293.88	0.9941	32.53

CORE SAMPLE NO 4A RUN 6 REVERSE DIRECTION
RE=0.15256 RW=0.00820 H=0.02600 POROSITY=0.22714

PE (PSI)	PW (PSI)	CP (PSI)	PB (CMHG)	TCE (MV)	TCW (MV)	TS (SEC)
836.00	819.00	820.00	70.430	0.8140	0.8210	18.800
814.00	798.20	800.00	70.440	0.8110	0.8190	19.400
786.00	773.00	800.00	70.440	0.8090	0.8190	20.500
747.00	734.30	800.00	70.440	0.8050	0.8150	20.900
694.00	682.00	800.00	70.440	0.8090	0.8150	21.500
652.00	640.50	800.00	70.440	0.8070	0.8140	22.000
606.00	595.20	800.00	70.440	0.8060	0.8140	22.680
557.00	546.10	800.00	70.440	0.8100	0.8150	23.000
514.00	504.00	800.00	70.440	0.8080	0.8140	23.850
454.00	444.40	800.00	69.700	0.8020	0.8130	25.000
402.00	394.00	800.00	69.700	0.8020	0.8100	26.800
346.00	338.50	800.00	69.700	0.8040	0.8100	28.000
313.40	306.30	800.00	69.670	0.8040	0.8100	29.200
273.60	266.50	800.00	69.620	0.8040	0.8070	30.700
222.60	215.20	800.00	69.620	0.8040	0.8080	31.900
174.40	167.30	800.00	69.620	0.8050	0.8100	34.450
139.30	132.00	800.00	70.360	0.7730	0.7760	36.800
100.00	91.400	800.00	70.360	0.7710	0.7760	38.600
60.000	48.100	800.00	70.400	0.7700	0.7760	40.600
32.000	17.000	800.00	70.460	0.7720	0.7760	47.400
20.000	7.1000	800.00	70.460	0.7750	0.7800	68.000
12.000	4.4000	800.00	70.460	0.7770	0.7790	127.20

PE (KPA)	PW (KPA)	RD	VIS (U-PAS)	T (DEG K)	ZA	QO (M3/D)
5857.9	5740.7	0.214	18.642	293.88	0.9941	32.53
5706.2	5597.3	0.209	18.605	293.82	0.9941	31.53
5513.2	5423.6	0.202	18.561	293.80	0.9940	29.84
5244.3	5156.7	0.192	18.497	293.70	0.9939	29.27
4878.9	4796.1	0.179	18.420	293.75	0.9939	28.45
4589.3	4510.0	0.168	8.358	293.71	0.9940	27.80
4272.1	4197.7	0.156	18.293	293.70	0.9941	26.97
3934.3	3859.1	0.144	18.229	293.76	0.9942	26.59
3637.8	3568.9	0.133	18.171	293.72	0.9944	25.65
3223.1	3157.0	0.118	18.090	293.64	0.9947	24.47
2864.6	2809.5	0.105	18.024	293.60	0.9951	22.82
2478.5	2426.8	0.090	17.958	293.62	0.9955	21.84
2253.7	2204.7	0.082	17.919	293.62	0.9958	20.95
1979.2	1930.3	0.072	17.871	293.59	0.9962	19.92
1627.6	1576.6	0.059	17.813	293.60	0.9968	19.17
1295.3	1246.3	0.047	17.761	293.64	0.9974	17.75
1054.2	1003.9	0.038	17.684	292.82	0.9977	16.62
783.28	723.99	0.028	17.639	292.80	0.9983	15.85
507.54	425.50	0.017	17.593	292.78	0.9989	15.07
314.57	211.15	0.010	17.562	292.81	0.9994	12.90
231.83	142.89	0.007	17.554	292.89	0.9996	8.995
176.68	124.28	0.006	17.549	292.91	0.9996	4.809

CORE SAMPLE NO 4A RUN 7 FORWARD DIRECTION
RE=0.15256 RW=0.00820 H=0.02600 POROSITY=0.22714

PE (PSI)	PW (PSI)	CP (PSI)	PB (CMHG)	TCE (MV)	TCW (MV)	TS (SEC)
30.000	.25500E-01	800.00	69.400	0.7870	0.7840	13002.
37.000	.31600E-01	800.00	69.400	0.7860	0.7850	9860.0
41.000	.47900E-01	800.00	69.400	0.7890	0.7870	8588.8
46.000	.51900E-01	800.00	69.450	0.7895	0.7850	7398.5
49.700	.59100E-01	800.00	69.400	0.7790	0.7860	6678.0
56.000	.77200E-01	800.00	69.400	0.7890	0.7850	5665.0
65.000	.97400E-01	800.00	69.440	0.7860	0.7860	4602.5
78.000	.14680	800.00	69.500	0.7890	0.7860	3585.0
89.000	.16640	800.00	69.500	0.7890	0.7860	2958.0
100.30	.17280	800.00	69.500	0.7900	0.7860	2465.8
108.50	.22000	800.00	69.730	0.7460	0.7500	2166.3
124.00	.26000	800.00	69.730	0.7410	0.7460	1748.0
140.00	.30350	800.00	69.730	0.7440	0.7450	1446.3
159.00	.40110	800.00	69.730	0.7410	0.7450	1188.0
179.00	.51670	800.00	69.730	0.7410	0.7450	988.92
201.00	.68890	800.00	69.730	0.7410	0.7440	834.00
225.00	.85780	800.00	69.730	0.7450	0.7410	698.50

PE (KPA)	PW (KPA)	RD	VIS (U-PAS)	T (DEG K)	ZA	QO (M3/D)
299.37	92.701	0.007	17.564	293.09	0.9995	0.4704E-01
347.63	92.743	0.008	17.568	293.09	0.9995	0.6203E-01
375.21	92.856	0.009	17.573	293.15	0.9994	0.7121E-01
409.75	92.950	0.009	17.575	293.14	0.9994	0.8267E-01
435.19	92.933	0.010	17.572	293.02	0.9994	0.9159E-01
478.63	93.058	0.011	17.580	293.13	0.9993	0.1080
540.74	93.250	0.012	17.584	293.10	0.9993	0.1329
630.45	93.671	0.013	17.593	293.14	0.9992	0.1706
706.29	93.806	0.015	17.599	293.14	0.9991	0.2068
784.20	93.850	0.016	17.605	293.15	0.9990	0.2481
841.05	94.482	0.017	17.565	292.17	0.9989	0.2823
947.92	94.758	0.019	17.568	292.05	0.9988	0.3499
1058.2	95.058	0.021	17.578	292.08	0.9986	0.4229
1189.2	95.731	0.024	17.587	292.04	0.9985	0.5149
1327.1	96.528	0.026	17.598	292.04	0.9983	0.6185
1478.8	97.715	0.029	17.610	292.03	0.9982	0.7334
1644.3	98.880	0.032	17.624	292.04	0.9980	0.8757

CORE SAMPLE NO 4A RUN 8 FORWARD DIRECTION
RE=0.15256 RW=0.00820 H=0.02600 POROSITY=0.22714

PE (PSI)	PW (PSI)	CP (PSI)	PB (CMHG)	TCE (MV)	TCW (MV)	TS (SEC)
20.000	.17500E-01	800.00	69.400	0.7880	0.7840	15258.
26.000	.21600E-01	800.00	69.400	0.7860	0.7840	11590.
34.000	.20160	800.00	69.400	0.7860	0.7850	8868.0
42.000	.11000E-01	800.00	69.400	0.7890	0.7860	7133.0
48.000	.18000E-01	800.00	69.400	0.7890	0.7850	6144.0
56.000	.77400E-01	800.00	69.440	0.7860	0.7860	5333.5
66.000	.16200E-01	800.00	69.440	0.7900	0.7900	4498.0
76.000	.50400E-01	800.00	69.500	0.7910	0.7860	3994.0
84.000	.10080	800.00	69.500	0.7890	0.7860	3584.0
92.000	.10440	800.00	69.500	0.7890	0.7860	3188.0
100.00	.82800E-01	800.00	69.500	0.7900	0.7860	2898.8
110.00	.20600	800.00	69.730	0.7460	0.7500	2597.3
124.00	.20600	800.00	69.730	0.7410	0.7460	2230.0
140.00	.30350	800.00	69.730	0.7440	0.7450	1795.3
160.00	.40110	800.00	69.730	0.7410	0.7450	1375.0
180.00	.51670	800.00	69.730	0.7410	0.7450	967.92
200.00	.75890	800.00	69.730	0.7410	0.7440	654.00
226.00	.95760	800.00	69.730	0.7450	0.7410	363.50
230.00	.98770	800.00	69.730	0.7400	0.7410	218.50

PE (KPA)	PW (KPA)	RD	VIS (U-PAS)	T (DEG K)	ZA	QO (M3/D)
230.42	92.646	0.006	17.559	293.10	0.9996	0.4009E-01
271.79	92.674	0.007	17.562	293.08	0.9996	0.5277E-01
326.95	93.915	0.008	17.567	293.09	0.9995	0.6897E-01
382.11	92.601	0.009	17.573	293.14	0.9994	0.8575E-01
423.47	92.650	0.009	17.576	293.13	0.9994	0.9955E-01
478.69	93.112	0.011	17.579	293.10	0.9993	0.1147
547.63	92.690	0.012	17.589	293.20	0.9993	0.1360
616.66	93.006	0.013	17.593	293.17	0.9992	0.1531
671.82	93.354	0.014	17.596	293.14	0.9991	0.1707
726.98	93.379	0.015	17.600	293.14	0.9991	0.1919
782.13	93.230	0.016	17.605	293.15	0.9990	0.2110
851.39	94.386	0.017	17.566	292.17	0.9989	0.2355
947.92	94.386	0.019	17.568	292.05	0.9988	0.2743
1058.2	95.058	0.021	17.578	292.08	0.9986	0.3407
1196.1	95.731	0.024	17.588	292.04	0.9985	0.4448
1334.0	96.528	0.026	17.599	292.04	0.9983	0.6319
1471.9	98.198	0.029	17.609	292.03	0.9982	0.9352
1651.2	99.568	0.032	17.624	292.04	0.9980	1.683
1678.8	99.775	0.033	17.624	291.98	0.9979	2.799

CORE SAMPLE NO 4A RUN 9 REVERSE DIRECTION
RE=0.15256 RW=0.00820 H=0.02600 POROSITY=0.22714

PE (PSI)	PW (PSI)	CP (PSI)	PB (CMHG)	TCE (MV)	TCW (MV)	TS (SEC)
292.00	.49100E-01	700.00	69.780	0.8630	0.8600	23.500
286.00	.49100E-01	700.00	69.780	0.8630	0.8600	25.400
280.00	.49100E-01	700.00	69.780	0.8630	0.8600	28.100
274.00	.98200E-01	700.00	69.780	0.8630	0.8580	33.500
264.00	[illegible]	700.00	69.780	0.8620	0.8580	41.400
252.00	[illegible]	700.00	69.780	0.8600	0.8580	61.100
240.00	[illegible]	700.00	69.780	0.8600	0.8580	80.600
224.00	[illegible]	700.00	69.780	0.8600	0.8550	107.18
212.00	[illegible]	700.00	69.780	0.8590	0.8550	122.35
200.00	[illegible]	700.00	70.120	0.8150	0.8140	137.15
180.00	[illegible]	700.00	70.140	0.8340	0.8340	159.50
160.00	.98200E-01	700.00	70.140	0.8400	0.8430	189.20
140.00	.49100E-01	700.00	70.140	0.8470	0.8450	221.30
120.00	.98200E-01	700.00	70.140	0.8530	0.8530	268.10
100.00	.73700E-01	700.00	70.140	0.8530	0.8500	330.10
80.000	.49100E-01	700.00	70.140	0.8560	0.8530	424.60
60.000	.98200E-01	700.00	70.140	0.8590	0.8590	576.90
40.000	.49100E-01	700.00	70.140	0.8600	0.8570	884.00
20.000	.49100E-01	700.00	70.140	0.8600	0.8560	1830.5

PE (KPA)	PW (KPA)	RD	VIS (U-PAS)	T (DEG K)	ZA	QO (M3/D)
2106.3	93.371	0.040	17.794	294.97	0.9978	26.03
2064.9	93.371	0.040	17.790	294.97	0.9978	24.08
2023.6	93.371	0.039	17.787	294.97	0.9979	21.77
1982.2	93.709	0.038	17.782	294.95	0.9979	18.26
1913.2	93.371	0.037	17.776	294.93	0.9980	14.77
1830.5	94.217	0.035	17.769	294.91	0.9980	10.01
1747.8	93.709	0.034	17.762	294.91	0.9981	7.589
1637.5	93.709	0.032	17.751	294.87	0.9982	5.707
1554.7	93.371	0.030	17.744	294.86	0.9983	4.999
1472.4	95.179	0.029	17.690	293.81	0.9983	4.460
1334.6	94.528	0.026	17.701	294.29	0.9985	3.835
1196.7	94.189	0.024	17.698	294.48	0.9986	3.233
1058.8	93.851	0.021	17.692	294.59	0.9988	2.764
920.88	94.189	0.019	17.689	294.76	0.9989	2.281
782.99	94.020	0.016	17.677	294.72	0.9990	1.853
645.09	93.851	0.014	17.669	294.80	0.9992	1.441
507.20	94.189	0.011	17.663	294.91	0.9993	1.060
369.30	93.851	0.008	17.652	294.90	0.9995	0.6919
281.41	93.851	0.006	17.641	294.88	0.9996	0.3341

CORE SAMPLE NO 2 RUN 1 FORWARD DIRECTION
RE=0.15225 RW=0.00815 H=0.02803 POROSITY=0.23432

PE (PSI)	PW (PSI)	CP (PSI)	PB (CMHG)	TCE (MV)	TCW (MV)	TS (SEC)
10.000	.30000	600.00	69.930	0.8150	0.8390	539.00
20.000	5.4000	600.00	69.930	0.8140	0.8450	285.10
30.000	6.2000	600.00	69.930	0.8180	0.8450	154.50
40.000	13.000	600.00	69.930	0.8190	0.8500	114.37
60.000	38.900	600.00	69.930	0.8220	0.8500	100.65
80.000	60.800	600.00	69.930	0.8250	0.8520	90.000
110.00	91.800	600.00	69.930	0.8260	0.8520	77.530
145.00	127.60	600.00	69.900	0.8310	0.8540	67.600
179.00	159.00	600.00	69.900	0.8350	0.8540	56.300
208.00	186.80	600.00	69.900	0.8370	0.8550	50.400
252.00	231.20	600.00	69.900	0.8380	0.8550	46.500
297.00	276.30	600.00	69.900	0.8440	0.8530	43.000
348.00	327.50	600.00	69.900	0.8440	0.8530	39.800
368.00	342.50	600.00	69.500	0.8230	0.8410	34.200
393.00	367.00	600.00	69.880	0.8460	0.8550	32.450
413.00	386.00	600.00	69.500	0.8260	0.8480	29.730
456.00	430.00	600.00	69.500	0.8260	0.8550	26.750
511.00	487.00	600.00	69.500	0.8300	0.8550	23.660
551.00	528.00	600.00	69.500	0.8330	0.8530	22.230
592.00	570.00	600.00	69.500	0.8360	0.8500	20.000
617.00	596.00	604.00	69.500	0.8360	0.8480	17.730

PE (KPA)	PW (KPA)	RD	VIS (U-PAS)	T (DEG K)	ZA	QO (M3/D)
162.18	95.301	0.005	17.600	294.12	0.9997	1.135
231.13	130.46	0.007	17.611	294.18	0.9996	2.145
300.07	135.98	0.008	17.619	294.23	0.9995	3.959
369.02	182.86	0.010	17.632	294.30	0.9994	5.348
506.92	361.44	0.016	17.659	294.34	0.9990	6.077
644.81	512.43	0.021	17.684	294.40	0.9987	6.796
851.66	726.17	0.029	17.718	294.41	0.9983	7.889
1092.9	972.96	0.038	17.761	294.50	0.9979	9.048
1327.4	1189.5	0.046	17.800	294.55	0.9975	10.86
1527.3	1381.1	0.053	17.834	294.59	0.9972	12.14
1830.7	1687.3	0.065	17.885	294.60	0.9967	13.15
2140.9	1998.2	0.076	17.939	294.65	0.9962	14.22
2492.6	2351.2	0.089	17.989	294.65	0.9958	15.37
2629.9	2454.1	0.094	18.002	294.24	0.9956	17.88
2802.8	2623.5	0.100	18.052	294.70	0.9955	18.85
2940.2	2754.0	0.105	18.061	294.36	0.9952	20.57
3236.7	3057.4	0.116	18.119	294.45	0.9950	22.87
3615.9	3450.4	0.130	18.193	294.50	0.9947	25.85
3891.7	3733.1	0.140	18.247	294.51	0.9945	27.51
4174.4	4022.7	0.151	18.303	294.51	0.9944	30.58
4346.7	4201.9	0.157	18.337	294.49	0.9943	34.50

CORE SAMPLE NO 2 RUN 2 REVERSE DIRECTION
RE=0.15225 RW=0.00815 H=0.02803 POROSITY=0.23432

PE (PSI)	PW (PSI)	CP (PSI)	PB (CMHG)	TCE (MV)	TCW (MV)	TS (SEC)
631.00	608.00	605.00	69.840	0.7860	0.7650	16.820
609.00	583.00	600.00	69.840	0.7870	0.7600	18.200
557.00	528.00	600.00	69.840	0.7850	0.7680	20.240
516.00	486.00	600.00	69.840	0.7890	0.7650	21.780
477.00	448.00	600.00	69.840	0.7890	0.7690	24.360
435.00	405.00	600.00	69.840	0.7900	0.7700	25.600
393.00	361.60	600.00	70.000	0.7900	0.7700	26.950
340.00	306.00	600.00	70.000	0.7900	0.7700	28.280
300.00	263.70	600.00	70.000	0.7900	0.7730	29.680
270.00	234.40	600.00	70.080	0.7910	0.7670	32.600
235.00	201.00	600.00	70.080	0.7900	0.7640	37.300
200.00	171.00	600.00	70.140	0.7910	0.7630	48.030
176.50	147.00	600.00	70.140	0.7910	0.7560	52.400
147.00	115.00	600.00	70.150	0.7910	0.7550	56.500
113.00	80.200	600.00	70.160	0.7910	0.7530	69.220
90.400	56.000	600.00	70.160	0.7900	0.7530	81.150
63.600	32.000	600.00	70.230	0.7910	0.7540	118.88
45.800	5.4800	600.00	70.340	0.7870	0.7510	141.80
25.800	1.3000	600.00	70.340	0.7860	0.7550	313.60

PE (KPA)	PW (KPA)	RD	VIS (U-PAS)	T (DEG K)	ZA	QO (M3/D)
4443.7	4285.1	0.162	18.280	292.84	0.9937	36.36
4292.0	4112.8	0.156	18.246	292.80	0.9937	33.61
3933.5	3733.5	0.142	18.176	292.87	0.9940	30.22
3650.8	3444.0	0.131	18.122	292.88	0.9942	28.08
3381.9	3182.0	0.121	18.075	292.93	0.9944	25.11
3092.3	2885.5	0.111	18.022	292.96	0.9947	23.89
2803.0	2586.5	0.100	17.970	292.96	0.9951	22.70
2437.5	2203.1	0.086	17.905	292.96	0.9956	21.63
2161.8	1911.5	0.075	17.858	292.99	0.9960	20.61
1955.0	1709.6	0.068	17.821	292.93	0.9963	18.76
1713.7	1479.3	0.059	17.780	292.88	0.9967	16.40
1472.5	1272.5	0.051	17.743	292.88	0.9971	12.73
1310.4	1107.0	0.045	17.712	292.80	0.9974	11.67
1107.1	886.42	0.037	17.677	292.78	0.9978	10.83
872.65	646.50	0.028	17.638	292.76	0.9983	8.836
716.82	479.65	0.022	17.612	292.75	0.9986	7.537
532.14	314.26	0.016	17.586	292.77	0.9990	5.145
409.56	131.56	0.010	17.557	292.68	0.9994	4.313
271.66	102.74	0.007	17.546	292.72	0.9995	1.950

CORE SAMPLE NO 2 RUN 3 FORWARD DIRECTION

RE=0.15225 RW=0.00815 H=0.02803 POROSITY=0.23432

PE (PSI)	PW (PSI)	CP (PSI)	PB (CMHG)	TCE (MV)	TCW (MV)	TS (SEC)
10.000	.25000E-01	600.00	71.040	0.7630	0.7710	1419.1
20.000	.25000E-01	600.00	71.040	0.7650	0.7710	617.90
30.000	.44000E-01	600.00	71.040	0.7650	0.7750	370.40
42.000	.12300	600.00	71.040	0.7650	0.7710	243.10
54.000	.37000E-01	600.00	71.040	0.7670	0.7710	175.20
66.000	.61000E-01	600.00	71.040	0.7670	0.7690	136.25
82.000	.10000	600.00	71.040	0.7660	0.7600	103.30
100.00	.74000E-01	600.00	71.040	0.7660	0.7700	80.550
120.00	.12000	600.00	71.040	0.7660	0.7660	63.600
140.00	.49000E-01	600.00	71.040	0.7660	0.7630	53.400
160.00	.25000E-01	600.00	71.040	0.7660	0.7660	45.300
180.00	.25000E-01	600.00	71.040	0.7660	0.7670	39.530
200.00	.25000E-01	600.00	71.040	0.7660	0.7590	34.530
220.00	.25000E-01	600.00	71.040	0.7660	0.7590	31.000
240.00	.25000E-01	600.00	71.040	0.7650	0.7640	28.300
260.00	.25000E-01	600.00	71.040	0.7650	0.7570	25.880
280.00	.25000	600.00	71.040	0.7650	0.7560	23.820
300.00	.54000	600.00	71.040	0.7640	0.7560	21.860

PE (KPA)	PW (KPA)	RD	VIS (U-PAS)	T (DEG K)	ZA	QO (M3/D)
163.66	94.884	0.005	17.533	292.63	0.9997	0.4310
232.61	94.884	0.006	17.540	292.66	0.9996	0.9899
301.55	95.015	0.007	17.547	292.71	0.9995	1.651
384.29	95.560	0.009	17.552	292.66	0.9994	2.516
467.03	94.967	0.010	17.559	292.68	0.9993	3.491
549.77	95.133	0.012	17.565	292.66	0.9992	4.489
660.08	95.401	0.014	17.568	292.54	0.9991	5.921
784.19	95.222	0.016	17.583	292.66	0.9990	7.593
922.08	95.539	0.019	17.592	292.61	0.9988	9.617
1060.0	95.050	0.021	17.601	292.57	0.9987	11.45
1197.9	94.884	0.024	17.614	292.61	0.9985	13.50
1335.8	94.884	0.026	17.625	292.62	0.9984	15.47
1473.7	94.884	0.029	17.632	292.52	0.9982	17.71
1611.6	94.884	0.032	17.643	292.52	0.9981	19.73
1749.5	94.884	0.034	17.656	292.57	0.9979	21.61
1887.3	94.884	0.037	17.663	292.49	0.9978	23.63
2025.2	96.436	0.039	17.674	292.47	0.9976	25.68
2163.1	98.435	0.042	17.684	292.46	0.9975	27.98

CORE SAMPLE NO 2   RUN 4   REVERSE DIRECTION
RE=0.15225 RW=0.00815 H=0.02803 POROSITY=0.23432

PE (PSI)	PW (PSI)	CP (PSI)	PB (CMHG)	TCE (MV)	TCW (MV)	TS (SEC)
300.00	.22000	600.00	70.820	0.7530	0.7610	19.500
280.00	.12000	600.00	70.820	0.7540	0.7610	21.530
260.00	.74000E-01	600.00	70.820	0.7550	0.7660	24.350
240.00	.74000E-01	600.00	70.820	0.7560	0.7660	27.250
220.00	.61000E-01	600.00	70.820	0.7600	0.7630	30.600
200.00	.49000E-01	600.00	70.820	0.7600	0.7610	35.340
180.00	.49000E-01	600.00	70.810	0.7710	0.7730	41.170
160.00	.27000	600.00	70.810	0.7740	0.7760	48.830
140.00	.49000E-01	600.00	70.810	0.7740	0.7770	58.370
120.00	.49000E-01	600.00	70.810	0.7770	0.7750	71.930
100.00	.19600	600.00	70.810	0.7770	0.7750	88.670
80.000	.49000E-01	600.00	70.810	0.7800	0.7790	113.30
60.000	.25000E-01	600.00	70.810	0.7800	0.7800	16[illegible].80
40.000	.25000E-01	600.00	70.810	0.7840	0.7760	255.20
30.000	.25000E-01	600.00	70.810	0.7840	0.7790	360.28
20.000	.25000E-01	600.00	70.810	0.7870	0.7840	555.20
10.000	.98000E-01	600.00	70.810	0.7890	0.7860	1240.8

PE (KPA)	PW (KPA)	RD	VISA (U-PAS)	T (DEG K)	ZA	QO (M3/D)
2162.8	95.935	0.042	17.681	292.39	0.9975	31.37
2025.0	95.246	0.039	17.670	292.40	0.9976	28.41
1887.1	94.929	0.037	17.662	292.47	0.9978	25.12
1749.2	94.929	0.034	17.652	292.49	0.9979	22.45
1611.3	94.839	0.032	17.641	292.50	0.9981	19.99
1473.4	94.756	0.029	17.629	292.47	0.9982	17.31
1335.5	94.743	0.026	17.631	292.76	0.9984	14.86
1197.6	96.267	0.024	17.624	292.83	0.9985	12.53
1059.7	94.743	0.021	17.613	292.84	0.9987	10.48
921.78	94.743	0.019	17.603	292.86	0.9988	8.503
783.88	95.757	0.016	17.592	292.86	0.9990	6.898
645.99	94.743	0.014	17.585	292.94	0.9991	5.398
508.09	94.578	0.011	17.575	292.96	0.9993	3.780
370.20	94.578	0.009	17.564	292.96	0.9994	2.397
301.25	94.578	0.007	17.560	292.99	0.9995	1.698
232.30	94.578	0.006	17.559	293.09	0.9996	1.102
163.35	95.081	0.005	17.556	293.14	0.9997	0.4929

Index